Influence of field properties and space-boundaries on quantum entanglement between Unruh-DeWitt detectors

Dipankar Barman

A thesis
submitted for the degree of

Doctor of Philosophy

Supervisor

Dr. Bibhas Ranjan Majhi

Department of Physics
Indian Institute of Technology Guwahati
Guwahati - 781039, Assam, India

Influence of field properties and space-boundaries on quantum entanglement between Unruh-DeWitt detectors

A thesis submitted by

DIPANKAR BARMAN

SUPERVISOR: **DR. BIBHAS RANJAN MAJHI**

Department of Physics
INDIAN INSTITUTE OF TECHNOLOGY GUWAHATI

A thesis submitted to Indian Institute of Technology Guwahati in accordance with the requirements of the degree of DOCTOR OF PHILOSOPHY in the Department of Physics.

SEPTEMBER 1, 2025

STATEMENT

Dipankar Barman
Roll No. 206121013
Department of Physics
IIT Guwahati
Guwahati, India

I hereby declare that works presented in the thesis entitled "**Influence of field properties and space-boundaries on quantum entanglement between Unruh-DeWitt detectors**" has been carried out by me under the supervision of Dr. Bibhas Ranjan Majhi at the Department of Physics, Indian Institute of Technology Guwahati, India. The thesis has not been submitted anywhere else for any degree. Works presented in the thesis are all my own unless referenced to the contrary in the thesis.

Dipankar Barman

Dipankar Barman

Date: September 1, 2025

DISCLAIMER

The bibliography included in this thesis is, by no means complete but contains the ones which are consulted thoroughly by me. I apologize for inadvertently missing out some of the research papers, review articles and other scientific documents pertaining to the focus of this thesis which should also have been cited.

Dipankar Barman

– Dipankar Barman

CERTIFICATE

Dr. Bibhas Ranjan Majhi
Associate Professor
Department of Physics
Indian Institute of Technology Guwahati
Guwahati, India
email:bibhas.majhi@iitg.ac.in

It is certified that the work contained in the thesis entitled **"Influence of field properties and space-boundaries on quantum entanglement between Unruh-DeWitt detectors"** by Mr. Dipankar Barman (Roll No - 206121013), a Ph.D. student in the Department of Physics, Indian Institute of Technology Guwahati is carried out under my supervision and has not been submitted elsewhere for the award of any other degree.

Dr. Bibhas Ranjan Majhi

Date: September 1, 2025

List of publications

1⋆. **Role of thermal field in entanglement harvesting between two accelerated Unruh-DeWitt detectors**
Dipankar Barman, Subhajit Barman and Bibhas Ranjan Majhi
JHEP 07 (2021) 124 [arXiv:2104.11269 [gr-qc]].

2. **Constructing an entangled Unruh Otto engine and its efficiency**
Dipankar Barman and Bibhas Ranjan Majhi
JHEP 05 (2022) 046 [arXiv:2111.00711 [quant-ph]].

3. **Entanglement harvesting from conformal vacuums between two Unruh-DeWitt detectors moving along null paths**
Subhajit Barman, **Dipankar Barman** and Bibhas Ranjan Majhi
JHEP 09 (2022) 106 [arXiv:2112.01308 [gr-qc]].

4⋆. **Entanglement harvesting between two inertial Unruh-DeWitt detectors from nonvacuum quantum fluctuations**
Dipankar Barman, Subhajit Barman and Bibhas Ranjan Majhi
Phys.Rev.D 106, 045005 (2022) [arXiv:2205.08505 [gr-qc]].

5⋆. **Spontaneous entanglement leakage of two static entangled Unruh-DeWitt detectors**
Dipankar Barman, Angshuman Choudhury, Bhushan Kad and Bibhas Ranjan Majhi
Phys.Rev.D 107, 045001 (2023) [arXiv:2211.00383 [quant-ph]].

6. **Field theory in Rindler frame and more on the correspondence with thermal field theory formalisms**
   Dipankar Barman and Bibhas Ranjan Majhi
   Annals Phys. 465 (2024) 169678 [arXiv:2303.16022 [hep-th]].

7⋆. **Are multiple reflecting boundaries capable of enhancing entanglement harvesting?**
   Dipankar Barman and Bibhas Ranjan Majhi
   Phys.Rev.D 108, 085007 (2023) [arXiv:2306.09943 [gr-qc]].

8. **Mirror-enhanced acceleration-induced geometric phase**
   Dipankar Barman, Debasish Ghosh and Bibhas Ranjan Majhi
   Eur.Phys.J.C 85, 410 (2025) [arXiv:2405.07711 [quant-ph]].

9. **Entanglement Harvesting in Accelerated Systems: Field Temperature and Boundary Effects**
   Dipankar Barman and Bibhas Ranjan Majhi
   Conference proceedings Seventeenth Marcel Grossmann Meeting, Italy (7-12 July 2024).

10. **Can spacetime fluctuations generate entanglement between co-moving accelerated detectors?**
    Dipankar Barman and Bibhas Ranjan Majhi
    Phys.Lett.B 868 (2025) 139631 [arXiv:2504.12674 [gr-qc]].

Note: ⋆ marked publications are included in the thesis.

WORKS PRESENTED IN THE CONFERENCES/SEMINARS

1. Presented a poster titled **"Constructing an entangled Unruh Otto engine and its efficiency"**, at *Avenues of Quantum Field Theory*, at Genoa, Italy during $8th - 10th$ February, 2022.

2. Delivered a talk, titled **"Role of thermal field in entanglement harvesting between two accelerated Unruh-DeWitt detectors"**, at *32nd meeting of Indian Association for General Relativity and Gravitation (IAGRG)* organized by the Department of Physical Sciences, Indian Institute of Science and Research (IISER) Kolkata during $19th - 21st$ December, 2022.

3. Delivered a talk, titled **"Are multiple reflecting boundaries capable of enhancing entanglement harvesting?"**, at *the 10th International Conference on Gravitation and Cosmology (ICGC)* organized by the Department of Physics, the Indian Institute of Technology (IIT) Guwahati during $6th - 9th$ December, 2023.

4. Delivered a talk, titled **"Entanglement Harvesting in Accelerated Systems: Field Temperature and Boundary Effects"**, at *Seventeenth Marcel Grossmann Meeting* organized by the 'Gabriele d'Annunzio' University and ICRANet during $7th - 12th$ July, 2024.

5. Delivered a talk, titled **"Entanglement Harvesting in Accelerated Systems: Field Temperature and Boundary Effects"**, at *7th International Conference in Holography and String Theory in Da Nang*, organized by Duy Tan University during $22th - 26th$ August, 2024.

6. Delivered a seminar talk, titled **"Entanglement Harvesting in Accelerated Systems: Field Temperature and Boundary Effects"**, organized by the Department of Physical Sciences, Indian Institute of Science and Research (IISER) Mohali on $14th$ November, 2024.

ACKNOWLEDGEMENTS

First and foremost, I would like to express my deepest gratitude to my supervisor, Dr Bibhas Ranjan Majhi, who has supported me in every step of my PhD journey. His expertise, commitment to his work, and example of a well-balanced life as a researcher have always inspired me. I am grateful to my doctoral committee members - Dr. Debaprasad Maity, Dr. Sayan Chakrabarti and Dr. Tarak Nath Dey for their valuable suggestions during the yearly assessments of my research work. I would like to thank all the technical support personnel and academic and non-academic members of the department who assisted me in different ways throughout my research period. I thank my other collaborators and co-authors, Subhajit Da, Angshuman, Bhushan and Debasish. I am especially thankful to my former and present group members cum friends Subhajit Da, Surojit Da, Sumit Da, Samik Da, Gopal Da, Soumya Da, Subhankar, Bhera, Pradeep and Mainak for many stimulating intellectual discussions.

I am also thankful to Dr. Manisha Phukan and Dr. Gitanjali Devi for their support while performing external teaching duty in LCB College for PMRF requirement. I especially thank Aritra and Anterdipan for helping me out during this period.

For being a part of my PhD journey, I would like to thank my fellow batch mates and dear friends Anterdipan, Aritra, Ankan, Ayan, Himanshu, Madan, Mouli, Nayan, Rajesh, Sanjib, Sourav and Subhankar. I acknowledge every bit of your help during this voyage. I would want to express my gratitude to a few of my close friends, including Adarsh, Bhupen, Keshav, Ranjith, Rohan, Shivam, Shivaprasad, Tanmay, and Uma Shankar, whom I have known since I started my master's programme. I would like to thank some special friends from my college days to this date who are very close to my heart, including Chitradeep, Krishnendu, Kuntal, Rajeswar and Santanu. The list would not be complete if I don't mention my childhood friends, Santanu, Debabrata, Madhusudan, Noor and Shiblal.

I owe a deep debt of gratitude to my parents, for their unwavering love, encouragement, and support throughout my life. I am also deeply thankful to my sister, Banashree and brother-in-law, Koushik, for their continual care and encouragement. Finally, I thank

Rima – for her love, her selflessness, and for making these years filled with happiness.

Abstract

In recent years, the fascinating phenomenon of quantum entanglement has garnered significant interest in the scenarios of relativistic particles in flat and curved spacetimes. It is well known that the vacuum of a quantum field is an entangled state from a local observer's point of view. This entanglement in the vacuum is key behind the famous Hawking radiation and the Unruh effect. In these studies, one usually considers two two-level UDW detectors or atoms, which do not interact with each other but interact with the background quantum field. The detectors are initially unentangled; they can get entangled through the interaction, popularly known as entanglement harvesting. The nature of entanglement harvesting depends on the background spacetime, boundary conditions, motion of the detectors, etc. Entanglement harvesting is possible even if the atoms are in causally disconnected regions. Also, the detectors may lose entanglement if they are initially entangled, a process known as entanglement leakage.

This thesis aims to understand the phenomenon of entanglement harvesting and leakage in various inertial and non-inertial systems by considering different field properties and boundary conditions. First, we consider two accelerated detectors interacting with the background massless real scalar field. Since reality is thermal in nature, we consider the quantum field to be a thermal field. Through the interaction, the atoms get entangled, and how the nature of entanglement varies with temperature is studied. Next, we consider the situation where one or two reflecting boundaries are placed in the background space, which changes the field's density of modes. We studied how the presence of reflecting boundaries influences entanglement harvesting between the atoms. This aims to determine if reflecting boundaries enhance entanglement harvesting compared to the free space scenario. The higher the degree of entanglement, the higher the possibility of operationally realising it. We then consider the scenario where the detectors move with constant velocity and are coupled to a massless real scalar field. However, the field is in an excited state. Since, in nature, it is not guaranteed that the quantum field will always remain in the ground state. Therefore, it is important to investigate if one can extract entanglement from a non-vacuum field state. We observed that entanglement from a non-vacuum state is always less than the vacuum counterpart. It aligns with the earlier known fact that the vacuum contains maximum entanglement content among all field states. Finally, we have investigated what will happen if two static detectors are initially entangled but interacting with the background quantum field. These detectors will lose entanglement due to spontaneous emission and vacuum fluctuations.

Table of Contents

List of Figures

Figure **Page**

CHAPTER 1

INTRODUCTION

In 1905, Einstein authored the foundation of the Special Theory of Relativity, which was incompatible with Newton's gravitational theory. This conflict led Einstein to his groundbreaking masterwork; after a decade, he presented the world with the General Theory of Relativity. It is considered one of the most outstanding intellectual achievements of human history. The General Theory of Relativity grew from Einstein's remarkably simple thought experiment on the (local) equivalence of gravitation and acceleration, known as the Equivalence Principle. It led him to conclude that, unlike the other natural forces, gravity is a manifestation of the curvature of spacetime. It is the physics of large and heavy objects. On the other hand, quantum physics – physics of small and light objects, grew up by holding the hands of several experimental and theoretical physicists. These are two of the most indispensable parts of the modern physics. These branches of physics involve two realms – one meant for very large and heavy, another meant for very small and light, which makes them entirely incompatible from the fundamental level. Coupling these two pillars of modern physics is a notoriously tricky challenge and has yet to produce a pretty acceptable solution. This dilemma has led many physicists to turn to the field of quantum field theory in curved space. In this approach, one studies quantum field theory imposed onto classical background geometry, presuming the back-reaction of the field to be negligible. This profound approach is an intermediate step towards the quantum theory of gravity and essential in understanding the quantum nature of gravity until a complete quantum gravity theory arrives.

1.1 Black holes and the equivalence principle

"The breakthrough came suddenly one day. I was sitting on a chair in my patent office in Bern. Suddenly a thought struck me: If a man falls freely, he would not feel his weight. I was taken aback. This simple thought experiment made a deep impression on me. This led me to the theory of gravity."
– Einstein

The foundation of Einstein's General Theory of Relativity was led by a simple thought experiment involving an observer in an elevator. He imagined two observers in two elevators; one rests on the surface of the Earth and another uniformly accelerating upward with acceleration g will not be able to distinguish whether they are in one situation or the other. Einstein's *equivalence principle* is the idea that says no experiment that can distinguish a uniform acceleration from a uniform gravitational field. The two are fully "*equivalent*". This understanding of physics in accelerated frames revealed the physics of gravity.

Einstein's General Theory of Relativity (GR) is widely considered the most acceptable theory for explaining gravity. Despite its complicated non-linear field equation, several attempts have been made to understand the closed-form solution of Einstein's field equation. Just a few months after Einstein's discovery, Karl Schwarzschild [1] discovered an exact solution of Einstein's vacuum field equations for a point mass. This solution predicts the existence of supermassive compact astrophysical objects which features peculiar singularity in the spacetime. John Archibald Wheeler named these peculiar objects as '*black holes*' and the research on black holes became one of the most active fields of research till now. In a black hole, mass is compressed into a compact volume, so the gravitational pull at the surface is so strong that nothing, even light, can escape. After Schwarzschild, Johannes Droste [2], Hans Reissner [3], Gunnar Nordström [4], John Lighton Synge [5], David Finkelstein [6], Christian Fronsdal [7], Martin D Kruskal [8], György Szekeres [9], ID Novikov [10, 11] and Roy Kerr [12] contributed to the solution of Einstein's theory. The major lessons learned during these studies revealed the global features of the Einstein equation's peculiar singularities, known as '*black holes*'. Finkelstein identified that the very existence of such singularity comes with another exotic character, constituted by a hypothetical null surface called *event horizon*, from which nothing can come out, even the light. Any information that falls into the black hole will be lost from the outside universe; no information inside the *event horizon* can

reach an observer outside of it. In the scenario of a black hole, such global features are connected with its topology and the causal structure. The formation of black holes due to the gravitational collapse of supermassive objects has long been investigated. Astronomers often found evidence supporting the presence of black holes. The recent discoveries of gravitational waves [13–16] from the binary black holes merger in 2015 and the first-ever image of black hole produced by *Event Horizon Telescope* collaboration [17] in 2019, have resolved the long-standing debate over the existence of black holes in reality.

1.2 The Hawking radiation and the Unruh effect

"Consideration of particle emission from black holes would seem to suggest that God not only plays dice, but also sometimes throws them where they cannot be seen."
– Stephen Hawking

It was Jacob Bekenstein, who first realised some similarities between black-hole physics and thermodynamics. If an object with some temperature and entropy falls into a black hole, the entropy of that object will be entirely lost from the outside universe. This will lead to a violation of the second law of thermodynamics. It was Bekenstein's observation that black holes must have some entropy, which increases with the mass of the black hole; only then the second law of thermodynamics will be preserved. His most striking observation was that, like entropy, the area of the black hole always tends to increase irreversibly. Indeed, the entropy of the black hole is proportional to the area of the black hole [18]. Later, Hawking shows the proportionality constant is precisely one-quarter of the horizon area in Planck units [19]. Hence, in SI units, the BH entropy turns out to be

$$S = \frac{k_B A}{4 l_p^2}, \tag{1.1}$$

where A is the horizon area. This discovery of Bekenstein-Hawking entropy for black holes led Hawking to his most profound insight about black holes. Black holes not only have entropy, but also have temperature [19, 20]. Due to quantum vacuum fluctuations, black holes emit particles with a Planckian thermal distribution upto a grey-body factor. For a Schwarzschild black hole, the temperature associated with this distribution turns

out to be

$$T_H = \frac{\hbar c^3}{8\pi G k_B M}\,. \tag{1.2}$$

Here M is the mass of the black hole. This temperature can re-expressed in terms of the surface gravity (κ) as

$$T_H = \frac{\hbar \kappa}{2\pi c k_B}\,. \tag{1.3}$$

The original idea of Hawking was based on the properties of quantum field theory in curved spacetime, and it is still one of the pioneering results of this theory. Near the event horizon, quantum field's vacuum after the black hole formation is compared with the vacuum at the asymptotic past (before formation of black hole) through the Bogoliubov coefficients. It turns out that the two vacuum states are not the same. Consequently, an observer at the future null infinity will observe a flux of particles emitting out from the immediate vicinity of the event horizon of the black hole. Hawking heuristically explained this phenomenon utilising the concept of vacuum fluctuations. The quantum field vacuum is known to spontaneously create particle-antiparticle pairs, which annihilate very rapidly after their emergence. However, in the vicinity of the event horizon, the members of the virtual pair become separated by the existence of the horizon, and the annihilation process is prevented. In that case, one member of that pair escapes away from the black hole with positive energy, contributing to the Hawking radiation. At the same time, the black hole absorbs the other one with negative energy. This phenomenon of black hole radiation was quite astonishing since black holes are known only to absorb and not emit particles. Along with this, it also leads to a problematic situation in the quantum regime, known as "*black hole information paradox*", which we will discuss in the next section.

Let us now return to *the equivalence principle*, which says that accelerated frames can mimic gravity locally. Even though this principle was originally introduced for classical systems, there may be a counterpart in quantum regime, since *the Hawking effect* is a frame-dependent phenomenon. It has a counterpart in accelerated system, known as the Unruh effect. At the similar time frame of the discovery of *the Hawking radiation*, Stephen Fulling observed non-uniqueness in the notion of particles in quantum field theories, even in absence of a real gravitational field *i.e.,* quantum fields in Rindler frames [21]. Particle notion for a uniformly accelerating observer in Rindler coordinates differs from the Minkowski counterpart. After that, Paul CW Davies [22] shows that the procedure used by Hawking [19] to demonstrate the creation of particles by black holes

can be implemented in the Rindler coordinate system in flat spacetime. He finds that a uniformly accelerating observer apparently can see a fixed surface radiating thermally. Subsequently, William G Unruh introduced the concept of particle detectors [23] to realize the notion of particles. He examined the behaviour of particle detectors under acceleration motion of the detector. He observed that an accelerated detector would detect a thermal bath of particles in the vacuum even in flat spacetime. Later these detectors are popularly known as the Unruh DeWitt detectors [24]. Moreover, this phenomenon of particle production from the point of view of a Rindler observer is well-known as the Fulling–Davies–Unruh effect or the Unruh effect. The temperature corresponding to the Unruh thermal bath is

$$T_U = \frac{\hbar a}{2\pi c k_B} \,. \tag{1.4}$$

Here the surface gravity of the black hole (κ) in Eq. (1.3) is replaced by the acceleration of the detector (a). More specifically, from the point of view of a Rindler observer, the Minkowski spacetime seems to have a horizon, known as *Rindler horizon*. The core of the Unruh effect lies in the fact that in a non-inertial system, the background quantum field can be quantized in a non-unique manner. Field quantization in different coordinate systems leads to different vacua, which are generally not equivalent. Therefore, observers in different coordinate systems will not agree on the particle content in the field. In the context of the Unruh effect, the vacuum of an accelerated observer is not equivalent to the vacuum of an inertial observer, the Minkowski vacuum. As a consequence, the accelerated observer sees particles in the Minkowski vacuum. Similar non-uniqueness in quantization is also present in gravitational fields. In the context of Schwarzschild black hole spacetime, the vacuum of a far-distant, static observer is different from the vacuum of a free-falling observer near the horizon. Here, the static observer sees particles in the vacuum of the free-falling observer. Both of these effects are also consequence of lacking the Lorentz symmetry of special relativistic quantum field. Furthermore, these effects are closely related to each other by *the equivalence principle*. The accelerated observer is analogous to the static observer far away from the black hole, and the Minkowski observer is analogous to the free-falling observer near the black hole horizon. Therefore, the similarity between these two effects is vividly discernible.

1.3 The information paradox

There are various repercussions of the Hawking radiation. The temperature of the black hole is inversely proportional to the mass of the black hole, as shown in Eq. (1.2). As the black hole emits Hawking radiation, its mass decreases. Because the black hole loses mass throughout the radiation process, it finally evaporates. However, as the black hole shrinks and temperature increases. At the time when its mass reaches the Planck mass, its temperature shall rise to a temperature near the temperature at the beginning of the Big Bang ($\sim 10^{32}$ K). At the last phases of black hole evaporation, no one can say anything about what is supposed to happen, as the existing physical theories are likely to fail when the black hole's mass reaches the order of Planck mass.

As matters get absorbed by the black holes, the information (or quantum state) of this matter disappears from the outside universe. Then black holes emits a radiation, which is thermal in nature. This radiation is essentially a mixed state and does not contain any imprint of the initial information. As the black hole eventually evaporates, this information is irretrievably lost [19]. However, one of the most fundamental principles of quantum mechanics – *unitarity* asserts that information cannot be created or destroyed; it must be conserved. Thus, the Hawking radiation violates the unitarity principle of quantum physics [25] and leads to a paradox known as "*the black hole information paradox*". This paradox, which came from Hawking's discovery, puzzled physicists for decades. One may think that no one will ever employ the Hawking radiation for any practical purposes. Even worse, unlike elementary particle physics or astrophysics – subjects which may never have any functional applications, the quantum radiation of black holes will never lead to any exploratory observances. Then, why should one be concerned if information is lost due to Hawking radiation? Furthermore, the evaporation of black holes is so imperceptive that no one ever may witness any black hole shrinking. The significance of the Hawking radiation lies in the history of the evolution of physics. Maxwell's electromagnetic theory of light was one of the most successful theories describing optics. However, the profound conflict between Maxwell's theory and the principles of Newtonian physics disturbs many physicists like Einstein. It was Einstein, who resolved the conflict between these two theories, and a new paradigm of the special theory of relativity emerged. Thereafter, the apparent conflict between the special theory of relativity and the Newtonian gravitational principle was found, which led Einstein to the general theory of relativity, Einstein's most splendid masterwork. Particularly, whenever there is a clash of fundamental principles, a new paradigm comes out. For decades till now,

many efforts are going on to resolve this paradox *e.g.,* introducing concepts of firewalls [26], fuzzballs [27, 28] and remnants [29, 30], black hole information loss but no paradox [31], wormhole replica tricks [32–34], *etc*. It is believed that a fully quantum theory of gravity is required to resolve this paradox, which is yet to come out. Till then, physicists are employing the quantum field theory in curved space to uncover several quantum attributes associated with gravity. It became unavoidable to understand how various quantum information theory-related quantities behave under the influence of gravity. Due to the equivalence principle, it is also essential to understand how acceleration influences various information theoretic quantities, which is very important to us in the context of comprehending quantum features on the gravitational backgrounds. In this regard, it turns out that quantum entanglement phenomena in a gravitational system can play a significant role in enlightening the quantum nature of gravity. Some recent studies have shown that two objects can get entangled while interacting through their gravitational potential. This implies that gravity may have an intrinsic quantum nature [35, 36]. Moreover, this phenomenon became very important to understand the quantum nature of gravity [35, 36], the black hole information paradox [19, 26, 37–40], black hole thermodynamics [41, 42], *etc*. In this regard, it is essential to understand the phenomenon of quantum entanglement in the context of gravity.

1.4 Quantum entanglement: '*spooky action at a distance*'

"Those who are not shocked when they first come across quantum theory cannot possibly have understood it."
– Niels Bohr

Quantum entanglement, originally termed by Einstein as – "*spooky action at a distance*" – has turned out to be a resource of the quantum information theory. It is one of the predictions of quantum theory, which shows fascinating non-local properties. If two quantum subsystems are entangled, then the measurement of a physical observable in one subsystem will immediately influence the measurement on the other subsystem, even if they are space-like separated. Any entangled states violate the Bell's inequalities [43], which were mathematically formalized as a working hypothesis to test the paradox of Einstein, Podolsky and Rosen (EPR) – that *quantum description of physical reality*

is not complete [44]. Thus quantum entanglement fundamentally differs from classical correlations, which satisfy the Bell's inequalities. Since then, many precise experimental tests have been conducted to confirm the violation of the Bell inequalities in systems with photons and even with electrons [45–59]. All these tests strongly confirmed the existence of such non-local quantum description. Due to these properties, entanglement acts as a ground for the development of secure information transmission and is crucial to many quantum information theoretic processes, such as quantum teleportation [60–63], quantum cryptography [48, 64–66], and computation [67], *etc*.

Even though the fundamental non-local aspect of entanglement was recognized already after the famous EPR work [68], there was still no operational or generalizable measure to qualify and quantify the entangled nature of a state for a long time. In the 1930s, von Neumann first introduced the idea of the von Neumann entropy to measure the uncertainty of a quantum state. He generalized the Shannon entropy of classical information theory in the context of quantum physics [69]. The von Neumann entropy vanishes for pure state and non-zero for mixed state. A half-century later, in 1989, Rainer Werner introduced an entanglement measure known as *entanglement entropy* [70], using the idea of the von Neumann entropy. An entangled state cannot be written as a product of the states of the individual subsystems and contains information about the total system as a whole. If we consider a reduced density state of one subsystem, we lose the information about how it is correlated with the other subsystem. Therefore, individual subsystems are generally a mixed state and will have some non-zero von Neumann entropy. For maximally entangled Bell states, measuring a single subsystem gives maximum entropy. Moreover, for a separable state, this entropy becomes zero. However this measure is primarily suited for pure entangled states. For mixed states, it is insufficient to describe quantum entanglement. Later, [71, 72] demonstrated that for 2×2 and 2×3 systems, the positivity of the partial transposition of a general state is necessary and sufficient for its separability. Furthermore, if the partial transposition of the state has any negative eigenvalues, then the system is entangled. This criterion is popularly known as *the Peres–Horodecki criterion* or *the positive partial transpose (PPT) criterion*. Also, the sum of absolute values of all negative eigenvalues given a quantitative measure of entanglement, known as *negativity* [73]. Another measure named *logarithmic negativity* [73] is defined using the idea of *negativity*. At the same time, a generalization of the entanglement entropy is introduced, known as *entanglement of formation* [74]. The entanglement of formation is the same as entanglement entropy for the pure states.

For mixed states, it extends the idea of entanglement entropy. It utilizes convex roof minimization over all possible pure-state decomposition of the mixed state. It provides a meaningful path to quantify entanglement. However, this quantity is generally challenging to compute. William K. Wootters shows that the entanglement of formation for a two-qubit system can be calculated using a computable quantity known as *the concurrence* [75]. Later, concurrence [75–77] turns out to be an independent measure of entanglement for two-qubit systems. For such systems, the concurrence is one of the simplest and most widely applicable measures of quantum entanglement, whether pure or mixed. We primarily utilize quantities like concurrence and negativity for the studies discussed in this thesis. The relevant mathematical expressions will be discussed in chapter 2. Let us now discuss the entanglement phenomena in the context of quantum field theory.

1.4.1 Vacuum as an Entangled state

In free quantum field theory, we treat field as a sum of modes with wave-vector $\mathbf{k}$. Each modes behave as mathematical simple harmonic oscillators [1]. The quantum field's vacuum state is a product of each oscillator's ground state and corresponds to a field state with *no-particle or empty state*. However in reality, vacuum is not '*empty*'. Even in the absence of real particles, the quantum field undergoes continuous, random fluctuations due to the Heisenberg uncertainty principle $\Delta E \Delta t \gtrsim \hbar$. The vacuum energy fluctuations manifest as the creation and annihilation of virtual particle pairs, which annihilate in a very short-duration to conserve energy. This process is evident in the Schwinger effect [78]. In the electric field, virtual particle and anti-particle pairs (electron and positron) are created due to vacuum fluctuations. However, if the electric field is strong enough, these pairs start to move apart and gain enough energy to become real particles. Even if this process does not occur, the pairs remain virtual; they should conserve momentum, spin, charge , *etc*. These conservation laws make the pairs to be highly correlated or entangled, *i.e.,* if the particle in the spin-up state ($|\uparrow\rangle$), then the anti-particle must be in spin-down state ($|\downarrow\rangle$) and *vice versa*. Thus, the pair's spin state is generally expected to

[1] This is explicitly valid for free fields, not for any strongly interacting fields. For strongly interacting fields it is not possible as mathematical simple harmonic oscillators as the interaction term in the Hamiltonian couples all momentum modes strongly. In such a scenario, our obtained results will be modified, as one has to consider the Greens' functions for interacting field theory instead of the free-field Greens' functions. In such a case, one has to obtain the final density matrix and its elements by following a similar procedure, as discussed in the thesis.

be an entangled state [25, 79–81]

$$|spin\rangle_{\text{pair}} = \delta\,|\uparrow\downarrow\rangle + \sqrt{1-\delta^2}\,|\downarrow\uparrow\rangle\,. \tag{1.5}$$

These entangled particle-antiparticle pairs are direct manifestation of the field's vacuum fluctuations. This signifies that the vacuum state of a quantum field is inherently entangled. This entanglement ensures that vacuum fluctuations exhibit long-range correlations across space ($\langle 0|\hat{\phi}(x)\hat{\phi}(y)|0\rangle \neq 0$). Indeed, Summers and Werner [82–85] showed the maximal violation of the Bell-CHSH inequality in a vacuum of any quantum field theory, which implies that a vacuum intrinsically includes the non-locality that cannot be explained by any local realistic means.

This entangled nature of pair production due to the vacuum fluctuations also plays a crucial role in understanding the Hawking effect and the Unruh effect. In the case of Hawking radiation, there are two observers: a far-distant observer and a free-falling observer near the horizon. The coordinate frame of a free-falling observer can cover the whole black hole spacetime, and the vacuum of this observer is Kruskal vacuum ($|0\rangle_K$), which is the global vacuum of the whole black hole spacetime. Whereas the distant observer can access only the region outside the event horizon, hence vacuum corresponds to this observer is different from the Kruskal vacuum. There are two such exterior regions: one in right side of the black hole, and another is in left side of the black hole. These exterior regions are causally inaccessible to each other. The global Kruskal vacuum can expressed as entangled state of field modes of left-exterior ($|n_k^{in}\rangle$) and right-exterior ($|n_k^{out}\rangle$) regions as [23, 24, 86]

$$|0\rangle_K = \prod_k \frac{1}{\sqrt{Z_k}} \sum_{n_k} e^{-\pi n_k c\omega_k/\kappa} |n_k^{out}\rangle \otimes |n_k^{in}\rangle\,. \tag{1.6}$$

where Z_k is a normalization factor. In Hawking radiation, the distant observer in right-exterior region sees the vacuum of the in-falling observer ($|0\rangle_K$). However, since the observer in the right-exterior region cannot access the degrees of freedom in the left-exterior region, these inaccessible modes has to be traced out, providing a thermal bath over the degrees of freedom in the right-exterior region as

$$\rho_{out} = \frac{1}{Z_k} \sum_{n_k} e^{-2\pi c\omega_k n_k/\kappa} |n_k^{out}\rangle\langle n_k^{out}|\,, \tag{1.7}$$

with temperature $T = \frac{\hbar\kappa}{2\pi k_B c}$ as already seen in Eq. (1.3). Here Z_k is a normalization factor. Similarly, in the case of Unruh effect, the accelerated observer sees the Minkowski

vacuum ($|0\rangle_M$), which is the natural vacuum state for an inertial observer in Minkowski spacetime. However, for an accelerated observer whole Minkowski spacetime is not accessible. The structure of Minkowski spacetime in presence of an accelerating observer is divided by the left-moving and right-moving null paths (also known as Rindler horizons) that pass through the origin, known as Rindler wedges. An accelerating observer, moving along positive x-direction remain confined in the region ($x > |t|$), known as right Rindler wedge (RRW). While accelerating observer along negative x-direction remain confined in the region ($-x > |t|$), known as Left Rindler wedge (LRW). These two regions, RRW and LRW are causally disconnected. In Section 3.2, the Rindler coordinate systems will be discussed in greater detail. The Minkowski vacuum, when expressed in the Rindler frame, can be expressed in terms of the number-states ($|n_k^{R/L}\rangle$) of LRW and RRW as [23, 87–90]

$$|0\rangle_M = \prod_k \frac{1}{\sqrt{Z_k}} \sum_{n_k} e^{-\pi n_k c\omega_k/a} |n_k^R\rangle \otimes |n_k^L\rangle, \tag{1.8}$$

where Z_k is a normalization factor. Thus, the Minkowski vacuum is an entangled state concerning a Rindler observer's local modes. Since the degrees of freedom of LRW are inaccessible for the accelerated observer in RRW, they shall be traced out. The reduced density matrix is perceived as a thermal state as [87]

$$\rho_R = \frac{1}{Z_k} \sum_{n_k} e^{-2\pi c\omega_k n_k/a} |n_k^R\rangle\langle n_k^R|, \tag{1.9}$$

with temperature $T = \frac{\hbar a}{2\pi k_B c}$ as mentioned in Eq. (1.4). In this way, the Hawking radiation and the Unruh effect arise due to the entanglement structure of the quantum vacuum. However, both these effects involve multiple observers. One observer looks at the vacuum associated with the other observer for the thermal effects. No thermallity or particles will be evident if they look at their own vacuum. Therefore, these phenomena are highly observer-dependent phenomena. The entanglement structure of the vacuum behind these phenomena also depends on the point of view of a local observer [91]. Understanding entanglement in the vacuum is crucial for studying observer-dependent phenomena like Unruh and Hawking radiation. In this regard, the above-mentioned entanglement of vacuum is unlike that of other quantum systems or particles in a lab. It involves particles in regions inaccessible to a single observer. Therefore, a direct observation of vacuum entanglement is extremely challenging.

Earlier, it was known that in non-relativistic quantum mechanical systems, entanglement does not depend on observers as a system's quantum state has global validity.

All observers will agree on a measure of an entangled system. However in relativistic quantum systems, all observers may not agree on this global nature of the entangled state, even for an inertial system [91, 92]. In the case of a spin-spin entangled state, this observer-dependent feature is evident under transformations like Lorentz boost. Two maximally entangled rest particles, the entanglement measure decreases as seen by a Lorentz boosted observer [92–94]. This is because a spin state itself is not an invariant quantity under Lorentz boost. Also, particle momentum is changed under Lorentz boost. However, a combination of spin and momentum ($p \cdot \sigma$) is a Lorentz invariant quantity [95]. For systems with much lower (non-relativistic) velocities, these effects seem negligible, leading to global validation of spin-spin entangled state. Similarly, some other studies [96, 97] shows that a maximally entangled state in an inertial frame loses entanglement if the observers are relatively accelerated. Thus, we see that entanglement is observer-dependent in relativistic regime.

1.5 Quantum entanglement in Relativistic set-up

The presence of entanglement within the quantum vacuum has far-reaching and profound implications, affecting various physical and conceptual domains, including the Unruh effect and Hawking radiation. The observer-dependent nature of vacuum entanglement reveals a fundamentally non-classical and context-dependent nature of reality. It has significant implications for understanding the quantum nature of gravity and may help to illuminate the black hole information paradox. Since entanglement is a major resource in quantum information theory, entanglement in a relativistic framework is crucial from both fundamental and practical perspectives. Despite having several profound physical consequences, it was extremely challenging to probe this entanglement structure of the vacuum directly.

The particle production in the Unruh effect is one of the direct consequences of vacuum entanglement. It was Unruh [23] who conceptualized an idea to realize the produced particles using external atoms operationally. These atoms are considered point-like quantum systems with two energy levels. They are coupled to a background real scalar field through monopole coupling, where a monopole operator corresponds to the detector is coupled to the scalar field. Operationally, this coupling mimics the dipole coupling, where dipole moment operators of an atom are coupled to the electric field. The

coupling between the field and detector will promote a transition between two energy levels of the detector along with excitation or de-excitation of the background quantum field. An upward transition in the atom by absorbing a quantum of energy from the field is interpreted as detecting a particle. These simplified two-level particle detectors are popularly known as the Unruh-DeWitt (UDW) detectors [23, 24]. A more physically intriguing circumstance appears when considering a system with two detectors; these detectors are locally correlated with the background quantum field at different spacetime points. Since the vacuum of the background field is entangled over the spacetime, this entanglement may get transferred or swapped to the two initially uncorrelated detectors. In this way, two mutually non-interacting detectors may extract entanglement from the quantum field's vacuum.

The seminal work of Antony Valentini [98] first analyzed this possibility of entanglement extraction, and advanced our understanding of the fundamental role of entanglement in relativistic quantum field theory. He utilized atoms locally coupled to background electric field with dipole operators. Two atoms are initially considered non-entangled and not allowed to interact with each other. Due to the local interaction with the field, these atoms develop entanglement between them. The entanglement in the vacuum of the background field is swapped into a system of two atomic detectors, revealing operational insights into the vacuum entanglement. Valentini's work inspired further research into the play of entanglement in the relativistic setups. Later, the pioneering works by Reznik [99, 100] solidified the formal and systematic approach to articulate the phenomena of entanglement harvesting from the field's vacuum state. In these works, he explored entanglement extraction in a system of two accelerated atoms by considering point-like two-level Unruh-DeWitt particle detectors interacting with background massless scalar filed. He showed that entanglement extraction was possible between two causally disconnected anti-parallelly accelerated detectors in the left and right Rindler wedges. This emphasized that the vacuum can be a source of entanglement generation between two space-like separated observers. This study gave an operational interpretation to vacuum entanglement. His groundbreaking exploration of how entanglement contained in the vacuum can be harnessed through localized measurements, inspired a large number of follow-up studies, where the focus is on understanding how vacuum entanglement changes in different curved spacetimes, near black hole horizons, or in cosmological expanding universes.

Entanglement extraction by accelerated detectors from the Minkowski vacuum is quite intriguing as an accelerated observer perceives the Minkowski vacuum as a thermal bath. Earlier, it was known that thermality introduces randomness in a system, which is counter to entanglement. However, in some specific occasions, a distinct class of heat baths can enhance entanglement in a system [101–105]. The thermality in the Unruh effect seems to have similar influences on entanglement [106], which is interestingly much aligned with the entangling nature of field vacuum. This indicates that studying quantum entanglement in the relativistic framework can provide a much deeper perspective towards reality and broaden our conceptual horizon. Furthermore, understanding observer-dependent vacuum entanglement can deliver a testing ground for the interface of quantum mechanics and general relativity.

Due to the unsurpassed consequences, investigations to understand quantum entanglement for relativistic particles have gained significant momentum. The formulation of entanglement extraction by Reznik further improved in [107–109], where proper time-ordering is introduced into the picture. The non-local term behind the entanglement extraction became dependent on the Feynman propagator instead of the earlier known Wightman function. These recent methods provide a meticulous and more general formulation for understanding entanglement extraction from vacuum. This process of entanglement extraction is now popularly known as '*entanglement harvesting*'. Moreover, if the detectors are already entangled, then due to the interaction with the field, entanglement may be degraded [110]. This phenomenon is known as "*entanglement leakage*". Entanglement harvesting is possible even if the detectors are causally disconnected and independent of the internal structure of the detectors. This process of swapping field entanglement to detectors turns out to be sensitive to the type of motion of the detectors [96, 107, 108, 111–125], the switching function of the interactions [108, 126–128], the nature of the background fields [129–133], the presence of black holes [134–145] and other curved spacetimes [142, 146–157], *etc*. These studies reveal several intriguing characteristics of entanglement harvesting or extraction from the vacuum. Entanglement harvesting acquires additional significance from the possibility of its experimental verification and utilization of the extracted entanglement in quantum information-related purposes [60, 61, 63]. The experimental verification of entanglement in systems with photons and even in electrons makes these possibilities all the more lucrative. In this regard, one should note that it is practically almost impossible to set up for entanglement harvesting from any black hole vacuum or cosmological vacuum;

however, for inertial and acceleration motion, it may be possible to create such a setup in the future. For this reason, we primarily focus on both inertial and non-inertial systems in the Minkowski spacetime, following the prescription presented in [108, 113], where a concrete operational formalism of entanglement harvesting with initially uncorrelated detectors is presented. Also, various measures of harvested entanglement are discussed.

In [113], the authors considered a set-up similar to [99]. They considered two initially non-entangled, accelerating UDW detectors interacting with a real scalar field. In the asymptotic future, the detectors get entangled for anti-parallel acceleration, not for parallel acceleration. Many studies have been done to understand entanglement harvesting with accelerating detectors considering parallel and anti-parallel accelerations of the detectors. For parallel motion of the detectors, they get entangled for finite time switching function [107, 117–119], however they remain non-entangled for infinite time switching function [113]. Therefore, the results varies with the choice of switching functions. Here, it should be noted that the original idea of particle detectors was introduced to detect particle production in the quantum field vacuum. In Minkowski spacetime, particle production is only possible for acceleration motion; not for inertial motion. However, considering finite time switching functions, the detector even clicks for inertial motion, where there is no actual particle production. This is due to the fact that finite time switching functions introduce oscillatory transient effects, which vanish for sufficiently extended periods of interaction. Even for an accelerating detector, the transition rate will have dominating contributions from transient effects compared to the contributions due to particle production in the vacuum, failing the actual motivation of conceptualizing the UDW detectors [158]. For these reasons, we consider an infinite switching function for our studies, following the original work on UDW detectors [23]. This helps to suppress spurious transient effects [24, 89]. In reality, no interaction can persist for an infinite time duration. This infinite interaction time in an actual set-up should be an extensive time duration compared to the time associated with the energy gap of the detectors ($\Delta\tau >> \hbar/\Delta E$) (see [158]). In this situation, the transition rate (or rate of any other relevant quantity) is a meaningful observable for the detector interacting with the field. This consideration of much longer interaction time enables us to understand the underlying physical processes in entanglement harvesting and to find out the roles played by the vacuum of the field in different systems under consideration. We will also study the phenomenon of entanglement leakage and try to understand the underlying elementary physical processes with a simple inertial system, which can reveal some

intriguing consequences of vacuum fluctuations on an entangled system of two detectors.

In our study, we consider two point-like, two-level Unruh-DeWitt (UDW) detectors to investigate the entanglement content in the vacuum of a quantum field. These detectors, labeled A and B, are carried by two observers, *Alice* and *Bob*, respectively. Since gravitational systems are analytically challenging, we primarily focus on accelerated systems, as acceleration can locally mimic gravitational effects. As previously discussed, an accelerated observer perceives the Minkowski vacuum as an entangled state of field modes in the left and right Rindler wedges (LRW and RRW). Motivated by this, we explore scenarios where the two detectors are accelerating in such a way that: one detector is in the RRW and the other in the LRW, making them causally disconnected. Can they still extract entanglement from the Minkowski vacuum? Also if both detectors move within the same Rindler wedge (either RRW or LRW), how does this effect entanglement harvesting? Since quantum fields in realistic environments are thermal in general, we analyse how background temperature influences entanglement harvesting between the accelerated detectors. Additionally, it is well known that the presence of reflecting boundaries in spacetime modifies the field's density of modes. As a result, we expect significant alterations in entanglement harvesting when boundaries are introduced. Depending on the configuration, these modifications may either enhance or suppress entanglement extraction. To explore this, we consider the effect of single or double reflecting boundaries and comparatively analyse how these boundaries influence the entanglement between the detectors. For simplicity, in this part of the study, we do not include a thermal background.

So far, our analysis has focused on entanglement extraction from the vacuum state of the quantum field. However, in realistic scenarios, the background field may not always be in the ground state. To address this, we investigate how entanglement harvesting changes if the background field is in a singly excited state rather than in vacuum. We conduct this study with inertial detectors instead of accelerated systems to show the effect of excited field states in a simpler way. We compare the entanglement content in excited field states with that in the vacuum, providing insight into the feasibility of entanglement harvesting in more general settings.

Until now, our analysis has focused on how two initially non-entangled detectors become entangled via local interaction with the background field. Next, we shift our attention to scenarios where the detectors are initially entangled. For simplicity, we consider static detectors and examine how vacuum fluctuations and spontaneous emission

influence their entanglement over time. We demonstrate that, due to these interactions, the detectors gradually lose entanglement.

In a nutshell, the current thesis aims to investigate how a system of two uncorrelated detectors interacting with a background quantum field can get entangled or lose entanglement due to vacuum fluctuations. The entire thesis consists of three parts, excluding the introduction and conclusion. The first chapter introduces some well-known results of black hole physics. Many of the topics discussed here are not directly connected with the main subjects of this thesis. However, their purpose is to offer a comprehensive introduction to the contemplation of entanglement in the system of two detectors and connections to the quantum field vacuum, which is the motivation behind the thesis. Now comes Part I, which includes Chapter Two, in which we present the detailed formalism for entanglement harvesting or leakage. Part II contains only three chapters (chapters three, four and five), where we study the entanglement harvesting phenomenon. We try to figure out how a thermal background and the presence of reflecting boundaries influence entanglement harvesting between two accelerated detectors. We also try to understand what happens to entanglement harvesting if the background field is in an excited field state rather than the vacuum. Part III, which consists of one chapter (chapter six), studies the entanglement leakage phenomenon. Here, we try to understand what happens to an initially entangled pair of detectors when they interact with the background quantum field. Chapter seven presents a brief conclusion and future directions for our findings.

1.6 Chapter-wise overview: Outline of the thesis

The results discussed in this thesis are based on the works in [159–162]. In this section, we have outlined the research guidelines of the thesis as follows

Chapter 2:

This chapter begins with a brief overview of quantum field theory in Minkowski space and curved space to highlight their key differences, including the vacuum space's non-uniqueness property. We briefly discuss the key concepts of the Unruh-DeWitt (UDW) detector model, introducing the detector response function and the transition rate. Then the whole formalism of entanglement harvesting or leakage is developed based on the detector model. We discuss the time evolution of two detector systems locally interacting with a background real, scalar field. For generality, here we start with an entangled state of the detectors as an initial state, which gets reduced to a separable state with a limiting condition. Then, we deduce the general conditions for entanglement between the detectors from the later time density matrix. We finally discuss the quantitative measures of quantum entanglement between two detectors.

Chapter 3:

We have already mentioned that the Minkowski vacuum is entangled concerning accelerated frame modes. Many works have already been performed to understand the entanglement extraction by uniformly accelerated detectors from the Minkowski vacuum. However, the environment is always thermal. Furthermore, it is known that, in general, background temperature has depreciating effects on quantum entanglement, except for some specific cases [101–105]. This chapter aimed to understand how background temperature influences entanglement harvesting between two uniformly accelerated detectors. We observe that even in the presence of a thermal bath, the detectors can get entangled only when they are in anti-parallel acceleration, as seen in [113]. We found that background temperature depreciates the range of accelerations for which the particles get entangled. Depending on the temperature, entanglement harvesting is possible after some finite value of primary detector acceleration. The amount of entanglement also gets suppressed with increasing temperature. However, entanglement harvesting increases with temperature after a specific (critical) acceleration value. There is only one critical acceleration in the $(1+1)$ dimension. In the $(1+3)$ dimension, there is one

(multiple) critical point(s) for both detectors having the same (different) magnitude(s) of acceleration.

Chapter 4:

The higher the degree of entanglement, the higher the probability of experimental detection. Therefore, asking how one may enhance the entanglement harvesting between the accelerated detectors is natural. It is well-known that modifying the field's density of modes can significantly influence the detector's transition rate, which may also influence the entanglement harvesting between two accelerated detectors. In this chapter, we consider systems with – (i) double reflecting boundaries and (ii) single reflecting boundaries and perform a comparative study of entanglement harvesting with respect to a no-boundary system. We observe that the reflecting boundaries can play double roles. In some parameter spaces, it causes suppression; in others, it can enhance entanglement. However, whether it is enhancement or degradation, double boundaries have more influence compared to single-reflecting boundaries.

Chapter 5:

The motivation for entanglement extraction from the vacuum arises from both foundational and practical considerations in quantum field theory, quantum information science, and the study of spacetime. This chapter considers a slightly different system for understanding entanglement harvesting between two inertial detectors interacting with the background field, which is initially in a non-vacuum field state. This venture gains its motivation as, in nature, it is not guaranteed that the background field will be in a vacuum state. Furthermore, if the background field state is indeed excited, how much do the results concerning the entanglement harvesting change compared to the vacuum fluctuations? Our main observation asserts that entanglement harvesting is suppressed compared to the vacuum fluctuations in this situation. Our other observations confirm a non-zero individual detector transition probability in this background and vanishing entanglement harvesting for parallel co-moving detectors.

Chapter 6:

This chapter considers two initially entangled, static UDW detectors coupled with the background field. They spontaneously lose entanglement when at least one is not isolated

from the quantum field. For eternal interaction between the detectors and the field, the spontaneous emission from the detectors' exited states and vacuum fluctuations of the field influence this adverse effect. Consequently, it suggests that two entangled qubits become less communicated during their free fall towards the black hole horizon.

Chapter 7:

We dedicate this final chapter of our thesis to the possible extensions of the results discussed in the thesis and a list of new problems that can be addressed in the future. Also, we have highlighted several important conclusions related to our work.

From the next chapter onwards, we have a detailed analysis of the studies. Each chapter of the thesis contains several appendices, added at the end of the respective chapters. We shall use natural units $c = G = k_{\mathrm{B}} = 1$. Here c is the velocity of light, G is the Newtonian constant of gravitation, and k_B is the Boltzmann constant. Here, we will consider the signature of the Lorentzian metric to be $(-,+,+,+)$.

Part I

Formalism

CHAPTER 2

THE FORMALISM: SYSTEM OF TWO DETECTORS

This chapter presents the formulation for understanding the possibility of two uncorrelated atomic Unruh-DeWitt detectors getting entangled over time while interacting with a general field state. Primarily, we are interested in finding the condition for the detectors to be entangled and the quantification of entanglement after time evolution is done. The whole analysis will be valid up to the second-order perturbative series of the system's density matrix, where the expansion is done order by order in terms of interaction strength. Before proceeding, we briefly discuss the differences between quantum field theory in flat and curved spacetime, from which the non-unique nature of vacuum will be discussed. Then, we will discuss how to prove this non-uniqueness of vacuum, introducing simplified two-level atoms (Unruh-DeWitt detectors). Finally, we will understand how a system of two detectors evolves with time while locally interacting with a background quantum field.

2.1 Scalar Fields in Minkowski Spacetime

Let us consider a real scalar field $\phi(t,\mathbf{x})$ defined at all points $(t,\mathbf{x})$ of n-dimensional Minkowski spacetime. The Lagrangian density is known as

$$\mathscr{L}(x) = \frac{1}{2}\left(\eta^{\alpha\beta}\phi_{,\alpha}\phi_{,\beta} - m^2\phi^2\right). \tag{2.1}$$

Here $\eta^{\alpha\beta} = (1,-1,-1,-1)$ [1] and the quantity m is identified as mass of the field quanta. For simplicity we define x as abbreviation of the spacetime point $(t,\mathbf{x})$ throughout the manuscript. From it one can construct an action

$$S = \int \mathscr{L}(x)\mathrm{d}^n x\,, \tag{2.2}$$

and demanding that for variations with respect to ϕ to be *zero*, i.e., $\delta S = 0$, one obtain the field equation

$$(\partial^\mu \partial_\mu + m^2)\phi = 0. \tag{2.3}$$

One set of solutions of Eq. (2.3) is known as

$$u_k(x) \propto \mathrm{e}^{i\mathbf{k}\cdot\mathbf{x} - \mathrm{i}\omega t}\,, \tag{2.4}$$

where $\omega \equiv \left(|\mathbf{k}|^2 + m^2\right)^{\frac{1}{2}}$ and the Cartesian components of $\mathbf{k}$ can take the values $-\infty < k_i < \infty, \quad i = 1,\ldots,n-1$. The modes in Eq. (2.4) are said to be positive frequency with respect to t, being eigenfunctions of the operator $\partial/\partial t$ as

$$\frac{\partial}{\partial t} u_k(x) = -\mathrm{i}\omega u_{\mathbf{k}}(x), \quad \text{with } \omega > 0\,. \tag{2.5}$$

Also the mode functions has to be orthogonal, which can be examined by using the following definition of scalar product

$$\begin{aligned}\left(\phi_1,\phi_2\right) &= -\mathrm{i}\int_\mu \left\{\phi_1(x)\partial_\mu\phi_2^\star(x) - \phi_2^\star(x)\partial_\mu\phi_1(x)\right\}\mathrm{d}\Sigma^\mu \\ &= -\mathrm{i}\int_t \phi_1(x)\overleftrightarrow{\partial_t}\phi_2^\star(x)\mathrm{d}\Sigma^t\,,\end{aligned} \tag{2.6}$$

where $\mathrm{d}\Sigma^t$ denotes the integration over a spacelike hyper-surface of simultaneity at instant t. Then the modes in Eq. (2.4) can be shown orthogonal if

$$\left(u_{\mathbf{k}}, u_{\mathbf{k}'}\right) = \delta^{n-1}\left(\mathbf{k}-\mathbf{k}'\right). \tag{2.7}$$

Using this condition one normalise the modes in Eq. (2.4), and the normalised modes can be expressed as

$$u_{\mathbf{k}}(x) = \left[2\omega(2\pi)^{n-1}\right]^{-\frac{1}{2}}\mathrm{e}^{\mathbf{i}\mathbf{k}\cdot\mathbf{x}-\mathrm{i}\omega t}\,. \tag{2.8}$$

[1] In general we use the sign convention $(-,+,+,+)$. Only here we use the convention $(+,-,-,-)$, as we follow the book by Birrell and Davies (1982). Use of different sign convention will not effect any results obtained in the thesis.

The field modes in Eq. (2.8) and their complex conjugates form a complete orthonormal basis with scalar product Eq. (2.6). The quantum field $\hat{\phi}(x)$ can be expanded using these field modes as

$$\hat{\phi}(x) = \sum_{\mathbf{k}} \left[\hat{a}_{\mathbf{k}} u_{\mathbf{k}}(x) + \hat{a}^{\dagger}_{\mathbf{k}} u^{\star}_{\mathbf{k}}(x) \right], \tag{2.9}$$

where, $\hat{a}_{\mathbf{k}}$, $\hat{a}^{\dagger}_{\mathbf{k}}$ are the annihilation and creation operators of the scalar field. The equal time commutation relations for field ($\hat{\phi}$) and conjugate momenta ($\hat{\Pi} = \partial_t \hat{\phi}$) are given by

$$\begin{aligned} &[\hat{\phi}(t,\mathbf{x}), \hat{\phi}(t,\mathbf{x}')] = [\hat{\Pi}(t,\mathbf{x}), \hat{\Pi}(t,\mathbf{x}')] = 0; \\ &[\hat{\phi}(t,\mathbf{x}), \hat{\Pi}(t,\mathbf{x}')] = i\delta^{n-1}(\mathbf{x}-\mathbf{x}'). \end{aligned} \tag{2.10}$$

Using explicit expression of $\hat{\phi}$ from Eq. (2.9) in these relations leads to the commutation relations for $\hat{a}_{\mathbf{k}}$ and $\hat{a}^{\dagger}_{\mathbf{k}}$, which are given by

$$\begin{aligned} &[\hat{a}_{\mathbf{k}}, \hat{a}_{\mathbf{k}'}] = [\hat{a}^{\dagger}_{\mathbf{k}}, \hat{a}^{\dagger}_{\mathbf{k}'}] = 0 \\ &[\hat{a}_{\mathbf{k}}, \hat{a}^{\dagger}_{\mathbf{k}'}] = \delta_{\mathbf{k}\mathbf{k}'} \,. \end{aligned} \tag{2.11}$$

In the Heisenberg picture of quantum mechanics, the quantum states span a Hilbert space. A convenient basis in this Hilbert space is given as the so-called Fock representation. The normalised basis ket vectors, denoted as $|n_{\mathbf{k}}\rangle$, can be constructed from the state $|0\rangle$, called the vacuum or no-particle state. The state $|0\rangle$ has the property that it is annihilated by all the $a_{\mathbf{k}}$ operators

$$a_{\mathbf{k}}|0\rangle = 0, \quad \forall \mathbf{k}. \tag{2.12}$$

Since our Lagrangian satisfies the Lorentz invariance, the vacuum state is consistent across all inertial frames. Hence all inertial observers will observe the vacuum as lowest energy state or no-particle state of the field.

The state with n number of particles with momentum $\mathbf{k}$ (denoted as $|n_{\mathbf{k}}\rangle$) is obtained from $|0\rangle$ with operation of $\left(\hat{a}^{\dagger}_{\mathbf{k}}\right)^n$ as

$$|n_{\mathbf{k}}\rangle = \frac{1}{\sqrt{n!}} \left(a^{\dagger}_{\mathbf{k}}\right)^n |0\rangle. \tag{2.13}$$

The Hamiltonian for the quantum field turns out to be

$$\hat{H} = \sum_{\mathbf{k}} \left(\hat{a}^{\dagger}_{\mathbf{k}} \hat{a}_{\mathbf{k}} + \frac{1}{2} \right) \omega_{\mathbf{k}} = \sum_{\mathbf{k}} \left(\hat{N}_{\mathbf{k}} + \frac{1}{2} \right) \omega_{\mathbf{k}}, \tag{2.14}$$

where $\hat{N}_{\mathbf{k}} = \hat{a}^{\dagger}_{\mathbf{k}}\hat{a}_{\mathbf{k}}$ is known number operator. Expectation value of this operator with respect to any state provides number of particles associated with the state. For the vacuum state and n-particle state, expectation of this operator gives

$$\begin{aligned} \langle 0|\hat{N}_{\mathbf{k}}|0\rangle &= 0 \\ \langle n_{\mathbf{k}}|\hat{N}_{\mathbf{k}}|n_{\mathbf{k}}\rangle &= n. \end{aligned} \tag{2.15}$$

2.2 Quantum field theory in curved space

This section briefly discusses the generalisation of the Minkowskian (flat) quantum field theory (QFT) in curved spacetime. Since we do not have a fully quantum theory of gravity; therefore, we use the semi-classical QFT methods in curved spacetime. By '*semi-classical*', one refers to the quantum fields are embedded on a background curved spacetime. To a great extent, the features of quantum fields in curved spacetime have direct correspondance to the quantum field theory in flat spacetime. However, there are some discrepancies are also apparent, *i.e.,* the quantum vacuum no longer remain unique due to lack of global inertial frames (*the Poincaré symmetry* is broken). Different observers in different coordinate systems in curve spacetime do not agree on the vacuum state [21, 24, 163]. In other words, the vacuum of one frame can be perceived as many particle state or thermal state in another frame.

Before we proceed to this topics, let us start with a Lagrangian density in gravitational field background [24]

$$\mathscr{L}(x) = \frac{1}{2}\sqrt{-g(x)}\left\{g^{\mu\upsilon}(x)\phi(x)_{,\mu}\phi(x)_{,\upsilon} - \left[m^2 + \xi R(x)\right]\phi^2(x)\right\}. \tag{2.16}$$

Here the coupling between the real scalar field and the gravitational field is represented by the term $\xi R\phi^2$, where ξ is the coupling constant, and $R(x)$ is the Ricci scalar curvature. Again one can construct an action corresponding to this Lagrangian and one obtains the scalar field equation by setting the variation with respect to ϕ equal to *zero*

$$\left[\Box_x + m^2 + \xi R(x)\right]\phi(x) = 0 \tag{2.17}$$

where $\Box = \nabla^{\mu}\nabla_{\mu} = (1/\sqrt{-g})\partial_{\mu}[\sqrt{-g}\,g^{\mu\nu}\partial_{\nu}]$. Here we use two particular values of ξ: $\xi = 0$, known as *minimal coupling* and $\xi = (n-2)/4(n-1)$, known as *conformal coupling*. The conformal coupling with consideration of massless scalar fields leads to mode functions similar to flat spacetime modes except a conformal factor [24].

The solutions of this field equation has to form a complete set of basis vectors. Hence, the solutions need to be orthogonal, which can be examined by utilising the definition of

scalar product. If ϕ_1, ϕ_2 are two solutions of the field equation in Eq. (2.17), then the scalar product is provided as

$$(\phi_1, \phi_2) = -i \int_\Sigma \phi_1(x) \overleftrightarrow{\partial_\mu} \phi_2^\star(x) \sqrt{-g_\Sigma(x)}\, \mathrm{d}\Sigma^\mu \tag{2.18}$$

where $\mathrm{d}\Sigma^\mu = n^\mu d\Sigma$, with n^μ is a future directed unit vector orthogonal to spacelike hypersurface Σ, $d\Sigma$ is volume element in Σ. There exists a complete set of mode solutions $u_i(x)$ of (2.17), which are orthogonal in the inner product in Eq. (2.18), satisfying

$$(u_i, u_j) = \delta_{ij},\ (u_i^\star, u_j^\star) = -\delta_{ij},\ (u_i, u_j^\star) = 0\ . \tag{2.19}$$

The field modes $u_j(x)$ and it's complex conjugates form a complete orthonormal basis with Eq. (2.19), hence the quantum field $\hat{\phi}(x)$ can be expanded as

$$\hat{\phi}(x) = \sum_j \left[\hat{a}_j u_j(x) + \hat{a}_j^\dagger u_j^\star(x) \right] \tag{2.20}$$

where $\hat{a}_j$, $\hat{a}_j^\dagger$ are the *annihilation* and *creation* operators, satisfying the commutator relations, $[\hat{a}_i, \hat{a}_j^\dagger] = \delta_{ij}$, etc. The no-particle state or the vacuum state $|0\rangle_u$ associated with the set of basis $\{u_j\}$, is defined as

$$\hat{a}_j |0\rangle_u = 0, \quad \text{for all } j. \tag{2.21}$$

Here also one can construct a n-particle state as constructed in Eq. (2.13). Number operator is defined as $\hat{N}_i = \hat{a}_i^\dagger \hat{a}_i$, provides $\langle n_i | \hat{N}_i | n_i \rangle = n_i$, as observers in quantum field theory in flat space.

In curved spacetime, the Poincaré group is no longer a symmetry group. The general relativity is based on *the principle of general covariance*, thus no coordinate system is more preferreble than any other. Hence, there can exist another complete set of orthonormal modes $\bar{u}_i(x)$ for the expansion of field operator. The expansion of $\hat{\phi}$ in these modes is expressed as

$$\hat{\phi}(x) = \sum_j \left[\hat{\bar{a}}_j \bar{u}_j(x) + \hat{\bar{a}}_j^\dagger \bar{u}_j^\star(x) \right] \tag{2.22}$$

where $\hat{\bar{a}}_j$, $\hat{\bar{a}}_j^\dagger$ are annihilation and creation operators for this new set of basis vectors, satisfying the commutator relations, $[\hat{\bar{a}}_i, \hat{\bar{a}}_j^\dagger] = \delta_{ij}$. The vacuum state corresponding to this modes is defined by

$$\hat{\bar{a}}_j |0\rangle_{\bar{u}} = 0 \quad \text{for all } j. \tag{2.23}$$

Both sets of mode functions are complete, and they span the same Hilbert space. Hence, any later mode, $\bar{u}_j$ can be written as linear superposition of u_j modes (or *vice versa*) as a vector expressed in terms of basis vectors. Hence one can write

$$\bar{u}_j = \sum_i \left(\alpha_{ji} u_i + \beta_{ji} u_i^\star\right). \tag{2.24}$$

Conversely one can write

$$u_i = \sum_j \left(\alpha_{ji}^\star \bar{u}_j - \beta_{ji} \bar{u}_j^\star\right). \tag{2.25}$$

These relations are known as *the Bogolubov transformations* [164]. The coefficients α_{ij}, β_{ij} are called *the Bogolubov coefficients*, and by using Eq. (2.24) and Eq. (2.19) they can be evaluated as

$$\alpha_{ij} = \left(\bar{u}_i, u_j\right), \quad \beta_{ij} = -\left(\bar{u}_i, u_j^\star\right). \tag{2.26}$$

These Bogolubov coefficients always satisfies the following relations [24]

$$\sum_k \left(\alpha_{ik}\alpha_{jk}^* - \beta_{ik}\beta_{jk}^*\right) = \delta_{ij}, \quad \sum_k \left(\alpha_{ik}\beta_{jk} - \beta_{ik}\alpha_{jk}\right) = 0. \tag{2.27}$$

Equating the above two mode expansions of the field $\hat{\phi}(x)$ in Eqs. (2.20) and (2.22) and making use the Bogolubov transformations in Eqs. (2.24) and (2.25) and the orthonormality of the modes in Eq. (2.19), one obtains the relation between the creation and annihilation operators associated with the basis sets as

$$\hat{a}_i = \sum_j \left(\alpha_{ji}\hat{\bar{a}}_j + \beta_{ji}^\star \hat{\bar{a}}_j^\dagger\right), \quad \hat{\bar{a}}_j = \sum_i \left(\alpha_{ji}^\star \hat{a}_i - \beta_{ji}^\star \hat{a}_i^\dagger\right). \tag{2.28}$$

It follows immediately from Eq. (2.28) that, the expectation value of the operator $\hat{N}_i = \hat{a}_i^\dagger \hat{a}_i$ for the number of u_i mode particles in the state $|0\rangle_{\bar{u}}$ is

$${}_{\bar{u}}\langle 0|\hat{N}_i|0\rangle_{\bar{u}} = \sum_j \left|\beta_{ji}\right|^2 \geq 0, \tag{2.29}$$

which is to say that the vacuum of the $\bar{u}_j$ modes contains $\Sigma_j \left|\beta_{ji}\right|^2$ particles according to an observer in the other frame. This means that, two observers quantising in different frames even in flat spacetime will not in general agree about the particle content of the field, unless they are both in specially related frames – such as inertial frames.

For example, an observer uniformly accelerating through the Minkowski vacuum observes a thermal bath of particles. This phenomenon is known as *the Unruh Effect*

[21, 23, 24]. Similarly, in black hole spacetime, a static Boulware observer at spatial infinity observes particles in the vicinity of the Horizon. This is known as *the Hawking Radiation* [19, 20, 24]. The similar particle productions in flat and curved spacetimes are also discussed in [165–171].

2.3 The Unruh-DeWitt Detectors

In the last section, we have seen that particle number in curved spacetime does not have global significance. Vacuum of one observer is perceived as a multi-particle state from another observer's point of view. Now, one can try to understand how to operationally realise these particles. Here, one can utilise the idea of measurement apparatus in quantum physics. If state of a quantum system is unknown, one can get informations about this system using a measurement apparatus, coupled with the system of interest. One example is: an electric dipole interacting with electrostatic field (the light-matter interaction). Observing transitions of the dipole (the pointer system), one can try to understand excitation or de-excitation of the electric field. Since through the dipole, one detects excitation or de-excitation of the field, one can call it as dipole detector.

In our works, we have considered the field to be scalar field. Thus the detectors in our case will be scalar operators, known as monopole detectors. The original idea of monopole detectors were introduced to provide an operational definition to the concept of a particle [23, 24, 172]. These detectors are conceptualised as point-like, two-level quantum systems. They have ground and excited states ($|g\rangle$ and $|e\rangle$) with a energy gap ΔE. The monopole operator is given by

$$\hat{m}(\tau) = e^{i\hat{H}\tau}\left(|g\rangle\langle e| + |e\rangle\langle g|\right)e^{-i\hat{H}\tau}. \tag{2.30}$$

These monopole detectors are popularly known as the Unruh-DeWitt detectors. The motion of a detector is described by a classical world-line. One can consider a detector that is moving along a trajectory $x(\tau)$, where τ is the proper time of the detector. The detector is coupled with the local quantum field via the interaction Hamiltonian, given by

$$\hat{H}_{int} = c\ \hat{m}(\tau)\hat{\phi}(x(\tau)), \tag{2.31}$$

where c is coupling constant. This interaction Hamiltonian mimics the light-matter interactions like $\hat{\mathbf{p}}\cdot\hat{\mathbf{A}}$ (or $\hat{\boldsymbol{\mu}}\cdot\hat{\mathbf{E}}$) when angular momentum is not involved [173]. The coupling between field and detector will promote transition between two energy levels of detector along with excitation or de-excitation of the background quantum field. Operationally,

this interaction is the simplification of the well-known light-matter interaction for scalar fields. When a detector detects a particle creation or destruction in the field, it beeps.

Let us consider the quantum field $\hat{\phi}$ is initally in the vacuum state $|0\rangle$ and the detector is in ground state $|g\rangle$. Up to the first order in perturbation theory, the transition amplitude from initial state $|g,0\rangle$ to final state $|e,\psi\rangle$ is given by

$$\mathscr{A} = ic\ \langle e,\psi| \int d\tau\ \hat{m}(\tau)\hat{\phi}(x(\tau))|g,0\rangle = ic\ \int d\tau e^{i\Delta E\tau}\langle\psi|\hat{\phi}(x(\tau))|0\rangle\,; \tag{2.32}$$

where $|\psi\rangle$ is the state of the field after the interaction with the detector. We will have quantity $\langle e|\hat{m}(0)|g\rangle$ to be unity (in natural unit). In generally, this term only depends on the internal structure of the detector, not on the motion or size of the detector. The transition probability of the detector to all possible final states $|\psi\rangle$ of the quantum field is given by

$$\mathscr{P}(\Delta E) = c^2 \int_{-\infty}^{\infty} d\tau \int_{-\infty}^{\infty} d\tau'\ e^{-i\Delta E\Delta(\tau-\tau')}\ G(x(\tau),x(\tau')) = c^2\mathscr{F}(\Delta E)\,. \tag{2.33}$$

The function $\mathscr{F}(\Delta E)$ is called the *detector response function*, can be expressed as

$$\mathscr{F}(\Delta E) = \int_{-\infty}^{\infty} dT \int_{-\infty}^{\infty} d(\Delta\tau)\ e^{-i\Delta E\Delta\tau}\ G(x(\tau),x(\tau')) \tag{2.34}$$

where, $\Delta\tau = \tau - \tau'$ and $T = (\tau+\tau')/2$. Here $G(x(\tau),x(\tau'))$ is the Wightman function, given by $\langle 0|\hat{\phi}(x(\tau))\hat{\phi}(x(\tau'))|0\rangle$. The detector response function only requires the *positive frequency Wightman function* as an input, which carries the information of the background field and the motion of the detector. For a uniformly accelerated detector with acceleration a, we have the Wightman function $G(\Delta\tau) = -a^2/16\pi^2\sinh^2(a(\Delta\tau - i\epsilon)/2)$. The detector response function turns out to be [23, 24, 172]

$$\mathscr{F}(\Delta E) = \frac{\delta(0)}{2\pi}\frac{\Delta E}{e^{2\pi\Delta E/a}-1}\,. \tag{2.35}$$

Thus, the accelerated observer sees a bath of thermal radiation at the temperature $k_B T_U = a/2\pi$. This temperature T_U is known as *the Unruh temperature*, and k_B is *the Boltzmann constant* (we use natural unit $k_B = \hbar = c = 1$). Here *the Dirac delta function* $\delta(0)$ appears because the interaction is on for *infinite time*. One can define detector response per unit time $\mathscr{F}(\Delta E)/T$ to avoid this delta function. Another possible way to avoid this delta function is by allowing interaction only for some finite time, introducing an interaction switching function [174–178]. However, for finite-time switching functions, there is always some additional contributions due to switching effect. For example, in case of inertial detector, excitation probability with eternal interaction is vanishing,

which is consistent with the vanishing expectation value of number operator. However, introduction of finite-time switching functions, the excitation probability is *non-zero* [179, 180]. This Unruh-DeWitt particle detector models are extensively studied in literature for various flat and curved spacetime backgrounds to operationally realise the particle production phenomena [87, 175, 176, 179, 181–204].

2.4 Evolution of combined state of the detectors

In previous section, we have discussed interaction of a single detector with background scalar field. In this section, we will consider the system of two detectors (say A and B) locally interacting with the quantum field. However, these detectors do not interact with each other. The interaction Hamiltonian is given by

$$\hat{H}_{int} = \sum_{j=A,B} c_j \hat{m}_j(\tau_j)\hat{\phi}(x_j(\tau_j)). \tag{2.36}$$

The interaction action $\hat{S}_{int}$ is given by

$$\hat{S}_{int} = \sum_{j=A,B} \int c_j \chi_j(\tau_j)\hat{m}_j(\tau_j)\hat{\phi}(x_j(\tau_j))d\tau_j \tag{2.37}$$

where c_j and $\hat{m}_j(\tau_j)$ are the coupling constant and the monopole operator of the j^{th} detector, respectively. $\chi(\tau)$ is interaction switching function, which can restricts the time-interval of the interaction. For eternal interactions, one uses $\chi(\tau) = 1$. For practical set-ups this time-interval need not has to be *infinite*, it has to be much larger than the time scale associated with the detector's energy gap. Then, the spurious, oscillatory finite-time switching effects become negligible compared to the actual transitions, and one obtains the results corresponding to the infinite time switching [158]. Only then, the experimental outcomes can be compared with the theoretical predictions. In our studies, we will always use $\chi(\tau) = 1$ for this reason. Later, we will define the rate of quantities as physical quantities.

Let us consider the initial state of the total system at the asymptotic past is given by

$$|in\rangle = |D\rangle|\Psi\rangle \ , \tag{2.38}$$

where $|D\rangle$ is the initial composite state of the detectors' (A and B), and $|\Psi\rangle$ is the initial state of the field (we will consider $|\Psi\rangle$ as vacuum state of the field $|0\rangle$, except in chapter 5). The final state at the asymptotic future can be expressed in terms of unitary evolution in interaction picture as [205]

$$|out\rangle = Te^{i\hat{S}_{int}}|in\rangle \ . \tag{2.39}$$

One can construct the final density matrix of the total system as $|out\rangle\langle out|$ (since the state of the total system is a pure state). Tracing the field degrees of freedom, one obtain the density matrix of two detector system as

$$\hat{\rho}_{AB} = Tr_{\phi}\{|out\rangle\langle out|\}\,. \tag{2.40}$$

Using the (2.39) and (2.40), we calculate $\hat{\rho}_{AB}$ up to second order in coupling constant as

$$\begin{aligned}\hat{\rho}_{AB} =& Tr_{\phi}\left\{[1+i\hat{S}_{int} - T(\hat{S}_{int}\hat{S'}_{int})/2]|\Psi\rangle|D\rangle\langle D|\langle\Psi|[1-i\hat{S}_{int} - T(\hat{S}_{int}\hat{S'}_{int})^{\dagger}/2]\right\}\\ =&|D\rangle\langle D|\,Tr_{\phi}\{|\Psi\rangle\langle\Psi|\} + Tr_{\phi}\left\{i\hat{S}_{int}|\Psi\rangle|D\rangle\langle D|\langle\Psi|\right\} - Tr_{\phi}\left\{|\Psi\rangle|D\rangle\langle D|\langle\Psi|i\hat{S}_{int}\right\}\\ &+ Tr_{\phi}\left\{\hat{S}_{int}|\Psi\rangle|D\rangle\langle D|\langle\Psi|\hat{S}'_{int}\right\} - Tr_{\phi}\left\{T(\hat{S}_{int}\hat{S'}_{int})/2|\Psi\rangle|D\rangle\langle D|\langle\Psi|\right\}\\ &- Tr_{\phi}\left\{|\Psi\rangle|D\rangle\langle D|\langle\Psi|T(\hat{S}_{int}\hat{S'}_{int})^{\dagger}/2\right\} + O(c^3)\,.\end{aligned} \tag{2.41}$$

Trace on the first term yields *unity*, the second and the third terms will vanish (see Appendix 2.A.1). The density operator $\hat{\rho}_{AB}$ become

$$\hat{\rho}_{AB} = |D\rangle\langle D| + [\hat{R}^{(1)} + \hat{R}^{(2)} + \hat{R}^{(2)\dagger}] + O(c^3)\,. \tag{2.42}$$

Here the first term represents the initial density matrix of the composite system of two detectors. The next term is given as

$$\begin{aligned}\hat{R}^{(1)} =& Tr_{\phi}[\hat{S}_{int}|\Psi\rangle|D\rangle\langle D|\langle\Psi|\hat{S}_{int}]\\ =& Tr_{\phi}\left[\sum_{i=A,B}\int c_i\chi_i(\tau_i)\hat{m}_i(\tau_i)\hat{\phi}(x_i)d\tau_i\right]|\Psi\rangle|D\rangle\langle D|\langle\Psi|\left[\sum_{j=A,B}\int c_j\chi_j(\tau'_j)\hat{m}_j(\tau'_j)\hat{\phi}(x'_j)d\tau'_j\right]\\ =& \sum_{i,j=A,B} c_ic_j\iint d\tau_i d\tau'_j\chi_i(\tau_i)\chi_j(\tau'_j)\left[\hat{m}_i(\tau_i)|D\rangle\langle D|\hat{m}_j(\tau'_j)\right]\langle\Psi|\hat{\phi}(x'_j)\hat{\phi}(x_i)|\Psi\rangle\,.\end{aligned} \tag{2.43}$$

Consider the initial composite state of two detectors as

$$|D\rangle = \alpha|g_Ag_B\rangle + \gamma|e_Ae_B\rangle\,, \tag{2.44}$$

one can calculate the quantity inside the square bracket in Eq. (2.43). For these calculations, one can check Appendix 2.A.2. Using the results from Appendix 2.A.2, the quantity $\hat{R}^{(1)}$ turns out to be

$$\begin{aligned}
\hat{R}^{(1)} &= |e_A g_B\rangle\langle e_A g_B|\{\alpha^2 c_A^2 \mathscr{P}_A(\Delta E) + \gamma^2 c_B^2 \mathscr{P}_B(-\Delta E) + \alpha\gamma c_A c_B(\bar{\mathscr{P}}_{AB}(\Delta E) + \bar{\mathscr{P}}^{\star}_{AB}(\Delta E))\} \\
&+ |g_A e_B\rangle\langle g_A e_B|\{\gamma^2 c_A^2 \mathscr{P}_A(-\Delta E) + \alpha^2 c_B^2 \mathscr{P}_B(\Delta E) + \alpha\gamma c_A c_B(\bar{\mathscr{P}}_{AB}(-\Delta E) + \bar{\mathscr{P}}^{\star}_{AB}(-\Delta E))\} \\
&+ |e_A g_B\rangle\langle g_A e_B|\{\alpha\gamma(c_A^2 \bar{\mathscr{P}}_{AA}(\Delta E) + c_B^2 \bar{\mathscr{P}}_{BB}(-\Delta E)) + c_A c_B(\alpha^2 \mathscr{P}_{AB}(\Delta E) + \gamma^2 \mathscr{P}^{\star}_{AB}(-\Delta E))\} \\
&+ |g_A e_B\rangle\langle e_A g_B|\{\alpha\gamma(c_A^2 \bar{\mathscr{P}}_{AA}(-\Delta E) + c_B^2 \bar{\mathscr{P}}_{BB}(\Delta E)) + c_A c_B(\alpha^2 \mathscr{P}^{\star}_{AB}(\Delta E) + \gamma^2 \mathscr{P}_{AB}(-\Delta E))\} \\
&= b_1 |e_A g_B\rangle\langle e_A g_B| + b_2 |e_A g_B\rangle\langle g_A e_B| + h_1 |g_A e_B\rangle\langle e_A g_B| + h_2 |g_A e_B\rangle\langle g_A e_B|; \qquad (2.45)
\end{aligned}$$

where we have defined the following functions:

$$\mathscr{P}_j(\Delta E) = \iint d\tau_j d\tau'_j \chi_j(\tau_j)\chi_j(\tau'_j) e^{i\Delta E_j \Delta\tau_j} \langle\Psi|\hat{\phi}(x'_j)\hat{\phi}(x_j)|\Psi\rangle, \qquad (2.46)$$

$$\bar{\mathscr{P}}_{jj}(\Delta E) = \iint d\tau_j d\tau_j \chi_j(\tau_j)\chi_j(\tau_j) e^{i\Delta E_j(\tau_j+\tau_j)} \langle\Psi|\hat{\phi}(x_j)\hat{\phi}(x_j)|\Psi\rangle, \qquad (2.47)$$

$$\bar{\mathscr{P}}_{AB}(\Delta E) = \iint d\tau_A d\tau_B \chi_A(\tau_A)\chi_B(\tau_B) e^{i\Delta E_A\tau_A + i\Delta E_B\tau_B} \langle\Psi|\hat{\phi}(x_B)\hat{\phi}(x_A)|\Psi\rangle, \qquad (2.48)$$

$$\mathscr{P}_{AB}(\Delta E) = \iint d\tau_A d\tau_B \chi_A(\tau_A)\chi_B(\tau_B) e^{i\Delta E_A\tau_A - i\Delta E_B\tau_B} \langle\Psi|\hat{\phi}(x_B)\hat{\phi}(x_A)|\Psi\rangle. \qquad (2.49)$$

The expressions of b_1, b_2, h_1 and h_2 are given later (see Eq. 2.65). Here $\mathscr{P}_j(\Delta E)$, $\bar{\mathscr{P}}_{jj}(\Delta E)$ are local quantities, depends on coordinates of only one detector. The quantity $\mathscr{P}_j(\Delta E)$ is the transition probability of j^{th} detector as discussed in Sec. 2.3. The other quantities $\bar{\mathscr{P}}_{AB}(\Delta E)$, $\mathscr{P}_{AB}(\Delta E)$ are non-local, depends on coordinates of both detectors. Also note that among these quantities, only $\bar{\mathscr{P}}_{AB}(\Delta E)$ is symmetric under exchange of (x_A, x_B) if the detectors have equal energy gap $\Delta E_A = \Delta E_B = \Delta E$.

The next term is obtained as

$$\begin{aligned}
\hat{R}^{(2)} &= -Tr_\phi T(\hat{S}_{int}\hat{S}'_{int})/2|\Psi\rangle|D\rangle\langle D|\langle\Psi| \\
&= -\frac{1}{2} Tr_\phi T\left(\sum_{i=A,B} c_i \int d\tau_i \chi_i(\tau_i)\hat{m}_i(\tau_i)\hat{\phi}(x_i)\right)\left(\sum_{j=A,B} c_j \int d\tau'_j \chi_j(\tau'_j)\hat{m}_j(\tau'_j)\hat{\phi}(x'_j)\right) \\
&\quad \times |\Psi\rangle|D\rangle\langle D|\langle\Psi|.
\end{aligned} \qquad (2.50)$$

After some rearrangement we obtain

$$\hat{R}^{(2)} = -\sum_{i,j=A,B} \frac{c_i c_j}{2} \iint d\tau_i d\tau'_j \chi_i(\tau_i)\chi_i(\tau'_j)\hat{m}_i(\tau_i)\hat{m}_j(\tau'_j)|D\rangle\langle D|\left[Tr_\phi T\left(\hat{\phi}(x_i)\hat{\phi}(x'_j)|\Psi\rangle\langle\Psi|\right)\right]. \qquad (2.51)$$

Here before tracing out field degrees of freedom, we need to remove the *time-ordering*. Thus we will use the following relation [205]

$$\frac{1}{2}\iint d\tau d\tau' T[\hat{O}(\tau)\hat{O}(\tau')] = \iint d\tau d\tau' \hat{O}(\tau)\hat{O}(\tau')\theta(\tau-\tau'). \qquad (2.52)$$

After that we can simply take trace over field degrees of freedom using Eq. (2.A.5) from Appendix 2.A.1. The quantity $\hat{R}^{(2)}$ in Eq. (2.51) then becomes

$$\begin{aligned}\hat{R}^{(2)} &= -\sum_{i,j=A,B} c_i c_j \iint d\tau_i d\tau'_j \chi_i(\tau_i)\chi_j(\tau'_j)\theta(\tau_i-\tau'_j)[\hat{m}_i(\tau_i)\hat{m}_j(\tau'_j)|D\rangle\langle D]\langle\Psi|\hat{\phi}(x_i)\hat{\phi}(x'_j)|\Psi\rangle \\ &= -\sum_{j=A,B} c_j^2 \iint d\tau_j d\tau'_j \chi_j(\tau_j)\chi_j(\tau'_j)\theta(\tau_j-\tau'_j)[\hat{m}_j(\tau_j)\hat{m}_j(\tau'_j)|D\rangle\langle D|]\langle\Psi|\hat{\phi}(x_j)\hat{\phi}(x'_j)|\Psi\rangle \\ &\quad - c_A c_B \iint d\tau_A d\tau_B \chi_A(\tau_A)\chi_B(\tau_B)[\hat{m}_A(\tau_A)\hat{m}_B(\tau_B)|D\rangle\langle D|]\langle\Psi|T\hat{\phi}(x_A)\hat{\phi}(x_B)|\Psi\rangle\,.\end{aligned} \tag{2.53}$$

Here in the last line we dropped prime ($'$) symbol from the dummy variables. Also used the property that $\hat{m}_A(\tau_A)\hat{m}_B(\tau_B)|D\rangle\langle D| = \hat{m}_B(\tau_B)\hat{m}_A(\tau_A)|D\rangle\langle D|$ (see Appendix 2.A.3). Here the time-ordered two-point function (the Feynman propagator) is appeared as we know that

$$\langle\Psi|T\hat{\phi}(x_A)\hat{\phi}(x_B)|\Psi\rangle = \theta(\tau_A-\tau_B)\langle\Psi|\hat{\phi}(x_A)\hat{\phi}(x_B)|\Psi\rangle + \theta(\tau_B-\tau_A)\langle\Psi|\hat{\phi}(x_B)\hat{\phi}(x_A)|\Psi\rangle\,. \tag{2.54}$$

For our considered initial composite state of two detectors $|D\rangle = \alpha|g_A g_B\rangle + \gamma|e_A e_B\rangle$, we have

$$\begin{aligned}\hat{R}^{(2)} = &-|g_A g_B\rangle\langle g_A g_B|\{\alpha^2(c_A^2\mathscr{P}_{A,+}(\Delta E)+c_B^2\mathscr{P}_{B,+}(\Delta E)) - \alpha\gamma c_A c_B \mathscr{E}(-\Delta E)\} \\ &-|e_A e_B\rangle\langle e_A e_B|\{\gamma^2(c_A^2\mathscr{P}_{A,+}(-\Delta E)+c_B^2\mathscr{P}_{B,+}(-\Delta E)) - \alpha\gamma c_A c_B \mathscr{E}(\Delta E)\} \\ &-|g_A g_B\rangle\langle e_A e_B|\{\alpha\gamma(c_A^2\mathscr{P}_{A,+}(\Delta E)+c_B^2\mathscr{P}_{B,+}(\Delta E)) - \gamma^2 c_A c_B \mathscr{E}(-\Delta E)\} \\ &-|e_A e_B\rangle\langle g_A g_B|\{\alpha\gamma(c_A^2\mathscr{P}_{A,+}(-\Delta E)+c_B^2\mathscr{P}_{B,+}(-\Delta E)) - \alpha^2 c_A c_B \mathscr{E}(\Delta E)\}\,;\end{aligned} \tag{2.55}$$

where we have defined

$$\mathscr{P}_j(\Delta E) = \mathscr{P}_{j,+}(\Delta E) + \mathscr{P}^{\star}_{j,+}(\Delta E), \tag{2.56}$$

$$\mathscr{P}_{j,+}(\Delta E) = \iint d\tau_j d\tau'_j \chi_j(\tau_j)\chi_j(\tau'_j)\theta(\tau_j-\tau'_j)e^{i\Delta E_j \Delta\tau_j}\langle\Psi|\hat{\phi}(x'_j)\hat{\phi}(x_j)|\Psi\rangle\,, \tag{2.57}$$

$$\begin{aligned}M_j &= \mathscr{P}_{j,+}(\Delta E_j) + \mathscr{P}^{\star}_{j,+}(-\Delta E_j) \\ &= \iint d\tau_j d\tau'_j \chi_j(\tau_j)\chi_j(\tau'_j)\theta(\tau_j-\tau'_j)e^{i\Delta E_j\Delta\tau_j}\langle\Psi|\{\hat{\phi}(x'_j),\hat{\phi}(x_j)\}|\Psi\rangle\,,\end{aligned} \tag{2.58}$$

$$\mathscr{E}(\Delta E) = -\iint d\tau_A d\tau_B \chi_A(\tau_A)\chi_B(\tau_B)e^{i\Delta E_A\tau_A + i\Delta E_B\tau_B}\langle\Psi|T\hat{\phi}(x_B)\hat{\phi}(x_A)|\Psi\rangle\,. \tag{2.59}$$

In Eq. (2.57), there is a discontinuity of the Heaviside function at the limit $\tau_j \to \tau'_j$. In this coincidence limit ($x_j(\tau) \to x_j(\tau')$), there exists a distributional singularity of the two-point function.

Here the dummy integration variables τ_j and τ'_j can be re-expressed in terms of new variables $u_j = \tau_j - \tau'_j$ and $v_j = \tau_j + \tau'_j$. Also, the two-point function of the j^{th} detector can be expressed as a function of u_j. Then the integrals in Eq. (2.57) can be expressed as

$$\mathscr{P}_{j,+} = \text{Limit}_{\epsilon\to 0}\int_{-\infty}^{\infty} dv_j \int_{0+\epsilon}^{\infty} du_j\, e^{i\Delta E_j u_j} G_\Psi(u_j); \tag{2.60}$$

where $G_\Psi(u_j) = \langle\Psi|\hat{\phi}(x'_j)\hat{\phi}(x_j)|\Psi\rangle$ and the switching functions $\chi_j(\tau_j) = 1$. In the integration limit, one introduces a minimal parameter ϵ (> 0), such that $u_j \geq \epsilon$, and after the integration takes the limit $\epsilon \to 0$. While performing the integrals, one also utilises the $i\epsilon$-prescription in the two-point function. For example, in the case of the Minkowski space, the two-point function usually can be expressed as [24]

$$G_{vac}(x,x') = -\frac{1}{4\pi^2}\frac{1}{(t-t'-i\epsilon)^2 - |x-x'|^2}. \tag{2.61}$$

After the integrations are performed, one set $\epsilon \to 0$. In this way, the discontinuity of the Heavisine function at $u = 0$ does not affect the integrations.

Following the earlier methods, we obtain $R^{(2)\dagger}$ as

$$\begin{aligned}
\hat{R}^{(2)\dagger} = &-|g_A g_B\rangle\langle g_A g_B|\{\alpha^2(c_A^2\mathscr{P}^\star_{A,+}(\Delta E) + c_B^2\mathscr{P}^\star_{B,+}(\Delta E)) - \alpha\gamma c_A c_B \mathscr{E}^\star(-\Delta E)\}\\
&-|e_A e_B\rangle\langle e_A e_B|\{\gamma^2(c_A^2\mathscr{P}^\star_{A,+}(-\Delta E) + c_B^2\mathscr{P}^\star_{B,+}(-\Delta E)) - \alpha\gamma c_A c_B \mathscr{E}^\star(\Delta E)\}\\
&-|e_A e_B\rangle\langle g_A g_B|\{\alpha\gamma(c_A^2\mathscr{P}^\star_{A,+}(\Delta E) + c_B^2\mathscr{P}^\star_{B,+}(\Delta E)) - \gamma^2 c_A c_B \mathscr{E}^\star(-\Delta E)\}\\
&-|g_A g_B\rangle\langle e_A e_B|\{\alpha\gamma(c_A^2\mathscr{P}^\star_{A,+}(-\Delta E) + c_B^2\mathscr{P}^\star_{B,+}(-\Delta E)) - \alpha^2 c_A c_B \mathscr{E}^\star(\Delta E)\}.
\end{aligned} \tag{2.62}$$

Thus adding the quantities $\hat{R}^{(2)}$, $\hat{R}^{(2)\dagger}$ with initial reduced density matrix $|D\rangle\langle D|$, we obtain

$$\begin{aligned}
&|D\rangle\langle D| + \hat{R}^{(2)} + \hat{R}^{(2)\dagger}\\
&= |g_A g_B\rangle\langle g_A g_B|\{\alpha^2 - \alpha^2(c_A^2\mathscr{P}_A(\Delta E) + c_B^2\mathscr{P}_B(\Delta E)) + \alpha\gamma c_A c_B(\mathscr{E}^\star(-\Delta E) + \mathscr{E}(-\Delta E))\}\\
&+ |e_A e_B\rangle\langle e_A e_B|\{\gamma^2 - \gamma^2(c_A^2\mathscr{P}_A(-\Delta E) + c_B^2\mathscr{P}_B(-\Delta E)) + \alpha\gamma c_A c_B(\mathscr{E}^\star(\Delta E) + \mathscr{E}(\Delta E))\}\\
&+ |e_A e_B\rangle\langle g_A g_B|\{\alpha\gamma - \alpha\gamma(c_A^2 M_A^\star + c_B^2 M_B^\star) + \gamma^2 c_A c_B \mathscr{E}^\star(-\Delta E) + \alpha^2 c_A c_B \mathscr{E}(\Delta E)\}\\
&+ |g_A g_B\rangle\langle e_A e_B|\{\alpha\gamma - \alpha\gamma(c_A^2 M_A + c_B^2 M_B) + \alpha^2 c_A c_B \mathscr{E}^\star(\Delta E) + \gamma^2 c_A c_B \mathscr{E}(-\Delta E)\}\\
&= a_1|e_A e_B\rangle\langle e_A e_B| + a_2|e_A e_B\rangle\langle g_A g_B| + d_1|g_A g_B\rangle\langle e_A e_B| + d_2|g_A g_B\rangle\langle g_A g_B|
\end{aligned} \tag{2.63}$$

Therefore, from Eqs. (2.42), (2.45) and (2.63), we obtain the final reduced density matrix of two detector system upto second order in coupling constant as [110]

$$\hat{\rho}_{AB} = \begin{pmatrix} a_1 & 0 & 0 & a_2 \\ 0 & b_1 & b_2 & 0 \\ 0 & h_1 & h_2 & 0 \\ d_1 & 0 & 0 & d_2 \end{pmatrix} + O(c^4); \tag{2.64}$$

with matrix elements obtained as follows

$$\begin{aligned}
a_1 &= \gamma^2 - \gamma^2(c_A^2\mathscr{P}_A(-\Delta E) + c_B^2\mathscr{P}_B(-\Delta E)) + \alpha\gamma c_A c_B(\mathscr{E}^\star(\Delta E) + \mathscr{E}(\Delta E)),\\
a_2 &= \alpha\gamma - \alpha\gamma(c_A^2 M_A^\star + c_B^2 M_B^\star) + \gamma^2 c_A c_B \mathscr{E}^\star(-\Delta E) + \alpha^2 c_A c_B \mathscr{E}(\Delta E),\\
d_1 &= \alpha\gamma - \alpha\gamma(c_A^2 M_A + c_B^2 M_B) + \alpha^2 c_A c_B \mathscr{E}^\star(\Delta E) + \gamma^2 c_A c_B \mathscr{E}(-\Delta E),\\
d_2 &= \alpha^2 - \alpha^2(c_A^2\mathscr{P}_A(\Delta E) + c_B^2\mathscr{P}_B(\Delta E)) + \alpha\gamma c_A c_B(\mathscr{E}^\star(-\Delta E) + \mathscr{E}(-\Delta E)),\\
b_1 &= \alpha^2 c_A^2\mathscr{P}_A(\Delta E) + \gamma^2 c_B^2\mathscr{P}_B(-\Delta E) + \alpha\gamma c_A c_B(\bar{\mathscr{P}}_{AB}(\Delta E) + \bar{\mathscr{P}}_{AB}^\star(\Delta E)),\\
b_2 &= \alpha\gamma(c_A^2\bar{\mathscr{P}}_{AA}(\Delta E) + c_B^2\bar{\mathscr{P}}_{BB}(-\Delta E)) + c_A c_B(\alpha^2\mathscr{P}_{AB}(\Delta E) + \gamma^2\mathscr{P}_{AB}^\star(-\Delta E)),\\
h_1 &= \alpha\gamma(c_A^2\bar{\mathscr{P}}_{AA}(-\Delta E) + c_B^2\bar{\mathscr{P}}_{BB}(\Delta E)) + c_A c_B(\alpha^2\mathscr{P}_{AB}^\star(\Delta E) + \gamma^2\mathscr{P}_{AB}(-\Delta E)),\\
h_2 &= \gamma^2 c_A^2\mathscr{P}_A(-\Delta E) + \alpha^2 c_B^2\mathscr{P}_B(\Delta E) + \alpha\gamma c_A c_B(\bar{\mathscr{P}}_{AB}(-\Delta E) + \bar{\mathscr{P}}_{AB}^\star(-\Delta E)).
\end{aligned} \tag{2.65}$$

Note that the elements a_1, a_2, d_1 and d_2 have contributions from both c^0 and c^2-orders. However, the all other elements b_1, b_2, h_1 and h_2 have contributions from only c^2-order. This general analysis has been given in [110].

There is one more thing we need to check before we proceed further. We need to ensure that the matrix $\hat{\rho}_{AB}$ is positive, as it is a density matrix [206]. Thus all the eigenvalues of $\hat{\rho}_{AB}$ has to be positive.

For the density matrix in Eq. (2.64), the eigenvalues of are

$$\begin{aligned}
\lambda_{1,2} &= \frac{1}{2}\left\{a_1 + d_2 \pm \sqrt{(a_1+d_2)^2 + 4(a_2 d_1 - a_1 d_2)}\right\},\\
\lambda_{3,4} &= \frac{1}{2}\left\{b_1 + h_2 \pm \sqrt{(b_1+h_2)^2 + 4(b_2 h_1 - b_1 h_2)}\right\}.
\end{aligned} \tag{2.66}$$

These eigenvalues are all positive, provided the following conditions are satisfied

$$a_1 d_2 \geq a_2 d_1, \quad b_1 h_2 \geq b_2 h_1. \tag{2.67}$$

2.4.1 Initially detectors are non-entangled

Now, if we consider the initial composite state of two detector system as *non-entangled state* and the detectors are in their ground states $|D\rangle = |g_A g_B\rangle$, then the final reduced

density matrix in Eq. (2.64) is simplified to [108, 109]

$$\hat{\rho}_{AB} = \begin{pmatrix} 0 & 0 & 0 & c_A c_B \mathscr{E} \\ 0 & c_A^2 \mathscr{P}_A & c_A c_B \mathscr{P}_{AB} & 0 \\ 0 & c_A c_B \mathscr{P}_{AB}^{\star} & c_B^2 \mathscr{P}_B & 0 \\ c_A c_B \mathscr{E}^{\star} & 0 & 0 & 1 - c_A^2 \mathscr{P}_A - c_B^2 \mathscr{P}_B \end{pmatrix} + O(c^4). \tag{2.68}$$

It is obtained by setting $\alpha = 1$ and $\gamma = 0$ in Eqs. (2.65) and (2.64). Here the elements always have the argument '$+\Delta E$', *i.e.,* $\mathscr{P} := \mathscr{P}(\Delta E)$ and $\mathscr{E} := \mathscr{E}(\Delta E)$. This implies that the time evolution of detectors in this scenario is only related to the excitation of detectors. When the initial state is entangled, the detectors are initially both in excited and ground states, then elements of the later time density matrix will be related to both excitation and emission of the detectors. In this thesis, we will focus more on the systems where the initial state of the detectors is $|g_A g_B\rangle$, which is a separable state. We will primarily investigate how in presence of different background spacetime and motion of the detectors, this state get evolved in to an entangled state. Only in entanglement leakage study (see chapter 6), we will consider the initially entangled state of the detectors, where we will deal with density matrix in Eq. (2.64).

Up to c^2-order perturbation, the density matrix $\hat{\rho}_{AB}$ in Eq. (2.68) has $a_1 = 0$. However this term will remain non-zero for higher order perturbations. We can take simply take contribution from c^4-order perturbation, $a_1 = c^4\chi \equiv \langle e_A e_B|\hat{\rho}_{AB}|e_A e_B\rangle$. Then both $a_1 d_2$ and $a_2 d_1$ from the *first condition* in Eq. (2.67) will be in c^4-order. Therefore $\hat{\rho}_{AB}$ in Eq. (2.68) can again satisfy the conditions in Eq. (2.67). This will be clear if we calculate the eigenvalues of the density matrix in Eq. (2.68). The corresponding eigenvalues are given by

$$1 + O(c^2),\ c^4(\chi - |\mathscr{E}|^2) + O(c^6),\ \frac{c^2}{2}\left[\mathscr{P}_A + \mathscr{P}_B \pm \sqrt{(\mathscr{P}_A - \mathscr{P}_B)^2 + 4|\mathscr{P}_{AB}|^2}\right] + O(c^4). \tag{2.69}$$

Here the $c^4\chi$ term is present in the second eigenvalue, which is in c^4-order. Since our whole calculation is done up to c^2-order, this c^4-order eigenvalue should not play any role in our analysis. This term is only considered to make all eigenvalues of our density matrix positive. Also note that as the quantities $\mathscr{P}_A, \mathscr{P}_B$'s are detector transition probabilities, these are always positive. These eigenvalues are always positive, provided the following conditions

$$c^4\left(\chi - |\mathscr{E}|^2\right) \geq 0, \qquad c^2\left(\mathscr{P}_A \mathscr{P}_B - |\mathscr{P}_{AB}|^2\right) \geq 0\ . \tag{2.70}$$

Here these conditions also can be directly obtained from Eq. (2.67).

2.5 Entanglement in two detector systems

In the previous section, we discussed the time evolution of the composite system consisting of two detectors. We considered two scenarios for the initial state of the detectors: (i) an entangled state and (ii) a non-entangled state. Using these initial states, we determined the state of the detectors at a later time. In this section, our aim to analyse the entanglement between the detectors in their evolved state. To do so, we first briefly discuss some well-known measures of entanglement for two qubit systems. A necessary and sufficient condition for determining entanglement in such systems was introduced by Peres. According to this criterion, the evolved state is entangled if there is at least one negative eigenvalue of the partial transpose of the density matrix of the detectors [72, 207]. However, Peres's condition does not provide quantification of entanglement. To measure the degree of entanglement, we consider the established measures - *negativity* [207] and *concurrence* [75, 76]. Let us briefly discuss them.

2.5.1 Separability Criterion

In 1996, Asher Peres discovered a criterion [72], which is a necessary condition, for the combined density matrix $\hat{\rho}_{AB}$ of two systems A and B, to be separable. If a density matrix is not separable, then it is an entangled state. This condition is also known as positive partial transpose (PPT) condition.

It is well-known that if a composite density matrix is separable, then we can write the total state as

$$\hat{\rho}_{AB} = \sum_j p_j \hat{\rho}_j^A \otimes \hat{\rho}_j^B , \tag{2.71}$$

where, $\hat{\rho}_j^A$ and $\hat{\rho}_j^B$ are density matrices of two subsystems. Applying partial transpose $(T_A \otimes I_B)$ operation (transpose of only subsystem A), we obtain

$$\hat{\rho}_{AB}^{T_A} := (T_A \otimes I_B)\hat{\rho}_{AB} = \sum_j p_j \left(\hat{\rho}_j^A\right)^T \otimes \hat{\rho}_j^B . \tag{2.72}$$

Since $\left(\hat{\rho}_j^A\right)^T$ has same eigenvalues as $\hat{\rho}_j^A$, the partial transposed matrix $(T_A \otimes I_B)\hat{\rho}$ has to be positive semidefinite. Therefore, all eigenvalues of $\hat{\rho}_{AB}^{T_A}$ are positive if $\hat{\rho}_{AB}$ is a separable state. In other words, if there is any negative eigenvalues of $\hat{\rho}_{AB}^{T_A}$, the state $\hat{\rho}_{AB}$ is an entangled state or non-separable state [72, 207].

In arbitrary dimensions of the two subsystems the PPT criterion provides only a necessary but not sufficient condition for separability. If instead the bipartite system has

dimension of the type $2\otimes 2$, $2\otimes 3$ (or $3\otimes 2$), then the PPT criterion provides a necessary and sufficient condition for separability.

Here for our density matrix in Eq. (2.64), taking partial transpose will swap the off-diagonal elements of the density matrix as

$$\langle g_A g_B|\rho_{AB}|e_A e_B\rangle \leftrightarrow \langle e_A g_B|\rho_{AB}|g_A e_B\rangle, \qquad \langle e_A e_B|\rho_{AB}|g_A g_B\rangle \leftrightarrow \langle g_A e_B|\rho_{AB}|e_A g_B\rangle\,. \tag{2.73}$$

The partial transpose of ρ_{AB} is

$$\hat{\rho}_{AB} = \begin{pmatrix} a_1 & 0 & 0 & b_2 \\ 0 & b_1 & a_2 & 0 \\ 0 & d_1 & h_2 & 0 \\ h_1 & 0 & 0 & d_2 \end{pmatrix} + O(c^4); \tag{2.74}$$

The eigenvalues of this partially transposed density matrix are

$$\begin{aligned} \lambda_{1,2} &= \frac{1}{2}\left\{a_1 + d_2 \pm \sqrt{(a_1+d_2)^2 + 4(b_2h_1 - a_1d_2)}\right\}, \\ \lambda_{3,4} &= \frac{1}{2}\left\{b_1 + h_2 \pm \sqrt{(b_1+h_2)^2 + 4(a_2d_1 - b_1h_2)}\right\}. \end{aligned} \tag{2.75}$$

Here the eigenvalues can be negative if any of the following conditions are satisfied

$$b_2h_1 > a_1d_2\,, \tag{2.76}$$

or,

$$a_2d_1 > b_1h_2\,. \tag{2.77}$$

Combining Eq. (2.67) and Eq. (2.76), we obtain

$$b_1h_2 \geq b_2h_1 > a_1d_2 \geq a_2d_1\,, \tag{2.78}$$

which contradicts Eq. (2.77). However, if we combine Eq. (2.67) and Eq. (2.77), we obtain

$$a_1d_2 \geq a_2d_1 > b_1h_2 \geq b_2h_1\,, \tag{2.79}$$

which contradicts Eq. (2.76). Therefore, either Eq. (2.76) or Eq. (2.77) provides the condition for entanglement between the detectors.

Here from Eq. (2.65), one can see that, the density matrix elements $a_1, a_2, d_1 d_2$ contains terms in both c^0 and c^2-orders. And the elements b_1, b_2, h_1, h_2 are only in c^2-order. Therefore, condition in Eq. (2.76) is impossible to be satisfied in a perturbation

theory. Thus, condition in Eq. (2.77) is the *only appropriate condition* for entanglement between the detectors. The only possible eigenvalue which can be negative is

$$\lambda_4 = \frac{1}{2}\left\{b_1 + h_2 - \sqrt{(b_1+h_2)^2 + 4(a_2 d_1 - b_1 h_2)}\right\}. \tag{2.80}$$

Similarly, the partial transpose of ρ_{AB} in Eq. (2.68) is

$$\rho_{AB}^{T_A} = \begin{pmatrix} c^4\chi & 0 & 0 & c^2\mathscr{P}_{AB} \\ 0 & c^2\mathscr{P}_A & c^2\mathscr{E} & 0 \\ 0 & c^2\mathscr{E}^\star & c^2\mathscr{P}_B & 0 \\ c^2\mathscr{P}^\star_{AB} & 0 & 0 & 1-c^2(\mathscr{P}_A+\mathscr{P}_B) \end{pmatrix}; \tag{2.81}$$

which has eigenvalues

$$1+O(c^2), \qquad c^4\left(\chi - |\mathscr{P}_{AB}|^2\right)+O(c^6), \qquad \frac{c^2}{2}\left[\mathscr{P}_A+\mathscr{P}_B \pm \sqrt{(\mathscr{P}_A-\mathscr{P}_B)^2+4|\mathscr{E}|^2}\right]+O(c^4). \tag{2.82}$$

Here the condition for the two detectors to become entangled can be found as [108]

$$\mathscr{P}_A\mathscr{P}_B < |\mathscr{E}|^2, \tag{2.83}$$

or,

$$\chi < |\mathscr{P}_{AB}|^2. \tag{2.84}$$

Again combining Eq. (2.70) and Eq. (2.83), we obtain

$$|\mathscr{P}_{AB}|^2 \le \mathscr{P}_A\mathscr{P}_B < |\mathscr{E}|^2 \le \chi, \tag{2.85}$$

which contradicts Eq. (2.84). However, if we combine Eq. (2.70) and Eq. (2.84), we obtain

$$|\mathscr{E}|^2 \le \chi < |\mathscr{P}_{AB}|^2 \le \mathscr{P}_A\mathscr{P}_B, \tag{2.86}$$

which contradicts Eq. (2.83). Therefore, either Eq. (2.83) or Eq. (2.84) provides the condition for entanglement between the detectors.

Here we will use the condition in Eq. (2.83) for our purpose since it contains terms, which are in the c^2-order only. Also it can be directly obtained from Eq. (2.77).

Therefore, the only possible eigenvalue which can be negative is [108]

$$\frac{c^2}{2}\left[\mathscr{P}_A+\mathscr{P}_B - \sqrt{(\mathscr{P}_A-\mathscr{P}_B)^2+4|\mathscr{E}|^2}\right]+O(c^4), \tag{2.87}$$

which also can be obtained directly from the eigenvalue in Eq. (2.80).

2.5.2 Negativity

The PPT criterion only provides the condition for examining if two detectors entangled or not. It does not provide any quantification of entanglement between the detectors. However, a quantification of entanglement is defined as sum of absolute value of negative eigenvalues of partial transpose of density matrix, known as *negativity* ($\mathcal{N}(\hat{\rho}_{AB})$) [207].

For the density matrix in Eq. (2.64), negativity is obtained form Eq. (2.80) as [110]

$$\mathcal{N}\left(\hat{\rho}_{AB}\right) = -\frac{1}{2}\left\{b_1 + h_2 - \sqrt{(b_1+h_2)^2 + 4(a_2 d_1 - b_1 h_2)}\right\}. \tag{2.88}$$

For the density matrix in Eq. (2.68), negativity is obtained form Eq. (2.87) as [108]

$$\mathcal{N}\left(\hat{\rho}_{AB}\right) = -\frac{c^2}{2}\left[\mathscr{P}_A + \mathscr{P}_B - \sqrt{(\mathscr{P}_A - \mathscr{P}_B)^2 + 4|\mathscr{E}|^2}\right]. \tag{2.89}$$

Larger the value of $\mathcal{N}\left(\hat{\rho}_{AB}\right)$, greater the degrees of the entanglement between the detectors.

2.5.3 Concurrence:

Another independent measure of entanglement is concurrence [75, 76, 208, 209], which was originally introduced to calculate entanglement of formation of $2\otimes 2$ quantum systems. Originally for $2\otimes 2$ quantum systems, definition of concurrence is given in terms of a special basis [76, 208]

$$|f_1\rangle = |\Phi_+\rangle, \qquad |f_2\rangle = i|\Phi_-\rangle, \qquad |f_3\rangle = i|\Psi_+\rangle, \qquad |f_4\rangle = |\Phi_-\rangle, \tag{2.90}$$

where the $|\Phi_\pm\rangle = (|g_A g_B\rangle \pm |e_A e_B\rangle)/\sqrt{2}$ and $|\Psi_\pm\rangle = (|g_A e_B\rangle \pm |e_A g_B\rangle)/\sqrt{2}$ are the well-known Bell states [208]. The concurrence $\mathscr{C}(\psi)$ for a pure state $|\psi\rangle$ is defined as

$$\mathscr{C}(\psi) = \left|\sum_i \langle f_i|\psi\rangle^2\right|. \tag{2.91}$$

Using Eq. (2.90), one can obtain $\sum_i |f_i^\star\rangle\langle f_i| = -\sigma_y \otimes \sigma_y$. Here σ_y is the second Pauli spin matrix, and $(^\star)$ is complex-conjugation operation. Thus $\mathscr{C}$ in Eq. (2.91) turns out to be

$$\mathscr{C}(\psi) = \left|\langle\psi^\star|\sigma_y\otimes\sigma_y|\psi\rangle\right| = \left|\langle\tilde{\psi}|\psi\rangle\right|, \tag{2.92}$$

where the state $|\tilde{\psi}\rangle = \sigma_y\otimes\sigma_y|\psi^\star\rangle$ is known as *spin-flipped* (or *time-reversed*) state. Similarly, for a density state $\hat{\rho}$, *spin-flipped* state is defined as $\hat{\tilde{\rho}} = (\sigma_y\otimes\sigma_y)\hat{\rho}^\star(\sigma_y\otimes\sigma_y)$.

Then the concurrence is defined as [77]

$$\mathscr{C}(\hat{\rho}) = \max\left\{0, \left(\lambda_{Max} - \sum_{i\neq Max}\lambda_i\right)\right\}, \tag{2.93}$$

where λ's are square root of eigenvalues of operator $\hat{\rho}\hat{\tilde{\rho}}$. Here λ^2_{Max} is the largest eigenvalue. The concurrence $\mathscr{C}$ can have values from *zero* to *one*. For a maximally entangled state, it is *one*.

For our density matrix in Eq. (2.64), we obtain

$$\tilde{\hat{\rho}} = \begin{pmatrix} d_2^\star & 0 & 0 & d_1^\star \\ 0 & h_2^\star & h_1^\star & 0 \\ 0 & b_2^\star & b_1^\star & 0 \\ a_2^\star & 0 & 0 & a_1^\star \end{pmatrix}, \quad \text{as} \quad \sigma_y\otimes\sigma_y = \begin{pmatrix} 0 & 0 & 0 & -1 \\ 0 & 0 & 1 & 0 \\ 0 & 1 & 0 & 0 \\ -1 & 0 & 0 & 0 \end{pmatrix}. \tag{2.94}$$

Thus

$$\hat{\rho}\tilde{\hat{\rho}} = \begin{pmatrix} |a_2|^2 + a_1 d_2^\star & 0 & 0 & a_1^\star a_2 + a_1 d_1^\star \\ 0 & |b_2|^2 + b_1 h_2^\star & b_1^\star b_2 + b_1 h_1^\star & 0 \\ 0 & b_2^\star h_2 + h_1 h_2^\star & |h_1^2 + b_1^\star h_2 & 0 \\ a_2^\star d_2 + d_1 d_2^\star & 0 & 0 & |d_1|^2 + a_1^\star d_2 \end{pmatrix}. \tag{2.95}$$

The eigenvalues of this matrix as

$$\begin{aligned} \lambda^2_{1,2} =& \frac{1}{2}\Big(|a_2|^2 + |d_1|^2 + a_1^\star d_2 + a_1 d_2^\star \\ & \pm\sqrt{(|a_2|^2 + |d_1|^2 + a_1^\star d_2 + a_1 d_2^\star)^2 - 4(|a_2 d_1|^2 - a_1 a_2^\star d_1^\star d_2 - a_1^\star a_2 d_1 d_2^\star + |a_1 d_2|^2)}\Big); \\ \lambda^2_{3,4} =& \frac{1}{2}\Big(|b_2|^2 + |h_1|^2 + b_1^\star h_2 + b_1 h_2^\star \\ & \pm\sqrt{(|b_2|^2 + |h_1|^2 + b_1^\star h_2 + b_1 h_2^\star)^2 - 4(|b_2 h_1|^2 - b_1 b_2^\star h_1^\star h_2 - b_1^\star b_2 h_1 h_2^\star + |b_1 h_2|^2)}\Big). \end{aligned} \tag{2.96}$$

Here again note that (from Eq. (2.65)), the density matrix elements $a_1, a_2, d_1 d_2$ contains terms in c^0 and c^2-orders. And the elements b_1, b_2, h_1, h_2 are in c^2-order. Thus the eigenvalue λ_1 (with '+' sgn) will the largest eigenvalue. Thus the concurrence is (using Eq. (2.96))

$$\mathscr{C}(\hat{\rho}) = \max\{0, (\lambda_1 - \lambda_2 - \lambda_3 - \lambda_4)\}. \tag{2.97}$$

For the density matrix in Eq. (2.68), we obtain

$$\begin{aligned} \lambda^2_{1,2} &= c^4(\sqrt{\chi} \pm |\mathscr{E}|)^2; \\ \lambda^2_{3,4} &= c^4(\sqrt{\mathscr{P}_A\mathscr{P}_B} \pm |\mathscr{P}_{AB}|)^2. \end{aligned} \tag{2.98}$$

From the PPT condition in Eq. (2.85), we know that $|\mathscr{E}|$ and $\sqrt{\chi}$ are both greater than $\sqrt{\mathscr{P}_A\mathscr{P}_B}$ and $|\mathscr{P}_{AB}|$, and hence $\sqrt{\mathscr{X}}+|\mathscr{E}| > \sqrt{\mathscr{P}_A\mathscr{P}_B}+|\mathscr{P}_{AB}|$. In this case, the maximal eigenvalue λ_{Max} is found to be $\lambda_1 = c^2(\sqrt{\chi}+|\mathscr{E}|)$. Thus, the concurrence is obtained as [108, 109]

$$\mathscr{C}(\hat{\rho}) = \max\left\{0, 2c^2\left(|\mathscr{E}| - \sqrt{\mathscr{P}_A\mathscr{P}_B}\right)\right\}. \tag{2.99}$$

This tells that two initially non-entangled detector will be entangled if $|\mathscr{E}|$ is greater than $\sqrt{\mathscr{P}_A\mathscr{P}_B}$, where $\mathscr{P}_j$ is transition probability of j^{th} detector. For this reason, the element $\mathscr{E}$ is therefore known as *the entangling term*. The same physics is also described by the negativity condition in Eq. (2.83). However, the negativity condition does not provide any quantitative measure of the entanglement as concurrence. Also the other measure, negativity in Eq. (2.89) has much complicated expression compared to the concurrence. Therefore in the subsequent studies of entanglement harvesting, we will mainly concentrate on the concurrence quantity $\mathscr{C}$. We will study the features of quantum entanglement between the detectors due the effect of different backgrounds and motions of the detectors.

2.6 Conclusion

In this chapter, we provided a brief overview of the key concepts relevant to studying entanglement harvesting or leakage in the presence of a general spacetime background and detector motion. We began by discussing the phenomenon of particle production in the vacuum of quantum fields in curved spacetime and how this effect can be operationally realised using simple quantum systems known as Unruh-DeWitt (UDW) detectors.

We then extended the discussion to a scenario involving two detectors, each locally interacting with the background quantum field. We explored how the interaction with the field drives the evolution of the two-detector system, leading to a final state that emerges from a given initial state of the composite system. Finally, we examined the characterisation and quantification of entanglement in the final state of the two detectors. In the following chapters, we will utilise the generalised expressions developed in this chapter to various physical set-ups.

Appendices

2.A Calculation of Later time density matrix

2.A.1 Calculation of traces of Eq. (2.41)

The trace quantities in Eq. (2.41) are elaborately calculated here.

$$\begin{aligned} Tr_\phi|\Psi\rangle\langle\Psi| &= \sum_n \langle n|\Psi\rangle\langle\Psi|n\rangle = \langle\Psi|\sum_n |n\rangle\langle n|\Psi\rangle = \langle\Psi|\hat{1}|\Psi\rangle \\ &= 1. \end{aligned} \tag{2.A.1}$$

$$\begin{aligned} Tr_\phi\hat{\phi}(x_A)|\Psi\rangle\langle\Psi| &= \sum_n \langle n|\hat{\phi}(x_A)|\Psi\rangle\langle\Psi|n\rangle = \langle\Psi|\sum_n |n\rangle\langle n|\hat{\phi}(x_A)|\Psi\rangle = \langle\Psi|\hat{\phi}(x_A)|\Psi\rangle \\ &= 0; \end{aligned} \tag{2.A.2}$$

$$\begin{aligned} Tr_\phi|\Psi\rangle\langle\Psi|\hat{\phi}(x_A) &= \sum_n \langle n|\Psi\rangle\langle\Psi|\hat{\phi}(x_A)|n\rangle = \langle\Psi|\hat{\phi}(x_A)\sum_n |n\rangle\langle n|\Psi\rangle = \langle\Psi|\hat{\phi}(x_A)|\Psi\rangle \\ &= 0; \end{aligned} \tag{2.A.3}$$

$$\begin{aligned} Tr_\phi\hat{\phi}(x_i)|\Psi\rangle\langle\Psi|\hat{\phi}(x_j) &= \sum_n \langle n|\hat{\phi}(x_i)|\Psi\rangle\langle\Psi|\hat{\phi}(x_j)|n\rangle = \langle\Psi|\hat{\phi}(x_j)\sum_n |n\rangle\langle n|\hat{\phi}(x_i)|\Psi\rangle \\ &= \langle\Psi|\hat{\phi}(x_j)\hat{\phi}(x_i)|\Psi\rangle; \end{aligned} \tag{2.A.4}$$

$$\begin{aligned} Tr_\phi\hat{\phi}(x_i)\hat{\phi}(x_j)|\Psi\rangle\langle\Psi| &= \sum_n \langle n|\hat{\phi}(x_i)\hat{\phi}(x_j)|\Psi\rangle\langle\Psi|n\rangle = \langle\Psi|\sum_n |n\rangle\langle n|\hat{\phi}(x_i)\hat{\phi}(x_j)|\Psi\rangle \\ &= \langle\Psi|\hat{\phi}(x_i)\hat{\phi}(x_j)|\Psi\rangle. \end{aligned} \tag{2.A.5}$$

2.A.2 Calculation of the $\hat{R}^{(1)}$ term:

We consider the initial state of the composite detector system is $|D\rangle = \alpha|g_A g_B\rangle + \gamma|e_A e_B\rangle$. Also the monopole operator is given as $\hat{m}_j(\tau_j) = e^{i\Delta E_j\tau_j}\hat{m}_j(0)e^{-i\Delta E_j\tau_j}$. Using these, one calculate the quantities $\left[\hat{m}_i(\tau_i)|D\rangle\langle D|\hat{m}_j(\tau'_j)\right]$ (with $i,j = A,B$) in Eq. (2.43).

$$\begin{aligned} &\hat{m}_A(\tau_A)|D\rangle\langle D|\hat{m}_A(\tau'_A) \\ &= [\alpha e^{i\Delta E_A\tau_A}|e_A g_B\rangle + \gamma e^{-i\Delta E_A\tau_A}|g_A e_B\rangle][\alpha e^{-i\Delta E_A\tau'_A}\langle e_A g_B| + \gamma e^{i\Delta E_A\tau'_A}\langle g_A e_B|] \\ &= \alpha^2 e^{i\Delta E_A\Delta\tau_A}|e_A g_B\rangle\langle e_A g_B| + \gamma^2 e^{-i\Delta E_A\Delta\tau_A}|g_A e_B\rangle\langle g_A e_B| \\ &\quad + \alpha\gamma(e^{i\Delta E_A(\tau_A+\tau'_A)}|e_A g_B\rangle\langle g_A e_B| + e^{-i\Delta E_A(\tau_A+\tau'_A)}|g_A e_B\rangle\langle e_A g_B|); \end{aligned} \tag{2.A.6}$$

$$\begin{aligned}
&\hat{m}_B(\tau_B)|D\rangle\langle D|\hat{m}_B(\tau'_B)\\
&=[\alpha e^{i\Delta E_B\tau_B}|g_Ae_B\rangle+\gamma e^{-i\Delta E_B\tau_B}|e_Ag_B\rangle][\alpha e^{-i\Delta E_B\tau'_B}\langle g_Ae_B|+\gamma e^{i\Delta E_B\tau'_B}\langle e_Ag_B|]\\
&=\alpha^2e^{i\Delta E_B\Delta\tau_B}|g_Ae_B\rangle\langle g_Ae_B|+\gamma^2e^{-i\Delta E_B\Delta\tau_B}|e_Ag_B\rangle\langle e_Ag_B|\\
&\quad+\alpha\gamma(e^{i\Delta E_B(\tau_B+\tau'_B)}|g_Ae_B\rangle\langle e_Ag_B|+e^{-i\Delta E_B(\tau_B+\tau'_B)}|e_Ag_B\rangle\langle g_Ae_B|);
\end{aligned}\tag{2.A.7}$$

$$\begin{aligned}
&\hat{m}_A(\tau_A)|D\rangle\langle D|\hat{m}_B(\tau'_B)\\
&=[\alpha e^{i\Delta E_A\tau_A}|e_Ag_B\rangle+\gamma e^{-i\Delta E_A\tau_A}|g_Ae_B\rangle][\alpha e^{-i\Delta E_B\tau'_B}\langle g_Ae_B|+\gamma e^{i\Delta E_B\tau'_B}\langle e_Ag_B|]\\
&=\alpha^2e^{i\Delta E_A\tau_A-i\Delta E_B\tau'_B}|e_Ag_B\rangle\langle g_Ae_B|+\gamma^2e^{-i\Delta E_A\tau_A+i\Delta E_B\tau'_B)}|g_Ae_B\rangle\langle e_Ag_B|\\
&\quad+\alpha\gamma(e^{i\Delta E_A\tau_A+i\Delta E_B\tau'_B}|e_Ag_B\rangle\langle e_Ag_B|+e^{-i\Delta E\tau_A-i\Delta E_B\tau'_B}|g_Ae_B\rangle\langle g_Ae_B|);
\end{aligned}\tag{2.A.8}$$

$$\begin{aligned}
&\hat{m}_B(\tau_B)|D\rangle\langle D|\hat{m}_A(\tau'_A)\\
&=[\alpha e^{i\Delta E_B\tau_B}|g_Ae_B\rangle+\gamma e^{-i\Delta E_B\tau_B}|e_Ag_B\rangle][\alpha e^{-i\Delta E_A\tau'_A}\langle e_Ag_B|+\gamma e^{i\Delta E_A\tau'_A}\langle g_Ae_B|]\\
&=\alpha^2e^{i\Delta E_B\tau_B-i\Delta E_A\tau'_A}|g_Ae_B\rangle\langle e_Ag_B|+\gamma^2e^{-i\Delta E_B\tau_B+i\Delta E_A\tau'_A}|e_Ag_B\rangle\langle g_Ae_B|\\
&\quad+\alpha\gamma(e^{i\Delta E_B\tau_B+i\Delta E_A\tau'_A}|g_Ae_B\rangle\langle g_Ae_B|+e^{-i\Delta E_B\tau_B-i\Delta E_A\tau'_A}|e_Ag_B\rangle\langle e_Ag_B|).
\end{aligned}\tag{2.A.9}$$

2.A.3 Calculation of the $\hat{R}^{(2)}$ term:

Here we calculate the quantities $\left[\hat{m}_i(\tau_i)\hat{m}_j(\tau'_j)|D\rangle\langle D|\right]$ (with $i,j=A,B$) in Eq. (2.53).

We use $|D\rangle=\alpha|g_Ag_B\rangle+\gamma|e_Ae_B\rangle$ and $\hat{m}_j(\tau_j)=e^{i\Delta E_j\tau_j}\hat{m}_j(0)e^{-i\Delta E_j\tau_j}$.

$$\begin{aligned}
&\hat{m}_j(\tau_j)\hat{m}_j(\tau'_j)|D\rangle\langle D|\\
&=[\alpha e^{-i\Delta E_j\Delta\tau_j}|g_Ag_B\rangle+\gamma e^{i\Delta E_j\Delta\tau_j}|e_Ae_B\rangle][\alpha\langle g_Ag_B|+\gamma\langle e_Ae_B|]\\
&=\alpha^2e^{-i\Delta E_j\Delta\tau_j}|g_Ag_B\rangle\langle g_Ag_B|+\gamma^2e^{i\Delta E_j\Delta\tau_j}|e_Ae_B\rangle\langle e_Ae_B|\\
&\quad+\alpha\gamma(e^{-i\Delta E_j\Delta\tau_j}|g_Ag_B\rangle\langle e_Ae_B|+e^{i\Delta E_j\Delta\tau_j}|e_Ae_B\rangle\langle g_Ag_B|);
\end{aligned}\tag{2.A.10}$$

$$\begin{aligned}
&\hat{m}_A(\tau_A)\hat{m}_B(\tau_B)|D\rangle\langle D|\\
&=[\alpha e^{i\Delta E_A\tau_A+i\Delta E_B\tau_B}|e_Ae_B\rangle+\gamma e^{-i\Delta E_A\tau_A-i\Delta E_B\tau_B}|g_Ag_B\rangle][\alpha\langle g_Ag_B|+\gamma\langle e_Ae_B|]\\
&=\alpha^2e^{i\Delta E_A\tau_A+i\Delta E_B\tau_B}|e_Ae_B\rangle\langle g_Ag_B|+\gamma^2e^{-i\Delta E_A\tau_A-i\Delta E_B\tau_B}|g_Ag_B\rangle\langle e_Ae_B|\\
&\quad+\alpha\gamma(e^{i\Delta E_A\tau_A+i\Delta E_B\tau_B}|e_Ae_B\rangle\langle e_Ae_B|+e^{-i\Delta E_A\tau_A-i\Delta E_B\tau_B}|g_Ag_B\rangle\langle g_Ag_B|)\\
&=\hat{m}_B(\tau_B)\hat{m}_A(\tau_A)|D\rangle\langle D|.
\end{aligned}\tag{2.A.11}$$

Part II

Entanglement Harvesting

CHAPTER 3

ACCELERATED OBSERVERS IN THERMAL BACKGROUND

3.1 Introduction and Motivation

Accelerated frames are known to mimic features of gravity locally. The quantum theoretical counterpart of this classical equivalence principle is featured by the discovery of the Unruh effect [21, 23], where an accelerated observer perceives a thermal bath of Rindler particles in the Minkowski vacuum. This effect is crucial in understanding the particle content in quantum fields in curved spacetime. It is related to the so-called Hawking radiation [19, 20] through the equivalence principle. The accelerated observer is analogous to the static observer far away from the black hole, and the static observer is analogous to the free-falling observer near the black hole horizon. In this way, detecting the Unruh effect backs the existence of the Hawking effect. Hence it may shed light on the quantum nature of strong gravity. On the other hand, this effect can be understood as a consequence of entangled nature of the Minkowski vacuum state. In Minkowski spacetime, the presence of an accelerated observer divides the whole spacetime into four parts, known as the Rindler wedges. These wedges are right Rindler wedge (RRW), left Rindler wedge (LRW), past Rindler wedge (PRW) and future Rindler wedge (FRW). These wedges are shown in Fig. 3.1. Among these, only RRW and LRW are physically accessible. These two wedges are also causally disconnected. Therefore the quantum fields in these two regions are independent to each other. These two quantum fields are usually expanded in terms of two independent sets of Rindler modes. Vacuum of the Minkowski spacetime can be expressed in terms of left and right Rindler particle

states as [88]

$$|0_M\rangle = \prod_i C_i \sum_{n_i=0}^{\infty} e^{-\frac{\pi n_i \omega_i}{a}} |n_i\rangle_R \otimes |n_i\rangle_L \,, \tag{3.1}$$

where $C_i = \sqrt{1 - e^{-2\pi\omega_i/a}}$. Thus the Minkowski vacuum is an entangled state in terms of field states of two disconnected regions. There have been several studies to understand whether this entanglement can be extracted to two accelerated atoms or UDW detectors through local interaction [99, 107, 113, 118, 210]. In initial works [99, 107] the authors noted that entangle measures depend on quantities estimated from positive frequency Wightman functions connecting different spacetime events of the same or different detectors. However, recent rigorous investigations [108, 109, 113] have suggested proper time ordering into the picture, which resulting in the inception of Feynman propagator rather than Wightman function in estimating the entanglement measures. These recent method described in Chapter 2 provide a meticulous and more general formulation for understanding entanglement harvesting. However, even with these changes, most previous perceptions regarding entanglement extraction corresponding to accelerated observers eternally interacting with the background field – like one can harvest entanglement between two anti-parallelly accelerated detectors but not for parallelly accelerated observers – remain the same. Although, the individual contributions of the retarded Green's function and the Wightman function from the Feynman propagator remain an interesting arena to venture further.

On the other hand, the effects of a thermal bath on entanglement harvesting remain equally interesting (see [211, 212]). In nature, an environment with thermal background is much more practical. Including the thermal nature in the model and investigating the effects in the physical quantities will approach a more realistic situation and thereby help to know the exact features of our surroundings. In this regard, one may mention that the thermal nature of fields has already been included in various investigations related to Unruh-De Witt detectors; like calculation of response functions in case of a single detector, [190, 213–215], and two entangled detectors [216]. In [114, 211, 212] it is predicted that the entanglement extraction gets depleted with increasing temperature of the thermal field. Then it will be pretty fascinating to study the situation of entanglement harvesting for accelerated observers interacting with thermal fields. In this regard, in literature [108, 113] the Feynman propagators and the positive frequency Wightman functions are necessary to understand entanglement extraction, are estimated in the Minkowski position space. Then for the calculations relating to accelerated observers, the relevant transformations to Rindler coordinates are made to those Green's functions,

and this method does not encounter any particular issue. However, consider a similar description of the Feynman propagators and the Wightman functions for thermal fields. The resulting Green's functions do not remain time translational invariant with the detectors' proper times. In [216] the authors have discussed this issue and considered Rindler modes with the vacuum for the Unruh modes to describe the Wightman functions corresponding to accelerated observers in a thermal bath, which are time translational invariant. This method circumvents the previously mentioned issue by expressing the Green's functions in terms of modes and their momentum space integrals rather than a position space representation, in line with the chain of thoughts also presented in [109].

In this chapter, we are going to investigate the condition for entanglement harvesting and study the concurrence [108, 113, 210], a measure of the harvested entanglement, for two accelerated Unruh-DeWitt detectors interacting with a massless thermal scalar field in $(1+1)$ and $(1+3)$ dimensions. In particular, we have considered the interaction between the two-level point-like detectors and the scalar field to be of monopole type as discussed in chapter 2. We consider the detectors to be initially in their ground states and the field state $|\psi\rangle$ to be the Minkowski vacuum. We use the prescription as provided in [216] for the construction of the Green's functions and follow the formulation of articles [108, 113] for entanglement harvesting. We arrive at the same assertions that entanglement extraction is possible only for the anti-parallelly accelerated detectors and not for the parallelly accelerated ones, and also encounter the phenomena of degrading entanglement extraction with increasing temperature of the thermal bath [211, 212]. However, here the situation is a bit more involved as we have observed that this degradation is happening in the low acceleration regimes. Above, a specific value of acceleration thermal bath enhances the entanglement harvesting for the two detectors with an equal magnitude of acceleration in both $(1+1)$ and $(1+3)$ dimensions. Therefore, for the equal magnitude of acceleration case of anti-parallel detectors, a notion of phase transition-like phenomena is encountered around a critical value of acceleration. However, we found that the range of acceleration in which entanglement harvesting is possible is always decreasing with the increasing temperature of the thermal bath. We also observed a non-vanishing contribution coming from the retarded part of the Feynman propagator when the detectors have unequal magnitudes of accelerations. While in $(1+1)$ dimensions, these contributions do not result in any new visible consequence, in $(1+3)$ dimensions, we encounter multiple transition points in accelerations a_A of the detector A, when a_B is fixed. Between these transition points, the nature of the measure of entanglement extraction with the temperature of the thermal bath flips compared to the adjacent

regions. In that case, entanglement harvesting becomes restricted to discrete ranges of acceleration a_A for a certain fixed temperature of the thermal bath, contrary to a single range of a_A for entanglement extraction of $(1+1)$ dimensions. We have also investigated the nature of mutual information $\mathscr{M}$ among the two detectors. We observed that $\mathscr{M}$ is non-vanishing for parallel motion, whereas it vanishes in the anti-parallel situation. For a non-vanishing case, $\mathscr{M}$ increases with the increase in temperature of the background field. On the other hand, it decreases with the growth of acceleration of the first detector.

In Sec. 3.2 we elucidate on accelerated observers in a thermal bath and provide the expressions of the Green's functions for the situation of parallelly and anti-parallelly accelerating observers, considering the Rindler field decomposition with the Unruh operators and Unruh mode vacuum. Subsequently, in Sec. 3.3 the condition for entanglement harvesting is analyzed first for two parallelly and then for two anti-parallelly accelerated observers in a thermal bath using the Green's functions of Sec. 3.2. In this section, we study the entanglement measure concurrence and, in Sec. 3.4 investigate the mutual information between the two detectors to discuss the notable outcomes. We conclude this article in Sec. 5.5 with a discussion of our results.

3.2 Accelerated observers in a thermal bath

This section discusses the relevant coordinate systems for our accelerated observers. We realized that the whole analysis is more convenient under the decomposition of field modes in the Rindler frame and writing the Rindler annihilation and creation operators in terms of those of Unruh modes. Finally, all the required positive frequency Wightman functions, both in $(1+1)$ and $(1+3)$ dimensions, for these fields will be evaluated with respect to the Minkowski vacuum, which is also the vacuum for Unruh modes.

3.2.1 Coordinate systems

The motion of a uniformly accelerated object is described by the Rindler coordinates which correspond to specific regions in the Minkowski spacetime, known as the Riddler wedges [24, 88]. There are four Rindler wedges: *left, right, past* and *future* Rindler wedges. Out of these, only left and right Rindler wedges are physically accessible. One can move to these Rindler coordinates from the Minkowski coordinates (t, x, y, z) in $(1+3)$ dimensions, with the line element

$$ds^2 = -dt^2 + dx^2 + dy^2 + dz^2 \ , \tag{3.2}$$

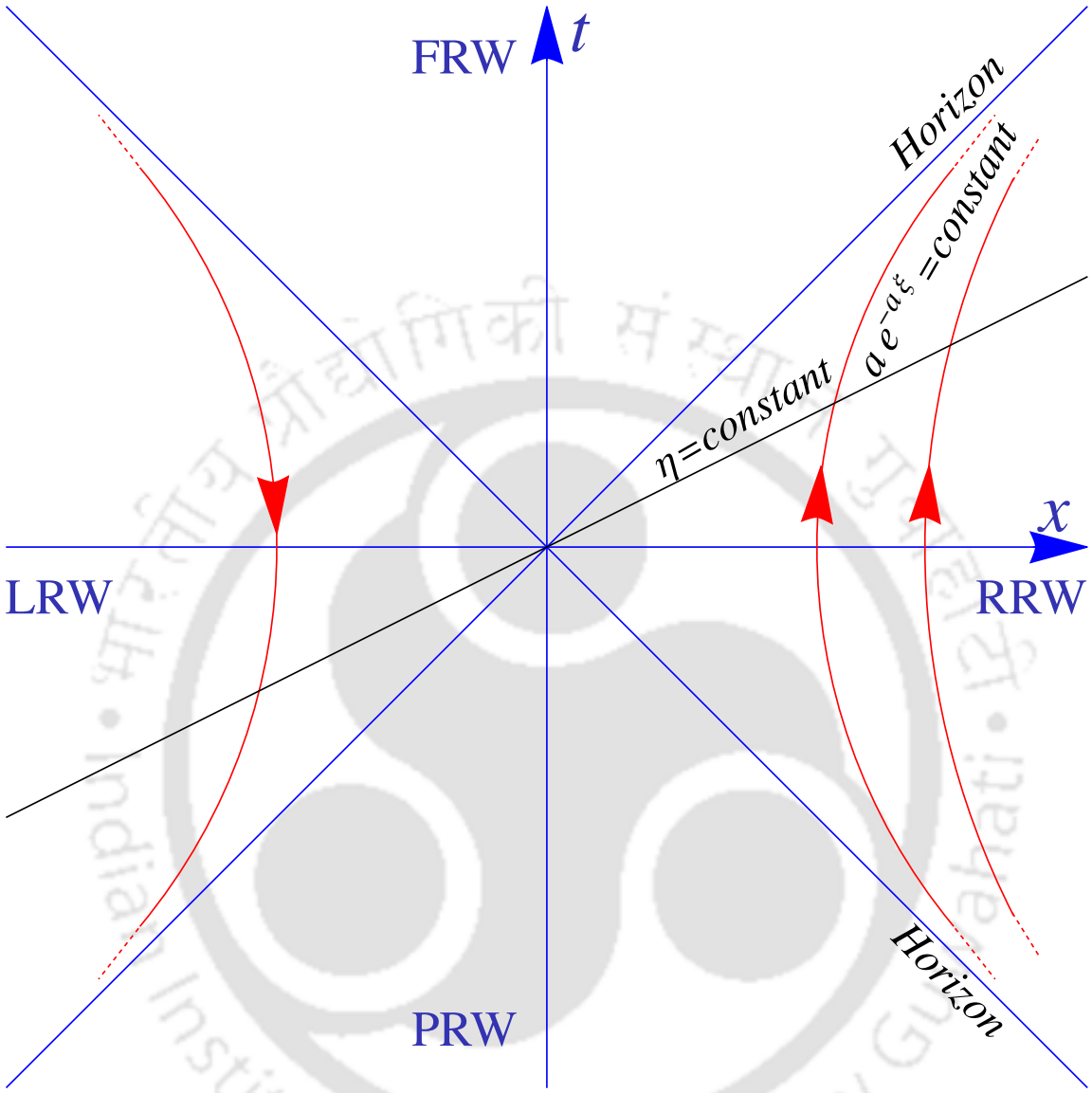

Figure 3.1: Trajectories of accelerated observers confined in right and left Rindler wedges (RRW and LRW).

by a coordinate transformation relating the time t and the spatial direction in which the object is accelerated. Without loss of generality we consider that particular axis of acceleration to be along the x-direction. Then the other two coordinates (y, z) remain unchanged by the Rindler transformation. The transformations to the coordinates (η, ξ) in the right Rindler wedge (RRW), *i.e.,* the region $|t| < x$ in the Minkowski spacetime; and to (η', ξ') in the left Rindler wedge (LRW), confined in a region $|t| < -x$ of the Minkowski

spacetime, are

$$\begin{aligned} t &= \frac{e^{a\xi}}{a}\sinh a\eta, \qquad x = \frac{e^{a\xi}}{a}\cosh a\eta \qquad \text{in RRW ;} \\ t &= -\frac{e^{a\xi'}}{a}\sinh a\eta', \quad x = -\frac{e^{a\xi'}}{a}\cosh a\eta' \qquad \text{in LRW.} \end{aligned} \tag{3.3}$$

Both of these transformations lead to the same line-element corresponding to an accelerated observer in terms of the Rindler coordinates, expressed as

$$ds^2 = e^{2a\xi}\left[-d\eta^2 + d\xi^2\right] + dy^2 + dz^2 \,. \tag{3.4}$$

One can perceive that these transformations in $(1+1)$ dimensions are trivially same as in that case the coordinates (y, z) cease to exist. In RRW and LRW one can estimate the proper times and proper accelerations to be

$$\begin{aligned} \tau &= e^{a\xi}\eta, \qquad b = ae^{-a\xi} \qquad \text{in RRW ;} \\ \tau' &= -e^{a\xi'}\eta', \quad b' = ae^{-a\xi'} \qquad \text{in LRW .} \end{aligned} \tag{3.5}$$

Then the coordinate transformations in Eq. (3.3) in terms of proper time and acceleration become

$$\begin{aligned} t &= \frac{1}{b}\sinh b\tau, \qquad x = \frac{1}{b}\cosh b\tau \qquad \text{in RRW;} \\ t &= \frac{1}{b'}\sinh b'\tau', \quad x = -\frac{1}{b'}\cosh b'\tau' \qquad \text{in LRW.} \end{aligned} \tag{3.6}$$

One can notice that η, $-\eta'$ denote the proper times in RRW and LRW respectively while a is the proper acceleration of the observer when $\xi = 0 = \xi'$. If both the detectors are moving in same Rindler wedge, we call this as the parallel motion. While one detector is moving in RRW and other one in LRW, we refer this as anti-parallel motion. The trajectories are shown in Fig. 3.1, where (y, z) coordinates are suppressed.

These right and left Rindler wedges (RRW and LRW) are two causally disconnected regions in global Minkowski spacetime, separated by two Rindler horizons (see Fig. 3.1). No event in one wedge can be witnessed in the other wedge. Since the Pauli-Jordan function, $i\Delta(x-y) = [\hat{\phi}(x), \hat{\phi}^\dagger(y)]$ vanishes for any spacelike intervals, the quantum fields in these wedges behave as two independent quantum fields [24]. These two quantum fields are usually expanded in terms of two independent sets of Rindler modes. One set of modes is only confined to RRW, and the other is confined to LRW. These quantum fields in RRW and LRW have their own vacuum states (known as Rindler vacuums), which are physically inequivalent to the Minkowski vacuum. Thus, an accelerated observer in RRW (LRW) does not see particles in the right (left) Rindler vacuum but in the Minkowski vacuum. This phenomenon is known as the Unruh effect [23, 87].

3.2.2 Scalar field decomposition corresponding to an accelerated observer

To understand the effect of temperature in accelerated systems, one usually utilises the Minkowski mode decomposition of the quantum fields. One can consider expressing the thermal two-point function in terms of the Minkowski modes and then make the Rindler coordinate transformation from Eq. (3.6). Or one can express the Rindler modes in terms of the Minkowski modes or vice versa, using the Bogoliubov coefficients [88]. Here, the positive frequency Minkowski modes combine the Rindler modes with both positive and negative frequencies. Therefore, the Wightman functions are not time translational invariance in Rindler time [216]. In this situation, the system does not remain in equilibrium. To avoid this situation, one can use the Unruh modes [23, 24], which are constructed as linear combinations of Rindler modes such that positive and negative frequencies do not mix. These modes are also analytic in the whole Minkowski spacetime. Alternatively, one can express the Rindler creation and annihilation operators as linear combinations of the Unruh operators. Therefore, one can write two quantum fields in RRW and LRW in terms of the Unruh operators. Note that the Unruh quantisation [23] is established such that the Unruh annihilation operators can annihilate the Minkowski vacuum state ($\hat{d}_k^{1,2}|0_M\rangle = 0$). Therefore, the Minkowski vacuum is the vacuum for both Minkowski and Unruh fields. However, the Unruh and Minkowski particles are not equivalent, even though they are excitations of the same vacuum [88]. To construct the thermal Wightman functions, thermal ensemble average will be done utilising the Unruh quantization. The thermal ensemble average of an observable $\hat{\phi}(x)\hat{\phi}(x')$ at inverse temperature β will consist the expectation value the observable over all possible Unruh particle states (including the Unruh vacuum), weighted by their Boltzmann factors (we will discuss this elaborately in the later subsection). Hence, the thermal bath here is an Unruh thermal bath, not a Minkowski thermal bath. However, this way of construction preserves the proper time translation invariance, unlike the Minkowski thermal bath [217]. Here we also mention that in $\beta \to \infty$ limit, the thermal this ensemble average will have only non-zero contribution from the Unruh vacuum (equivalently, Minkowski vacuum), then the Wightman function will be equivalent to non-thermal Minkowski Wightman function.

The procedure of decomposing the scalar field in terms of the Unruh operators is elaborately discussed in [24, 218]. Here we give a brief recollection of the construction and refer to the article [216] for further understandings. We first consider the case in

$(1+1)$ dimensions and the $(1+3)$ dimensional result will follow accordingly. The equation of motion for a minimally coupled, massless free scalar field ϕ is expressed as $\Box\phi = 0$.

3.2.2.1 $(1+1)$ dimensions

In terms of the Rindler coordinates in $(1+1)$ dimensions this equation has solutions, suggesting set of modes in the right and left Rindler wedges as [24, 218]

$$\begin{aligned} {}^{R}u_k &= \frac{1}{\sqrt{4\pi\omega}} e^{ik\xi - i\omega\eta} && \text{in RRW} \\ &= 0 && \text{in LRW}\,, \\ {}^{L}u_k &= \frac{1}{\sqrt{4\pi\omega}} e^{ik\xi + i\omega\eta} && \text{in LRW} \\ &= 0 && \text{in RRW.} \end{aligned} \tag{3.7}$$

The scalar field is expressed in terms of the Rindler modes and operators, see [24], as $\hat{\phi}(x) = \sum_{k=-\infty}^{\infty}\left[\hat{b}_k^R\, {}^{R}u_k + \hat{b}_k^{R^\dagger}\, {}^{R}u_k^\star + \hat{b}_k^L\, {}^{L}u_k + \hat{b}_k^{L^\dagger}\, {}^{L}u_k^\star\right]$, where superscript L and R correspond to the left and the right Rindler wedges respectively, and the annihilation operators annihilate the Rindler vacuum $|0_R\rangle$, *i.e.,* $\hat{b}_k^R|0_R\rangle = 0 = \hat{b}_k^L|0_R\rangle$. In the right or left Rindler wedges where the field modes ${}^{L}u_k = 0$ or ${}^{R}u_k = 0$, the scalar field takes the form

$$\begin{aligned} \hat{\phi}^R(x) &= \sum_{k=-\infty}^{\infty}\left[\hat{b}_k^R\, {}^{R}u_k + \hat{b}_k^{R^\dagger}\, {}^{R}u_k^\star\right]\,, \\ \text{or} \qquad \hat{\phi}^L(x) &= \sum_{k=-\infty}^{\infty}\left[\hat{b}_k^L\, {}^{L}u_k + \hat{b}_k^{L^\dagger}\, {}^{L}u_k^\star\right]\,. \end{aligned} \tag{3.8}$$

One can use this scalar field decomposition in terms of the Rindler modes and operators to obtain a two-point function corresponding to an accelerated observer in Minkowski vacuum. Here, it should be noted that the operators $\hat{b}_k^R$ and $\hat{b}_k^L$ in Eq. (3.8) do not annihilate the Minkowski vacuum, and the operations of the Rindler ladder operators on the Minkowski vacuum is obtained from the cumbersome calculations of Bogoliubov transformation. However, there is a simpler way out of this situation as provided by Unruh [23] in 1976, where he prescribed field modes out of these Rindler modes which are analytic in the whole region of the Minkowski spacetime. These Unruh modes have the positive frequency analyticity property with respect to the Minkowski time, same as the Minkowski modes. This enables one to decompose the scalar field in terms of these Unruh modes and operators, which annihilate the Minkowski vacuum. The Unruh modes are obtained from the combination of the Rindler modes ${}^{R}u_k + e^{-\pi\omega/a}\, {}^{L}u_{-k}^*$ and ${}^{R}u_{-k}^* + e^{\pi\omega/a}\, {}^{L}u_k$, see [24]. In terms of the Unruh modes and operators the scalar field is

expressed as [24]

$$\hat{\phi}(x)=\sum_{k=-\infty}^{\infty}\frac{1}{\sqrt{2\sinh\frac{\pi\omega}{a}}}\left[\hat{d}_k^1\left(e^{\frac{\pi\omega}{2a}}\,{}^R u_k+e^{-\frac{\pi\omega}{2a}}\,{}^L u_{-k}^{\star}\right)+\hat{d}_k^2\left(e^{-\frac{\pi\omega}{2a}}\,{}^R u_{-k}^{\star}+e^{\frac{\pi\omega}{2a}}\,{}^L u_k\right)\right]+h.c.\,, \tag{3.9}$$

where $h.c.$ stands for Hermitian conjugate. The Unruh annihilation operators annihilate the Minkowski vacuum $\hat{d}_k^1|0_M\rangle=\hat{d}_k^2|0_M\rangle=0$. To obtain the positive frequency Green's function using the field decompositions of Eq. (3.8), one needs a transformation between the Rindler operators and the Unruh operators, see [24], which is

$$\begin{aligned}\hat{b}_k^R&=\frac{1}{\sqrt{2\sinh\frac{\pi\omega}{a}}}\left[e^{\frac{\pi\omega}{2a}}\hat{d}_k^1+e^{-\frac{\pi\omega}{2a}}\hat{d}_{-k}^{2^\dagger}\right]\,,\\ \hat{b}_k^L&=\frac{1}{\sqrt{2\sinh\frac{\pi\omega}{a}}}\left[e^{\frac{\pi\omega}{2a}}\hat{d}_k^2+e^{-\frac{\pi\omega}{2a}}\hat{d}_{-k}^{1^\dagger}\right],\end{aligned} \tag{3.10}$$

and, it is similar to the Bogoliubov transformation. Then putting this transformation in Eq. (3.8) one can get the expression of the field in the RRW and LRW in terms of the Unruh operators as

$$\begin{aligned}\hat{\phi}^R(x)&=\sum_{k=-\infty}^{\infty}\frac{1}{\sqrt{2\sinh\frac{\pi\omega}{a}}}\left[\hat{d}_k^1\,e^{\frac{\pi\omega}{2a}}\,{}^R u_k+\hat{d}_k^2\,e^{-\frac{\pi\omega}{2a}}\,{}^R u_{-k}^{\star}\right]+h.c.\,,\\ \hat{\phi}^L(x)&=\sum_{k=-\infty}^{\infty}\frac{1}{\sqrt{2\sinh\frac{\pi\omega}{a}}}\left[\hat{d}_k^1 e^{-\frac{\pi\omega}{2a}}\,{}^L u_{-k}^{\star}+\hat{d}_k^2 e^{\frac{\pi\omega}{2a}}\,{}^L u_k\right]+h.c.\,.\end{aligned} \tag{3.11}$$

Now these expression of the scalar fields in RRW and LRW can be used to obtain the expressions of the positive frequency Wightman function corresponding to accelerated observers in thermal bath.

3.2.2.2 $(1+3)$ dimensions

Like the above analysis, in $(1+3)$ dimensions also, one can proceed in a similar manner to get the Scalar field in terms of the Unruh operators. In particular, from the equation of motion $\Box\phi=0$ one can get the Rindler modes in the right and the left Rindler wedges as

$$\begin{aligned}{}^R u_{\omega,\mathbf{k}_\perp}&=\frac{1}{2\pi^2}\sqrt{\frac{\sinh\left(\frac{\pi\omega}{a}\right)}{a}}\,\mathcal{K}\left[\frac{i\omega}{a},\frac{|k_p|e^{a\xi}}{a}\right]e^{-i\omega\eta+i\mathbf{k}_\perp\cdot\mathbf{x}_\perp} && \text{in RRW}\\ &=0 && \text{in LRW,}\\ {}^L u_{\omega,\mathbf{k}_\perp}&=\frac{1}{2\pi^2}\sqrt{\frac{\sinh\left(\frac{\pi\omega}{a}\right)}{a}}\,\mathcal{K}\left[\frac{i\omega}{a},\frac{|k_p|e^{a\xi}}{a}\right]e^{i\omega\eta+i\mathbf{k}_\perp\cdot\mathbf{x}_\perp} && \text{in LRW}\\ &=0 && \text{in RRW}\,,\end{aligned} \tag{3.12}$$

where, $\mathcal{K}[n,z]$ denotes the modified Bessel function of the second kind of order n, and $\mathbf{x}_\perp$ is perpendicular to the direction of acceleration, *i.e.,* in the $y-z$ plane, see [88, 90, 219], and $\mathbf{k}_\perp$ denotes the transverse wave vector in the $y-z$ plane. Like the $(1+1)$ dimensional case here also one can construct the Unruh modes [88] out of the Rindler modes, which are analytic in the whole Minkowski spacetime and gives positive frequency mode solutions with respect to the Minkowski time. Then in $(1+3)$ dimensions the scalar field in the RRW and LRW using the Unruh operators, see [88, 216] for a detailed description, can be expressed in forms

$$\hat{\phi}^R(x) = \sum_{\omega=0}^{\infty}\sum_{\mathbf{k}_\perp=-\infty}^{\infty} \frac{1}{\sqrt{2\sinh\frac{\pi\omega}{a}}}\left[\hat{d}^1_{\omega,\mathbf{k}_\perp} e^{\frac{\pi\omega}{2a}} {}^R u_{\omega,\mathbf{k}_\perp} + \hat{d}^2_{\omega,\mathbf{k}_\perp} e^{-\frac{\pi\omega}{2a}} {}^R u^\star_{\omega,-\mathbf{k}_\perp}\right] + h.c.\,,$$
$$\hat{\phi}^L(x) = \sum_{\omega=0}^{\infty}\sum_{\mathbf{k}_\perp=-\infty}^{\infty} \frac{1}{\sqrt{2\sinh\frac{\pi\omega}{a}}}\left[\hat{d}^1_{\omega,\mathbf{k}_\perp} e^{-\frac{\pi\omega}{2a}} {}^L u^\star_{\omega,-\mathbf{k}_\perp} + \hat{d}^2_{\omega,\mathbf{k}_\perp} e^{\frac{\pi\omega}{2a}} {}^L u_{\omega,\mathbf{k}_\perp}\right] + h.c. \quad (3.13)$$

This is exactly same as the $(1+1)$ dimensional expression with the Rindler field modes ${}^R u_{\omega,\mathbf{k}_\perp}$ and ${}^L u_{\omega,\mathbf{k}_\perp}$ are now given by different expressions, and the sum is now on ω and two components of $\mathbf{k}_\perp$ rather than one wave vector k of the $(1+1)$ dimensional case.

3.2.3 Two-point correlators for thermal field

Considering a scalar field $\hat{\phi}(x) = \hat{\phi}(t,\mathbf{x})$ in equilibrium with a thermal bath of temperature $T^{(f)} = 1/(k_B\beta)$, where k_B is the *Boltzmann constant* ($k_B = 1$ for our analysis), the thermal Green's (Wightman) function can be obtained by taking Gibbs ensemble average of the operator $\hat{\phi}(x_2)\hat{\phi}(x_1)$ as

$$\begin{aligned} G^\beta(x_2;x_1) &= \langle\hat{\phi}(x_2)\hat{\phi}(x_1)\rangle_\beta \\ &= \frac{1}{Z}\,\mathrm{Tr}\left[e^{-\beta\hat{H}}\hat{\phi}(x_2)\hat{\phi}(x_1)\right], \end{aligned} \quad (3.14)$$

where, x_1 and x_2 are two events in the spacetime, $Z = \mathrm{Tr}[\exp(-\beta\hat{H})]$ denotes the partition function, and $\hat{H}$ denotes the Hamiltonian of free massless scalar field.

3.2.3.1 $(1+1)$-dimensions

In $(1+1)$ dimensions to obtain the thermal Green's function corresponding to accelerated observers, with respect to Rindler modes, we consider massless scalar field where $\omega = \omega_k = |k|$. The Hamiltonian related to the k^{th} excitation corresponding to the Unruh operators, which respect the Unruh vacuum, is $\hat{H}_k = \left(\hat{d}^{1^\dagger}_k \hat{d}^1_k + \hat{d}^{2^\dagger}_k \hat{d}^2_k\right)\omega$. To calculate the trace in Eq. (3.14), we will utilise the Unruh particle states and express the observable

Rindler fields $(\hat{\phi}(x_2)\hat{\phi}(x_1))$ in terms of Unruh operators. Using the above Hamiltonian one will obtain the trace as $\mathrm{Tr}[e^{-\beta\hat{H}}\hat{d}_k^{1,2\dagger}\hat{d}_k^{1,2}]/Z = 1/(e^{\beta\omega}-1)$. Then the thermal Green's function, defined by Eq. (3.14), corresponding to an accelerated observer, see [216], can be expressed as

$$
\begin{aligned}
&G^{\beta}_{W_R}\left(\Delta\xi_{jl},\Delta\eta_{jl}\right)\\
&=\langle 0_M|\hat{\phi}^R(x)\hat{\phi}^R(x')|0_M\rangle_\beta\\
&=\int_{-\infty}^{\infty}\frac{dk}{8\pi\omega\sqrt{\sinh\frac{\pi\omega}{a_j}\sinh\frac{\pi\omega}{a_l}}}\times\\
&\left[\frac{1}{1-e^{-\beta\omega}}\left\{e^{ik\Delta\xi_{jl}-i\omega\Delta\eta_{jl}}\;e^{\frac{\pi\omega}{2}\left(\frac{1}{a_j}+\frac{1}{a_l}\right)}+e^{ik\Delta\xi_{jl}+i\omega\Delta\eta_{jl}}\;e^{-\frac{\pi\omega}{2}\left(\frac{1}{a_j}+\frac{1}{a_l}\right)}\right\}\right.\\
&\left.+\frac{1}{e^{\beta\omega}-1}\left\{e^{-ik\Delta\xi_{jl}+i\omega\Delta\eta_{jl}}\;e^{\frac{\pi\omega}{2}\left(\frac{1}{a_j}+\frac{1}{a_l}\right)}+e^{-ik\Delta\xi_{jl}-i\omega\Delta\eta_{jl}}\;e^{-\frac{\pi\omega}{2}\left(\frac{1}{a_j}+\frac{1}{a_l}\right)}\right\}\right],
\end{aligned}
\tag{3.15}
$$

where, j, l denote different detectors, and $\Delta\xi_{jl}=\xi_{j,2}-\xi_{l,1}$, $\Delta\eta_{jl}=\eta_{j,2}-\eta_{l,1}$. For observers in the left Rindler wedge immersed in a thermal bath the Wightman function $G^{\beta}_{W_L}\left(\Delta\xi_{jl},\Delta\eta_{jl}\right)$ is obtained from the expression of Eq. (3.15) with $\Delta\eta_{jl}\to-\Delta\eta_{jl}$.

Similarly for observers with one in the right Rindler wedge and one in the left Rindler wedge immersed in a thermal bath the Wightman function can be expressed, using the appropriate field modes from Eq. (3.11), as

$$
\begin{aligned}
&G^{\beta}_{W_{LR}}\left(\Delta\xi_{jl},\Delta\eta_{jl}\right)\\
&=\langle 0_M|\hat{\phi}^L(x)\hat{\phi}^R(x')|0_M\rangle_\beta\\
&=\int_{-\infty}^{\infty}\frac{dk}{8\pi\omega\sqrt{\sinh\frac{\pi\omega}{a_j}\sinh\frac{\pi\omega_k}{a_l}}}\times\\
&\left[\frac{1}{1-e^{-\beta\omega}}\left\{e^{ik\Delta\xi_{jl}-i\omega\Delta\eta_{jl}}\;e^{-\frac{\pi\omega}{2}\left(\frac{1}{a_j}-\frac{1}{a_l}\right)}+e^{ik\Delta\xi_{jl}+i\omega\Delta\eta_{jl}}\;e^{\frac{\pi\omega}{2}\left(\frac{1}{a_j}-\frac{1}{a_l}\right)}\right\}\right.\\
&\left.+\frac{1}{e^{\beta\omega}-1}\left\{e^{-ik\Delta\xi_{jl}+i\omega\Delta\eta_{jl}}\;e^{-\frac{\pi\omega}{2}\left(\frac{1}{a_j}-\frac{1}{a_l}\right)}+e^{-ik\Delta\xi_{jl}-i\omega\Delta\eta_{jl}}\;e^{\frac{\pi\omega}{2}\left(\frac{1}{a_j}-\frac{1}{a_l}\right)}\right\}\right],
\end{aligned}
\tag{3.16}
$$

where, we have considered the j^{th} detector to be in the left Rindler wedge and the detector denoted by l is in the right Rindler wedge. We also mention that the Wightman function $G^{\beta}_{W_{RL}}\left(\Delta\xi_{jl},\Delta\eta_{jl}\right)$, where the detectors denoted by j and l are in right and left Rindler wedges is obtained from the complex conjugate of the expression in the right hand side of Eq. (3.16). It should be noted that from Eq. (3.15) the thermal Green's function corresponding to a single accelerated detector can also be obtained by making $a_j=a_l$.

3.2.3.2 $(1+3)$ dimensions

One can obtain the thermal Green's function corresponding to accelerated observers, with respect to Rindler modes in $(1+3)$ dimensions in a similar manner. The field decomposition is taken from Eq. (3.13) and the Hamiltonian corresponding to the Unruh operators is $\hat{H}_{\omega,k_p} = \left(\hat{d}^{1^\dagger}_{\omega,\mathbf{k}_\perp}\hat{d}^{1}_{\omega,\mathbf{k}_\perp} + \hat{d}^{2^\dagger}_{\omega,\mathbf{k}_\perp}\hat{d}^{2}_{\omega,\mathbf{k}_\perp}\right)\omega$. For simplicity, we consider $\Delta\mathbf{x}_\perp = 0$. Then in RRW the Green's function corresponding to an accelerated observer in thermal bath [216] is

$$G^{\beta}_{W^{3D}_{R}}(\Delta\eta_{jl}) = \int_0^\infty d\omega \int \frac{d^2k_p}{(2\pi)^4}\frac{2}{\sqrt{a_j a_l}}\times \left[\frac{e^{-i\omega\Delta\eta_{jl}}\, e^{\frac{\pi\omega}{2}\left(\frac{1}{a_j}+\frac{1}{a_l}\right)} + e^{i\omega\Delta\eta_{jl}}\, e^{-\frac{\pi\omega}{2}\left(\frac{1}{a_j}+\frac{1}{a_l}\right)}}{1-e^{-\beta\omega}} + \frac{e^{i\omega\Delta\eta_{jl}}\, e^{\frac{\pi\omega}{2}\left(\frac{1}{a_j}+\frac{1}{a_l}\right)} + e^{-i\omega\Delta\eta_{jl}}\, e^{-\frac{\pi\omega}{2}\left(\frac{1}{a_j}+\frac{1}{a_l}\right)}}{e^{\beta\omega}-1}\right] \times \mathcal{K}\left[\frac{i\omega}{a_j}, \frac{|k_p|e^{a_j\xi_j}}{a_j}\right]\mathcal{K}\left[\frac{i\omega}{a_l}, \frac{|k_p|e^{a_l\xi_l}}{a_l}\right], \tag{3.17}$$

where, $\Delta\eta_{jl} = \eta_{j,2} - \eta_{l,1}$ and ξ_j is the fixed Rindler spatial coordinate corresponding to the j^{th} detector. It should be noted that the above Green's function is time translational invariant.

On the other hand, the Wightman function corresponding to two observers with anti-parallel acceleration is

$$G^{\beta}_{W^{3D}_{LR}}(\Delta\eta_{jl}) = \int_0^\infty d\omega \int \frac{d^2k_p}{(2\pi)^4}\frac{2}{\sqrt{a_j a_l}}\times \left[\frac{e^{-i\omega\Delta\eta_{jl}}\, e^{-\frac{\pi\omega}{2}\left(\frac{1}{a_j}-\frac{1}{a_l}\right)} + e^{i\omega\Delta\eta_{jl}}\, e^{\frac{\pi\omega}{2}\left(\frac{1}{a_j}-\frac{1}{a_l}\right)}}{1-e^{-\beta\omega}} + \frac{e^{i\omega\Delta\eta_{jl}}\, e^{-\frac{\pi\omega}{2}\left(\frac{1}{a_j}-\frac{1}{a_l}\right)} + e^{-i\omega\Delta\eta_{jl}}\, e^{\frac{\pi\omega}{2}\left(\frac{1}{a_j}-\frac{1}{a_l}\right)}}{e^{\beta\omega}-1}\right] \times \mathcal{K}\left[\frac{i\omega}{a_j}, \frac{|k_p|e^{a_j\xi_j}}{a_j}\right]\mathcal{K}\left[\frac{i\omega}{a_l}, \frac{|k_p|e^{a_l\xi_l}}{a_l}\right]. \tag{3.18}$$

Here also j and l denote detectors in left and in right Rindler wedges, and the Wightman function $G^{\beta}_{W^{3D}_{RL}}(\Delta\xi_{jl}, \Delta\eta_{jl})$, with j and l denoting detectors in right and left Rindler wedges, is obtained from the complex conjugate of the expression in Eq. (3.18). The thermal Green's function corresponding to a single accelerated detector can be obtained by making $a_j = a_l$ in Eq. (3.17).

Having equipped with all the necessary results we will next investigate the role of temperature of the field on the entanglement harvesting between the two uniformly

accelerated detectors. We will have particular interest here on two situations – (i) both the detectors are in right wedge and (ii) one is in right wedge and another one is in left wedge. This will be done in the next section.

3.3 Entanglement harvesting

We Have already discussed the formalism for entanglement harvesting in Chapter 2, which was originally introduced in [108, 109]. In this study, we consider the detectors are in their ground states *i.e.,* $|D\rangle = |g_A\, g_B\rangle$ and the background field is in the Minkowski vacuum state. Therefore, the final density matrix is given by the matrix in Eq. (2.68). The elements of the density matrix in terms of the Minkowski vacuum can be expressed as (from Eqs. (2.46), (2.49) and (2.59))

$$\mathscr{P}_j(\Delta E) = \iint d\tau_j d\tau'_j\, e^{i\Delta E_j(\tau'_j-\tau_j)} G_W(x_j,x'_j), \tag{3.19}$$

$$\mathscr{P}_{AB}(\Delta E) = \iint d\tau_A d\tau_B\, e^{i\Delta E_A\tau_A - i\Delta E_B\tau_B} G_W(x_B,x_A), \tag{3.20}$$

$$\mathscr{E}(\Delta E) = -\iint d\tau_A d\tau_B\, e^{i\Delta E_A\tau_A + i\Delta E_B\tau_B} \{i\,G_F(x_B,x_A)\}. \tag{3.21}$$

Here in these expressions, we set the switching functions $\chi_j(\tau_j) = 1$; i.e. the detectors are interacting with the background field all the time. On the other hand, the quantities $G_W(x_i,x_j)$ and $G_F(x_i,x_j)$ denote the positive frequency Wightman function with $t_i > t_j$ and the Feynman propagator, respectively. Their expressions are

$$\begin{aligned} G_W\left(x_i,x_j\right) &\equiv \langle 0_M|\hat{\phi}(x_i)\hat{\phi}\left(x_j\right)|0_M\rangle\ , \\ i\,G_F\left(x_I,x_j\right) &\equiv \langle 0_M|T\left\{\hat{\phi}(x_i)\hat{\phi}\left(x_j\right)\right\}|0_M\rangle \\ &= \theta\left(t_i-t_j\right) G_W\left(x_i,x_j\right) + \theta(t_j-t_i) G_W\left(x_j,x_i\right)\ . \end{aligned} \tag{3.22}$$

Now one can re-express the Feynman propagator as $iG_F\left(x_i,x_j\right) = G_W\left(x_i,x_j\right) + \theta(t_j - t_i)\left\{G_W\left(x_j,x_i\right) - G_W\left(x_i,x_j\right)\right\}$ to simplify the calculation of the integral $\mathscr{E}$. The quantity $\theta(t_j-t_i)\left\{G_W\left(x_j,x_i\right) - G_W\left(x_i,x_j\right)\right\}$ is known as the retarded greens function $iG_R\left(x_j,x_i\right)$. We can now express this integral as

$$\mathscr{E} = -\int_{-\infty}^{\infty} d\tau_B \int_{-\infty}^{\infty} d\tau_A\, e^{i(\Delta E^B\tau_B + \Delta E^A\tau_A)}[G_W(x_B,x_A) + \theta(t_A-t_B)\{G_W(x_A,x_B) - G_W(x_B,x_A)\}]. \tag{3.23}$$

However, for verification of the condition in Eq. (2.83) for entanglement harvesting, we only need to evaluate the transition probability and the entangling term ($\mathscr{P}_j$ and $\mathscr{E}$). If

this condition ($\mathscr{P}_A\mathscr{P}_B < |\mathscr{E}|^2$) is satisfied, then we can study the entanglement measures: negativity (see Eq. (2.89)) or concurrence (see Eq. (2.99)). This quantities also depends on only $\mathscr{P}_j$ and $\mathscr{E}$. In this analysis, we will only study the concurrence quantity. Since we are interested to the entanglement between the detectors due to motion of the detectors and background temperature, it is only relevant to study the nature of the quantity

$$\mathscr{C}_{\mathscr{J}} = \left(|\mathscr{E}| - \sqrt{\mathscr{P}_A\mathscr{P}_B}\right). \tag{3.24}$$

Particularly, by this we will be investigating the nature of entanglement harvesting with respect to different parameters of our system.

3.3.1 Transition probability

In this subsection, we will calculate the transition probability in Eq. (3.19) in both $(1+1)$ and $(1+3)$ dimensions. Due to our choice $\xi'_j = 0 = \xi_j$, from Eq. (3.5) we have $\eta'_j = \tau'_j$, $\eta_j = \tau_j$. We consider the change of variables $v_j = \tau'_j + \tau_j$, $u_j = \tau_j - \tau'_j = \Delta\eta_j$. Jacobian for this transformation is obtained as 1/2. Thus from Eq. (3.19) and (3.15), we obtain

$$\mathscr{P}_j(\Delta E^j) = \frac{1}{2}\int_{-\infty}^{\infty} dv_j \int_{-\infty}^{\infty} du_j e^{-i\Delta E^j u_j} \int_{-\infty}^{\infty} \frac{dk}{8\pi\omega \sinh\frac{\pi\omega}{a_j}} \times \left[\frac{1}{1-e^{-\beta\omega}}\left\{e^{-i\omega u_j}\, e^{\frac{\pi\omega}{a_j}} + e^{i\omega u_j}\, e^{-\frac{\pi\omega}{2a_j}}\right\} + \frac{1}{e^{\beta\omega}-1}\left\{e^{i\omega u_j}\, e^{\frac{\pi\omega}{2a_j}} + e^{-i\omega u_j}\, e^{-\frac{\pi\omega}{2a_j}}\right\}\right] \tag{3.25}$$

To evaluate the u_j-integral we utilise the following relation

$$\frac{1}{2\pi}\int_{-\infty}^{\infty} dq\, e^{i(\Delta E \pm \omega)q} = \delta(\Delta E \pm \omega). \tag{3.26}$$

Then the k-integral can be performed easily. Since both ΔE^j and ω are positive quantities, terms with $\delta(\Delta E^j + \omega)$ will vanish. Another Dirac delta function will be obtained as $(1/2\pi)\int_{-\infty}^{\infty} d\gamma_j = \delta(0)$, where $\gamma_j = a_j v_j$ is a dimensionless parameter characterising the proper time of the detector. Therefore we obtain

$$\mathscr{P}_j(\Delta E^j) = \delta(0)\frac{\pi}{2\Delta E^j a_j}\frac{1}{\sinh\frac{\pi\Delta E^j}{a_j}}\left[\frac{e^{-\frac{\pi\Delta E^j}{a_j}}}{1-e^{-\beta\Delta E^j}} + \frac{e^{\frac{\pi\Delta E^j}{a_j}}}{e^{\beta\Delta E^j}-1}\right]. \tag{3.27}$$

On the other hand, in a similar manner in LRW also one can estimate the integral $\mathscr{P}_j(\Delta E^j)$ using the complex conjugate of the Wightman function from Eq. (3.15). Note that the complex conjugate of the Wightman function with $\xi'_j = 0 = \xi_j$ and $\eta'_j = -\tau'_j$, $\eta_j = -\tau_j$ is same as the Wightman function in RRW *i.e.*, $\left(G^{\beta}_{W_R}(\Delta\eta_j)\right)^{\star} = G^{\beta}_{W_L}(u_j)$ with

$\Delta\eta_j = -u_j$ (in LRW). Thus in $(1+1)$ dimensions this expression comes out to be the same as the one obtained for the observer in RRW (Eq. (3.25)), i.e., we get $\mathscr{P}_j^L(\Delta E^j) = \mathscr{P}_j^R(\Delta E^j)$.

Similarly, in $(1+3)$ dimensions also one can find out the quantities $\mathscr{P}_j^R(\Delta E^j)$ and $\mathscr{P}_j^L(\Delta E^j)$ using the Wightman function from Eq. (3.17). Here again, we first evaluate u_j-integral using Eq. (3.26) to get $\delta(\Delta E^j \pm \omega)$, which get integrated in ω-integral. Since the integrand is independent of v_j, the v_j-integration gives $\delta(0)$. We finally obtain

$$\begin{aligned}\mathscr{P}_j(\Delta E^j) &= \frac{1}{2}\int_{-\infty}^{\infty} dv_j \int_{-\infty}^{\infty} du_j\, e^{-i\Delta E^j u_j}\, G^{\beta}_{W_{3D}}(u_j) \\ &= \delta(0)\frac{1}{2\pi a_j^2}\left[\frac{e^{-\frac{\pi\Delta E^j}{a_j}}}{1-e^{-\beta\Delta E^j}} + \frac{e^{\frac{\pi\Delta E^j}{a_j}}}{e^{\beta\Delta E^j}-1}\right]\Upsilon\left(\Delta E^j, a_j, a_j\right), \end{aligned} \tag{3.28}$$

where, in this case the quantity $\Upsilon\left(\Delta E^j, a_j, a_j\right) = \pi a_j \Delta E^j/(2\sinh(\pi\Delta E^j/a_j))$ [1] , and it is obtained from a general expression of integral

$$\Upsilon\left(\bar{\varepsilon}, a_j, a_l\right) = \int_0^{\infty} k_p\, dk_p\, \mathscr{K}\left[\frac{i\bar{\varepsilon}}{a_j}, \frac{k_p}{a_j}\right]\mathscr{K}\left[\frac{i\bar{\varepsilon}}{a_l}, \frac{k_p}{a_l}\right]. \tag{3.29}$$

As observed in $(1+1)$ dimension, the transition probabilities in right and left Rindler wedges will be same as in LRW $\Delta\eta_j = -u_j$ and $\left(G^{\beta}_{W_R}(\Delta\eta_j)\right)^{\star} = G^{\beta}_{W_L}(u_j)$. Now it should be noted that the integrals representing transition probabilities from Eq. (3.25), and (3.28) can be multiplied on both sides by ΔE_j^2 to make them dimensionless. In this regard, we define other dimensionless parameters of the system as

$$\alpha_j = \frac{a_j}{\Delta E_j};\quad \sigma_j = \beta\Delta E_j\,. \tag{3.30}$$

It will be much more convenient to represent the necessary diagrams in our subsequent analysis with respect to these dimensionless parameters and quantities. In our subsequent analysis we specifically consider the situation of two observers accelerated parallelly or anti-parallelly in a thermal bath, and in particular, going to estimate the integrals $\mathscr{E}$. Then we shall analyse the condition of Eq. (2.83), and verify the possibility of entanglement extraction in those specific cases.

[1] Note that, Eqs. (3.27) and (3.28) represents transition probabilities of j^{th} detectors in $(1+1)$ and $(1+3)$ dimensions in thermal bath of inverse temperature β. Here if one takes $\beta \to \infty$, the expressions will reduced to transition probabilities in non-thermal Minkowski vacuum with temperature $a_j/2\pi$ (consistent with the Unruh effect [23]). On the other hand, Bisognano–Wichmann Theorem [220, 221] shows that the Minkowski vacuum induces on a Rindler wedge appears as a thermal state with dimensionless temperature $1/(2\pi)$. This difference is due to the fact that the evolution is done under the dimensionless boost Killing vector $x\partial_t + t\partial_x$, where the boost parameter t is a dimensionless quantity, and does not represent the physical proper time of the observer.

3.3.2 Parallel acceleration: No harvesting

In this subsection we consider the two observers *Alice* and *Bob* to be accelerated parallelly. We consider them to have the proper accelerations a_A and a_B and both of them to be in the right Rindler wedge. For convenience of calculation, in this case we express integral $\mathscr{E}$ from Eq. (3.23) as

$$\begin{aligned}\mathscr{E} &= -\int_{-\infty}^{\infty} d\tau_B \int_{-\infty}^{\infty} d\tau_A \; e^{i(\Delta E^B \tau_B + \Delta E^A \tau_A)} [G_W(x_B, x_A) + \theta(t_A - t_B)\{G_W(x_A, x_B) - G_W(x_B, x_A)\}] \\ &= \mathscr{E}^W + \mathscr{E}^R \,. \end{aligned} \tag{3.31}$$

Here the first integral $\mathscr{E}^W$ contains the Wightman function, while the second integral $\mathscr{E}^R$ represents the contribution of the retarded Green's function. We shall be using this expression to evaluate the integral $\mathscr{E}$ separately in $(1+1)$ and $(1+3)$ dimensions in our following studies.

3.3.2.1 $(1+1)$ dimensions

For the evaluation of $\mathscr{E}^W$ and $\mathscr{E}^R$ in $(1+1)$ dimensions we consider the positive frequency Wightman function (3.15). In particular, in the expression of this Green's function the indices j and l correspond to the detector A and B respectively. The relation between Rindler times and detector proper times are $\eta_A = \tau_A = t_A$ and $\eta_B = \tau_B = t_B$, considering $\xi_A = 0 = \xi_B$, i.e., assuming the accelerating detectors to be fixed at the origin of the respective Rindler frames, while the proper accelerations are $b_j = a_j$. Then the first integral $\mathscr{E}^W$ can be expressed as

$$\begin{aligned}\mathscr{E}^W &= -\int_{-\infty}^{\infty} d\tau_B \int_{-\infty}^{\infty} d\tau_A \; e^{i(\Delta E^B \tau_B + \Delta E^A \tau_A)} G^{\beta}_{W_R}(x_B, x_A) \\ &= -\delta\left(\frac{\Delta E^A + \Delta E^B}{\sqrt{a_A a_B}}\right) \frac{\pi}{\Delta\breve{E}\sqrt{a_A a_B}} \frac{1}{\sqrt{\sinh\frac{\pi\Delta\breve{E}}{a_B}\sinh\frac{\pi\Delta\breve{E}}{a_A}}} \left[\frac{e^{\frac{\pi\Delta\breve{E}}{2}\left(\frac{1}{a_B}+\frac{1}{a_A}\right)}}{1-e^{-\beta\Delta\breve{E}}} + \frac{e^{-\frac{\pi\Delta\breve{E}}{2}\left(\frac{1}{a_B}+\frac{1}{a_A}\right)}}{e^{\beta\Delta\breve{E}}-1}\right] \,, \end{aligned} \tag{3.32}$$

where the expression of $\Delta\breve{E}$ is given by $\Delta\breve{E} = (\Delta E^B - \Delta E^A)/2$. For the evaluation of this integral we have considered a change of variables $\tilde{v} = \tau_B + \tau_A$ and $\tilde{u} = \tau_B - \tau_A$. The Jacobian of this transformation from (τ_A, τ_B) to $(\tilde{v}, \tilde{u})$ is 1/2. We first evaluated the $\tilde{u}$-integral, followed by the ω-integral. The Dirac delta function comes from the $\tilde{v}$-integration as observed in the last subsection. Since $\Delta E^j > 0$, this delta function leads to vanishing $\mathscr{E}^W$. On the other hand, using the same Wightman function from Eq. (3.15) with proper identification of the indices j and l to the detectors A and B, and only

performing the $\tilde{v}$-integral, we obtain the integral $\mathscr{E}^R$ to be

$$\mathscr{E}^R = -\int_{-\infty}^{\infty} d\tau_B \int_{-\infty}^{\infty} d\tau_A \; e^{i(\Delta E^B \tau_B + \Delta E^A \tau_A)} \theta(\tau_A - \tau_B) \left\{ G^{\beta}_{W_R}(x_A, x_B) - G^{\beta}_{W_R}(x_B, x_A) \right\}$$
$$= -\delta\left(\frac{\Delta E^A + \Delta E^B}{\sqrt{a_A a_B}} \right) \int_0^{\infty} \frac{d\omega}{\omega \sqrt{a_A a_B}} \frac{\sinh\left[\frac{\pi\omega}{2} \left(\frac{1}{a_B} + \frac{1}{a_A} \right) \right]}{\sqrt{\sinh \frac{\pi\omega}{a_B} \sinh \frac{\pi\omega}{a_A}}} \int_0^{\infty} e^{-i\tilde{u}\Delta\breve{E}} \left(e^{-i\omega\tilde{u}} - e^{i\omega\tilde{u}} \right) . \quad (3.33)$$

Similar to Eq. (3.32), here also we have encountered expression $\delta((\Delta E^B + \Delta E^A)/\sqrt{a_A a_B})$, which definitely cannot give non-zero contribution when $\Delta E^j > 0$. Then we have $\mathscr{E} = 0$ due to the contributions of $\mathscr{E}^W$ and $\mathscr{E}^R$. Whereas from Eq. (3.25) we observe that $\mathscr{P}_j$ always are non-zero and also have $\delta(0)$ multiplied with them. This signifies that for two observers accelerated parallelly the condition for entanglement harvesting Eq. (2.83) is not satisfied in $(1+1)$ dimensions.

3.3.2.2 $(1+3)$ dimensions

We consider the positive frequency Wightman function in Eq. (3.17) for the estimation of the quantities $\mathscr{E}^W$ and $\mathscr{E}^R$ in $(1+3)$ dimensions. Furthermore, we have identified the indices j and l with the detectors A and B respectively. Then proceeding like the earlier way the first integral $\mathscr{E}^W$ becomes

$$\mathscr{E}^W = -\int_{-\infty}^{\infty} d\tau_B \int_{-\infty}^{\infty} d\tau_A \; e^{i(\Delta E^B \tau_B + \Delta E^A \tau_A)} G^{\beta}_{W^{3D}_R}(x_B, x_A)$$
$$= -\delta\left(\frac{\Delta E^A + \Delta E^B}{\sqrt{a_A a_B}} \right) \frac{1}{\pi a_A a_B} \Upsilon\left(\Delta\breve{E}, a_A, a_B \right) \left[\frac{e^{\frac{\pi\Delta\breve{E}}{2}\left(\frac{1}{a_B} + \frac{1}{a_A}\right)}}{1 - e^{-\beta\Delta\breve{E}}} + \frac{e^{-\frac{\pi\Delta\breve{E}}{2}\left(\frac{1}{a_B} + \frac{1}{a_A}\right)}}{e^{\beta\Delta\breve{E}} - 1} \right] . \quad (3.34)$$

Here expression of Υ is given in Eq. (3.29). Using the same Wightman function from Eq. (3.17) with the proper identification of the indices j and l to the detectors A and B, we get the second integral $\mathscr{E}^R$ to be

$$\mathscr{E}^R = -\int_{-\infty}^{\infty} d\tau_B \int_{-\infty}^{\infty} d\tau_A \; e^{i(\Delta E^B \tau_B + \Delta E^A \tau_A)} \theta(\tau_A - \tau_B) \left\{ G^{\beta}_{W^{3D}_R}(x_A, x_B) - G^{\beta}_{W^{3D}_R}(x_B, x_A) \right\}$$
$$= -\delta\left(\frac{\Delta E^B + \Delta E^A}{\sqrt{a_A a_B}} \right) \int_0^{\infty} \frac{d\omega}{\pi^2} \frac{\sinh\left[\frac{\pi\omega}{2} \left(\frac{1}{a_B} + \frac{1}{a_A} \right) \right]}{a_A a_B} \Upsilon\left(\Delta\breve{E}, a_A, a_B \right)$$
$$\times \int_0^{\infty} e^{-i\tilde{u}\Delta\breve{E}} \left(e^{-i\omega\tilde{u}} - e^{i\omega\tilde{u}} \right) . \quad (3.35)$$

Here also in both of the integrals from (3.34) and (3.35) we have $\delta((\Delta E^B + \Delta E^A)/\sqrt{a_A a_B})$ multiplied, which always gives zero contribution when $\Delta E^j > 0$. Then none of the above quantities $\mathscr{E}^W$ or $\mathscr{E}^R$ contribute to the non-zero expression of $\mathscr{E}$. This signifies that for

two observers accelerated parallelly, the condition for entanglement harvesting is not satisfied in $(1+3)$ dimensions.

In both $(1+1)$ and $(1+3)$ dimensions, considering parallelly accelerated detectors in a thermal bath, we observed that the condition for entanglement harvesting is not satisfied. This was also true in the case of accelerated detectors without a thermal bath, see [99, 113]. Then one can deduce that here *the thermal bath has no additional influence to make the entanglement harvesting possible*. One should also notice that, it is not possible to distinguish between thermal and non-thermal scalar fields only by analyzing the parallelly accelerated detectors using entanglement harvesting information.

3.3.3 Anti-parallel accelerations: harvesting possible

In this subsection we consider *Alice* (denoted by A) in right and *Bob* (denoted by B) in left Rindler wedge so that they are anti-parallelly accelerated while interacting with background thermal field. Here the relation between Rindler times and detector proper times are $\eta_A = \tau_A = t_A$ and $-\eta_B = \tau_B = t_B$, considering $\xi_A = 0 = \xi_B$. Here again we use the coordinates transformation $\tilde{v} = \tau_B + \tau_A$ and $\tilde{u} = \tau_B - \tau_A$. However, in this case the Green's function depends on $\tilde{v} = \eta_A - \eta_B = \tau_B + \tau_A$, not on $\tilde{u}$. We shall explicitly evaluate the integrals $\mathscr{E}^W$ and $\mathscr{E}^R$ from Eq. (3.31) in $(1+1)$ and $(1+3)$ dimensions to understand the possibility of entanglement extraction in our following studies.

3.3.3.1 (1+1)dimensions

Analytical results: – In $(1+1)$ dimensions the first part $\mathscr{E}^W$ of the integral $\mathscr{E}$, is estimated using the expression of the Wightman function from Eq. (3.16). Then the integral $\mathscr{E}^W$ becomes

$$\begin{aligned}\mathscr{E}^W &= -\int_{-\infty}^{\infty} d\tau_B \int_{-\infty}^{\infty} d\tau_A \, e^{i(\Delta E^B \tau_B + \Delta E^A \tau_A)} G^{\beta}_{W_{LR}}(x_B, x_A) \\ &= -\delta\left(\frac{\Delta E^B - \Delta E^A}{\sqrt{a_A a_B}}\right) \frac{1}{\sqrt{\sinh\frac{\pi\Delta\widetilde{E}}{a_A}\sinh\frac{\pi\Delta\widetilde{E}}{a_B}}} \frac{\pi}{\Delta\widetilde{E}\sqrt{a_A a_B}} \left[\frac{e^{\frac{\pi\Delta\widetilde{E}}{2}\left(\frac{1}{a_B}-\frac{1}{a_A}\right)}}{1-e^{-\beta\Delta\widetilde{E}}} + \frac{e^{-\frac{\pi\Delta\widetilde{E}}{2}\left(\frac{1}{a_B}-\frac{1}{a_A}\right)}}{e^{\beta\Delta\widetilde{E}}-1}\right],\end{aligned} \tag{3.36}$$

where, $\Delta\widetilde{E} = (\Delta E^B + \Delta E^A)/2$. To evaluate the integral, we first perform the coordinate transform, then evaluate the $\tilde{v}$-integral, followed by the ω-integral. The Dirac delta function $\delta\left(\frac{\Delta E^B - \Delta E^A}{\sqrt{a_A a_B}}\right)$ is obtained by performing the $\tilde{u}$-integral. One also may have considered moving to dimensionless variables $\gamma_j = \tau_j a_j$, and then make change of variables

$\bar{v} = \gamma_B + \gamma_A$ and $\bar{u} = \gamma_B - \gamma_A$ to obtain the same final result. The Jacobian corresponding to both of these change of variables is 1/2. Similarly one can evaluate the second integral $\mathscr{E}^R$. Then using the Wightman function of Eq. (3.16) the integral $\mathscr{E}^R$ can be evaluated to be

$$\begin{aligned}\mathscr{E}^R &= -\int_{-\infty}^{\infty} d\tau_B \int_{-\infty}^{\infty} d\tau_A \; e^{i(\Delta E^B \tau_B + \Delta E^A \tau_A)}\, \theta(\tau_A - \tau_B) \left\{ G^{\beta}_{W_{RL}}(x_A, x_B) - G^{\beta}_{W_{LR}}(x_B, x_A) \right\} \\ &= \frac{\sinh\frac{\pi\Delta\widetilde{E}}{2}\left(\frac{1}{a_B} - \frac{1}{a_A}\right)}{2\Delta\widetilde{E}} \frac{1}{\sqrt{\sinh\frac{\pi\Delta\widetilde{E}}{a_A}\sinh\frac{\pi\Delta\widetilde{E}}{a_B}}} \int_{-\infty}^{\infty} e^{-\frac{i}{2}(\Delta E^B - \Delta E^A)\tilde{u}}\; \theta(\tilde{u})\, d\tilde{u}\;, \end{aligned} \tag{3.37}$$

where, $\Delta\widetilde{E} = (\Delta E_A + \Delta E_B)/2$. One can evaluate this last integral as

$$\begin{aligned}\int_{-\infty}^{\infty} e^{-\frac{i}{2}(\Delta E^B - \Delta E^A)\tilde{u}}\; \theta(\tilde{u}) d\tilde{u} &= \int_0^{\infty} e^{-\frac{i}{2}(\Delta E^B - \Delta E^A - i\epsilon)\tilde{u}}\; d\tilde{u} \\ &= \frac{2}{i(\Delta E^B - \Delta E^A - i\epsilon)}\,, \end{aligned} \tag{3.38}$$

where a multiplicative regulator of $e^{-\epsilon\tilde{u}/2}$, with $\epsilon > 0$, is introduced in the integrand to evaluate this otherwise diverging integral. It is to be noted that the limit $\epsilon \to 0$ provides the actual value of the integral. One can express this quantity of Eq. (3.38) with the help of a consequence of the *Sokhotski-Plemelj theorem* [24]

$$\lim_{\epsilon \to 0+} \frac{1}{z - i\epsilon} = i\pi\, \delta(z) + P\left(\frac{1}{z}\right)\,, \tag{3.39}$$

where, $P(1/z)$ denotes the principal value of $(1/z)$, which is a finite quantity. Then the quantity $\mathscr{E}^R$ is

$$\mathscr{E}^R = \frac{\pi \sinh\left\{\frac{\pi\Delta\widetilde{E}}{2}\left(\frac{1}{a_B} - \frac{1}{a_A}\right)\right\}}{\Delta\widetilde{E}\sqrt{a_A a_B}\sqrt{\sinh\frac{\pi\Delta\widetilde{E}}{a_A}\sinh\frac{\pi\Delta\widetilde{E}}{a_B}}} \left[\delta\left(\frac{\Delta E^B - \Delta E^A}{\sqrt{a_A a_B}}\right) - \frac{i}{\pi} P\left(\frac{\sqrt{a_A a_B}}{\Delta E^B - \Delta E^A}\right)\right]. \tag{3.40}$$

The second quantity inside the square brackets in the right hand side denotes the principal value and it is a finite quantity. It should be mentioned that when $\Delta E^B \neq \Delta E^A$ the Dirac delta distribution from Eq. (3.40) vanishes and one is left out with only this finite second term. In this particular situation the integral $\mathscr{E}^W$ also vanishes and the whole $\mathscr{E} = \mathscr{E}^W + \mathscr{E}^R$ becomes finite. [2] However, from Eq. (3.25) it is observed that the integrals $\mathscr{P}_j$ still keeps the $\delta(0)$ terms in them. In that case it is obvious that the condition

[2] Note that the term $\mathscr{E}$ involves transition in both detectors, and has contributions from the two-detector cross correlators, which involve acceleration of both detectors. Thus, two different proper accelerations appeared in the expression. These terms are not directly related to any thermality as seen by individual detectors..

from (2.83) remains unfulfilled. On the other hand, when $\Delta E^B = \Delta E^A$ only the Dirac delta distribution contributes in the expression of $\mathscr{E}^R$. In this situation, $\mathscr{E}^W$ is also non zero, and there are multiplicative factors of $\delta(0)$ in $\mathscr{E}^W$ and $\mathscr{E}^R$ like the $\mathscr{P}_j$. Then it is evident that only for $\Delta E^B = \Delta E^A$ the condition (2.83) for entanglement harvesting may get satisfied. Since both $\mathscr{P}_j$ and $\mathscr{E}$ have multiplicative factors of $\delta(0)$, we can define a quantity C_I, which will represent concurrence per unit time when it is non-negative as

$$C_I = \left(|\mathscr{E}| - \sqrt{\mathscr{P}_A \mathscr{P}_B}\right)/\delta(0). \tag{3.41}$$

Let us now make a comment on the contribution related to the retarded Green's function. It is observed from (3.40) that the integral $\mathscr{E}^R$ in general vanishes when the two anti parallelly moving observers have equal magnitude of accelerations i.e. $a_A = a_B$. It is noticed that even in Green's function level when the accelerations of the anti-parallelly accelerated detectors are equal the quantity $G^{\beta}_{W_{RL}}(x_A, x_B) - G^{\beta}_{W_{LR}}(x_B, x_A) = 0$, denoting the vanishing of retarded Green's function in the integral of (3.37). This is expected as left Rindler wedge is causally disconnected from the right wedge. However, it remains non-zero for scenarios when $a_A \neq a_B$, although both are causally disconnected. The retarded Green's function with respect to Minkowski mode vanishes (or when $a_A = 0 = a_B$) when they are spacelike separated. It may be mentioned that when $a_A = a_B$ then they can be regarded as "similar frames" (as LRW is mirror image of RRW) and hence since retarded Green's function vanishes in Minkowski frame, it must vanish in any other frame. Whereas for $a_A \neq a_B$ we do not have such similarity and we may take this as investigations of field operators from two "dis-similar frames". In this case the commutator of the fields may not be the same as it was earlier. In the above exactly this thing has been reflected in $\mathscr{E}^R$. In summary, the relative acceleration between the frames introduces this non-triviality. We will see later that in $(1+3)$ case, compared to $(1+1)$ dimensional analysis, this has a big role to give a distinct feature in the entanglement harvesting.

From Eq. (3.36) and (3.40) we obtain the expression of the integral $\mathscr{E}$ corresponding to two anti-parallelly accelerated observers as $\mathscr{E} = \mathscr{E}^W + \mathscr{E}^R$. Also similar to $\mathscr{P}_j$, we shall multiply ΔE^2 with $\mathscr{E}$ to make it dimensionless. Since we have already discussed these expressions are non-zero and comparable to $\mathscr{P}_j$ only when $\Delta E^A = \Delta E^B = \Delta E$ (say), in that case we also have $\Delta \widetilde{E} = \Delta E$. The condition for entanglement harvesting from Eq.

(2.83) becomes

$$\left(\frac{e^{-\frac{\pi\Delta E}{a_A}}}{1-e^{-\beta\Delta E}}+\frac{e^{\frac{\pi\Delta E}{a_A}}}{e^{\beta\Delta E}-1}\right)\left(\frac{e^{-\frac{\pi\Delta E}{a_B}}}{1-e^{-\beta\Delta E}}+\frac{e^{\frac{\pi\Delta E}{a_B}}}{e^{\beta\Delta E}-1}\right)< 4\left[\frac{e^{\frac{\pi\Delta E}{2}\left(\frac{1}{a_B}-\frac{1}{a_A}\right)}}{1-e^{-\beta\Delta E}}+\frac{e^{-\frac{\pi\Delta E}{2}\left(\frac{1}{a_B}-\frac{1}{a_A}\right)}}{e^{\beta\Delta E}-1}-\sinh\left\{\frac{\pi\Delta E}{2}\left(\frac{1}{a_B}-\frac{1}{a_A}\right)\right\}\right]^2 . \quad (3.42)$$

From this expression (3.42) depicting the condition for entanglement harvesting for two

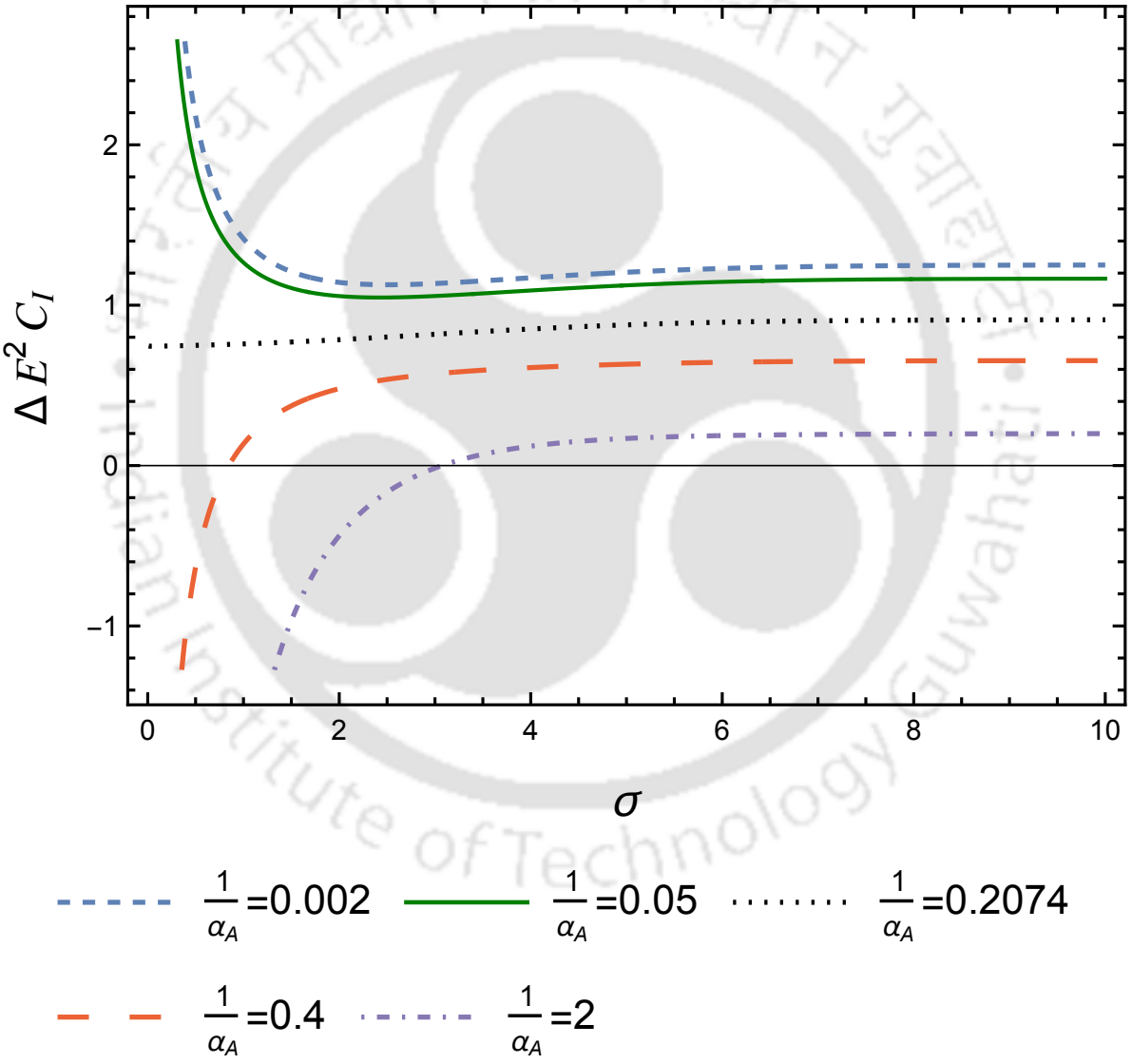

Figure 3.2: In $(1+1)$ dimensions the quantity $\Delta E^2 C_I$ is plotted for two anti-parallelly accelerating detectors with respect to the inverse temperature $\sigma = \beta\Delta E$ for different fixed $\alpha_A = a_A/\Delta E$. The other parameter is fixed at $\alpha_B = a_B/\Delta E = 1$.

anti-parallelly accelerated observers, we see that contribution of the retarded Green's function exists when the detectors have different magnitudes of acceleration, i.e., $a_A \neq a_B$.

Numerical analysis: – In Fig. 3.2 we have plotted the quantity C_I of (3.41) signifying the concurrence, with respect to σ, which is proportional to the inverse temperature of the thermal bath $\sigma = \beta\Delta E$, considering two anti-parallelly accelerated observers with different accelerations in $(1+1)$ dimensions. The curves in this figure correspond to fixed $a_B = a_B/\Delta E = 1$ and different fixed $a_A = a_A/\Delta E$. It is to be noted that the dimensionless quantity $\Delta E^2 C_I$ plotted in the figure is obtained using the expressions from (3.25), (3.36) and (3.40) when $\Delta E^B = \Delta E^A = \Delta E$. Removing the delta function, the quantity C_I can be interpreted as taking a rate per unit proper time, like discussed in literature [113]. From Fig. 3.2 we have the following observations.

- For low acceleration a_A of the first detector (e.g. $a_A = 1/2$) the quantity C_I is negative for very high temperature of the thermal bath, and it tends to increase with increasing β and becomes positive at some much larger β or low temperature of the thermal bath. Therefore thermal fields do not allow entanglement at high temperature. Entanglement can start only from certain value of temperature of thermal bath to lower values when the first detector moves with small acceleration.

- For high acceleration a_A of the first detector ($a_A = 1/0.002$) the quantity C_I is positive for very high temperature of the thermal bath, and it tends to decrease with increasing β but never becomes negative at much larger β or low temperature of the thermal bath. So for large values of acceleration, we will have entanglement at any temperature of bath.

- With these it is observed that there is a characteristic change in the nature of these curves depending on the value of a_A – for low values of a_A the entanglement increases with increase of β while after certain value of a_A entanglement decreases with increase of β. We call the value of acceleration $a_A = a_c$ as '*critical acceleration*' value around which these curves have different nature. In Fig. 3.2 this is given by the black dotted line ($a_A = 1/0.2074$), which is almost a straight line.

To find this critical value note that the change is nature is prominent for very low value of β; *i.e.,* at higher temperature of the bath. So it will be sufficient to investigate C_I for very low value of σ. Also in this regime the critical line (black dotted line in Fig. 3.2) is straight. Therefore the vanishing of the slope of the curve in low value of σ will yield

α_c. One can series expand the derivative of C_I with respect to σ in this case, in small σ regimes and observe that it is of the form $(\partial/\partial\sigma)C_I(\rho_{AB}) = (1/\sigma^2)C_1 + C_2 + \mathcal{O}(\sigma)$. Then in high temperature regime one can predict about the transition point α_c by making $C_1 = 0$ (this is leading term) with $\alpha_A = \alpha_c$, which provides us with the expression

$$C_1 = \frac{\pi}{\sqrt{\sinh\left(\frac{\pi}{\alpha_c}\right)\sinh\left(\frac{\pi}{\alpha_B}\right)}}\left(\sqrt{\cosh\left(\frac{\pi}{\alpha_c}\right)\cosh\left(\frac{\pi}{\alpha_B}\right)} - 2\cosh\left(\frac{\pi(\alpha_B-\alpha_c)}{2\alpha_c\alpha_B}\right)\right) = 0\,. \quad (3.43)$$

It can be checked that the above equation yields the value of α_c as 4.82026 for our choice of parameter value $\alpha_B = 1$. Note that this is exactly the value of α_A for which the critical curve (black dotted line in Fig. 3.2) was obtained numerically.

In Fig. 3.3 we have plotted C_I signifying the concurrence with respect to the acceleration of the first detector α_A for different fixed σ. From this figure one can observe that the temperature of the thermal bath has a diminishing effect on the entanglement measure for low values of the acceleration of the first detector α_A. It is observed that for smaller α_A with low β (if ΔE is kept fixed then β changes in unison with σ), *i.e.,* for very high temperature, the condition for entanglement harvesting is failing, while for high α_A the condition again gets satisfied. We have also depicted the same curves as shown in Fig. 3.3 in lower regimes of $1/\alpha_A$ in Fig. 3.4. From this curve we observe that, above a certain value of α_A, which is the critical value α_c, the thermal bath has an enhancing effect on concurrence (denoted by C_I). Then the plots depicted in Fig. 3.3 and 3.4 together predict the same phenomena provided by Fig. 3.2, *i.e.,* for low accelerations thermal bath has a diminishing effect and for high accelerations thermal bath has an enhancing effect on the entanglement measure, and there is a perceivable critical value of acceleration separating these two regimes of accelerations. In Fig. 3.5 and 3.6 we have further plotted the derivative of C_I with respect to σ for varying σ and α_A for the perception of α_c. Fig. 3.5 shows that some curves contains negative slope while others have positive slope for initial values of β. Similarly Fig. 3.6 signifies that slopes of each curve become same at the particular value of α_A. All these reassured the existence the aforesaid critical value of α_A.

It is to be noted that in the equal magnitude of acceleration limit the second integral from Eq. (3.40) coming from the retarded Green's function vanishes and one is left with only $\mathscr{E} = \mathscr{E}^W$. In this particular case we consider $a_A = a_B = a$, and the condition for entanglement harvesting from Eq. (2.83) is then given by

$$\frac{e^{-\frac{\pi\Delta E}{a}}}{1-e^{-\beta\Delta E}} + \frac{e^{\frac{\pi\Delta E}{a}}}{e^{\beta\Delta E}-1} < 2\,\frac{e^{\beta\Delta E}+1}{e^{\beta\Delta E}-1}\,, \quad (3.44)$$

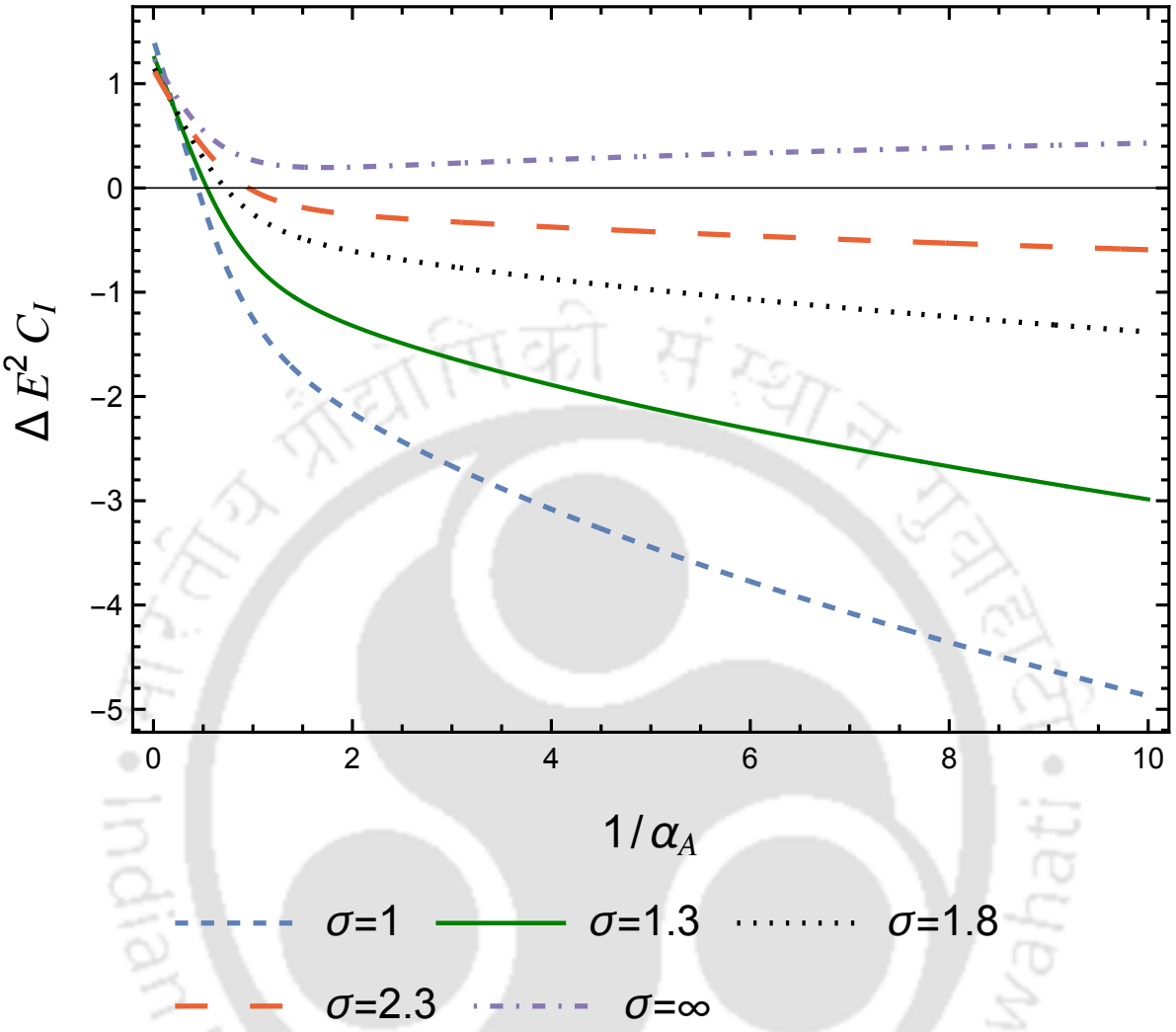

Figure 3.3: In $(1+1)$ dimensions the quantity $\Delta E^2 C_I$ is plotted for two anti-parallelly accelerating detectors with respect to the acceleration of the first detector α_A for different fixed inverse temperature of the thermal bath σ. The other parameters are fixed at $\alpha_B = 1$.

which for the zero temperature of the thermal bath, i.e., in the $\beta \to \infty$ limit, becomes $e^{\frac{\pi\Delta E}{a}} > 1/2$. This basically reinstates the fact that in the zero temperature case the entanglement can be harvested for anti-parallelly accelerated detectors with any possible equal acceleration, which is also observed from [99, 113] though considering the detectors in $(1+3)$ dimensions. In Fig. 3.7 and Fig. 3.8 we have plotted $C_I = \left(|\mathscr{E}| - \mathscr{P}_j\right)/\delta(0)$ respectively with respect to varying σ and α. From these figures also we observe the same phenomena as perceived before. Here also we see that below a certain critical α entanglement harvesting is not possible for low β or high temperature of the thermal

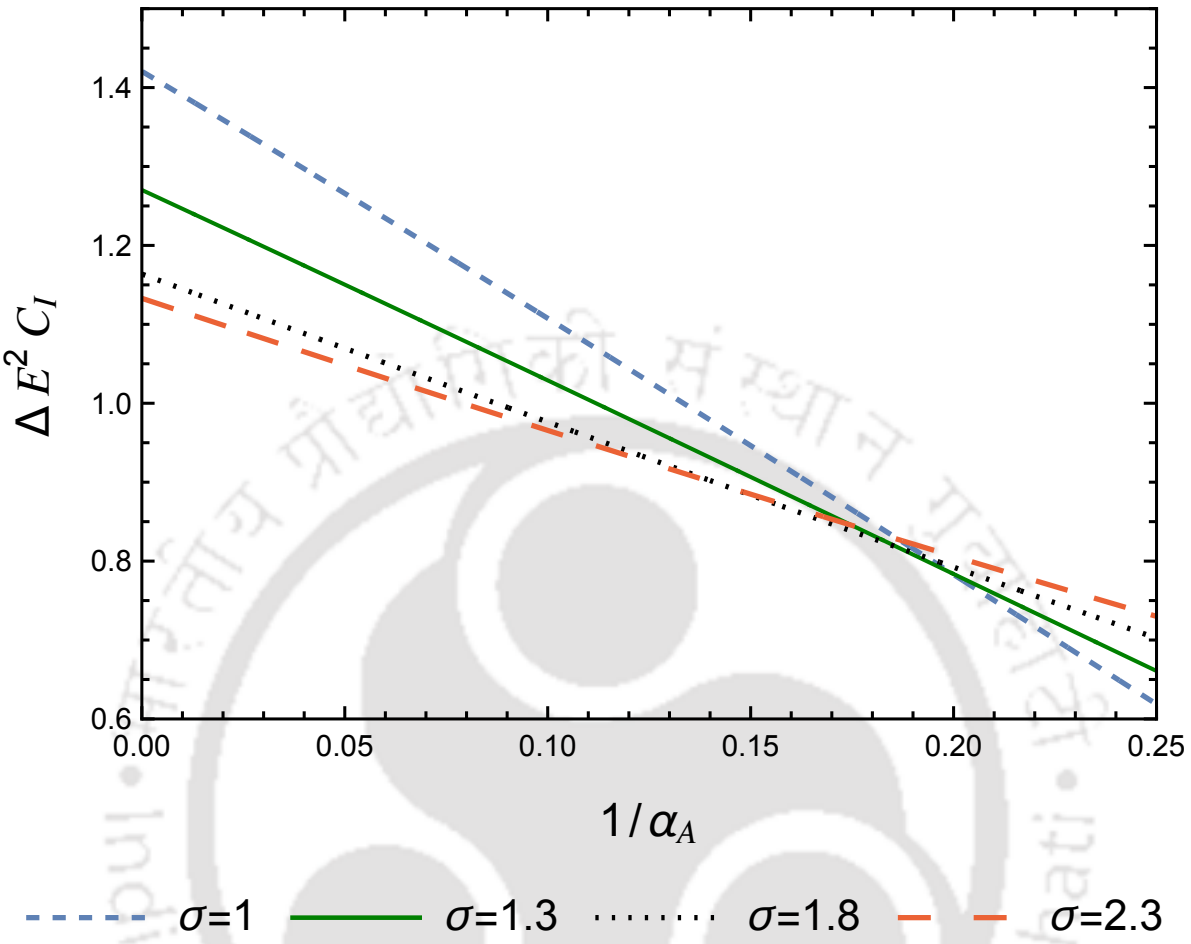

Figure 3.4: In $(1+1)$ dimensions the quantity $\Delta E^2 C_I$ is plotted for two anti-parallelly accelerating detectors with respect to the acceleration of the first detector α_A for different fixed inverse temperatures of the thermal bath σ. The other parameters are fixed at $\alpha_B = 1$. In particular we have depicted the curves of Fig. 3.3 in lower regime of $1/\alpha_A$.

bath and the entanglement measure increases with increasing β. On the other hand, above this critical acceleration entanglement measure decreases with increasing β, but remains positive. In Fig. 3.8 this behaviorial change of the curves after a certain critical acceleration α_c is much more prominent than the previous ones with different accelerations. It should be noted that in this equal acceleration case, by making the derivative of the quantity C_I with respect to σ equal to zero, one can obtain the critical value of acceleration $\alpha_c = \pi/\log[2+\sqrt{3}]$, which is around $\alpha_c \approx 2.385$ and is independent of σ. This is depicted by a straight line (black dotted line) in Fig. 3.7. In Fig. 3.9 and 3.10 the derivative of C_I is plotted with respect to varying α and σ, which also signifies the earlier mentioned slope change about the critical value of α. This reconfirms the existence of

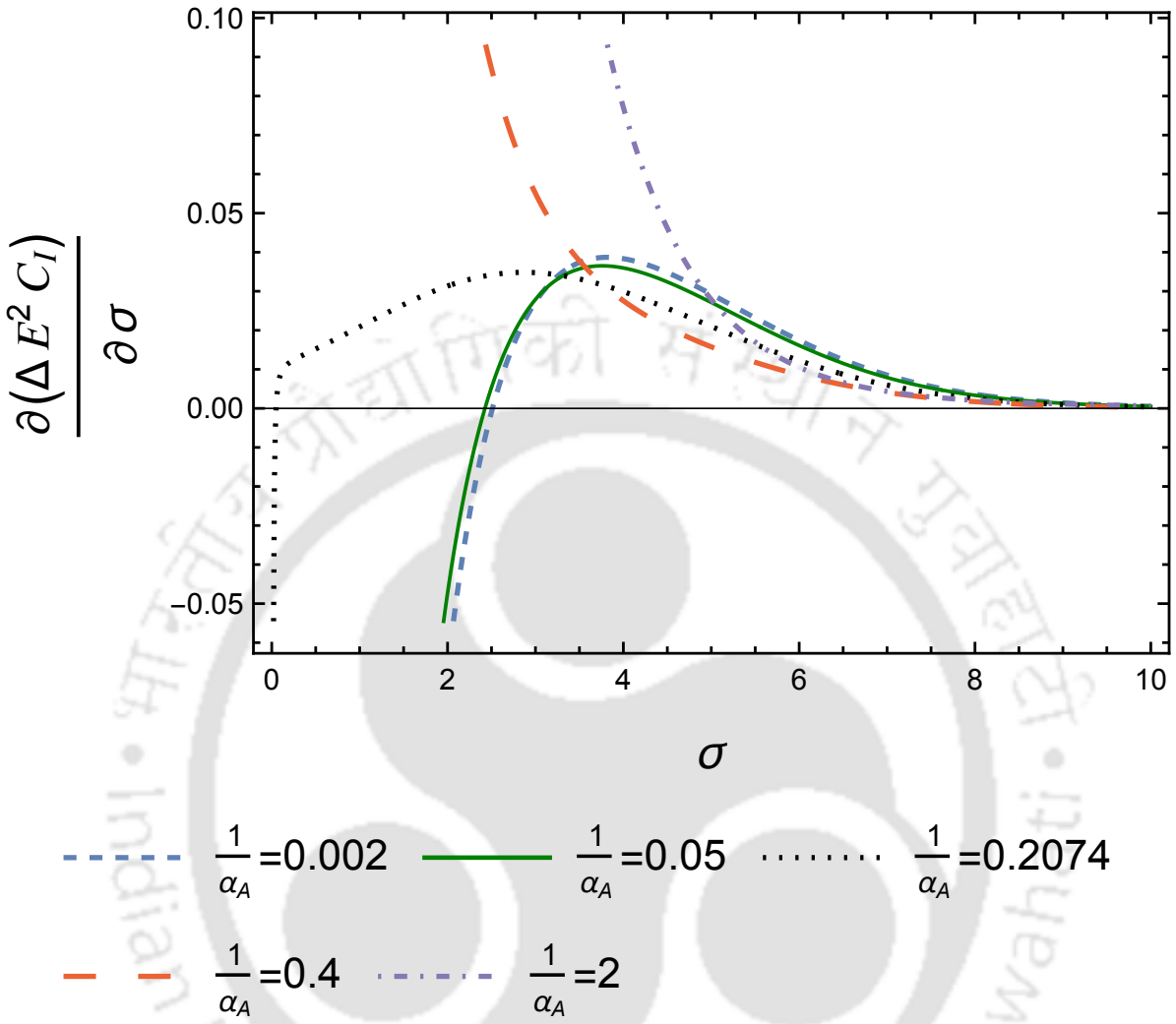

Figure 3.5: In $(1+1)$ dimensions the derivative with respect to $(\partial/\partial\sigma)\left(\Delta E^2 C_I\right)$ is plotted for two anti-parallelly accelerating detectors for varying σ. The other parameters $\alpha_B = 1$ and α_A are fixed.

the aforesaid criticality.

3.3.3.2 (1+3)dimensions

Analytical results: – From Eq. (3.23) we observe that there are two specific terms in the integral $\mathscr{E}$. One involving a Wightman function and another involving a retarded Green's function. The second term involving the retarded Green's function is recently conceived through rigorous analysis of the model for entanglement harvesting. Like the $(1+1)$ dimensional case in $(1+3)$ dimensions also we shall explicitly evaluate these terms. We

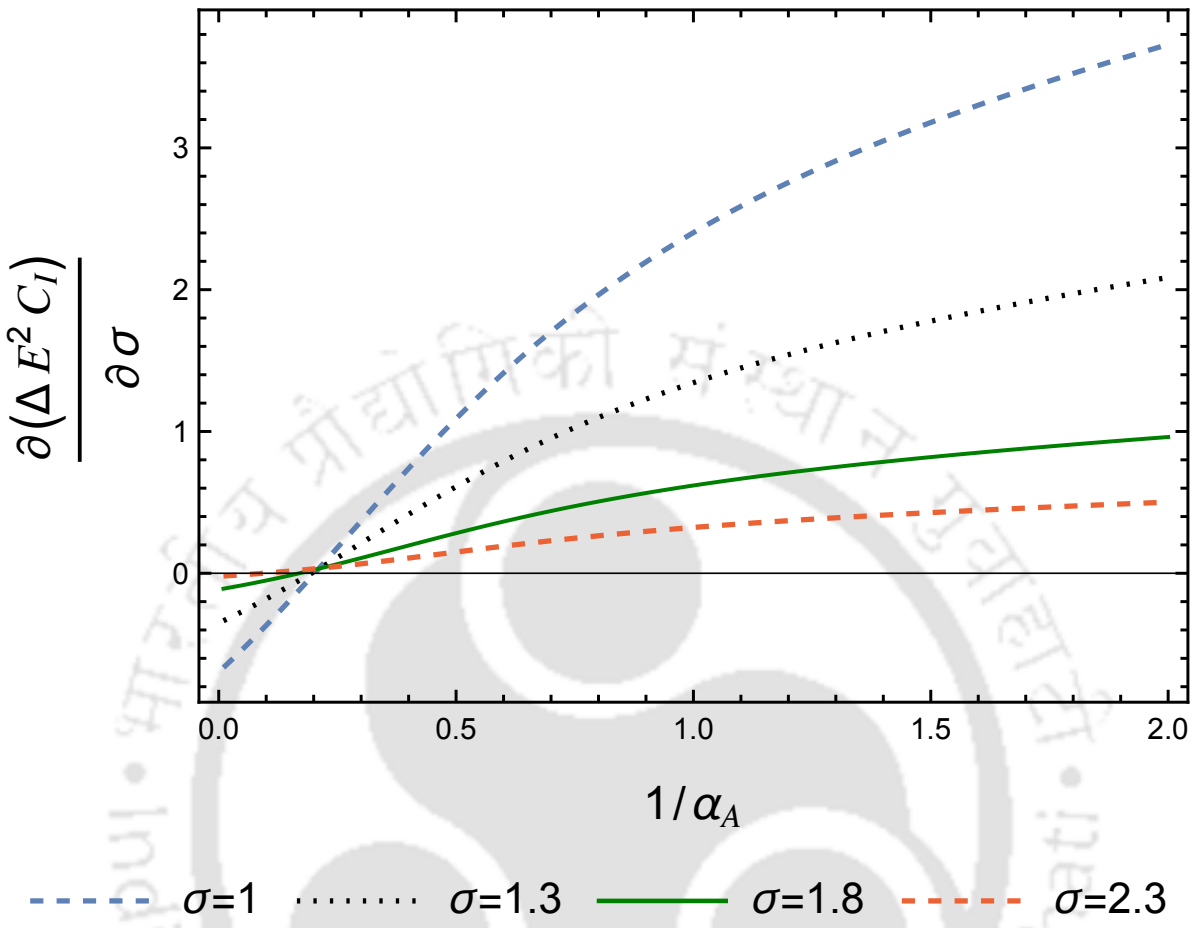

Figure 3.6: In $(1+1)$ dimensions the derivative with respect to σ of the quantity $(\partial/\partial\sigma)(\Delta E^2 C_I)$ is plotted for two anti-parallelly accelerating detectors for varying acceleration of the first detector α_A. The temperatures of the thermal bath σ and other parameter $\alpha_B = 1$ are fixed.

express the first quantity using the Wightman function of Eq. (3.18), *i.e.,* considering the observer B to be accelerating anti-parallelly in LRW with respect to observer A in RRW, as

$$\begin{aligned}\mathscr{E}^W &= -\int_{-\infty}^{\infty} d\tau_B \int_{-\infty}^{\infty} d\tau_A \; e^{i(\Delta E^B \tau_B + \Delta E^A \tau_A)} G^{\beta}_{W^{3D}_{LR}}(x_B, x_A) \\ &= -\delta\left(\frac{\Delta E^B - \Delta E^A}{\sqrt{a_A a_B}}\right) \frac{1}{a_A a_B} \frac{\Upsilon\left(\Delta\widetilde{E}, a_B, a_A\right)}{\pi} \left[\frac{e^{\frac{\pi\Delta\widetilde{E}}{2}\left(\frac{1}{a_B}-\frac{1}{a_A}\right)}}{1-e^{-\beta\Delta\widetilde{E}}} + \frac{e^{-\frac{\pi\Delta\widetilde{E}}{2}\left(\frac{1}{a_B}-\frac{1}{a_A}\right)}}{e^{\beta\Delta\widetilde{E}}-1}\right], \end{aligned} \tag{3.45}$$

where, $\Delta\widetilde{E} = (\Delta E^B + \Delta E^A)/2$, and expression of Υ is given in Eq. (3.29). For the evaluation of this integral we have considered change of variables $\tilde{v} = \tau_B + \tau_A$ and $\tilde{u} = \tau_B - \tau_A$, and we shall be using this same change of variables to evaluate the next integral also. Then

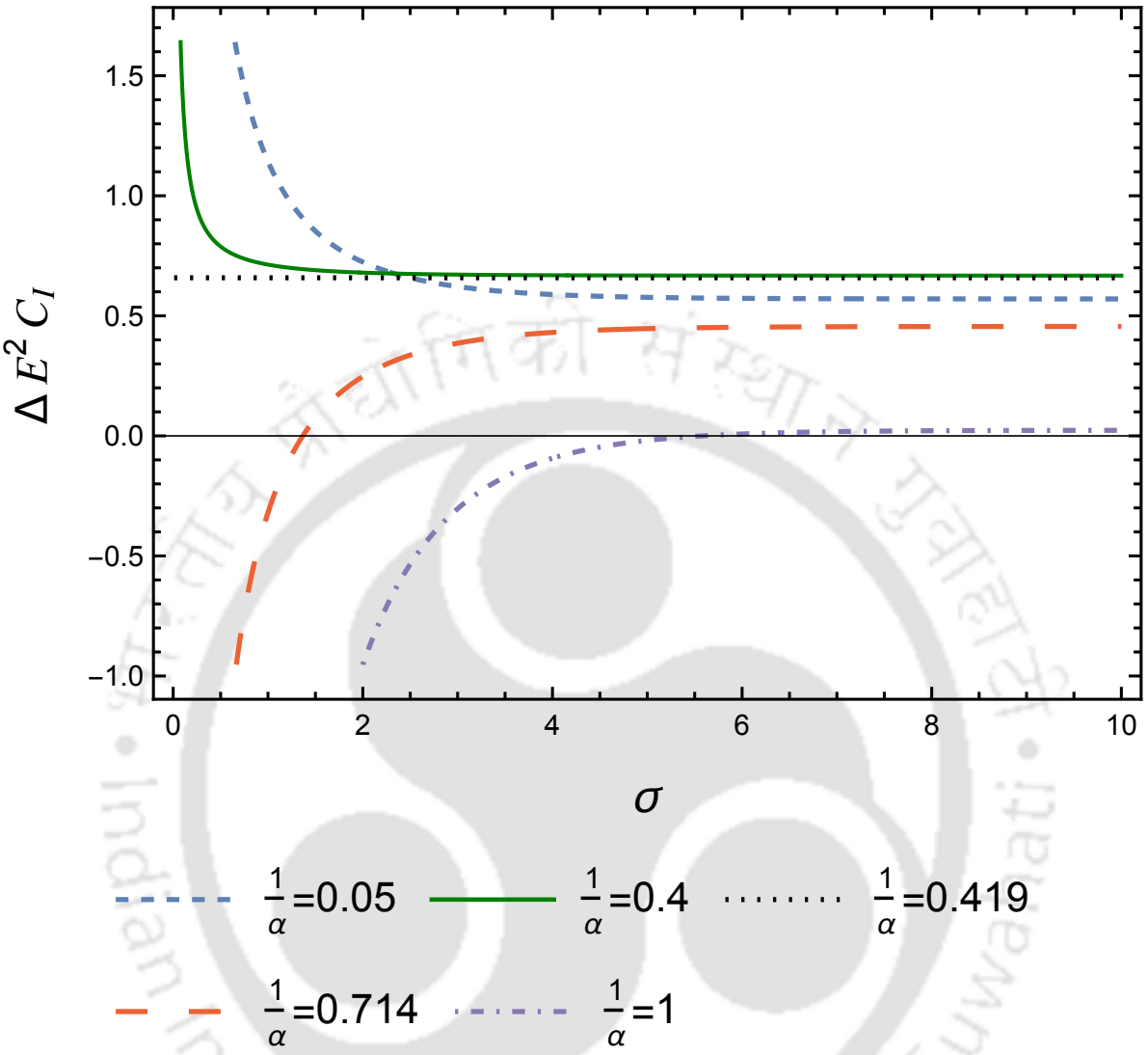

Figure 3.7: In $(1+1)$ dimensions the quantity $\Delta E^2 C_I$ is plotted for two anti-parallelly accelerating detectors with respect to the inverse temperature of the thermal bath σ for equal magnitude of proper accelerations, i.e., $a_A = a_B = a$.

one can evaluate the second part of the integral $\mathscr{E}$ from Eq. (3.23) as

$$\mathscr{E}^R = -\int_{-\infty}^{\infty} d\tau_B \int_{-\infty}^{\infty} d\tau_A \theta(\tau_A - \tau_B)\, e^{i(\Delta E^B \tau_B + \Delta E^A \tau_A)} \left[G^{\beta}_{W^{3D}_{RL}}(x_A, x_B) - G^{\beta}_{W^{3D}_{LR}}(x_B, x_A)\right]$$
$$= \sinh\left\{\frac{\pi \Delta\widetilde{E}}{2}\left(\frac{1}{a_B} - \frac{1}{a_A}\right)\right\} \frac{2\Upsilon\left(\Delta\widetilde{E}, a_B, a_A\right)}{(2\pi)^2\sqrt{a_A a_B}} \int_{-\infty}^{\infty} e^{-\frac{i}{2}(\Delta E^B - \Delta E^A)\tilde{u}}\, \theta(\tilde{u})\, d\tilde{u}\ . \qquad (3.46)$$

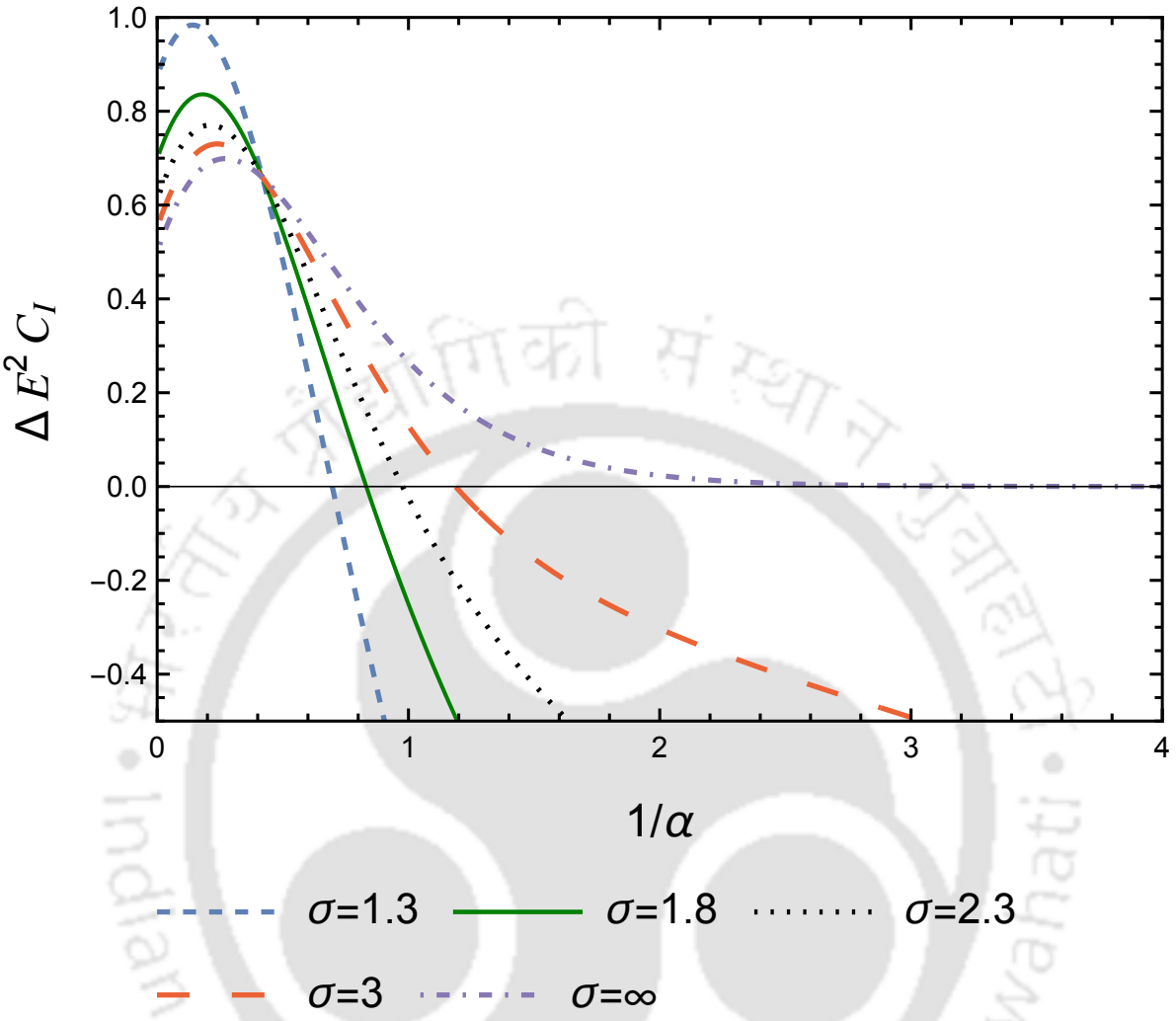

Figure 3.8: In $(1+1)$ dimensions the quantity $\Delta E^2 C_I$ is plotted for two anti-parallelly accelerating detectors with same magnitude of acceleration for varying acceleration of the detectors α and different fixed σ.

Like the previous $(1+1)$ dimensional case, using (3.39) the contributing part of this expression here can be evaluated to be

$$\mathscr{E}^R = \frac{\sinh\left\{\frac{\pi\Delta\widetilde{E}}{2}\left(\frac{1}{a_B}-\frac{1}{a_A}\right)\right\}\Upsilon\left(\Delta\widetilde{E},a_B,a_A\right)}{\pi a_A a_B}\left[\delta\left(\frac{\Delta E^B-\Delta E^A}{\sqrt{a_A a_B}}\right)-\frac{i}{\pi}P\left(\frac{\sqrt{a_A a_B}}{\Delta E^B-\Delta E^A}\right)\right]. \tag{3.47}$$

Like the $(1+1)$ dimensional case here also we observe that when $\Delta E^B \neq \Delta E^A$ the integral $\mathscr{E}^R$ becomes finite, whereas $\mathscr{E}^W$ vanishes. On the other hand, from (3.28) we observe that the integrals $\mathscr{P}_j$ have $\delta(0)$ multiplied with them. Then in this situation

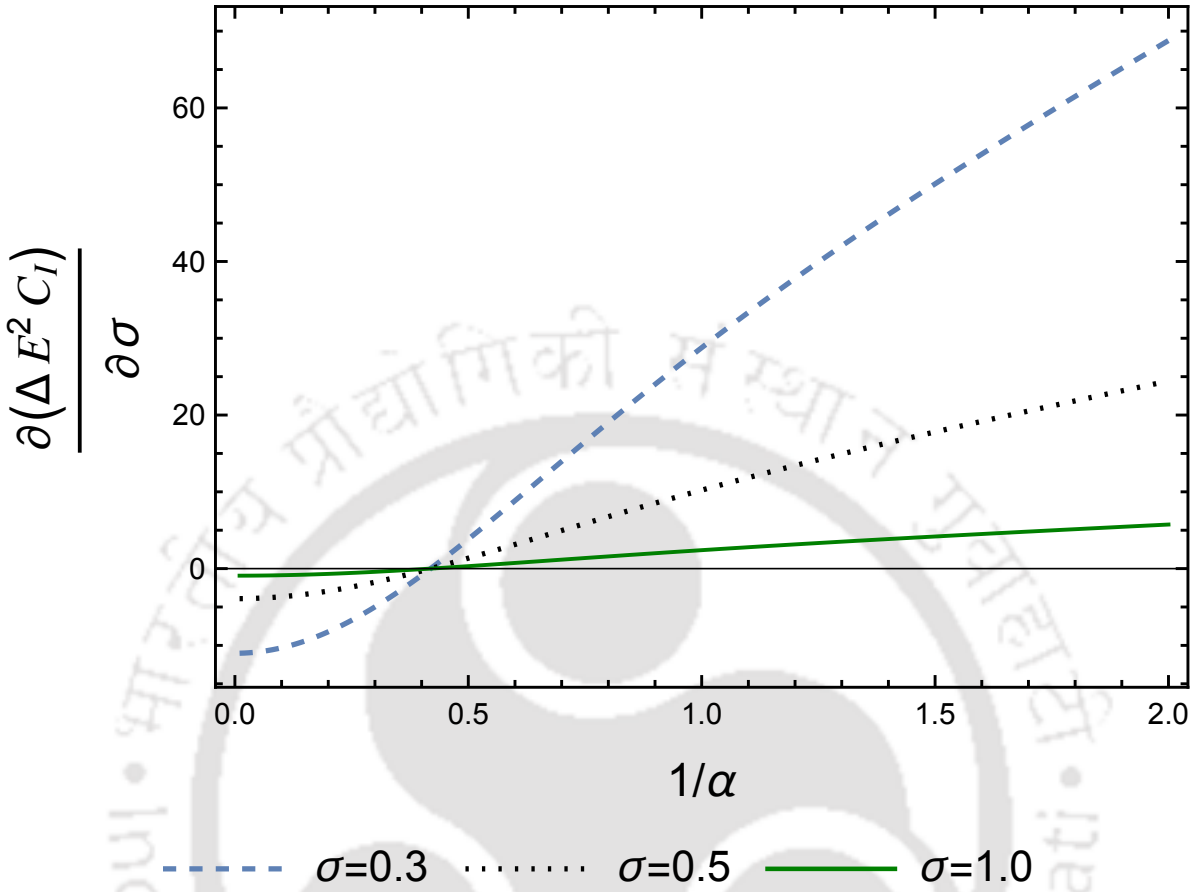

Figure 3.9: In $(1+1)$ dimensions the quantity $(\partial/\partial\sigma)\left(\Delta E^2 C_I\right)$ is plotted for two anti-parallelly accelerating detectors with respect to the equal magnitude of proper accelerations $a_A = a_B = a$ for fixed inverse temperature of the thermal bath σ. The critical acceleration, where this quantity is σ independent, is $a_c = 2.3854$.

one cannot harvest any entanglement. Entanglement harvesting may become possible only when $\Delta E^B = \Delta E^A$. In that case we consider $\Delta E^B = \Delta E^A = \Delta E$, which also results in $\Delta\widetilde{E} = \Delta E$. Then from Eq. (3.45) and (3.47) one can obtain the expression of the integral $\mathscr{E}$ corresponding to two anti-parallelly accelerated observers in $(1+3)$ dimensions as $\mathscr{E} = \mathscr{E}^W + \mathscr{E}^R$, and then get the condition for entanglement harvesting (2.83) to be

$$\left(\frac{e^{-\frac{\pi\Delta E}{a_A}}}{1-e^{-\beta\Delta E}} + \frac{e^{\frac{\pi\Delta E}{a_A}}}{e^{\beta\Delta E}-1}\right)\left(\frac{e^{-\frac{\pi\Delta E}{a_B}}}{1-e^{-\beta\Delta E}} + \frac{e^{\frac{\pi\Delta E}{a_B}}}{e^{\beta\Delta E}-1}\right)\Upsilon(\Delta E, a_A, a_A)\Upsilon(\Delta E, a_B, a_B) < 4\left[\frac{e^{\frac{\pi\Delta E}{2}\left(\frac{1}{a_B}-\frac{1}{a_A}\right)}}{1-e^{-\beta\Delta E}} + \frac{e^{-\frac{\pi\Delta E}{2}\left(\frac{1}{a_B}-\frac{1}{a_A}\right)}}{e^{\beta\Delta E}-1} - \sinh\left\{\frac{\pi\Delta E}{2}\left(\frac{1}{a_B}-\frac{1}{a_A}\right)\right\}\right]^2 \Upsilon(\Delta E, a_A, a_B)^2. \tag{3.48}$$

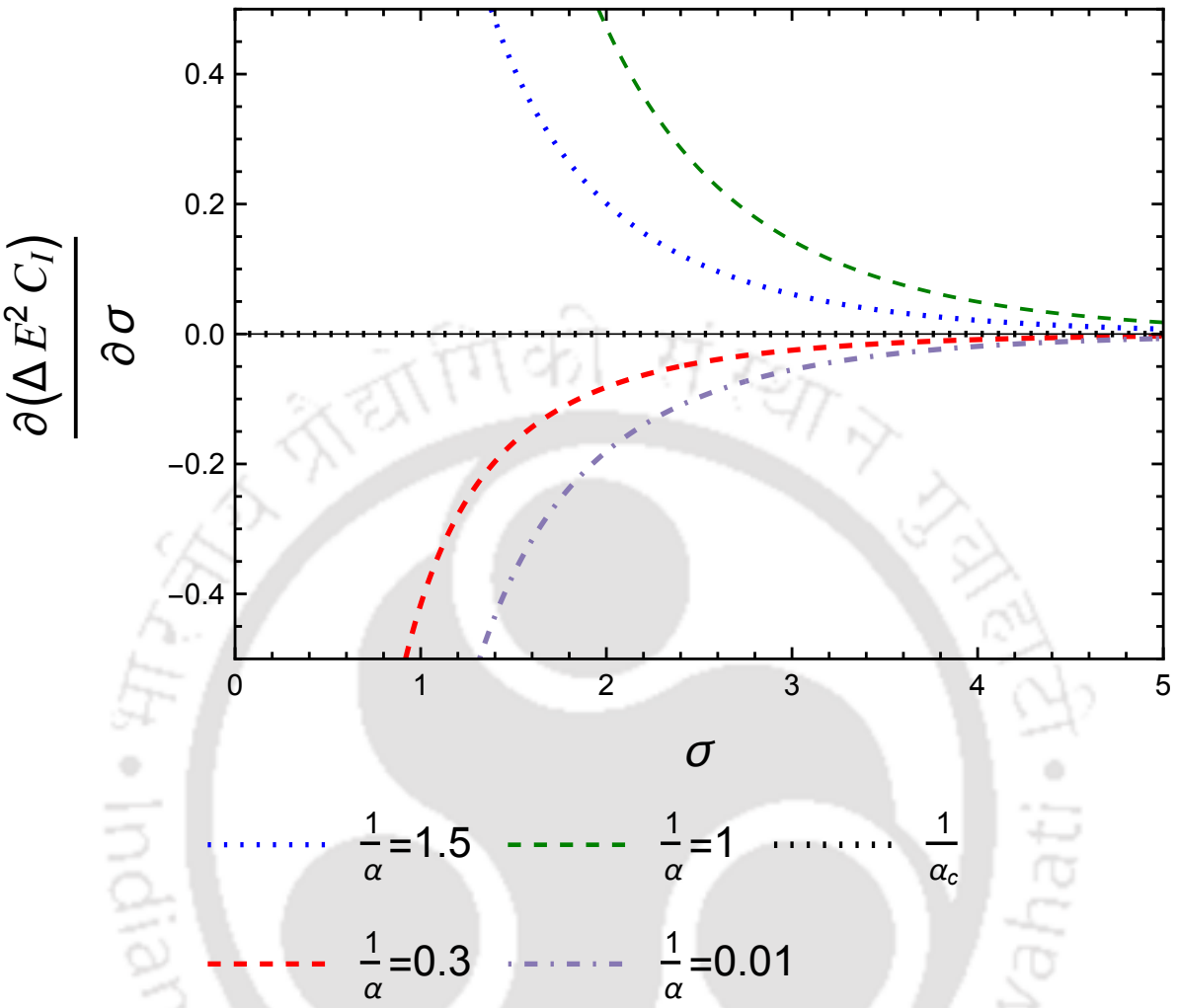

Figure 3.10: In $(1+1)$ dimensions the quantity $(\partial/\partial\sigma)\left(\Delta E^2 C_I\right)$ is plotted for two anti-parallelly accelerating detectors with respect to the inverse temperature of the thermal bath σ for equal magnitude of proper accelerations $\alpha_A = \alpha_B = \alpha$. The critical acceleration, where this quantity is σ independent, is $\alpha_c = 2.3854$.

Numerical analysis: – In Fig. 3.11 we have plotted the quantity $C_I = \left(|\mathscr{E}| - \sqrt{\mathscr{P}_A \mathscr{P}_B}\right)/\delta(0)$, which signifies the rate of concurrence per unit proper time, with respect to α_A for different fixed temperature of the thermal bath. On the other hand, in Fig. 3.12 and Fig. 3.13 we have plotted this C_I with respect to the inverse temperature of the thermal bath $\sigma = \beta\Delta E$ for different fixed α_A. From both of these figures we observe that higher temperature of the thermal bath results in a failure of the condition for entanglement harvesting, which is in agreement with the understandings gained from the $(1+1)$ dimensional analysis. However, the characteristics of the curves obtained from Fig. 3.11

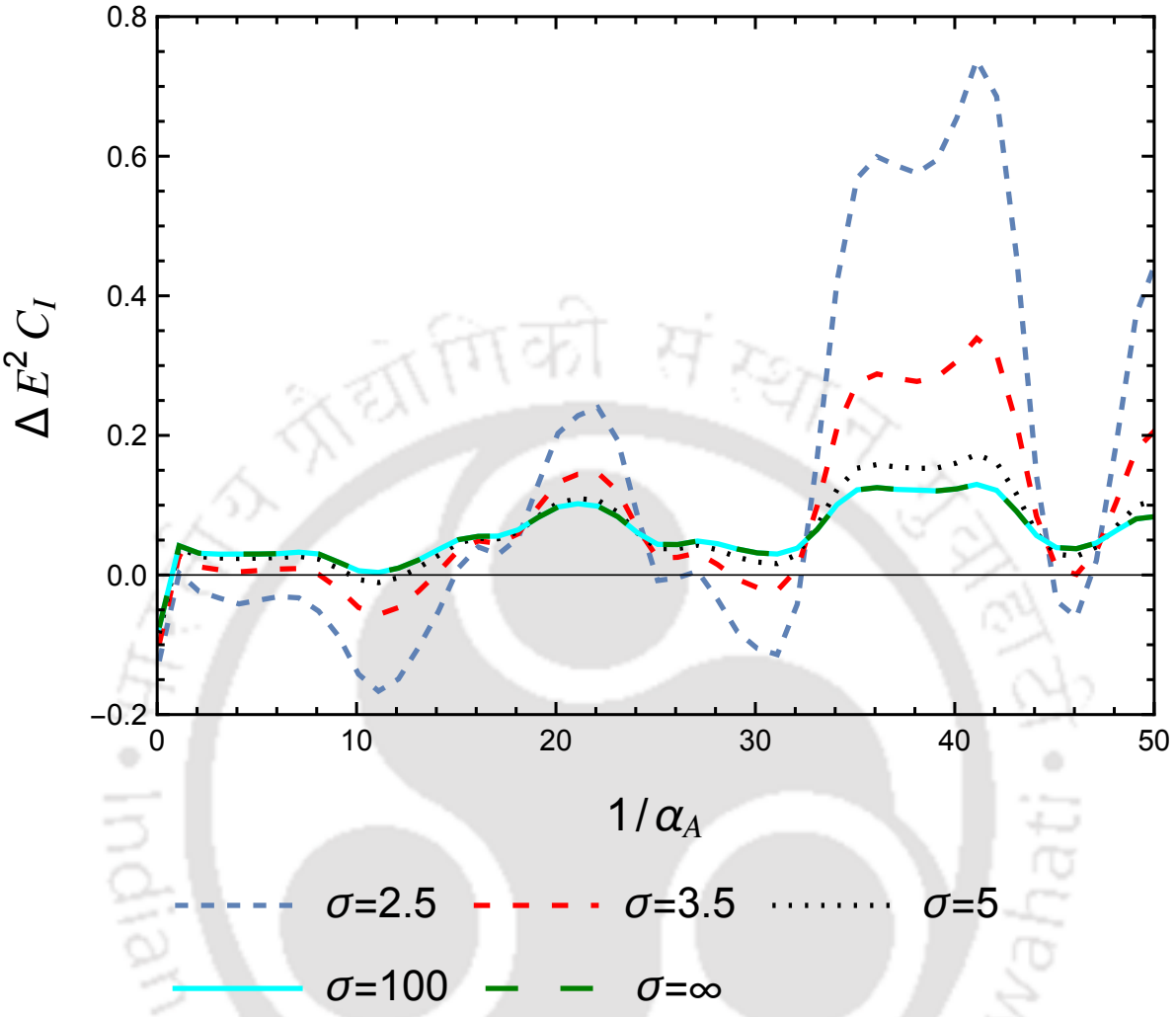

Figure 3.11: In $(1+3)$ dimensions the quantity $\Delta E^2 C_I$ is plotted for two anti-parallelly accelerating detectors with respect to the acceleration of the first detector α_A for different fixed σ. The other parameter is fixed at $\alpha_B = 1$.

are turbulent compared to the $(1+1)$ dimensional curves of Fig. 3.3 in similar situation. It is also noticed that unlike the $(1+1)$ dimensional case there are multiple transition points of α_A in curves of Fig. 3.11. After crossing each of these transition points the characteristics of C_I flips with respect to β, *i.e.,* in some of the regions, in between these transition points, C_I increases with increasing β, and in the neighboring regions C_I decreases with increasing β. In Fig. 3.14 and 3.15 we have plotted the derivative of C_I with respect to σ for varying σ and α_A to further confirm the positions of the transition points. Another intriguing thing to notice is that in $(1+1)$ dimensions for $\alpha_A \neq \alpha_B$ we observed that for a fixed temperature of the thermal field entanglement harvesting

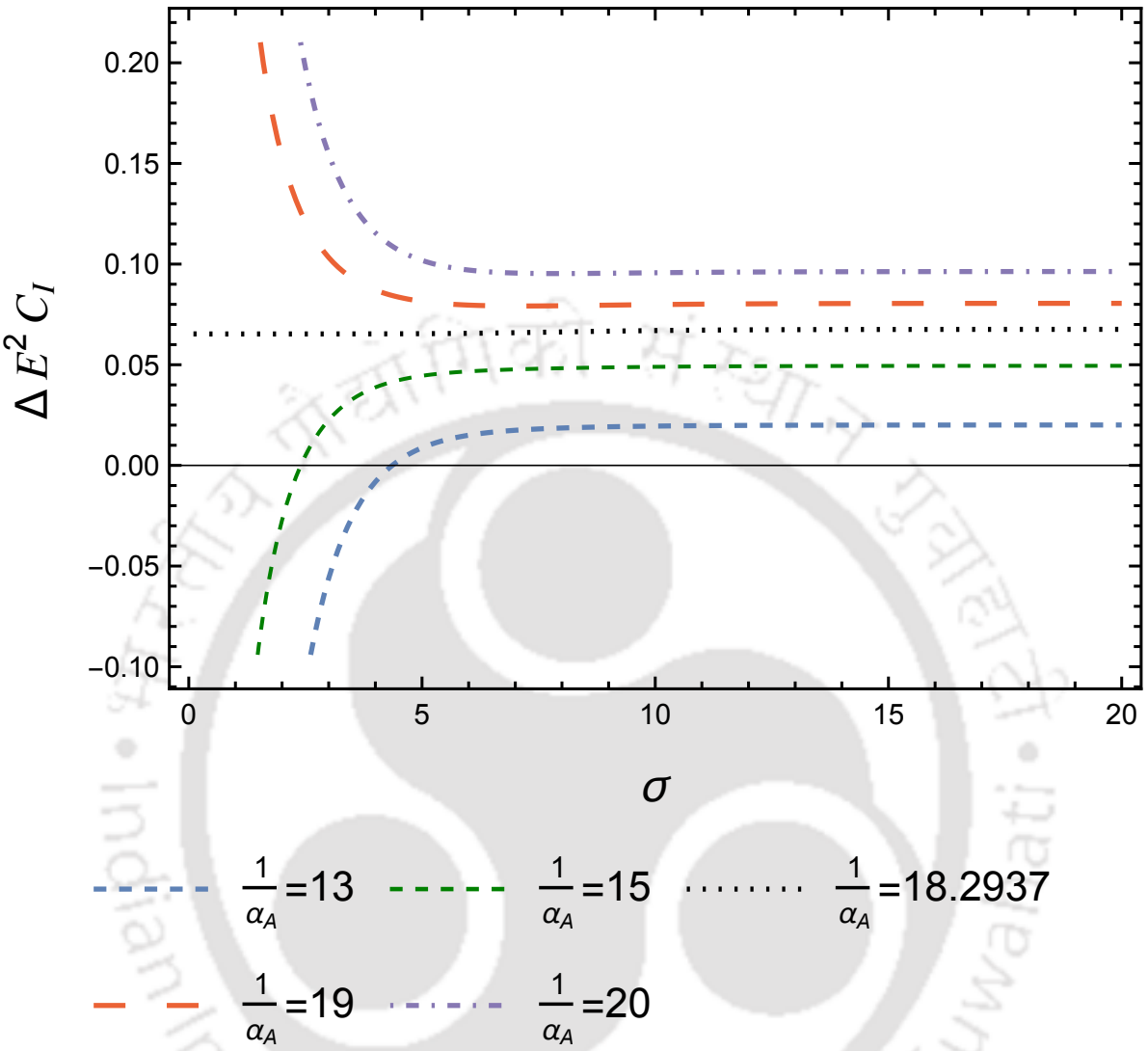

Figure 3.12: In $(1+3)$ dimensions the quantity $\Delta E^2 C_I$ is plotted for two anti-parallelly accelerating detectors with respect to the inverse temperature of the thermal bath σ for different fixed accelerations α_A. The other parameter is fixed at $\alpha_B = 1$.

is possible for any accelerations above a certain acceleration. However, here in $(1+3)$ dimensions this is not the case, as now entanglement harvesting is possible in discrete ranges of α_A for certain values of fixed temperatures of the thermal fields.

It is to be noted that in the equal magnitude of acceleration limit the second integral from Eq. (3.47) coming from the retarded Green's function vanishes and one is left with only $\mathscr{E} = \mathscr{E}^W$. In this particular case $a_A = a_B = a$, and the condition for entanglement harvesting from Eq. (3.48) becomes same as the one from the $(1+1)$ dimensional case

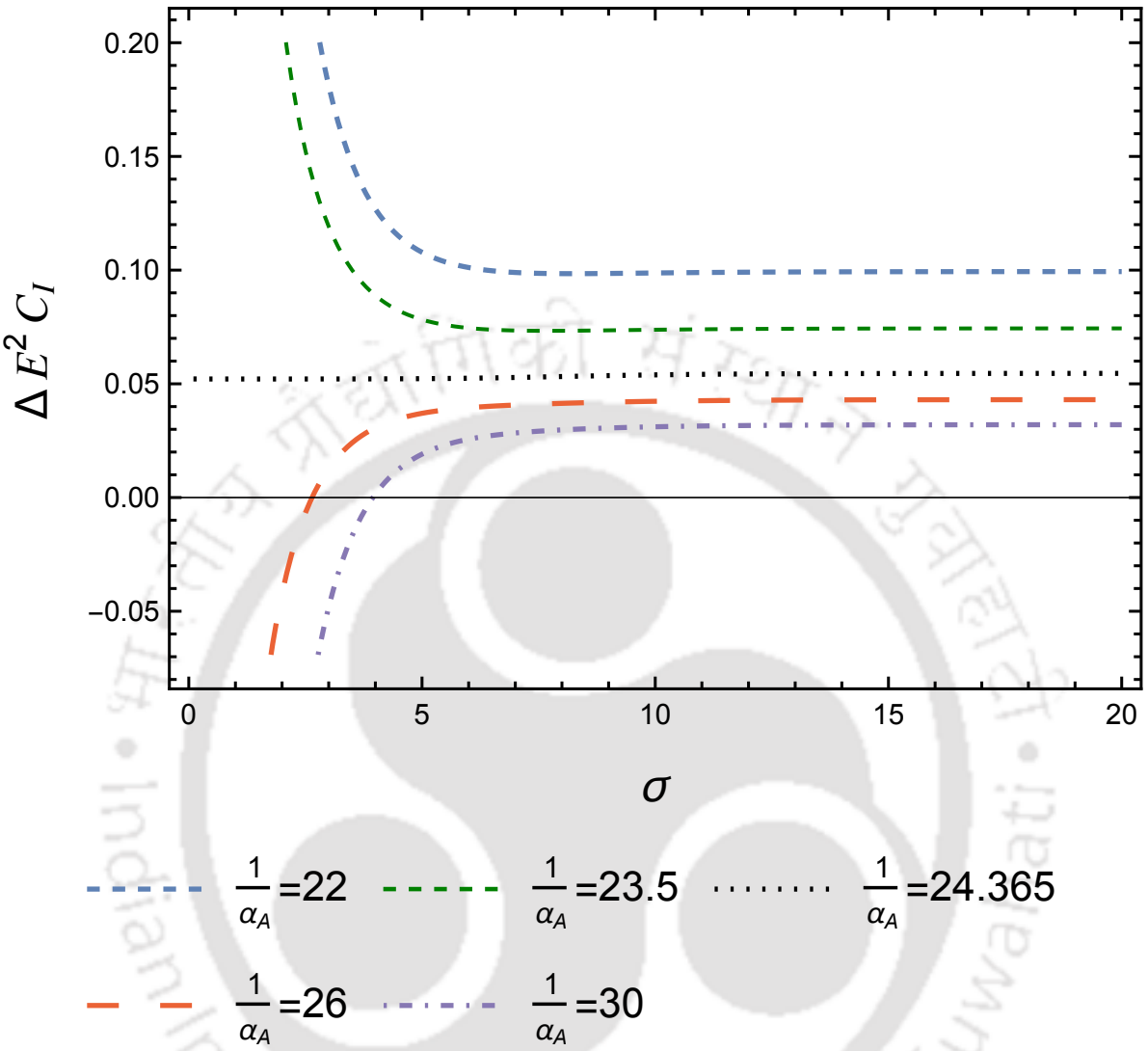

Figure 3.13: In $(1+3)$ dimensions the quantity $\Delta E^2 C_I$ is plotted for two anti-parallelly accelerating detectors with respect to the inverse temperature of the thermal bath σ for different fixed accelerations α_A, and α_B is fixed at $\alpha_B = 1$. Here the set of fixed α_A is different than the ones considered in Fig. 3.12. However, here also one can observe a transition in the nature of the curves as α_A changes.

of Eq. (3.44). Then it is expected that the entanglement measure C_I in $(1+3)$ should be qualitatively same as the one from $(1+1)$ dimensions. However, it is quantitatively different in the $(1+3)$ dimensional case compared to the $(1+1)$ dimensional case with equal acceleration. In Fig. 3.16 and 3.17 we have further plotted this quantity C_I signifying the concurrence, in this case in $(1+3)$ dimensions. Here also the concurrence shows similar characteristics as was observed in the $(1+1)$ dimensional case. From

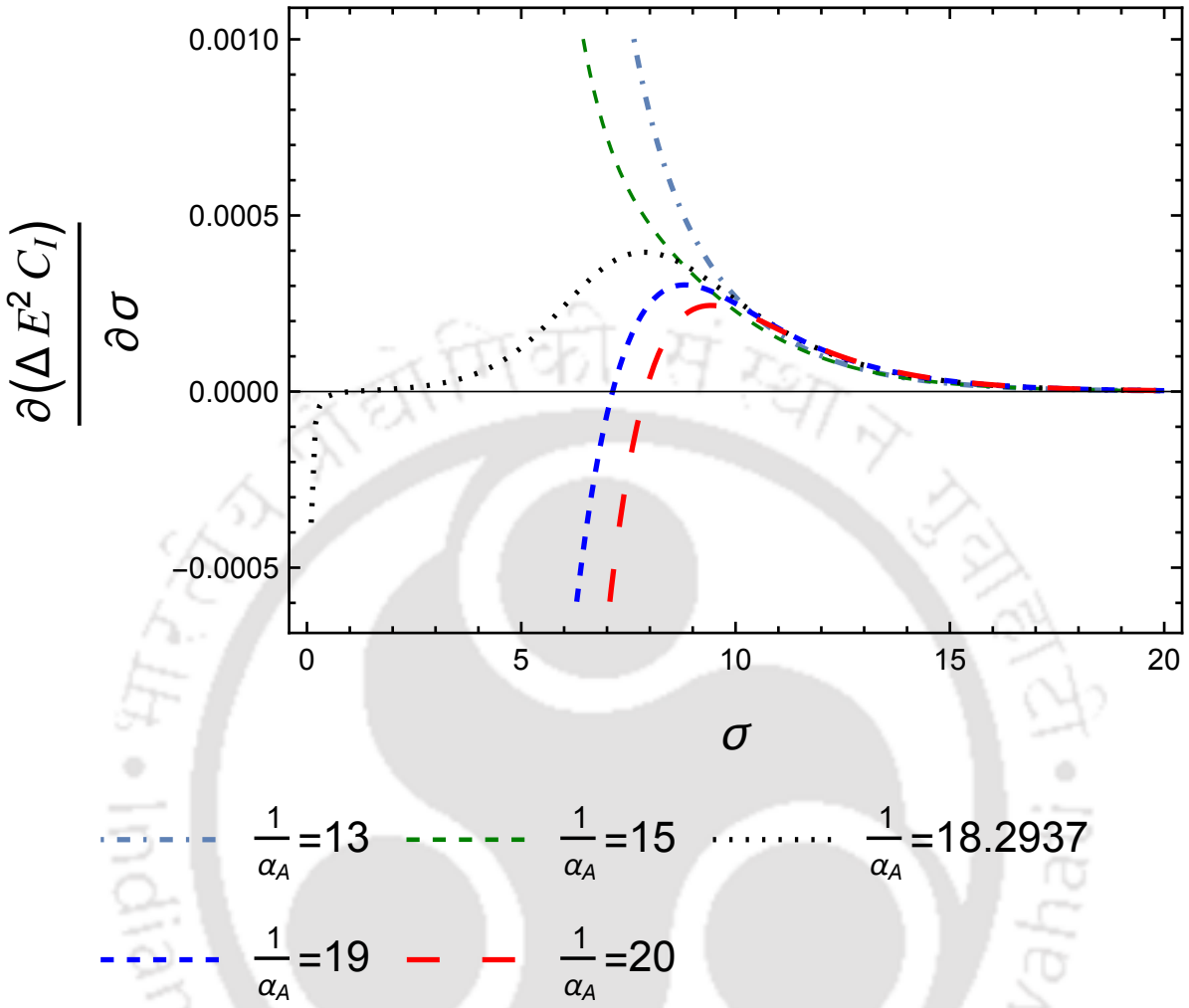

Figure 3.14: In $(1+3)$ dimensions the derivative with respect to σ of the quantity $(\partial/\partial\sigma)(\Delta E^2 C_I)$ is plotted for two anti-parallelly accelerating detectors for varying σ. The other parameters $\alpha_B = 1$ and α_A are fixed.

Fig. 3.17 it is clear that the temperature of the thermal bath diminishes the range of acceleration in which entanglement extraction is possible. However, it enhances the amount of concurrence above a certain value of acceleration thus enhancing the entanglement extraction in that region. Furthermore, in Fig. 3.18 and 3.19 we have plotted the derivative of C_I with respect to σ in this case for varying σ and α for the perception of α_c. It should be noted that in $(1+3)$ dimensions one is left out with only one transition point, contrary to multiple transition points in α_A from Fig. 3.11, when equal accelerations are considered.

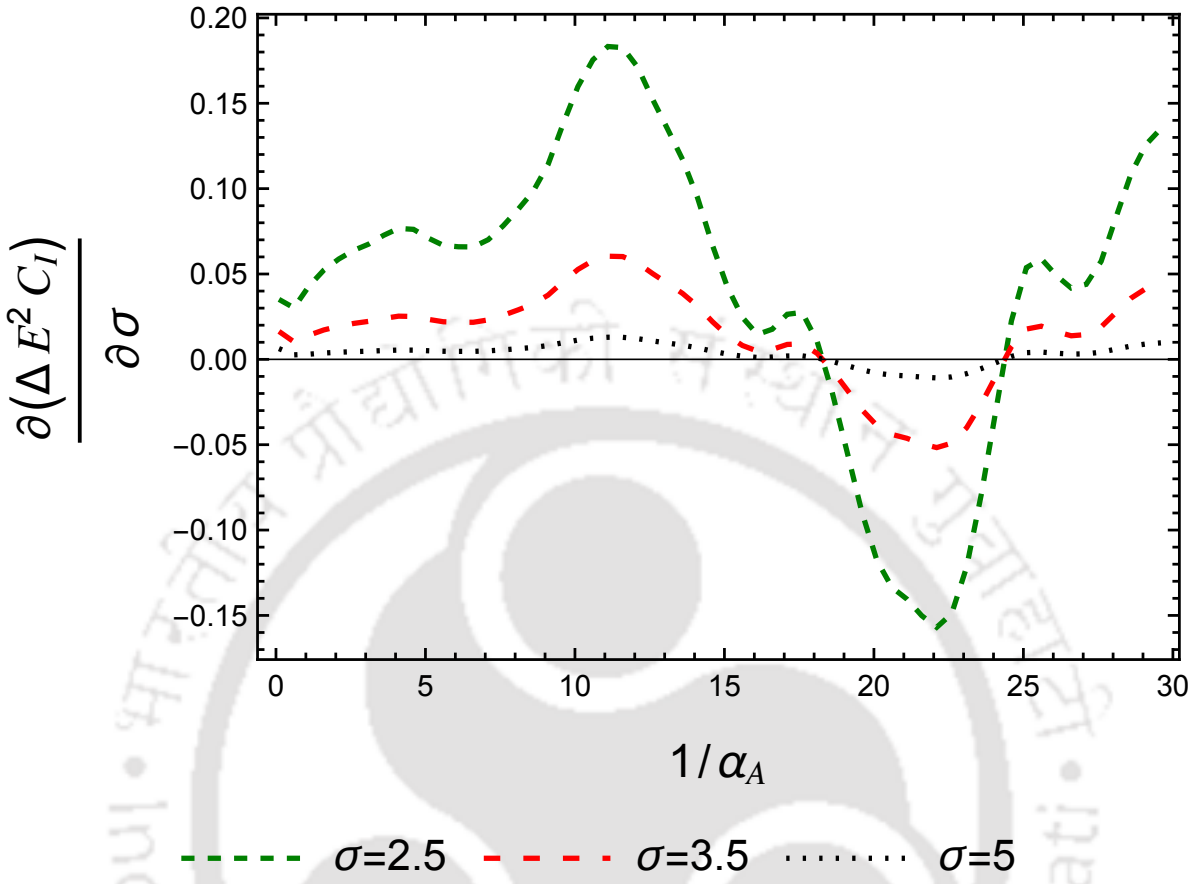

Figure 3.15: In $(1+3)$ dimensions the derivative with respect to σ of the quantity $(\partial/\partial\sigma)\left(\Delta E^2 C_I\right)$ is plotted for two anti-parallelly accelerating detectors for varying acceleration of the first detector α_A. The temperatures of the thermal bath σ and other parameter $\alpha_B = 1$ are fixed.

3.4 Mutual Information

In the last section, we have studied the quantum correlation between two detectors in terms of concurrence quantity. Now we will study the total correlation in the system *i.e.,* the entirety of classical and quantum correlations, between the two detectors A and B with the observers Alice and Bob is quantified by mutual information $\mathscr{M}$, defined as

$$\mathscr{M}(\rho_{AB}) \equiv S(\rho_A) + S(\rho_B) - S(\rho_{AB})\,, \tag{3.49}$$

where, $\rho_A \equiv Tr_B(\rho_{AB})$ and $\rho_B \equiv Tr_A(\rho_{AB})$ are the reduced density matrices corresponding to the detectors A and B, and $S(\rho) \equiv -Tr(\rho \ln \rho)$ is the von Neumann entropy corresponding to the state with ρ to be the density matrix. Using the expression of the density

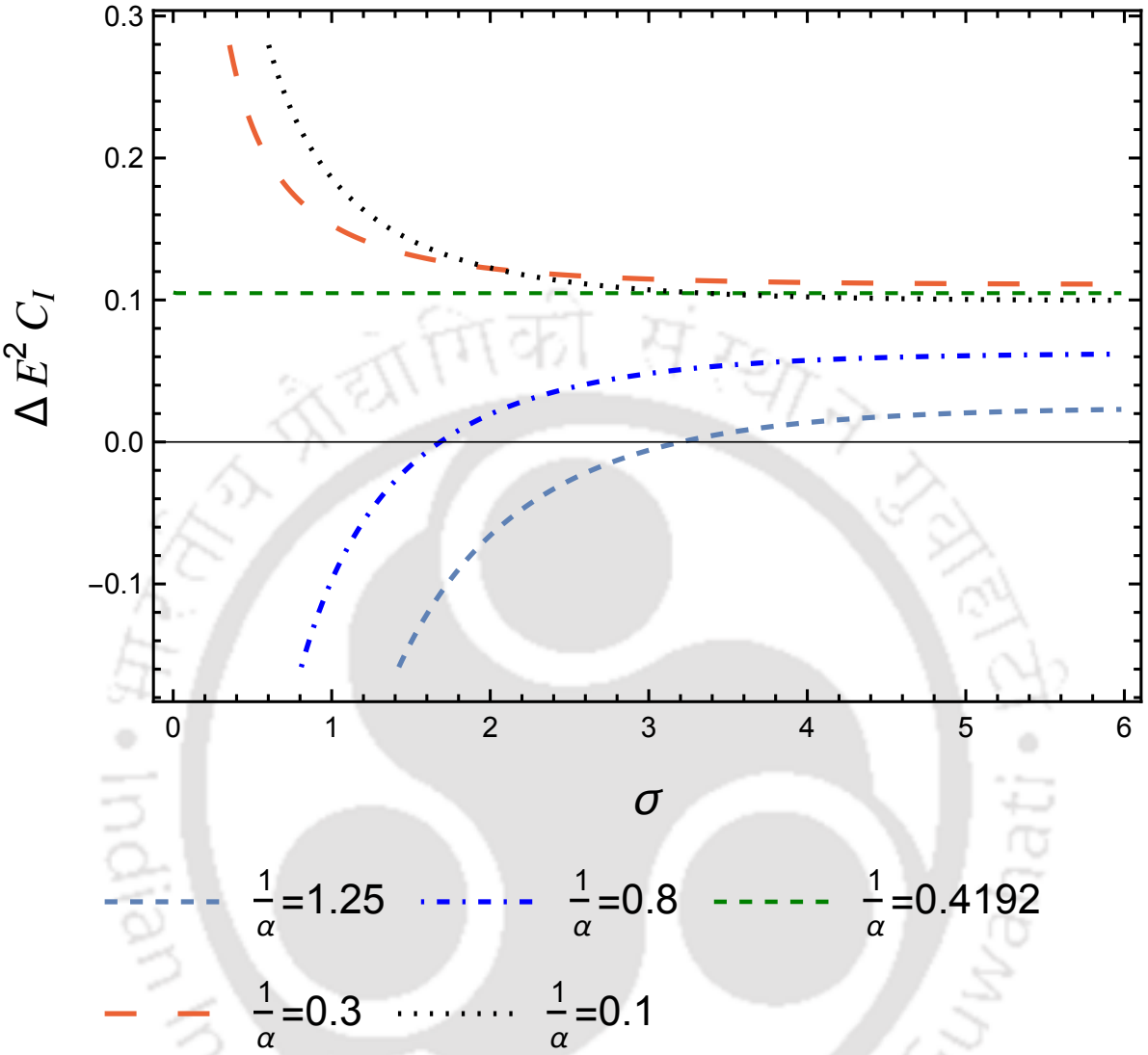

Figure 3.16: In $(1+3)$ dimensions the quantity $\Delta E^2 C_I$ is plotted for two anti-parallelly accelerating detectors with respect to the inverse temperature of the thermal bath σ for equal magnitude of proper accelerations, i.e., $\alpha_A = \alpha_B = \alpha$.

matrix at some later time from Eq. (2.68), and considering the couplings between the detectors and field to be the same for the two detectors $c_A = c_B = c$, one can express the mutual information of (3.49) as [212]

$$\mathscr{M}(\rho_{AB}) = c^2\left[\mathscr{P}_+ \ln \mathscr{P}_+ + \mathscr{P}_- \ln \mathscr{P}_- - \mathscr{P}_A \ln \mathscr{P}_A - \mathscr{P}_B \ln \mathscr{P}_B\right] + \mathscr{O}(c^4)\,, \tag{3.50}$$

where, the quantities $\mathscr{P}_\pm$ are given by

$$\mathscr{P}_\pm = \frac{1}{2}\left[\mathscr{P}_A + \mathscr{P}_B \pm \sqrt{(\mathscr{P}_A - \mathscr{P}_B)^2 + 4|\mathscr{P}_{AB}|^2}\right]. \tag{3.51}$$

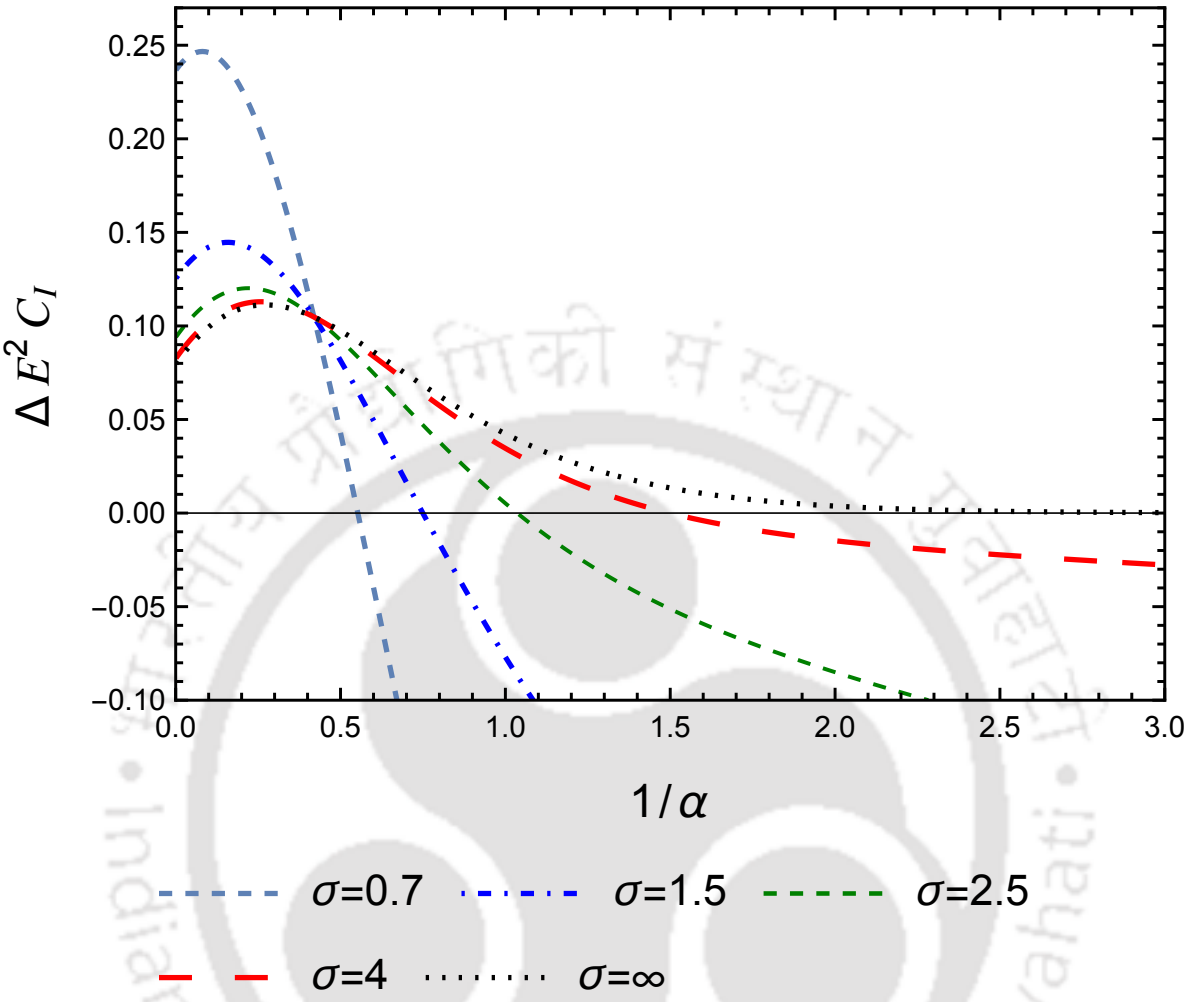

Figure 3.17: In $(1+3)$ dimensions the quantity $\Delta E^2 C_I$ is plotted for two anti-parallelly accelerating detectors with respect to $1/\alpha$ for fixed inverse temperatures of the thermal bath σ for equal magnitude of proper accelerations, i.e., $\alpha_A = \alpha_B = \alpha$.

A more useful quantity for our analysis is mutual information per unit time, can be defined as

$$M_I(\rho_{AB}) = \left[\mathscr{P}_+ \ln \mathscr{P}_+ + \mathscr{P}_- \ln \mathscr{P}_- - \mathscr{P}_A \ln \mathscr{P}_A - \mathscr{P}_B \ln \mathscr{P}_B\right]/\delta(0). \tag{3.52}$$

It should be mentioned that one may encounter situations when both the concurrence and mutual information are not simultaneously non-zero for a certain system. In that case when either only the concurrence or the mutual information is non-zero the correleation is found to be of quantum or classical origin respectively. Therefore, it becomes interesting to investigate both of these measures for the understanding of the nature of the correlation between the two detectors.

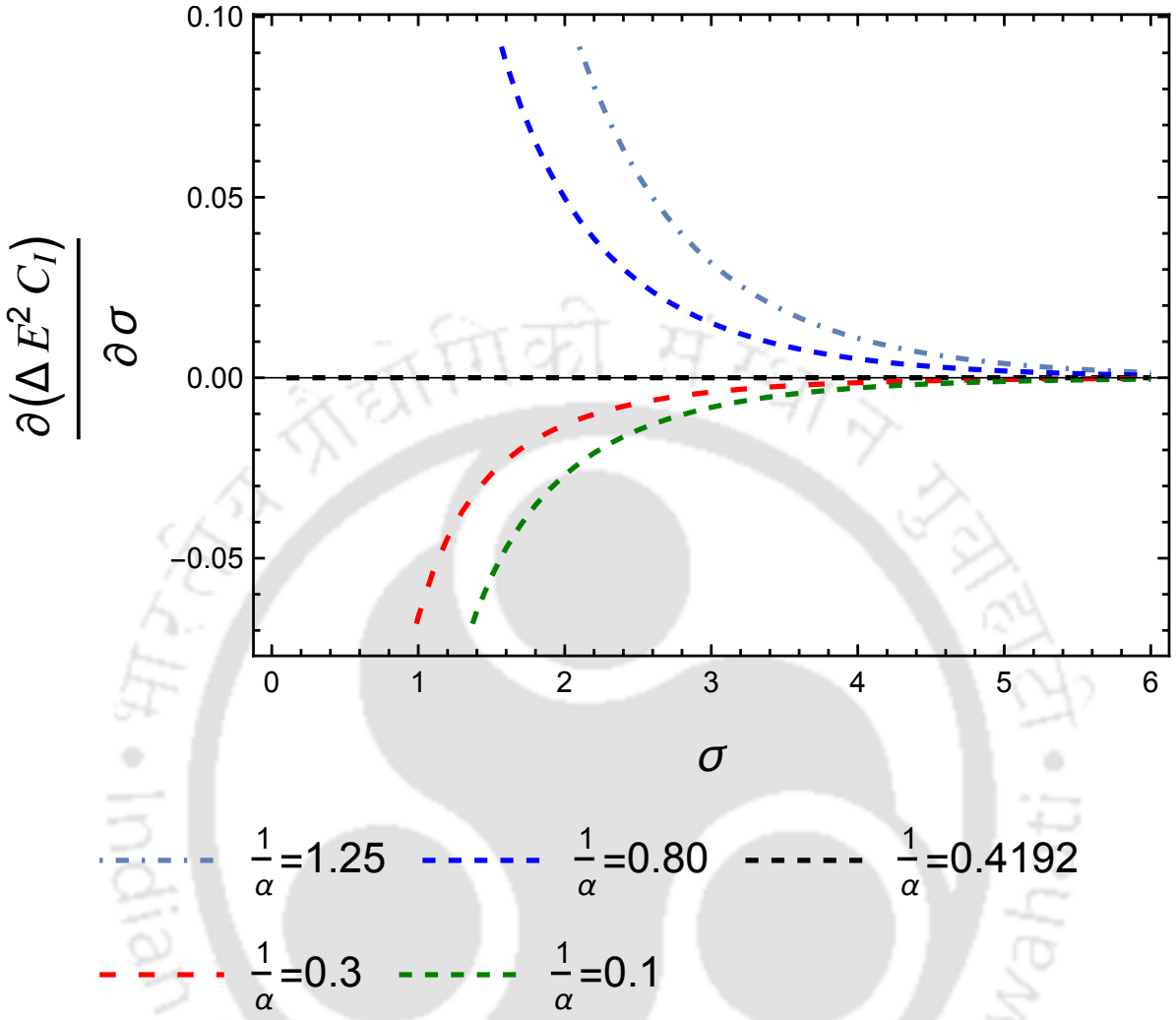

Figure 3.18: In $(1+3)$ dimensions the quantity $(\partial/\partial\sigma)\left(\Delta E^2 C_I\right)$ is plotted for two anti-parallelly accelerating detectors with respect to the inverse temperature of the thermal bath σ for equal magnitude of proper accelerations $\alpha_A = \alpha_B = \alpha$.

From Eq. (3.50) and (3.51) it is observed that the mutual information corresponding to the two accelerated detectors interacting with background thermal field can be estimated by estimating the quantities $\mathscr{P}_j$ and $\mathscr{P}_{AB}$. From Eq. (3.25) and (3.28) one can find out the expressions of $\mathscr{P}_j$ in $(1+1)$ and $(1+3)$ dimensions corresponding to observers accelerated parallelly or anti-parallelly. Then here we only have to find out the expression of $\mathscr{P}_{AB}$ to understand the nature of the mutual information for the considered detector pair. In particular we have to estimate $\mathscr{P}_{AB}$ in Eq. (3.20). If this quantity turns out to be zero, then $\mathscr{P}_{\pm}$ become $\mathscr{P}_A$ and $\mathscr{P}_B$. Therefore, the mutual information $\mathscr{M}(\rho_{AB})$ in Eq.

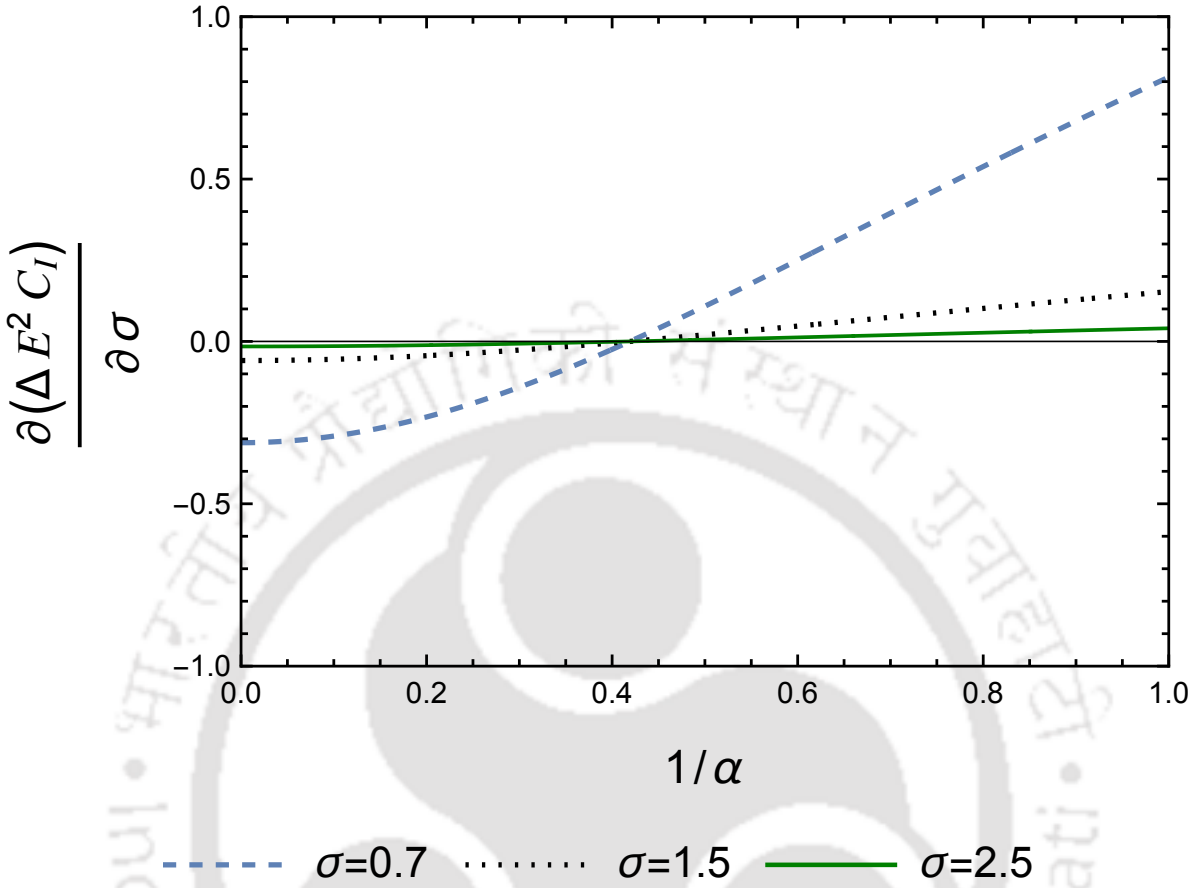

Figure 3.19: In $(1+3)$ dimensions the quantity $(\partial/\partial\sigma)\left(\Delta E^2 C_I\right)$ is plotted for two anti-parallelly accelerating detectors with respect to the equal magnitude of proper accelerations $\alpha_A = \alpha_B = \alpha$ for fixed inverse temperature of the thermal bath σ.

(3.50) vanishes. We shall first consider the prallelly and then anti-parallelly accelerated detectors to estimate these quantities.

3.4.1 Parallel acceleration

3.4.1.1 $(1+1)$ dimensions

We consider the Wightman function of Eq. (3.15) corresponding to parallelly accelerated detectors interacting with thermal fields, and consider a change of variables $\tilde{v} = \tau_B + \tau_A$

and $\tilde{u} = \tau_B - \tau_A$ to evaluate the integral $\mathscr{P}_{AB}$ as

$$\mathscr{P}_{AB} = \int_{-\infty}^{\infty} d\tau_B \int_{-\infty}^{\infty} d\tau_A \; e^{i(\Delta E^A \tau_A - \Delta E^B \tau_B)} \; G^{\beta}_{W_R}(x_B, x_A)$$
$$= \delta\left(\frac{\Delta E^A - \Delta E^B}{\sqrt{a_A a_B}}\right) \frac{\pi}{\Delta\widetilde{E}\sqrt{a_A a_B \sinh\frac{\pi\Delta\widetilde{E}}{a_B}\sinh\frac{\pi\Delta\widetilde{E}}{a_A}}} \left[\frac{e^{-\frac{\pi\Delta\widetilde{E}}{2}\left(\frac{1}{a_B}+\frac{1}{a_A}\right)}}{1-e^{-\beta\Delta\widetilde{E}}} + \frac{e^{\frac{\pi\Delta\widetilde{E}}{2}\left(\frac{1}{a_B}+\frac{1}{a_A}\right)}}{e^{\beta\Delta\widetilde{E}}-1}\right], \quad (3.53)$$

where $\Delta\widetilde{E} = (\Delta E^B + \Delta E^A)/2$. To evaluate this quantity, we first performed the $\tilde{u}$-integral, then ω-integral is performed. The Dirac delta function comes from the $\tilde{v}$-integration. It is to be noted that when $\Delta E^B \neq \Delta E^A$, due to the Dirac delta distribution $\delta\left(\frac{\Delta E^A - \Delta E^B}{\sqrt{a_A a_B}}\right)$ in front of the expression (3.53), the quantity $\mathscr{P}_{AB}$ vanishes. This leads to vanishing mutual information.

One has non vanishing mutual information only when $\mathscr{P}_{AB} \neq 0$, *i.e.,* when $\Delta E^B = \Delta E^A$. We get $\Delta\widetilde{E} = \Delta E$ by considering $\Delta E^B = \Delta E^A = \Delta E$. In that case it is observed that there will be a multiplicative $\delta(0)$ term in the expression of $\mathscr{P}_{AB}$ similar to the case of $\mathscr{P}_j$ of Eq. (3.25). Therefore, the final expression of the quantity M_I can be evaluated using Eq. (3.25), (3.53), (3.51) and (3.52). In Fig. 3.20 we have plotted the rate of mutual information with respect to the temperature of the thermal field $T^{(f)}$ ($\sim 1/\sigma$), which shows that with increasing temperature the mutual information increases. From this figure it is also observed that with increasing acceleration of the first detector (denoted by α_A) the mutual information decreases.

3.4.1.2 $(1+3)$ dimensions

We consider the positive frequency Wightman function of Eq. (3.17) for the estimation of the quantity $\mathscr{P}_{AB}$ in $(1+3)$ dimensions. Following the earlier analysis, we obtain

$$\mathscr{P}_{AB} = \int_{-\infty}^{\infty} d\tau_B \int_{-\infty}^{\infty} d\tau_A \; e^{i(\Delta E^A \tau_A - \Delta E^B \tau_B)} \; G^{\beta}_{W_R^{3D}}(x_B, x_A)$$
$$= \delta\left(\frac{\Delta E^A - \Delta E^B}{\sqrt{a_A a_B}}\right) \frac{1}{\pi a_A a_B} \Upsilon\left(\Delta\widetilde{E}, a_A, a_B\right) \left[\frac{e^{-\frac{\pi\Delta\widetilde{E}}{2}\left(\frac{1}{a_B}+\frac{1}{a_A}\right)}}{1-e^{-\beta\Delta\widetilde{E}}} + \frac{e^{\frac{\pi\Delta\widetilde{E}}{2}\left(\frac{1}{a_B}+\frac{1}{a_A}\right)}}{e^{\beta\Delta\widetilde{E}}-1}\right]. \quad (3.54)$$

Here also $\Delta\widetilde{E} = (\Delta E^B + \Delta E^A)/2$, and for $\Delta E^B \neq \Delta E^A$ Dirac delta distribution $\delta\left(\frac{\Delta E^A - \Delta E^B}{\sqrt{a_A a_B}}\right)$ in (3.54) provides vanishing $\mathscr{P}_{AB}$. This leads to vanishing mutual information.

The mutual information is non vanishing only when $\Delta E^B = \Delta E^A$. The final expression of the quantity M_I can be evaluated using Eq. (3.28), (3.54), (3.51) and (3.52). We plotted the rate of mutual information with respect to the temperature of the thermal field $T^{(f)}$ ($\sim 1/\sigma$) in Fig. 3.21. From this figure we conclude that in $(1+3)$ dimensions also

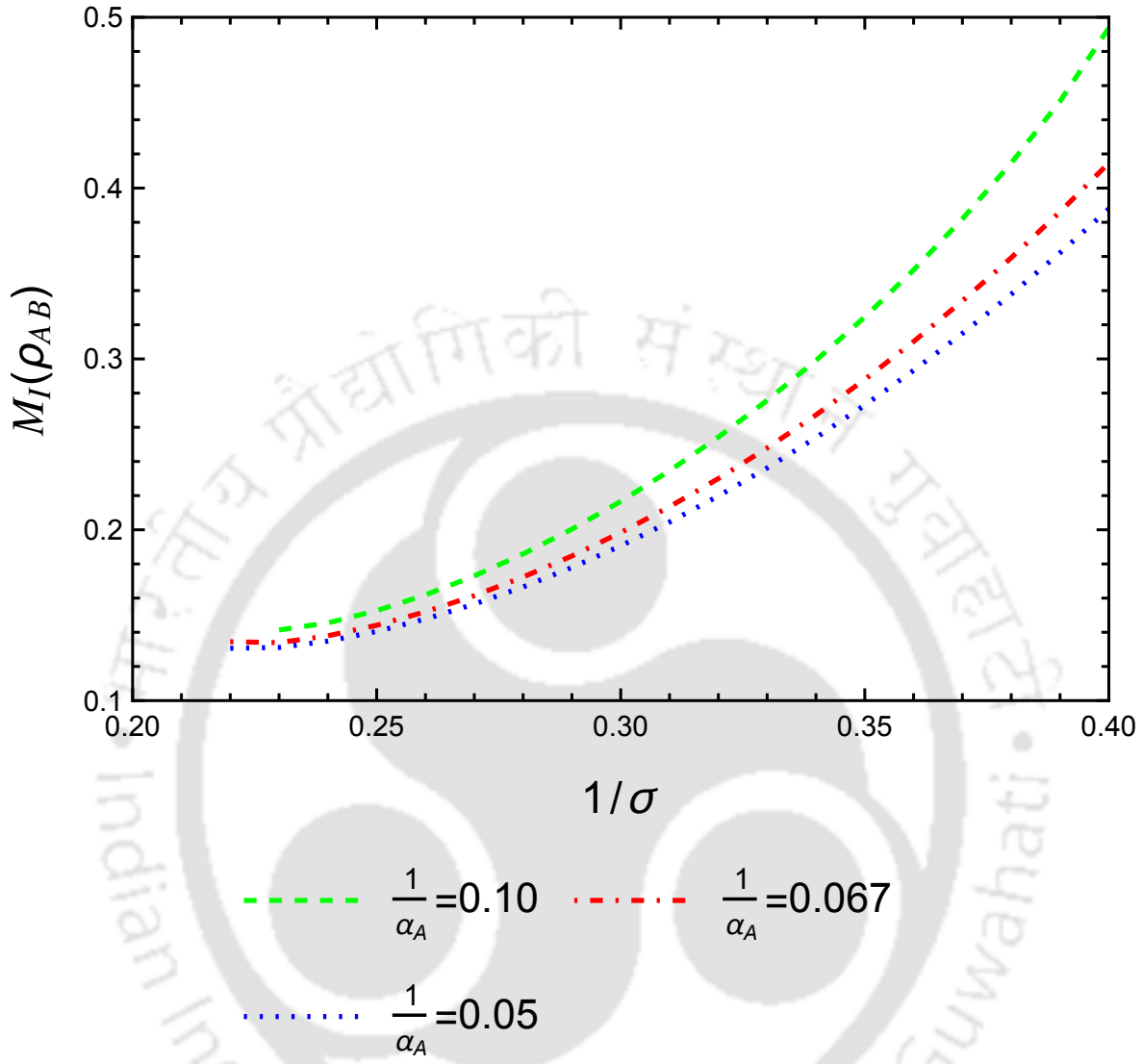

Figure 3.20: In $(1+1)$ dimensions the quantity $M_I(\rho_{AB})$ is plotted, which signifies the mutual information, for two parallelly accelerating detectors with respect to the temperature of the thermal field $T^{(f)}(\sim 1/\sigma)$ for different fixed proper accelerations α_A, where $\alpha_B = 1$.

the mutual information increases with increasing temperature of the thermal field and decreasing acceleration of the first detector (denoted by α_A).

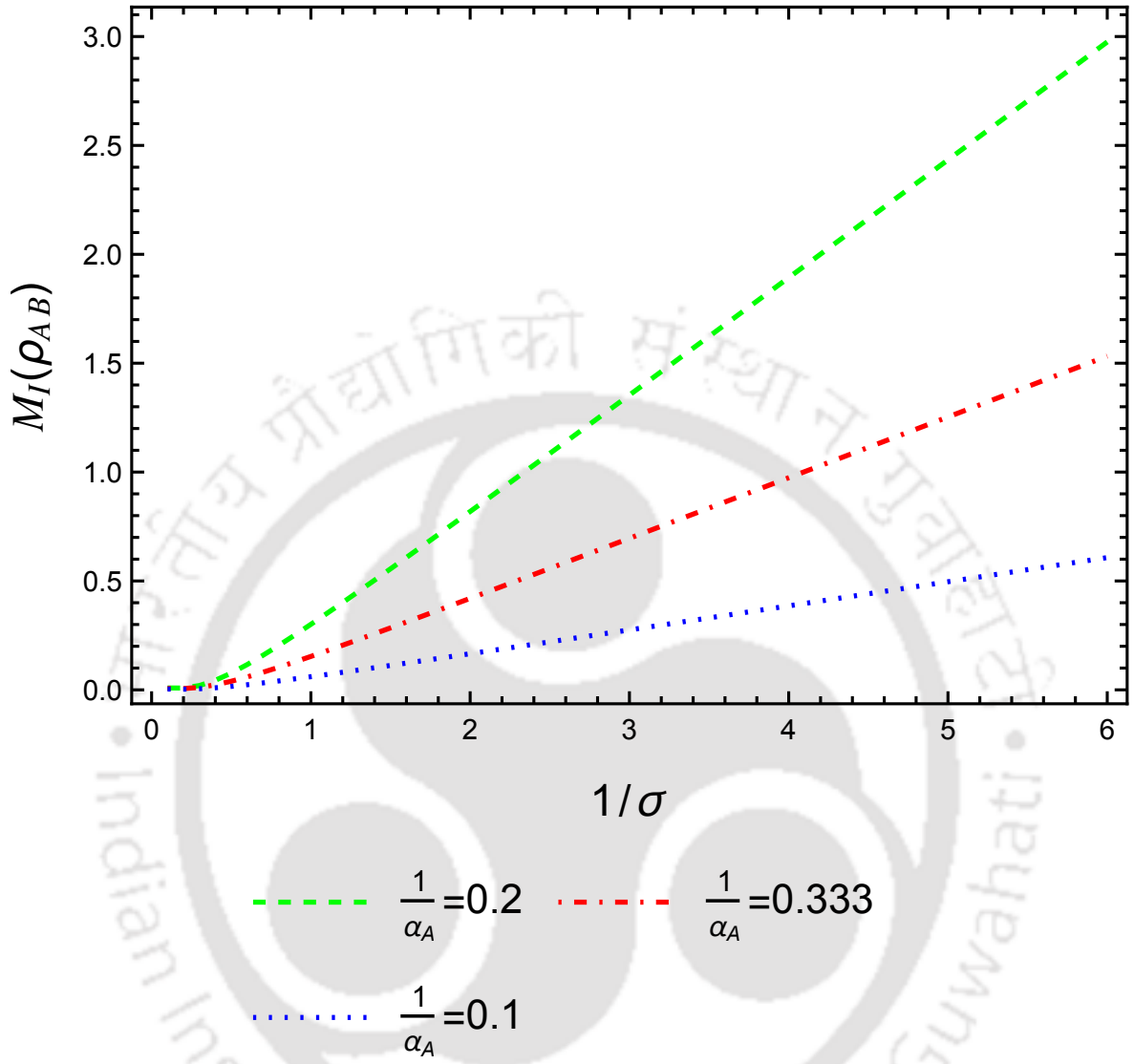

Figure 3.21: In $(1+3)$ dimensions the quantity $M_I(\rho_{AB})$ is plotted, which signifies the mutual information, for two parallelly accelerating detectors with respect to the temperature of the thermal field $T^{(f)}(\sim 1/\sigma)$ for different fixed proper accelerations α_A, where $\alpha_B = 1$.

3.4.2 Anti-parallel acceleration

3.4.2.1 $(1+1)$ dimensions

We consider the Wightman function from Eq. (3.16) corresponding to two anti-parallelly accelerated observers in $(1+1)$ dimensional thermal bath, and a change of variables $\tilde{v} = \tau_B + \tau_A$ and $\tilde{u} = \tau_B - \tau_A$ to evaluate the quantity $\mathscr{P}_{AB}$. Following the earlier analysis,

one can express this integral $\mathscr{P}_{AB}$ as

$$\mathscr{P}_{AB} = \int_{-\infty}^{\infty} d\tau_B \int_{-\infty}^{\infty} d\tau_A \; e^{i(\Delta E^A \tau_A - \Delta E^B \tau_B)} \; G^{\beta}_{W_{LR}}(x_B, x_A)$$
$$= \delta\left(\frac{\Delta E^A + \Delta E^B}{\sqrt{a_A a_B}}\right) \frac{\pi}{\Delta\breve{E}\sqrt{a_A a_B \sinh\frac{\pi\Delta\breve{E}}{a_B}\sinh\frac{\pi\Delta\breve{E}}{a_A}}} \left[\frac{e^{-\frac{\pi\Delta\breve{E}}{2}\left(\frac{1}{a_B}-\frac{1}{a_A}\right)}}{1-e^{-\beta\Delta\breve{E}}} + \frac{e^{\frac{\pi\Delta\breve{E}}{2}\left(\frac{1}{a_B}-\frac{1}{a_A}\right)}}{e^{\beta\Delta\breve{E}}-1}\right], \quad (3.55)$$

where $\Delta\breve{E} = (\Delta E^B - \Delta E^A)/2$. Then it is obvious that for $\Delta E^A > 0$ and $\Delta E^B > 0$ the Dirac delta distribution sitting in front of this expression $\delta\left(\frac{\Delta E^A + \Delta E^B}{\sqrt{a_A a_B}}\right)$ will provide a vanishing contribution. Thus $\mathscr{P}_{AB}$ vanishes. This leads to the expression of mutual information from (3.50) to be vanishing upto $\mathscr{O}(c^2)$. This result persuades one to conclude that the mutual information corresponding to two anti-parallelly accelerated detectors in a thermal bath is zero in $(1+1)$ dimensions.

3.4.2.2 $(1+3)$ dimensions

We consider the positive frequency Wightman function (3.18) corresponding to anti-parallelly accelerated observers for the estimation of the quantity $\mathscr{P}_{AB}$ in $(1+3)$ dimensions. Following the earlier analysis, we obtain

$$\mathscr{P}_{AB} = \int_{-\infty}^{\infty} d\tau_B \int_{-\infty}^{\infty} d\tau_A \; e^{i(\Delta E^A \tau_A - \Delta E^B \tau_B)} \; G^{\beta}_{W^{3D}_{LR}}(x_B, x_A)$$
$$= \delta\left(\frac{\Delta E^A + \Delta E^B}{\sqrt{a_A a_B}}\right) \frac{1}{\pi a_A a_B} \Upsilon\left(\Delta\breve{E}, a_A, a_B\right) \left[\frac{e^{-\frac{\pi\Delta\breve{E}}{2}\left(\frac{1}{a_B}-\frac{1}{a_A}\right)}}{1-e^{-\beta\Delta\breve{E}}} + \frac{e^{\frac{\pi\Delta\breve{E}}{2}\left(\frac{1}{a_B}-\frac{1}{a_A}\right)}}{e^{\beta\Delta\breve{E}}-1}\right]. \quad (3.56)$$

Here also $\Delta\breve{E} = (\Delta E^B - \Delta E^A)/2$ and similar to the $(1+1)$ dimensional case the Dirac delta distribution $\delta\left(\frac{\Delta E^A + \Delta E^B}{\sqrt{a_A a_B}}\right)$ sitting in front of this expression will provide a vanishing contribution. This leads to a vanishing $\mathscr{P}_{AB}$ and in turn vanishing mutual information upto $\mathscr{O}(c^2)$ from (3.50). Then in $(1+3)$ dimensions also one can conclude that the mutual information corresponding to two anti-parallelly accelerated detectors in a thermal bath is zero.

3.5 Summary and Discussions

The possibility of constructing a plausible experimental setup in contact with a thermal bath is much higher, as, in nature, the background is thermal than a purely non-thermal field vacuum. Therefore it is much more relevant to understand realistic situations in our surroundings to study physical phenomena in the presence of a thermal bath or by

considering the thermal fields. We have considered studying entanglement harvesting with two accelerated Unruh-DeWitt detectors interacting with a background thermal massless scalar field in this work. We have constructed the relevant Green's functions corresponding to accelerated observers in thermal bath considering the Rindler modes with the vacuum for the Unruh modes to avoid dealing with Wightman functions which are not time translational invariant. We used the prescription of [216] for constructing the thermal Green's functions. It is observed that for zero temperature of the thermal bath, *i.e.,* in the limit $\beta \to \infty$, in both $(1+1)$ and $(1+3)$ dimensions considering the equal magnitude of accelerations for the two observers but moving anti-parallelly, we always get the condition for entanglement harvesting to be satisfied. It ensures that entanglement extraction is possible for any finite non-zero acceleration in zero temperature background, which is in fact known from the earlier works of [99].

Furthermore, for non-zero temperature of the thermal bath with equal magnitude of acceleration of the anti-parallelly accelerated observers in both $(1+1)$ and $(1+3)$ dimensions we get identical conditions for entanglement harvesting (Eq. (2.83)). The quantity C_I signifying concurrence also shows similar behavior in $(1+1)$ and $(1+3)$ dimensions, which can be observed from Fig. 3.7, 3.8 and 3.16, 3.17. An interesting fact we noticed from Fig. 3.8 and 3.17 is that with increasing temperature of the thermal bath (decreasing β or σ), the range of acceleration, in which entanglement can be harvested, is decreasing, which is in agreement with the results of previous works [211, 212]. We observe that with the higher temperature of the thermal bath, higher acceleration is needed to initiate entanglement harvesting. However, once for a certain temperature, entanglement harvesting starts with some initial acceleration in this system; it keeps on harvesting for all other higher accelerations. On the other hand, above a certain critical acceleration $a = a_c$ we see the amount of entanglement harvested, denoted by concurrence, to be increasing with increasing temperature of the thermal bath, showing a characteristic opposite compared to the region below $a = a_c$, which is like a phase transition.

We also observe in $(1+1)$ dimensions from Eq. (3.36) and (3.40) that for $a_A = a_B = a$ and in the limit of $a \to 0$ the whole quantity $\mathscr{E}$ without the multiplicative delta distribution vanishes, making the condition for entangle extraction to break down. Then it is obvious that in the requirement of entanglement harvesting an accelerated observer and a static observer in thermal bath do not act in equal footing.

In particular it is observed that for $a_A \neq a_B$, the Retarded Green's function has a non-zero contribution. However, when $a_A = a_B$ the contributions from $G_F(x'_B, x_A)$ and

$G_W(x'_B, x_A)$ are the same. Finally it is to be noticed that when $a_A \neq a_B$, by observing the plots of C_I with respect to the acceleration of the first detector, it is possible to distinguish between the cases of $(1+1)$ and $(1+3)$ dimensions. Notably, in $(1+1)$ dimensions the curves of fixed σ (Fig. 3.3) shows monotonic nature, while in $(1+3)$ dimensions (Fig. 3.11) this is not the case with various peaks and valleys. In $(1+3)$ dimensions this results in multiple transition points of accelerations a_A between which the nature of concurrence with respect to the temperature of the thermal bath flips compared to the adjacent regions, also restricting the entanglement harvesting to discrete ranges of acceleration a_A for certain fixed temperature of the thermal bath.

An investigation of mutual information among the detectors has also been done in this chapter. We found that this vanishes for the anti-parallel situation whereas it is non-vanishing for parallel case. In the later situation, mutual information increases with the increase in background field temperature while it decreases with the increase of first detector's proper acceleration.

We want to mention here a nature of the curves in Fig. 3.8 and Fig. 3.17 which we did not discuss in the main text. In the equal acceleration case $a_A = a_B$ in both $(1+1)$ and $(1+3)$ dimensions it is observed that in very high acceleration regime the entanglement extraction rate tends to decrease with increasing acceleration. The possible reason can be as follows. When the acceleration of the detector is very large (i.e. $a_A \to \infty$), the detector moves very near to null surface denoted by $x = -t$ and $x = t$ and also feels a very high temperature due to its acceleration (temperature is given by Unruh expression $a/2\pi$). In this regime the thermal bath due to acceleration becomes equally relevant along with the real thermal bath on the nature of entanglement harvesting. Since we already observed that temperature can reduce the entanglement between the detectors, the presence of both the temperatures may play the role in the decreasing nature of concurrence. This is happening in very high acceleration regime as there the Unruh temperature also becomes appreciable to affect entanglement harvesting. So in this regime acceleration is showing its double standards – in one side it is helping in entanglement, but in other side it is also suppressing this phenomenon. On the other hand in earlier accelerations, the Unruh temperature is not so appreciable to give any effect on entanglement harvesting. Therefore there the acceleration plays only the role in helping entanglement. In this regard we point out that this reason is only a suggestive one. To find any conclusive explanation further investigation is needed.

Finally we mention that in this paper we deeply investigated the effect of background temperature on the harvesting of two uniformly accelerated detectors. As we mentioned

this situation mimics much more realistic situation and hence the results have practical importance. As we mentioned above, the background temperature introduces several interesting noticeable features which are completely absent when the temperature is taken to be zero. Therefore we feel that the present study is very important in the context of entanglement harvesting between the observers through their interaction with the background quantum fields and helps to progress the aforesaid subject.

CHAPTER 4

ACCELERATED OBSERVERS IN PRESENCE OF REFLECTING BOUNDARIES

4.1 Introduction and Motivation

Quantum entanglement is one of the predictions of quantum theory, which shows fascinating nonlocal properties. Two observers can be entangled, even if they are spacelike separated. This phenomenon is crucial to many quantum information theoretic processes, such as quantum teleportation [60–63], cryptography [64, 66], and computation [67]. In the last chapter, we have seen that two initially uncorrelated detectors can extract entanglement from the field's vacuum state. We observed that for lower accelerations, which are much more achievable in experimental setups, entanglement harvesting due to acceleration is suppressed due to background temperature. It is known that the higher the degree of entanglement between the atoms or detectors, the higher the probability of experimental detection. Therefore, it is natural to ask how one may enhance the entanglement harvesting between the accelerated detectors. It is well known that modifying the field's density of modes can significantly influence the detector's transition rate [198, 222]. It can be done by using cavity systems or reflecting boundaries, where the field modes satisfy the Dirichlet boundary conditions. Hence, it is natural to ask how this boundary can influence entanglement harvesting. In this chapter, we will investigate the influence of reflecting boundaries on entanglement harvesting between two accelerated detectors. We will primarily focus on the possibility of enhancement

of entanglement due to single and double boundaries compared to free space entanglement harvesting. In a recent study [117], the influence of a reflecting boundary on entanglement harvesting between two UDW detectors has been studied, where it is observed that entanglement between two UDW detectors can get suppressed or enhanced in the presence of a reflecting boundary. However, in that study, the finite-time interaction switching function is considered, where the harvested entanglement is not totally extracted from the vacuum; it contain modifications due to the switching effect. Also, the study is limited to a single boundary system. Understanding the role of reflecting boundaries is crucial due to its applicability to cavity quantum optomechanical systems (cavity QED) with numerous practical applications [223]. Reflecting boundaries also plays an essential role in the context of holographic entanglement entropy [224], secure quantum communication over long distances [225–227], the Casimir-Polder interaction [228–230], the radiative properties of atoms [222, 231–237], the geometric phase [238] and the modified entanglement dynamics [239, 240], etc.

As mentioned in the earlier work [117], presence of a reflecting boundary can suppress or enhance entanglement harvesting between two detectors, depending on the parameter space under consideration. One can ask whether the similar effect of boundary also holds in presence of multiple boundaries. Will these effects – entanglement suppression and enhancement due to the presence of a reflecting boundary be amplified if multiple reflecting boundaries are present there? It will be much interesting if one finds more enhancement in the harvested entanglement in presence of multiple boundaries. Till now, there has been no studies done so far, analysing the entanglement harvesting phenomena in presence of multiple reflecting boundaries. In this study, we have done a detailed analysis of such a phenomena, considering multiple reflecting boundaries. We compare the harvested entanglement in presence of double boundaries with the entanglement harvested in single and no boundary systems. Here we consider the reflecting boundaries are extended in the x-y plane and located at $z = 0$ and $z = L$. The detectors accelerate along the x-direction. We use Green's functions for two reflecting boundaries as provided in [24, 222, 241] and follow the formulation for entanglement harvesting utilized in [108, 113] (see chapter 2). To study the fate of entanglement between two detectors, we investigate the concurrence [75, 76, 208], as a measure of the harvested entanglement.

Here we consider three types of arrangements for detector trajectories to apprehend the effect of the boundaries.

Case I: We position one detector near the first boundary (at $z = 0$) and the other near the second boundary (at $z = L$), ensuring identical separation from the boundaries. If

detector A is z_A distance away from $z = 0$ plane, then detector B is also z_A distance away from $z = L$ plane. This symmetric configuration ensures that the reflecting boundaries for the double-boundary system equally influence both detectors. Here, we studied different z_A-values.
Case II: We consider both detectors to be in the same z-plane ($z_A = z_B$) so that each boundary each boundary influences them equally. Additionally, the perpendicular separation between the detectors remains fixed. Here, we studied for different values of $z_A = z_B$.
Case III: Here, we chose one detector to be fixed on a $z = constant$ plane and investigated how the perpendicular separation between the trajectory of a second detector and the boundaries affects entanglement harvesting.

We observe that entanglement enhancement and suppression are also possible is presence of double boundaries. The enhancement and suppression of harvested entanglement due to the presence of boundaries is more perceptible for the double boundary system.

This chapter is organized as follows. In Sec. 4.2, we discuss the trajectories and the green functions of the two accelerated UDW detectors in the presence of reflecting boundaries. Subsequently, in Sec. 4.3, we evaluate the necessary density matrix elements and discuss the possibility of entanglement harvesting between the detectors in parallel and anti-parallel motion. Also, the properties of the harvested entanglement are being analysed. Finally, in Sec. 4.4, we conclude with the overall discussion of the results.

4.2 Accelerated system with reflecting boundaries

Let us now discuss the system under consideration. Since we aim to understand the influence of reflecting boundaries on entanglement harvesting between two accelerated detectors, we cannot study it in $(1+1)$ dimensional spacetime. We shall only consider $(1+3)$ dimensional Minkowski spacetime with two parallel reflecting boundaries extended in the x-y plane – one is at $z = 0$ and another at $z = L$. In the context of cavity quantum electrodynamics, the quantity L is known as cavity length. Here for simplicity, we consider the background field temperature to be *zero*. Hence we do not need to utilise the Unruh modes as earlier (see chapter 3). Thus the field state is the Minkowski vacuum state $|0_M\rangle$. Also the massless real scalar field is constrained to vanish at the surface of the boundaries, satisfying the Dirichlet boundary condition ($\phi(x, y, z = 0, t) =$

$0 = \phi(x, y, z = L, t)$) [24]. Thus, without taking of the field decomposition, one may find the Green's function using the mirror image problem of classical electrodynamics. The Green's function may be computed as infinite sum of images due to reflections between the planes [24]. Here all images are outside the mirrors at $z_n = (-1)^n z' + 2nL$. The Green's function can be expressed using the free space Green's function as $G(\mathbf{x}, \mathbf{x}') = \sum_{n=-\infty}^{\infty} (1-)^2 G_{free}(x - x', y - y', z - z_n, t - t')$. The positive frequency Wightman function for a massless scalar field in $(3+1)$-dimensional Minkowski spacetime in the presence of reflecting boundaries is given by [24, 222, 241][1]

$$G_W(x, x') = -\frac{1}{4\pi^2} \sum_{n=-\infty}^{\infty} \left(\frac{1}{(t - t' - i\epsilon)^2 - (x - x')^2 - (y - y')^2 - (z - z' - 2Ln)^2} - \frac{1}{(t - t' - i\epsilon)^2 - (x - x')^2 - (y - y')^2 - (z + z' - 2Ln)^2} \right). \tag{4.1}$$

By construction, this green function vanishes at z (or z') $= 0$ or L. Considering only $n = 0$ term, one gets the Wightman function in presence of a single reflecting boundary at $z = 0$. In this particular situation, among two terms – the first term corresponds to the unbounded Minkowski space and the second term is due to the boundary effect.

The trajectories of the detectors uniformly accelerating along x-direction in terms of their proper times are given in Eq. (3.6) as (see also [24, 113, 159])

$$\begin{aligned} t_A &= \frac{1}{a_A} \sinh(a_A \tau_A), \quad x_A = \frac{1}{a_A} \cosh(a_A \tau_A), \quad y_A = 0, \quad z_A = z_A; \\ t_B &= \frac{1}{a_B} \sinh(a_B \tau_B), \quad x_B = \pm \frac{1}{a_B} \cosh(a_B \tau_B), \quad y_B = \Delta y, \quad z_B = z_B, \end{aligned} \tag{4.2}$$

where $0 < z_A, z_B < L$. a_A and a_B are respectively the acceleration of the detectors A and B. The "+(−)" sign in x_B corresponds to motion of the detector B in the right (left) Rindler wedge.

4.3 Entanglement harvesting

As in the earlier chapter, here we consider the detectors are initially in their ground states $|D\rangle = |g_A g_B\rangle$. In that situation, we have already discussed that understanding entanglement harvesting requires expression of two density matrix elements: $\mathscr{P}_j$ and $\mathscr{E}$ (see Eq. (3.19) and (3.21)). In this section we calculate these quantities and then check the entanglement harvesting condition in Eq. (2.83). Let us first evaluate the transition probability $\mathscr{P}_j$.

[1] In the book by Birrell and Davies [24], the factor of 2 with L in the green function of Eq.(4.1) is missing (we feel it is a typo). The same factor can be found in the original work [241], and in a recent work [222].

4.3.1 Transition Probability

To evaluate the quantity $\mathscr{P}_j$, we use the trajectories in Eq.(4.2) to find out the Wightman function in Eq. (4.1). The denominators of the Wightman function in (4.1) for a single detector (*i.e.,* any one of the detectors among A or B is moving either in left or in right Rindler wedge) are evaluated below. Here we can drop the detector subscripts as these quantities are same for any detector. We obtain the denominators of the first and second terms in the parenthesis of (4.1) as

$$\begin{aligned}(t-t'-i\epsilon)^2-(x-x')^2-(y-y')^2-(z-z'-2Ln)^2 &= \frac{4}{a^2}\Big\{\sinh^2(a(\tau-\tau')/2-i\epsilon)-a^2L^2n^2\Big\},\\ (t-t'-i\epsilon)^2-(x-x')^2-(y-y')^2-(z+z'-2Ln)^2 &= \frac{4}{a^2}\Big\{\sinh^2(a(\tau-\tau')/2-i\epsilon)\\ &\qquad -a^2(z-Ln)^2\Big\}.\end{aligned} \tag{4.3}$$

These two quantities have the same proper time dependence with different additional constants. Hence one can write them in a combined way as $4\{\sinh^2(a(\tau-\tau')/2-i\epsilon)-g_n^2\}/a^2$ with g_n as Lan and $a(z+Ln)$ for the first and second denominators, respectively. To calculate the transition probability, we need to perform time-integrations in Eq. (3.19) by using (4.1) and (4.3). The two terms in the Wightman function provide identical integrations and therefore performing the following form of integration is sufficient to achieve the goal. We use coordinate transform $u=\tau-\tau'$ and $v=\tau+\tau'$ to simplify the integrations. The Jacobian of the transformation is $|J|=1/2$. We define two new variables $\alpha=a/\Delta E$ and $s=au/2$. Then the transition probability becomes

$$-\frac{a^2}{16\pi^2}\int_{-\infty}^{\infty}\int_{-\infty}^{\infty}\frac{d\tau d\tau' e^{-i\Delta E(\tau-\tau')}}{\sinh^2(a(\tau-\tau')/2-i\epsilon)-g_n^2}=-\frac{a}{16\pi^2}\int_{-\infty}^{\infty}dv\int_{-\infty}^{\infty}\frac{ds\,e^{-i\frac{2}{\alpha}s}}{\sinh^2(s-i\epsilon)-g_n^2}. \tag{4.4}$$

To perform contour integral over s-variable we evaluate the poles as

$$s_n=i\epsilon+i\pi n\pm\sinh^{-1}(|g_n|)\,. \tag{4.5}$$

Taking all contributions from lower half of the complex s-plane ($\alpha>0$), we obtain

$$-\frac{1}{16\pi^2}\int_{-\infty}^{\infty}d(av)\int_{-\infty}^{\infty}\frac{ds\,e^{-i\frac{2}{\alpha}s}}{\sinh^2(s-i\epsilon)-g_n^2}=\frac{\delta(0)}{2\left(e^{\frac{2\pi}{\alpha}}-1\right)}\frac{\sin\left(\frac{2}{\alpha}\sinh^{-1}(|g_n|)\right)}{|g_n|\sqrt{g_n^2+1}}, \tag{4.6}$$

where, the Dirac delta function $\delta(0)$ is obtained from the integral $\int_{-\infty}^{\infty} d(av)$. Then the transition probability of j^{th}-detector is obtained as

$$\begin{aligned}\mathscr{P}_j &= \int\int d\tau d\tau' e^{i\Delta E(\tau-\tau')} G_W(x',x) \\ &= \frac{\delta(0)}{2\left(e^{\frac{2\pi}{a}}-1\right)} \sum_{n=-\infty}^{\infty} \left(\frac{\sin\left(\frac{2}{a}\sinh^{-1}(|La\,n|)\right)}{|La\,n|\sqrt{|La\,n|^2+1}} - \frac{\sin\left(\frac{2}{a}\sinh^{-1}(|a(z_j+Ln)|)\right)}{|a(z_j+Ln)|\sqrt{|a(z_j+Ln)|^2+1}} \right).\end{aligned} \tag{4.7}$$

This quantity will be needed for testing the validity of the entangling condition (2.83) and the calculation of concurrence (3.24).

Before proceeding to this, few comments are in order. First of all, note that when $Ln/z_j >> 1$, two term in (4.7) will cancel each other. This can happen for large values of n and therefore we may set a cut off on upper and lower limit of n in order to evaluate the summation in (4.7). Therefore later in numerical calculation we choose $\max|n|$ to a large finite value. Secondly, only $n=0$ term in (4.7) refers to the transition probability of an accelerated detector with single reflecting boundary. This corresponds to the only mirror image at $z_0 = -z'$ due the mirror at $z=0$ position along with the free space Green's function. In this case ($n=0$), the first part reproduces the same in free or unbounded Minkowski spacetime (see, [113]) as

$$\mathscr{P}_j = \frac{\delta(0)\Delta E}{a\left(e^{\frac{2\pi}{a}}-1\right)}. \tag{4.8}$$

4.3.2 Entangling term: parallel acceleration

In this subsection, we will evaluate the entangling term for the accelerated detectors. First we will calculate it for the parallel motion of the detectors, *i.e.,* the detectors are in same Rindler wedge, namely in right wedge. Then in the next subsection we evaluate it for the anti-parallel motion, *i.e.,* one detector is in right wedge and other one is in left wedge, will be considered.

The evaluation of the quantity $\mathscr{E}$ requires the Feynman propagator, which can be expressed as

$$\begin{aligned}G_F(x_A,x_B) = \frac{i}{4\pi^2}\sum_{n=-\infty}^{\infty}\Bigg(&\frac{1}{(t_A-t_B)^2-(x_A-x_B)^2-\rho_{n,-}^2-i\epsilon} \\ &- \frac{1}{(t_A-t_B)^2-(x_A-x_B)^2-\rho_{n,+}^2-i\epsilon}\Bigg),\end{aligned} \tag{4.9}$$

with $\rho_{n,\pm}^2 = \Delta y^2 + (z_A \pm z_B - 2Ln)^2$.

We need to numerically analyse the final outcomes for our later purpose to compare the concurrence quantity for different boundary systems. As mentioned earlier, we must have $0 < z_A, z_B < L$. Now for a finite fixed value of Δy, if we consider n is sufficiently large, then the last term in $\rho^2_{n,\pm}$ will dominate. Hence, one will have $\rho^2_{n,\pm} \approx 4L^2n^2$. Therefore the quantities inside the parenthesis of Eq. (4.9) corresponding to large n will cancel each other. Thus the infinite summation in Eq. (4.9) effectively can be replaced by a finite summation (the same is also true for the anti-parallel acceleration of the detectors).

The quantities in the denominators can be re-expressed using the detector trajectories given in Eq. (4.2). For parallel motion of the detectors (with '+' sign in x_B), one obtains

$$\begin{aligned}
&(t_A - t_B)^2 - (x_A - x_B)^2 - \rho^2_{n,\pm} - i\epsilon \\
&= \frac{1}{a_A a_B}\left[e^{a_A\tau_A - a_B\tau_B} + e^{-a_A\tau_A + a_B\tau_B} - \left(\frac{a_A}{a_B} + \frac{a_B}{a_A} + a_A a_B \rho^2_{n,\pm}\right)\right] - i\epsilon \\
&= \frac{1}{a_A a_B\, e^{\tilde{\tau}_A - \tilde{\tau}_B}}\left(e^{\tilde{\tau}_A - \tilde{\tau}_B} - M_{n,\pm} + \sqrt{M^2_{n,\pm} - 1} + i\epsilon\right)\left(e^{\tilde{\tau}_A - \tilde{\tau}_B} - M_{n,\pm} - \sqrt{M^2_{n,\pm} - 1} - i\epsilon\right) \\
&= \frac{1}{a_A a_B\, e^{\tilde{\tau}_A - \tilde{\tau}_B}}\left(e^{\tilde{\tau}_A - \tilde{\tau}_B} - e^{-\sigma_{n,\pm}} + i\epsilon\right)\left(e^{\tilde{\tau}_A - \tilde{\tau}_B} - e^{\sigma_{n,\pm}} - i\epsilon\right).
\end{aligned} \tag{4.10}$$

Here we defined $\tilde{\tau}_j = a_j \tau_j$ $(j = A, B)$ and

$$\sigma_{n,\pm} = \log\left(M_{n,\pm} + \sqrt{M^2_{n,\pm} - 1}\right); \tag{4.11}$$

$$M_{n,\pm} = \left(a_A/a_B + a_B/a_A + a_A a_B \rho^2_{n,\pm}\right)/2. \tag{4.12}$$

Thus we can rewrite the entangling term from Eq. (3.21) as

$$\mathscr{E} = -i\int_{-\infty}^{\infty}\frac{d\tilde{\tau}_B}{a_B}\int_{-\infty}^{\infty}\frac{d\tilde{\tau}_A}{a_A}\, e^{i\left(\frac{\tilde{\tau}_A}{a_A} + \frac{\tilde{\tau}_B}{a_B}\right)} G_F(x_B, x_A). \tag{4.13}$$

For single term (n^{th} term) of the Feynman propagator Eq. (4.9), we can write the integral as

$$\mathscr{E}_{n,\pm} = \frac{1}{(2\pi)^2}\int_{-\infty}^{\infty}\int_{-\infty}^{\infty}\frac{d\tilde{\tau}_B\, d\tilde{\tau}_A\;\; e^{i\left(\frac{\tilde{\tau}_A}{a_A} + \frac{\tilde{\tau}_B}{a_B}\right)}\;\; e^{\tilde{\tau}_A - \tilde{\tau}_B}}{\left(e^{\tilde{\tau}_A - \tilde{\tau}_B} - e^{-\sigma_{n,\pm}} + i\epsilon\right)\left(e^{\tilde{\tau}_A - \tilde{\tau}_B} - e^{\sigma_{n,\pm}} - i\epsilon\right)}. \tag{4.14}$$

We can only evaluate this term and sum over n to obtain the entangling term as $\mathscr{E} = \sum_{n=-\infty}^{\infty}(\mathscr{E}_{n,+} - \mathscr{E}_{n,-})$. To evaluate $\mathscr{E}_{n,\pm}$, we need to perform contour integral for $\tilde{\tau}_A$-variable. The integral has poles at

$$\tilde{\tau}_{A+\tilde{n}} = \left(\tilde{\tau}_B \pm \sigma_{n,\pm} + 2\pi i\tilde{n} \pm i\epsilon\right). \tag{4.15}$$

Since $\alpha_A > 0$, only poles from upper half of the complex $\tilde{\tau}_A$-plane will contribute. We obtain

$$\mathscr{E}_{n,\pm} = \frac{i}{4\pi\sinh\sigma_{n,\pm}}\left\{\sum_{\tilde{n}=0}^{\infty} e^{\frac{i}{\alpha_A}(\sigma_{n,\pm} + 2\pi\tilde{n}i)} + \sum_{\tilde{n}=1}^{\infty} e^{\frac{i}{\alpha_A}(-\sigma_{n,\pm} + 2\pi\tilde{n}i)}\right\}\int_{-\infty}^{\infty} d\tilde{\tau}_B e^{i\tilde{\tau}_B\left(\frac{1}{\alpha_A} + \frac{1}{\alpha_B}\right)} \tag{4.16}$$

The summation oven $\tilde{n}$ can be done using $\sum_{n=1}^{\infty} e^{-2\pi n/x} = 1/(e^{2\pi/x}-1)$. Then performing τ_B-integration, one obtain the final expression for $\mathscr{E}$ as

$$\mathscr{E} = \frac{\delta\left(\frac{1}{\alpha_A}+\frac{1}{\alpha_B}\right)}{1-e^{-\frac{2\pi}{\alpha_A}}} \sum_{n=-\infty}^{\infty} \left[\frac{i}{2\sinh\sigma_{n,-}} \left\{ e^{\frac{i\sigma_{n,-}}{\alpha_A}} - e^{-\frac{2\pi}{\alpha_A}} e^{-\frac{i\sigma^{n,-}}{\alpha_A}} \right\} - \frac{i}{2\sinh\sigma_{n,+}} \left\{ e^{\frac{i\sigma_{n,+}}{\alpha_A}} - e^{-\frac{2\pi}{\alpha_A}} e^{-\frac{i\sigma_{n,+}}{\alpha_A}} \right\} \right]. \tag{4.17}$$

The steps of the above calculation is not new. It has been followed from Sec. III of [113]. The expression in (4.17) contains the Dirac-delta function with argument $\frac{1}{\alpha_A}+\frac{1}{\alpha_B}$, which always vanishes as ΔE^A, ΔE^B, a_A, a_B all are positive quantities. On the other hand $\mathscr{P}_j$ is always positive and non-vanishing quantity with $\delta(0)$ multiplied. Since possibility of entanglement harvesting requires to satisfy the condition (2.83), entanglement harvesting is not possible for parallel motion of the detectors. This situation is similar to the case where no reflecting boundary is considered [113, 159]. The same result is also valid for the identical system with single reflecting boundary as well.

4.3.3 Anti-parallel acceleration

For the anti-parallel motion of the detectors, the trajectories are given in (4.2) with '–' sign in the x_B. Therefore we find

$$\begin{aligned}
&(t_A-t_B)^2-(x_A-x_B)^2-\rho_{n,\pm}^2-i\epsilon \\
&= -\frac{1}{a_A a_B}\left[e^{a_A\tau_A+a_B\tau_B} + e^{-a_A\tau_A-a_B\tau_B} + \left(\frac{a_A}{a_B}+\frac{a_B}{a_A}+a_A a_B\rho_{n,\pm}^2\right)\right] - i\epsilon \\
&= -\frac{1}{a_A a_B\, e^{\tilde{\tau}_A+\tilde{\tau}_B}} \left(e^{\tilde{\tau}_A+\tilde{\tau}_B} + M_{n,\pm} + \sqrt{M_{n,\pm}^2-1} + i\epsilon\right)\left(e^{\tilde{\tau}_A+\tilde{\tau}_B} + M_{n,\pm} - \sqrt{M_{n,\pm}^2-1} - i\epsilon\right) \\
&= -\frac{1}{a_A a_B\, e^{\tilde{\tau}_A+\tilde{\tau}_B}} \left(e^{\tilde{\tau}_A+\tilde{\tau}_B} + e^{\sigma_{n,\pm}} + i\epsilon\right)\left(e^{\tilde{\tau}_A+\tilde{\tau}_B} + e^{-\sigma_{n,\pm}} - i\epsilon\right).
\end{aligned} \tag{4.18}$$

For single term (n^{th} term) of the Feynman propagator Eq. (4.9), we can write the integral as

$$\mathscr{E}_{n,\pm} = \frac{1}{(2\pi)^2}\int_{-\infty}^{\infty}\int_{-\infty}^{\infty} \frac{d\tilde{\tau}_B\, d\tilde{\tau}_A \;\; e^{i\left(\frac{\tilde{\tau}_A}{\alpha_A}+\frac{\tilde{\tau}_B}{\alpha_B}\right)} \;\; e^{\tilde{\tau}_A+\tilde{\tau}_B}}{\left(e^{\tilde{\tau}_A+\tilde{\tau}_B}+e^{\sigma_{n,\pm}}+i\epsilon\right)\left(e^{\tilde{\tau}_A+\tilde{\tau}_B}+e^{-\sigma_{n,\pm}}-i\epsilon\right)}. \tag{4.19}$$

In this case the poles are at

$$\tilde{\tau}_{A\pm\tilde{n}} = -\tilde{\tau}_B \mp \sigma_{n,\pm} + (2\tilde{n}+1)i\pi \mp i\epsilon. \tag{4.20}$$

Since $\alpha_A > 0$, only poles from upper half of the complex $\tilde{\tau}_A$-plane will contribute (all $\tilde{n} \geq 0$). We obtain

$$\mathscr{E}_{n,\pm} = -\frac{\sin\left(\frac{\sigma_{n,\pm}}{\alpha_A}\right)}{4\pi \sinh\left(\frac{\pi}{\alpha_A}\right)\sinh\sigma_{n,\pm}} \int_{-\infty}^{\infty} d\tilde{\tau}_B e^{i\tilde{\tau}_B\left(\frac{1}{\alpha_B}-\frac{1}{\alpha_A}\right)} \tag{4.21}$$

Then performing the integration over the variable $\tilde{\tau}_B$, one obtain the final expression for $\mathscr{E}$ as

$$\begin{aligned}\mathscr{E}(\Delta E) &= -\frac{1}{2}\frac{\delta\left(\frac{1}{\alpha_A}-\frac{1}{\alpha_B}\right)}{\sinh\left(\frac{\pi}{\alpha_A}\right)} \sum_{n=-\infty}^{\infty}\left(\frac{\sin\left(\frac{\sigma_{n,-}}{\alpha_A}\right)}{\sinh(\sigma_{n,-})} - \frac{\sin\left(\frac{\sigma_{n,+}}{\alpha_A}\right)}{\sinh(\sigma_{n,+})}\right) \\ &= -\frac{1}{2}\frac{\delta\left(\frac{\Delta E^A}{a_A}-\frac{\Delta E^B}{a_B}\right)}{\sinh\left(\pi\frac{\Delta E^A}{a_A}\right)} \sum_{n=-\infty}^{\infty}\left(\frac{\sin\left(\frac{\Delta E^A\sigma_{n,-}}{a_A}\right)}{\sinh(\sigma_{n,-})} - \frac{\sin\left(\frac{\Delta E^A\sigma_{n,+}}{a_A}\right)}{\sinh(\sigma_{n,+})}\right).\end{aligned} \tag{4.22}$$

Here again, the steps of Sec. III in [113] have been followed.

For numerical analysis, practically we do not have to sum over infinite terms. In fact the terms up to $n = N$ (i.e. terms from $-N$ to N), where N is chosen to be sufficiently large such that conditions mentioned below Eq. (4.9) are satisfied, will be enough to consider. The reasons are as follows. First, notice that the entangling term contains the terms like $f(\sigma_{n,-}) - f(\sigma_{n,+})$ where $f(\sigma_{n,\pm}) = \sin\left(\Delta E\sigma_{n,\pm}/a_A\right)/\sinh(\sigma_{n,\pm})$. The numerator of this function can have values between -1 and 1. However, the denominator is a massive number for large value of Ln. Therefore the larger values of n, $f(\sigma_{n,\pm})$ becomes smaller and smaller, and ultimately can be negligible. Second, note that the quantities $\sigma_{n,\pm}$ have n-dependence through $\rho_{n,\pm}$ (defined below Eq. (4.9)). Moreover we already observed that $\rho_{n,+} \approx \rho_{n,-}$ for large value of Ln with Δy, z_A and z_B satisfy the earlier mentioned conditions (see the discussion after Eq. (4.9)). Thus, a finite summation will be sufficient for the numerical analysis. We have also verified this feature numerically, where it turns out that the quantity $\mathscr{E}$ becomes constant after a significantly large value of N. For instance corresponding to our chosen fixed-parameters, we found that $N = 2000$ is enough for our purpose. This is because just below $N = 2000$ and above it $\mathscr{E}$ becomes constant (see Fig. 4.8 in the Appendix 4.A).

As we mentioned earlier, only the $n = 0$ term provides us the effect of single reflecting boundary at $z = 0$. Using this we obtain the entangling term in the presence of a single reflecting boundary as

$$\mathscr{E}(\Delta E) = -\frac{1}{2}\frac{\delta\left(\frac{\Delta E^A}{a_A}-\frac{\Delta E^B}{a_B}\right)}{\sinh\left(\pi\frac{\Delta E^A}{a_A}\right)}\left(\frac{\sin\left(\frac{\Delta E^A\sigma_{0,-}}{a_A}\right)}{\sinh(\sigma_{0,-})} - \frac{\sin\left(\frac{\Delta E^A\sigma_{0,+}}{a_A}\right)}{\sinh(\sigma_{0,+})}\right). \tag{4.23}$$

Among the two terms of the above, the first term corresponds to the entangling term for the unbounded Minkowski space. Therefore the same with no boundary situation is given by

$$\mathscr{E}(\Delta E) = -\frac{1}{2}\frac{\delta\left(\frac{\Delta E^A}{a_A} - \frac{\Delta E^B}{a_B}\right)}{\sinh\left(\pi\frac{\Delta E^A}{a_A}\right)}\frac{\sin\left(\frac{\Delta E^A \sigma_{0,-}}{a_A}\right)}{\sinh(\sigma_{0,-})} \ . \tag{4.24}$$

Like the entangling terms with single or double boundaries, it also depends on the perpendicular separation between the detectors' trajectories. All of the entangling terms contain the Dirac-delta function with the argument of $\frac{\Delta E^A}{a_A} - \frac{\Delta E^B}{a_B}$. Since we consider the detectors to have same energy gap $\Delta E^A = \Delta E^B = \Delta E$. Therefore, to harvest a non-zero amount of entanglement, one must take $a_A = a_B$.

Note that when the entangling term is non-vanishing, it contains $\delta(0)$ (like $\mathscr{P}_j$ in Eq. (4.7)). Thus the quantity ($\mathscr{C}_J$) in (3.24) can be expressed as $\mathscr{C}_J = \delta(0)C_I$, where C_I is a finite quantity (also done in Eq. (3.41)). This is a well-known artefact of the choice eternal interaction between the detectors and the background quantum field. However, in order to quantify entanglement through concurrence it is legitimate to define concurrence per unit time, which is given by the positive values of C_I. This proposal is already well known in literature [24, 113, 159]. In our later analysis, we only focus on the quantity C_I. Now it is time to study C_I to understand the features of entanglement harvesting. This will be done numerically. For that we introduce dimensionless parameters $\bar{z}_j = z_j\Delta E$, $\Delta\bar{y} = \Delta y\Delta E$, $\alpha_j = a_j/\Delta E$, and $\bar{L} = L_0\Delta E$. Here we consider, $L_0 = L$ for the double boundary system (where L is position of the second boundary); otherwise L_0 is just a numerical parameter, which determines the intra-distance between the detectors. For our numerical analysis, we choose $\Delta\bar{y} = 0.1$ and use solid, dotted and dashed lines to represent no boundary, single boundary and double boundary systems, respectively.

Numerical Analysis: We discuss the numerical results in three cases as:

4.3.3.1 Case-I

We consider that both detectors are accelerating in an anti-parallel manner along the x-direction. The detector A is positioned near the boundary at $\bar{z} = 0$, and the detector B is near the boundary at $\bar{z} = \bar{L}$. Both detectors are equally distanced from the $\bar{z} = \bar{L}/2$ plane, which is implemented by the constraint $\bar{z}_A + \bar{z}_B = \bar{L}$. We also consider the same positions of the detectors for the no-boundary and single-boundary systems to compare the concurrence among them. Therefore we use the same constraint $\bar{z}_B = \bar{L} - \bar{z}_A$ in

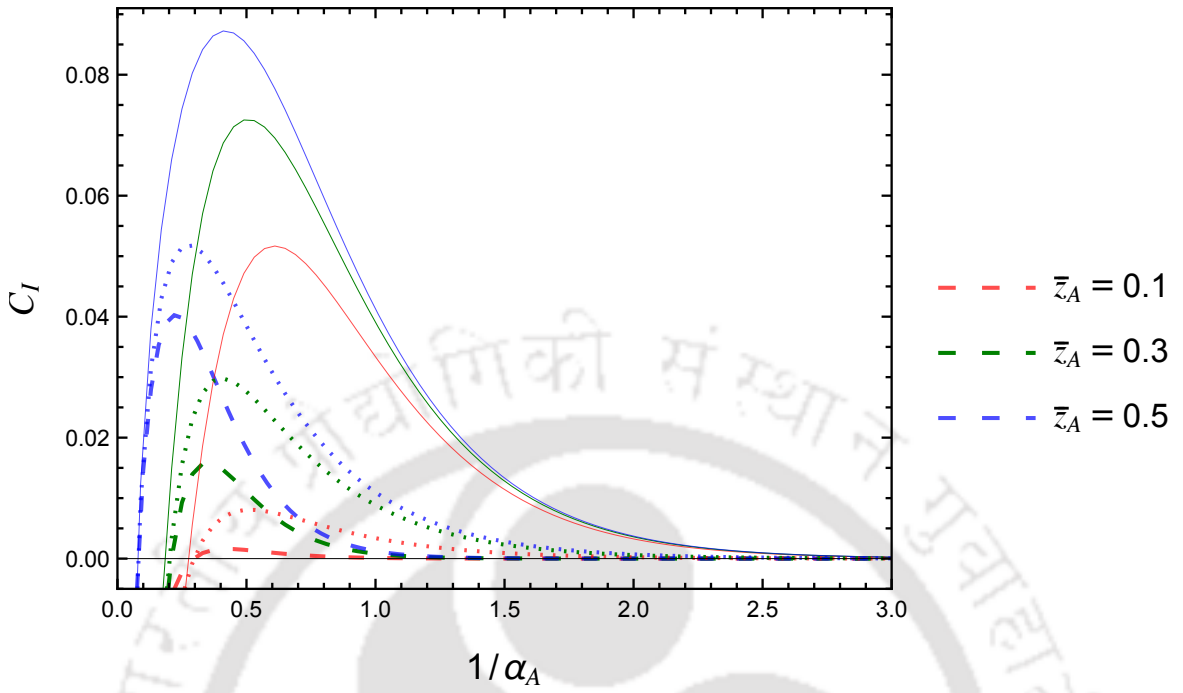

Figure 4.1: We plotted C_I with respect to the dimensionless inverse acceleration $1/\alpha_A$ for $\bar{L} = 1.0$. Different colours are used for different fixed values of $\bar{z}_A$ with the constraint $\bar{z}_A + \bar{z}_B = \bar{L}$. Here we used solid, dotted and dashed lines to represent no boundary, single boundary and double boundary systems, respectively.

the expressions of C_I for the single and no boundary systems with $0 < \bar{z}_A < \bar{L}$. Note that $\bar{L} = L_0 \Delta E = L \Delta E$ for the double boundary system and for single and no boundary systems, $\bar{L} = L_0 \Delta E$ is just a numerical parameter.

In Figs. 4.1, 4.2 and 4.3, we plot C_I with respect to the dimensionless inverse acceleration of the detector A (*i.e.,* $1/\alpha_A$) with $\bar{L} = 1.0$, $\bar{L} = 5.0$ and $\bar{L} = 10.0$, respectively. We also choose different colours to describe the results with different $\bar{z}_A$ values. In these plots, one can see that entanglement harvesting is possible only in a particular range of acceleration values, depending on the other parameters $\bar{L}$, $\bar{z}_A$ and number of boundaries in the considered systems. For lower separation between the boundaries ($\bar{L} = 1.0$) in Fig. 4.1, we observe that C_I for any particular value of $1/\alpha_A$ and $\bar{z}_A$, has maximum value for the no boundary system and minimum value for the two boundary system. Also, for a particular value of $\bar{z}_A$, the allowed range of acceleration for entanglement harvesting is much suppressed for the double boundary system and less suppressed for the single boundary system. However, as $\bar{L}$ increases, we can have different scenario. For instance, with $\bar{L} = 5.0$ and 10.0 (see, Figs. 4.2 and 4.3), one observes that the allowed

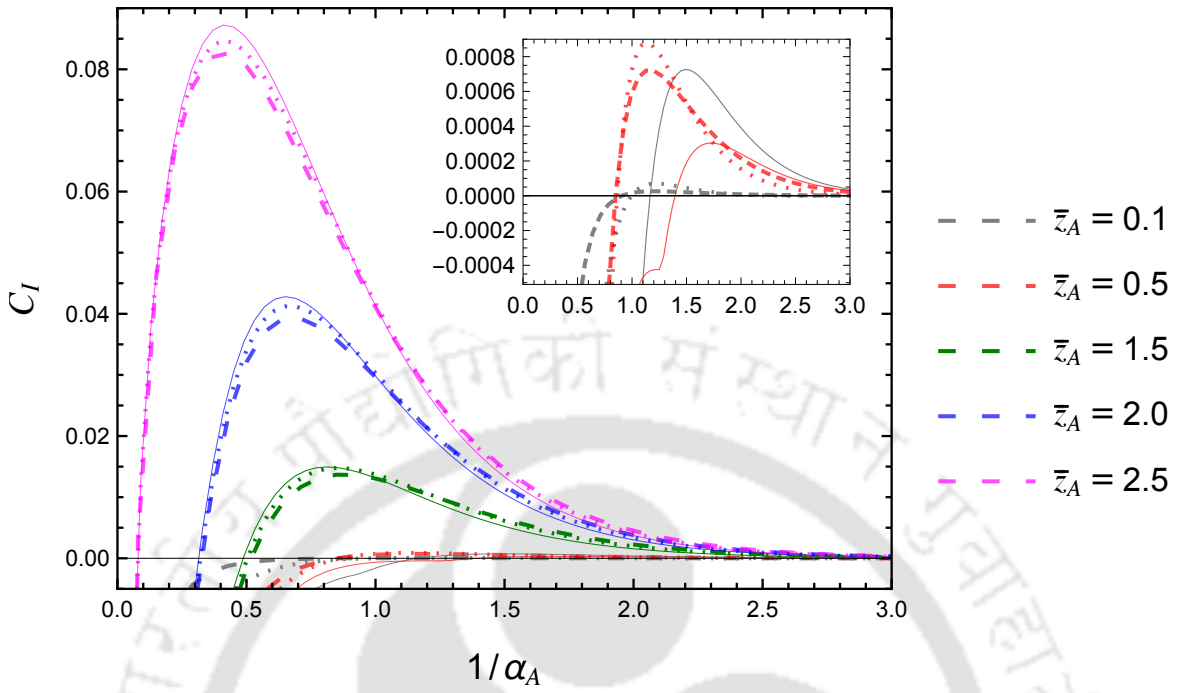

Figure 4.2: We plotted C_I with respect to the dimensionless inverse acceleration $1/\alpha_A$ for $\bar{L} = 5.0$. Different colours are used for different fixed values of $\bar{z}_A$ with the constraint $\bar{z}_A + \bar{z}_B = \bar{L}$. Here we used solid, dotted and dashed lines to represent no boundary, single boundary and double boundary systems, respectively.

range of accelerations for entanglement harvesting in the single and double boundary systems are almost equal to that of the no boundary system. Also, suppression of the peak of C_I for any particular value of $1/\alpha_A$ and $\bar{z}_A$ is very small for the single and double boundary systems compared to the no boundary system. For $\bar{L} = 5.0$, Fig. 4.2 shows that for any particular value of $\bar{z}_A$, the concurrence quantity has maximum suppression for the double boundary system for a smaller $1/\alpha_A$ value. However, for a higher $1/\alpha_A$ value (lower accelerations) and any fixed $\bar{z}_A$, there is enhancement in C_I quantity compared to the no boundary C_I quantity. The maximum enhancement is always for the double boundary system. The similar nature of enhancement in C_I is also observed for $\bar{L} = 10.0$ (see, Fig. 4.3). Thus it appears that the presence of reflecting boundaries suppresses entanglement harvesting between two detectors for small $\bar{L}$ values. However, compared to an unbounded situation, the entanglement harvesting can be enhanced by introducing reflecting boundaries with a large separation between them.

It is also perceivable that for any particular $\bar{L}$, as the value of $\bar{z}_A$ goes from 0 to $\bar{L}/2$ (also $\bar{z}_B$ goes from 0 to $\bar{L}/2$), the distance between the detectors decreases. As a

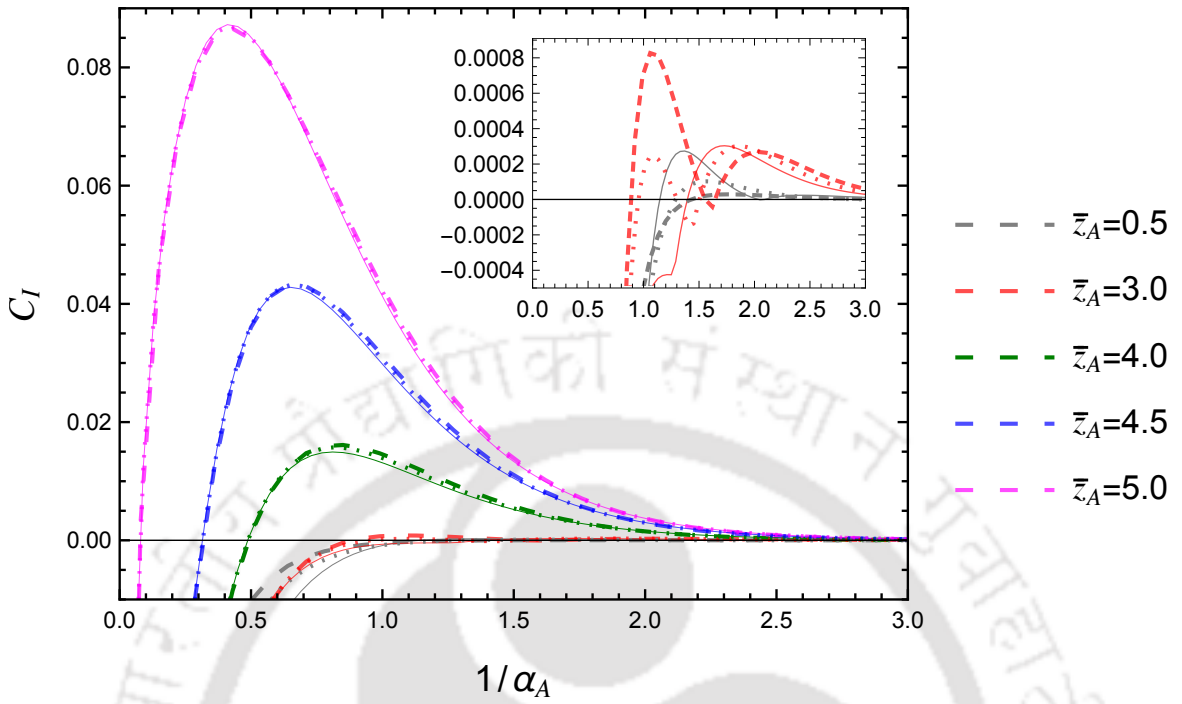

Figure 4.3: We plotted C_I with respect to the dimensionless inverse acceleration $1/\alpha_A$ for $\bar{L} = 10.0$. Different colours are used for different fixed values of $\bar{z}_A$ with the constraint $\bar{z}_A + \bar{z}_B = \bar{L}$. Here we used solid, dotted and dashed lines to represent no boundary, single boundary and double boundary systems, respectively.

consequence, the concurrence quantity for a particular $1/\alpha_A$ increase as $\bar{z}_A$ goes from 0 to $\bar{L}/2$ (in allowed parameter range, where $C_I > 0$). After crossing the value of $\bar{L}/2$, for any $\bar{z}_A = \bar{L}/2 + d$ ($\leq \bar{L}$), the concurrence quantity at any particular $1/\alpha_A$ will have the same value as it has for $\bar{z}_A = \bar{L}/2 - d$ (see, Fig. 4.4). This symmetrical nature of C_I around $\bar{z} = \bar{L}/2$ is expected due to the symmetry $(\bar{z}_A, \bar{z}_B) = (\bar{z}_B, \bar{z}_A)$ in the Wightman function in Eq. (4.1).

4.3.3.2 Case-II

After analysing the case where the detectors have a different perpendicular separation between them, here we consider the situation where the detectors have a fixed perpendicular separation ($\bar{z}_A = \bar{z}_B$; $\Delta\bar{y} = 0.1$). Again we consider the detectors to be accelerating in an anti-parallel manner along the x-axis. Keeping the separation between the detectors fixed, we take the $\bar{z}$-coordinates of both detectors between 0 and $\bar{L}/2$. Therefore, the change in C_I for different $\bar{z}_A = \bar{z}_B$ is solely due to the influence of the boundaries.

Therefore, for the no boundary system, C_I has the same value for a particular value

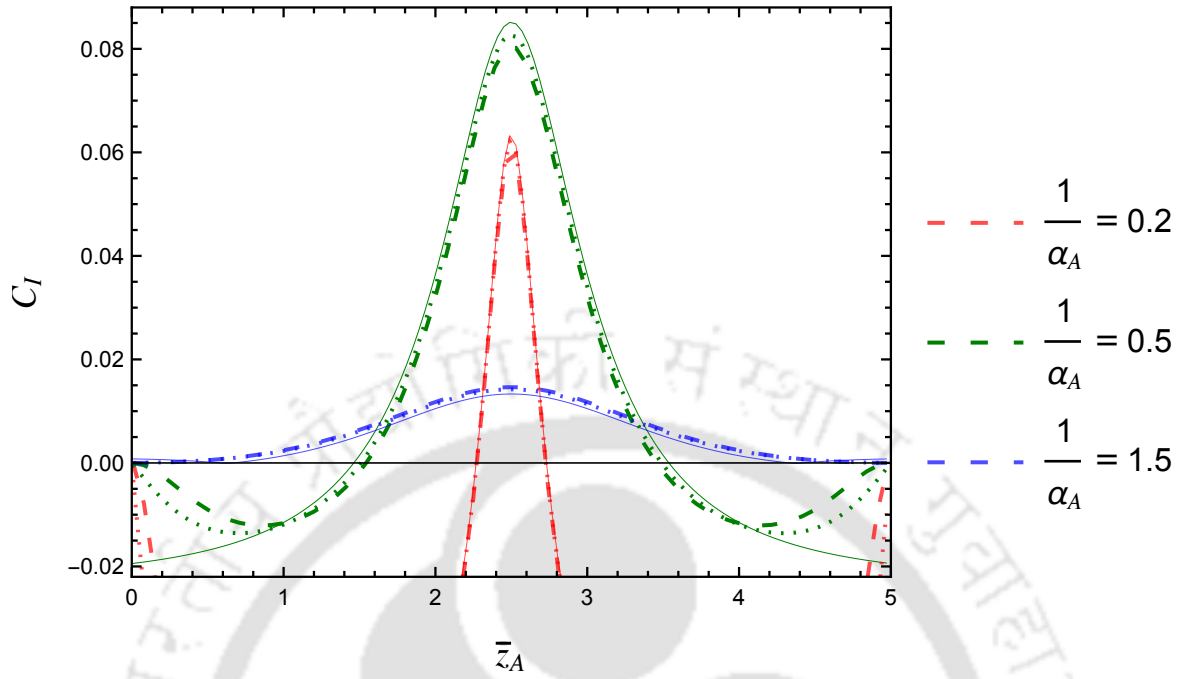

Figure 4.4: We plotted C_I with respect to $\bar{z}_A$ with $\bar{L} = 5.0$ and $\bar{z}_A + \bar{z}_B = \bar{L}$. Different colours are used for different fixed values of $1/\alpha_A$. Here we used solid, dotted and dashed lines to represent no boundary, single boundary and double boundary systems, respectively.

of $1/\alpha_A$ with any fixed $\bar{z}_A$. For smaller values of $\bar{L}$ (say, $\bar{L} = 1.0$), C_I will be suppressed due to the presence of boundary. The suppression of the C_I quantity for the single and double boundary system is already observed for $\bar{z}_{A,B} = \bar{L}/2$ (with $\bar{L} = 1$) in Fig. 4.1. The suppression will be even higher for other $\bar{z}_{A,B}$ values when $\bar{z}_{A,B} < \bar{L}/2$. Note that, the double boundary C_I has symmetrical nature around $\bar{z} = \bar{L}/2$ for any particular value of $1/\alpha_A$ (similar to the case-I). However, this is not true for the single boundary system as both detectors keep moving away from the boundary at $\bar{z} = 0$. Further increasing $\bar{z}_A$, the single boundary C_I will eventually become the same for the no boundary system.

However, the enhancement in the concurrence quantity is only possible for larger $\bar{L}$ values ($\bar{L} \gtrsim 5.0$). In Fig. 4.5, we have shown this no boundary C_I quantity in a black solid line, while the single and double boundary systems are shown in dotted and dashed lines, respectively. Here we observe that as $\bar{z}_{A,B}$ increases, the concurrence for single and double boundary systems at any particular $1/\alpha_A$ increase for any fixed value of $\bar{L}$. For fixed $\bar{z}_A = \bar{L}/2\,(= 2.5)$ and a higher value of $1/\alpha_A$, there is enhancement in concurrence quantity for the single and double boundary systems. However, the latter one enjoys slightly more. Also, the allowed ranges of accelerations for entanglement harvesting increase with

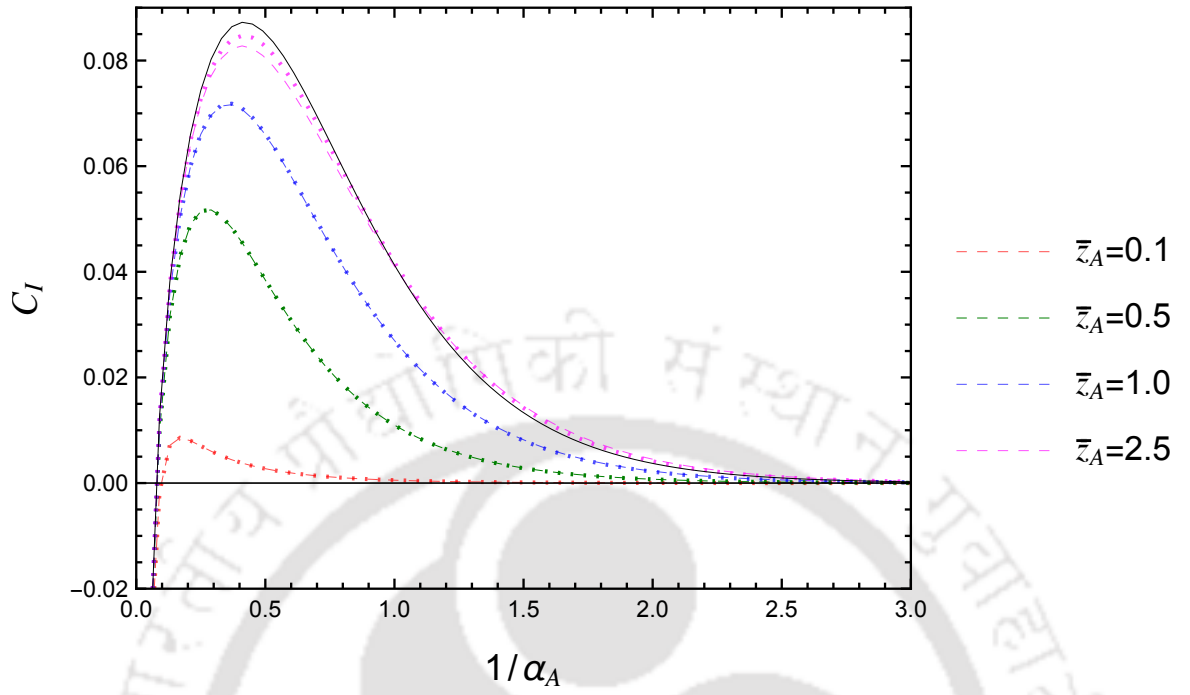

Figure 4.5: We plotted C_I with respect to $1/\alpha_A$ with $\bar{L} = 5.0$ and $\bar{z}_A = \bar{z}_B$. Different colours are used for different $\bar{z}_A$ values. Here we used solid, dotted and dashed lines to represent no boundary, single boundary and double boundary systems, respectively.

$\bar{z}_A$. In Fig. 4.6, we have plotted the concurrence quantity C_I with respect to $\bar{L}$ with consideration that $\bar{z}_{A,B} = \bar{L}/2$ (remember for double boundary systems $\bar{L} = L_0\Delta E = L\Delta E$, therefore both positions of the detectors and the second boundary is changing). Here we again see that C_I for single and double boundary systems increase with $\bar{L}$ for a fixed value of $1/\alpha_A$. Entanglement enhancement is observed for a large value of $1/\alpha_A$ (= 1.0), which is more for the double boundary system.

4.3.3.3 Case-III

Finally, we consider a situation where detector B is fixed at $\bar{z} = 5.0\,(\bar{L} = 10.0)$ and different $\bar{z}$-positions for detector A has taken in the range of $0 < \bar{z}_A < 5.0$. Here again, we consider the detectors to be accelerating in an anti-parallel manner along the x-axis. We observe a boundary-induced enhancement in C_I for any $1/\alpha_A$ value (in the allowed ranges of accelerations) with all fixed $\bar{z}_A$ values (see, Fig. 4.7). We also see that C_I for double, single and no boundary systems increase as $\bar{z}_A$ is approaching $\bar{z}_B$ for any choice of $\bar{L}$. The entanglement amplification due to the double boundary is more perceptible compared to the single boundary system. Like the previous cases, enhancement in C_I due to the

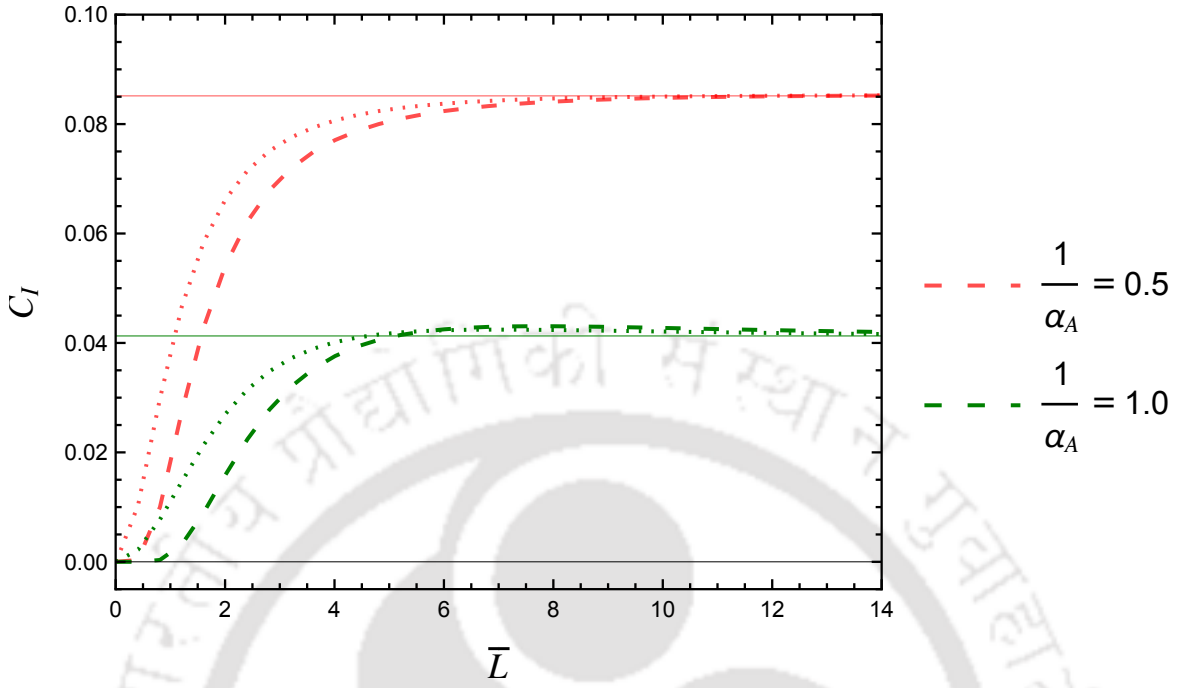

Figure 4.6: We plotted C_I with respect to $\bar{L}$ with consideration of $\bar{z}_A = \bar{z}_B = \bar{L}/2$. Different colours are used for different fixed $1/\alpha_A$ values. Here we used solid, dotted and dashed lines to represent no boundary, single boundary and double boundary systems, respectively.

presence of boundary is only possible for larger $\bar{L}$ values, not for smaller $\bar{L}$ values.

4.4 Summary and Discussions

In this chapter, we have investigated the influence of multiple reflecting boundaries on entanglement harvesting between two uniformly accelerated UDW detectors. In literature, existing studies suggest that entanglement harvesting in the presence of a single reflecting boundary can get suppressed or enhanced depending on the parameter space. However, no studies have been conducted on whether increasing the number of reflecting boundaries enhances similar features. Here we have done a comparative study on entanglement phenomena between two detectors in the presence of double, single and no reflecting boundaries. We considered the monopole coupling model with the eternal switching function of the interaction to obtain a simple analytic expression of the concurrence quantity. Due to this choice of the switching function, we found that entanglement extraction from the field vacuum is only possible for the anti-parallel motion of the detec-

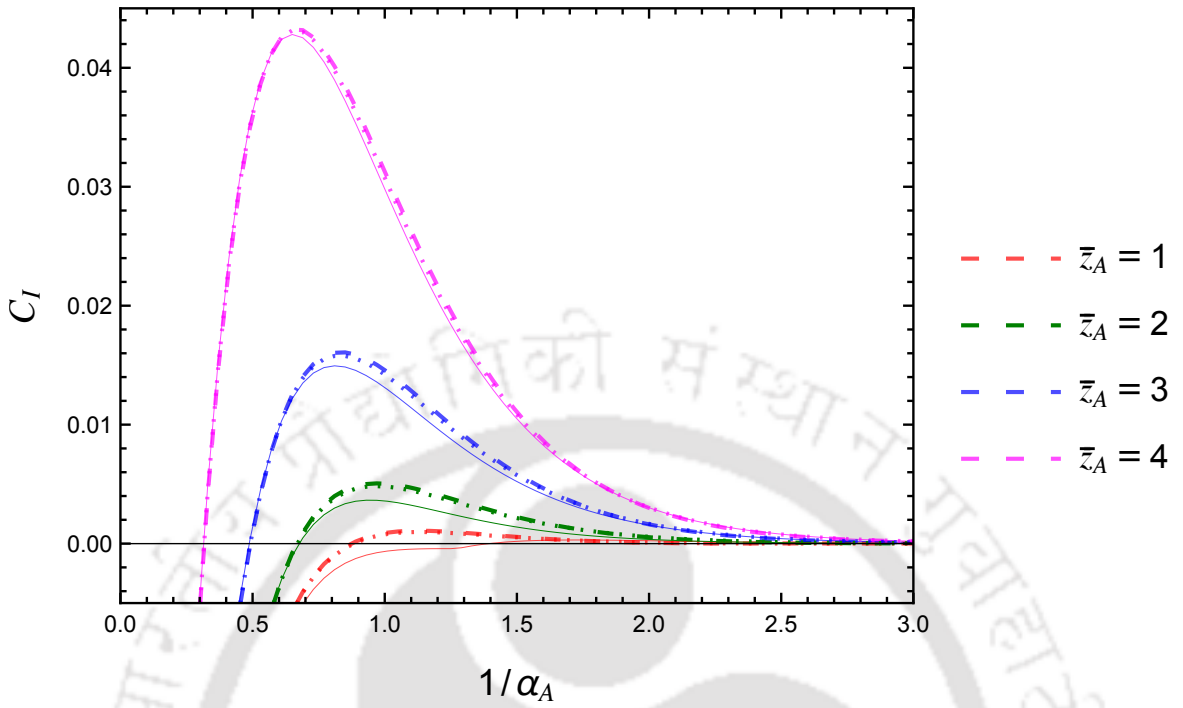

Figure 4.7: We plotted C_I with respect to $1/\alpha_A$ and fixed values of $\bar{z}_A$. Here we used $\bar{z}_B = 5.0$ and $\bar{L} = 10.0$. Different colours are used for different $\bar{z}_A$ values. Here we used solid, dotted and dashed lines to represent no boundary, single boundary and double boundary systems, respectively.

tors. Since we considered identical detectors with the same energy gap, their acceleration must have the same magnitude. We observe that detectors' entanglement increases as the vertical separation between them decreases for any number of boundaries. For the single and double boundary systems, the entanglement gets suppressed if any one or both of the detectors are near the boundary or boundaries. Entanglement degradation is much higher for the double boundary system than the single boundary system. Entanglement harvesting increases as the detectors move away from the boundary or boundaries. For small separations between the boundaries, the influence of the boundaries is strong, leading to higher degradation. As the separation increases, the boundary influence on the detectors decreases; the concurrence approaches the same for no boundary system. In some specific parameter spaces, the double boundary concurrence crosses the free space as well as the single boundary situations. Similar nature of concurrence is also found for the single boundary system, where the degradation and the enhancement of the entanglement only depend on distance from the first boundary. One of the important observations is – the double boundary concurrence degrades more whenever there is

a degradation. The same also holds for the enhancement of entanglement harvesting. Therefore an overall conclusion can be drawn that the presence of a more number of reflecting boundaries enhances the similar effect observed for a single reflecting boundary system.

Several possible setups have been proposed for the experimental verification of the Unruh effect. In these setups, a single accelerated atomic detector is considered, interacting with the background field. The Unruh–DeWitt (UDW) detector model is emulated using an atomic system restricted to two specific energy levels [198]. In such cases, one may choose either an electrostatic field ($\hat{\boldsymbol{E}}$) or an electromagnetic field ($\hat{\boldsymbol{A}}$) as a substitute for the scalar field. The corresponding interaction terms can then be taken as $\hat{\boldsymbol{d}} \cdot \hat{\boldsymbol{E}}$ or $\hat{\boldsymbol{p}} \cdot \hat{\boldsymbol{A}}$, where $\hat{\boldsymbol{d}}$ and $\hat{\boldsymbol{p}}$ represent the atomic dipole moment and momentum operators, respectively. Our monopole interaction ($\hat{m}\hat{\phi}$) is a simplified version of these interactions.

One must consider two such atomic detectors instead of one for the experimental verification of entanglement harvesting in similar setups. Large grounded conducting planes can be placed parallel to the direction of the atoms' acceleration to study the effect of mirrors on entanglement harvesting. Initially, the atoms are prepared in their ground states, and the interaction time is chosen such that $\Delta t \gg \Delta E^{-1}$, where ΔE denotes the atomic energy gap [158]. After the interaction, standard quantum protocols can be used to measure the entanglement between the detectors. Superconducting flux qubits (effective two-level systems) can also serve as UDW detectors in such setups.

Another promising approach to implementing entanglement harvesting between accelerated detectors involves superconducting circuit-QED models [242]. In this scheme, a pair of superconducting qubits is coupled to a one-dimensional resonator mode, where the "vacuum" is simulated by a superconducting transmission line prepared in its ground state. The two superconducting qubits, acting as effective UDW detectors, couple capacitively or inductively to the line at controllable positions x_A and x_B. The presence of a mirror can be realized physically by introducing an open-ended or short-circuited termination of the line, which imposes boundary conditions on the microwave field, analogous to a scalar-field mirror [243].

In this setup, the superconducting qubits are not physically accelerated to relativistic speeds. Instead, the coupling strength is modulated as $\lambda(t) = \lambda_0 e^{ikx(t)}$, effectively reproducing the same mathematical dependence as an accelerated detector [244]. After the interaction time, chosen such that $\Delta t \gg \Delta E^{-1}$, the amount of harvested entanglement

can be quantified by computing the concurrence up to second order in perturbation theory. A potential limitation of this setup is that it effectively simulates only a $(1+1)$-dimensional background field, since the transmission line supports photon propagation along a single spatial dimension.

Appendices

4.A Finite summation for Eq. (4.22)

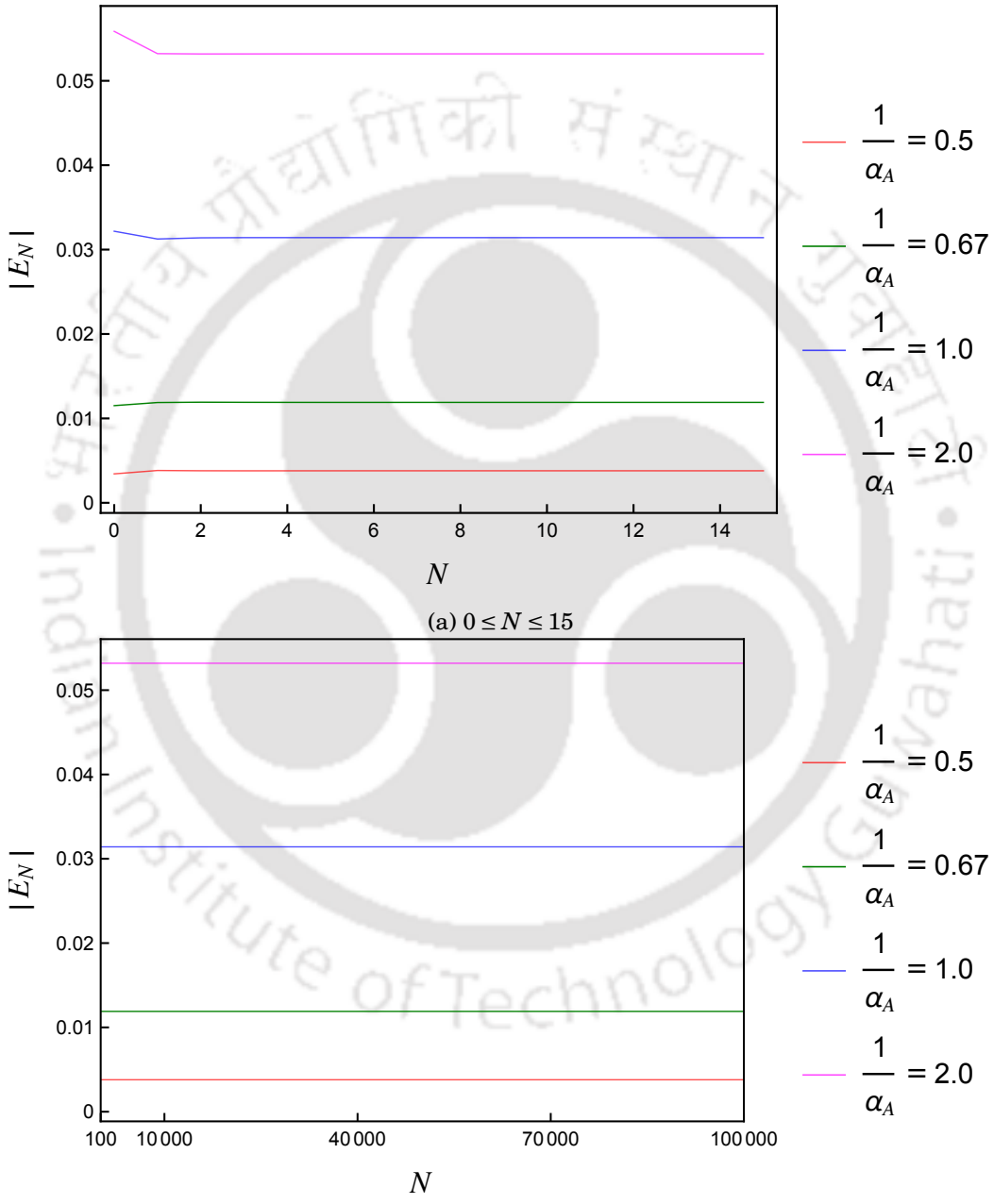

(a) $0 \le N \le 15$

(b) $100 \le N \le 100000$

Figure 4.8: In subfigures (a) and (b), we plotted $|E_N| = |\mathscr{E}(\Delta E)/\delta(0)|$ with respect to N for different $\Delta E/a_A$ values. Here we used $\bar{\Delta}y = 0.1$, $\bar{z}_A = 2.0$, $\bar{z}_B = 3.0$ and $\bar{L} = 5.0$. Different colours are used for different $1/\alpha_A$ values.

After Eq. (4.22), we analytically argued why one can perform a finite sum over n instead of the infinite sum. Here we give two plots in Fig. 4.8, which show how the absolute value of the entangling term changes with respect to $\max\{n\} = N$ with other parameters are fixed. Here we consider $\Delta\bar{y} = 0.1$, $\bar{z}_A = 2.0$, $\bar{z}_B = 3.0$, $\bar{L} = 5.0$ and $\Delta E/a_A = 0.5, 0.67, 1.0, 2.0$. We used different colours to represent different α_A values. These plots show that the entangling term changes for small values of N, while it remains constant for large N. Note that for $N = 0$, the quantity $|\mathscr{E}|$ corresponds to the single boundary system.

The same is also true for the other fixed parameter values.

CHAPTER 5

ENTANGLEMENT FROM NON-VACUUM FIELD STATES

5.1 Introduction and Motivation

The vacuum of the quantum fields maximally violates Bell's inequality [82–85]. In other words, vacuum of the quantum field shows maximal entangling properties. In the earlier chapters (chapter 2 and 3), we have already studied how this entanglement can be extracted to two space-like separated, initially uncorrelated atomic Unruh-DeWitt detectors, depending on system parameters. However, it is not guaranteed that the background field will be in a vacuum state. And if the background field state is indeed in some excited state, how much do the results concerning the entanglement harvesting change compared to the vacuum fluctuations. If the field state is not the vacuum, can we extract entanglement to two initially uncorrelated detectors? And if that is possible, how will it depend on the choice of excited field state? One such area is the possibility of entanglement harvesting from the non-vacuum quantum fluctuations, which may be relevant from the practical point of view. The non-vacuum field states also play very crucial roles in retrieving shock wave memory of spacetime [245] and in constructing quantum information of initial state from the black hole radiation, which can be a potential resolution to the black hole information paradox [246–249].

In this current chapter, we are going to investigate the entanglement harvesting condition for two UD detectors in inertial motion interacting with the *single-particle background field states* in $(1+1)$ and $(1+3)$ dimensions. This work is motivated from the work [191], where the detector's response function for an accelerated detector in

single particle excited state has been studied. In principle the field can be in any excited state; but here, following [191], we consider the simplest model where the fields are in single-particle excited state. We will see that this becomes an analytically tractable system. In particular, we have considered detectors in parallel inertial motion in $(1+1)$ dimensions, and in parallel and perpendicular inertial motions in $(1+3)$ dimensions. Our study involves detectors interacting for eternity with the background massless, minimally coupled scalar quantum field through monopole-type couplings. Here we aim to provide a rigorous formulation for entanglement harvesting with a background non-vacuum field state. In this regard, we have followed the formalism presented in chapter 2, where one can thoroughly understand entanglement harvesting conditions with detectors interacting with the field in a state $|\Psi\rangle$. For our present study, we consider this state to be a general *single-particle field state*.

In particular, our principal observation in this work is that the entanglement harvested with inertial detectors from the single-particle field states is lower than that harvested from the field vacuum. In this regard, we consider normalizable single-particle states with two specific types of distribution functions. Namely the exponential decaying and the Gaussian distribution functions (see [191] for elaborate discussions on these field states). We also observe that in both $(1+1)$ and $(1+3)$ dimensions, inertial UD detectors' self transition probabilities are non-zero due to the non-vacuum background fluctuations. In $(1+1)$ dimensions, our observations suggest that one cannot harvest entanglement between two comoving inertial detectors. In $(1+3)$ dimensions, two parallelly moving observers with equal velocity do not harvest entanglement. While in perpendicular motion, we do not confirm a similar situation. Furthermore, in this work, we elucidate the different characteristics of entanglement harvesting and study its dependence on the parameters of our considered system.

This chapter is organized as follows. In Sec. 5.2 we discuss the model consisting of two UD detectors interacting with a minimally coupled, massless scalar field through monopole couplings in the background of a non-vacuum field state. This section contains the discussion on the general density matrix elements and choice of excited field state. In Sec. 5.3 we shall consider two inertial Unruh-DeWitt detectors in $(1+1)$ dimensions and investigate the individual detector transition probabilities and entanglement harvesting conditions. Subsequently, in Sec. 5.4, UD detectors are considered in $(1+3)$ dimensions for studying the same relevant quantities. There are two special cases for $(1+3)$ dimensions; one is for parallel motion, and the other is for the perpendicular motion of the detectors. They constitute different subsections. We conclude by discussing our findings in Sec. 5.5.

5.2 The model and working formulas

This section presents the formulation for understanding the possibility of two uncorrelated atomic Unruh-DeWitt detectors getting entangled over time while interacting with an excited field state $|\Psi\rangle$. Here again we consider the detectors to be initially in their ground state $|D\rangle = |g_A g_B\rangle$. Therefore, the final density matrix is given by the matrix in Eq. (2.68). For eternal interaction between detectors and field ($\chi_j(\tau_j) = 1$) the elements of the density matrix can be expressed as (from Eqs. (2.46), (2.49) and (2.59))

$$\mathscr{P}_j = \iint d\tau_j d\tau'_j\, e^{i\Delta E_j(\tau'_j-\tau_j)} \langle\Psi|\hat{\phi}\left(x_j\right)\hat{\phi}\left(x'_j\right)|\Psi\rangle \tag{5.1}$$

$$\mathscr{P}_{AB} = \iint d\tau_A d\tau_B\, e^{i\Delta E_A\tau_A - i\Delta E_B\tau_B} \langle\Psi|\hat{\phi}(x_B)\hat{\phi}(x_A)|\Psi\rangle\,, \tag{5.2}$$

$$\mathscr{E} = -\iint d\tau_A d\tau_B\, e^{i\Delta E_A\tau_A + i\Delta E_B\tau_B} \langle\Psi|T\hat{\phi}(x_B)\hat{\phi}(x_A)|\Psi\rangle\,, \tag{5.3}$$

where, $\langle\Psi|\phi(x_i)\phi(x'_j)|\Psi\rangle$ is the two point function corresponding to an excited field state with $t_i > t'_j$. It is observed that one only needs the expressions of the integrals $\mathscr{P}_A$, $\mathscr{P}_B$ and $\mathscr{E}$ for verification of the condition (2.83) for entanglement harvesting ($|\mathscr{E}|^2 > \mathscr{P}_A\mathscr{P}_B$). The relevant concurrence quantity from Eq. (2.99) is (see also in Eq. (3.24))

$$\mathscr{C}_{\mathscr{J}} = \left(|\mathscr{E}| - \sqrt{\mathscr{P}_A\mathscr{P}_B}\right). \tag{5.4}$$

The general discussion regarding the entanglement harvesting condition as well as measurement of harvested entanglement will exactly follow from chapter 2. We are interested on excited states of field and so in principle $|\Psi\rangle$ can be chosen as any excited field state or combination of all field states. For simplicity of calculation and analysis, in this study, we will consider $|\Psi\rangle$ to be consisted of only single exited field states corresponding to modes $u_{\mathbf{k}}$. Such choice is mainly inspired from [191] where the detector's response function for its accelerated motion has been investigated. In $(1+d)$-dimensions, it can be expressed as [191]

$$|\Psi\rangle = \int \frac{d^d k}{(2\pi)^{d/2}\sqrt{2\omega_{\mathbf{k}}}} f(k)\hat{a}_{\mathbf{k}}|0_M\rangle\,. \tag{5.5}$$

where $\omega_{\mathbf{k}} = |\mathbf{k}|$ and $f(k)$ denotes the normalised probability amplitude of the distribution, which satisfies the normalization condition

$$\int \frac{d^d k}{(2\pi)^d 2\omega_{\mathbf{k}}} |f(k)|^2 = 1\,. \tag{5.6}$$

In a singly excited state the two point function (for explicit derivation, see [24, 191]) is given as

$$\langle\Psi|\hat{\phi}(x_j)\hat{\phi}(x'_j)|\Psi\rangle = G_W(x_j,x'_j) + \Phi_{\text{eff}}(x_j)\Phi^{\star}_{\text{eff}}(x'_j) + \Phi^{\star}_{\text{eff}}(x_j)\Phi_{\text{eff}}(x'_j). \tag{5.7}$$

Here, Φ_{eff} is called the effective field, defined by [191]

$$\Phi_{\text{eff}}(x_j) = \int \frac{d^d k}{(2\pi)^d 2\omega_k} f(k) e^{i\mathbf{k}\cdot\mathbf{x}_j}. \tag{5.8}$$

Now because of the fact that $f(k)$ is a scalar distribution it is convenient to consider $f(k) \equiv f(\omega_{\mathbf{k}})$. With this line of thought, one may express the time ordered field expectation value as

$$\begin{aligned}\langle\Psi|T\,\hat{\phi}(x_j)\hat{\phi}(x'_j)|\Psi\rangle &= \theta(t_j - t'_j)\langle\Psi|\hat{\phi}(x_j)\hat{\phi}(x'_j)|\Psi\rangle + \theta(t'_j - t_j)\langle\Psi|\hat{\phi}(x'_j)\hat{\phi}(x_j)|\Psi\rangle \\ &= i\,G_F(x_j,x'_j) + \Phi_{\text{eff}}(x_j)\Phi^{\star}_{\text{eff}}(x'_j) + \Phi^{\star}_{\text{eff}}(x_j)\Phi_{\text{eff}}(x'_j)\,,\end{aligned} \tag{5.9}$$

where, $\theta(t_j - t'_j)$ denotes the *Heaviside Theta function*, and we have used the expression of Eq. (5.7) to arrive at the last form. One should also note that here $G_F(x_j,x'_j) \equiv -i\langle 0_M|T\,\Phi(x_j)\Phi(x'_j)|0_M\rangle$ denotes the Feynman propagator associated with the Minkowski vacuum. Thus one can easily observe that the expressions given in Eqs. (5.1), (5.2) and (5.3) will contain two contributions – one from pure vacuum fluctuations and another part is due to the effect of choosing non-vacuum state. Therefore the entanglement harvesting phenomenon in this case effectively driven by vacuum fluctuation of the fields as well as by an effective field configuration emerged due to the non-vacuum property of field state. Hence we expect that the usual entanglement harvesting phenomenon through vacuum fluctuation suffers modification if the background field is in excited state.

Then one may express the density matrix elements relevant to entanglement harvesting: $\mathscr{P}_j$ and $\mathscr{E}$ from Eqs. (5.1) and (5.3) as

$$\mathscr{P}_j = \mathscr{P}_j^{vac} + \mathscr{P}_j^{nv}\,, \tag{5.10}$$

$$\mathscr{E} = \mathscr{E}^{vac} + \mathscr{E}^{nv}\,, \tag{5.11}$$

where the vacuum contributions are already known to us as (see chapter 3 and 4)

$$\mathscr{P}_j^{vac} = \int_{-\infty}^{\infty}\int_{-\infty}^{\infty} d\tau_j\, d\tau'_j\, e^{-i\Delta E(\tau_j - \tau'_j)} G_W(x_j,x'_j)\,, \tag{5.12a}$$

$$\mathscr{E}^{vac} = -i\int_{-\infty}^{\infty}\int_{-\infty}^{\infty} d\tau_B\, d\tau'_A\, e^{i\Delta E(\tau'_A + \tau_B)} G_F(x_B,x'_A)\,. \tag{5.12b}$$

Furthermore, using the relation between Feynman propagator and the Wightman function $iG_F(x,x') = G_W(x,x') + iG_R(x',x) = G_W(x,x') + \theta(t'-t)\{G_W(x',x) - G_W(x,x')\}$ one can simplify the calculation of the integral $\mathscr{E}^{vac}$ as

$$\mathscr{E}^{vac} = \mathscr{E}_W^{vac} + \mathscr{E}_R^{vac}, \tag{5.13}$$

with

$$\mathscr{E}_W^{vac} = -\int_{-\infty}^{\infty} d\tau_B \int_{-\infty}^{\infty} d\tau_A \; e^{i(\Delta E^B \tau_B + \Delta E^A \tau_A)} G_W(x_B, x_A), \tag{5.14a}$$

$$\mathscr{E}_R^{vac} = -\int_{-\infty}^{\infty} d\tau_B \int_{-\infty}^{\infty} d\tau_A \; e^{i(\Delta E^B \tau_B + \Delta E^A \tau_A)} \theta(t_A - t_B)\{G_W(x_A, x_B) - G_W(x_B, x_A)\}, \tag{5.14b}$$

where, $G_R(x,x') \equiv i\theta(t-t')\langle 0_M|\left[\hat{\phi}(x'), \hat{\phi}(x)\right]|0_M\rangle$ signifies the retarded Green's function. The non-vacuum contributions can be expressed as

$$\mathscr{P}_j^{nv} = |\mathscr{A}(\Delta E)|^2 + |\mathscr{B}(\Delta E)|^2 \,, \tag{5.15a}$$

$$\mathscr{E}^{nv} = -\int_{-\infty}^{\infty}\int_{-\infty}^{\infty} d\tau_B d\tau'_A \, e^{i\Delta E(\tau'_A + \tau_B)} [\Phi_{\text{eff}}(x_B)\Phi^{\star}_{\text{eff}}(x'_A) + \Phi^{\star}_{\text{eff}}(x_B)\Phi_{\text{eff}}(x'_A)] \,. \tag{5.15b}$$

where,

$$\mathscr{A}(\Delta E) = \int_{-\infty}^{\infty} d\tau'_j \, e^{i\Delta E \, \tau'_j} \, \Phi_{\text{eff}}(\tau'_j) \,, \tag{5.16a}$$

$$\mathscr{B}(\Delta E) = \int_{-\infty}^{\infty} d\tau'_j \, e^{i\Delta E \, \tau'_j} \, \Phi^{\star}_{\text{eff}}(\tau'_j) \,. \tag{5.16b}$$

We shall use these expressions for our purpose to obtain the explicit expression of $\mathscr{P}_j$ and $\mathscr{E}$.

5.3 Entanglement harvesting: Motion in $(1+1)$ dimensions

Here we consider two atomic Unruh-DeWitt detectors in uniform velocity in $(1+1)$ dimensional spacetime. We assume Alice and Bob to have velocities v_A and v_B respectively. In this scenario one is able to express the Minkowski time t_j and position x_j of these two detectors in terms of their respective proper times τ_j as

$$\begin{aligned} t_j &= \gamma_j \tau_j \,, \\ x_j &= v_j \gamma_j \tau_j \,, \end{aligned} \tag{5.17}$$

where, j denotes either A (corresponds to Alice) or B (corresponds to Bob), and γ_j is the Lorentz factor, $\gamma_j = 1/\sqrt{1-v_j^2}$.

Transition probability:

The integrals $\mathscr{P}_j$ signify individual detector transition probabilities. We shall be first evaluating these integrals. Note that in $(1+1)$ dimensions the expression of the scalar field mode function is given by $u_k(x_j) = (1/\sqrt{4\pi\omega_k})e^{-i\omega_k t_j + ikx_j}$ and so the Wightman function is

$$G_W(x_j, x_j') = \int_{-\infty}^{\infty} \frac{dk}{4\pi\omega_k} e^{-i\omega_k(t_j - t_j') + ik(x_j - x_j')}. \tag{5.18}$$

Here note that, for a massless field, Eq. (5.18) is ill defined because of an infrared divergence at small $|k|$. To avoid this divergence, we first insert this Wightman function in the expressions of density matrix elements without performing the momentum integral. In this way, one can easily perform the momentum integral without encountering the divergence in the Wightman function. Utilizing this Wightman function with the coordinate transformation from Eq. (5.17) one can find out the quantity $\mathscr{P}_j^{vac}$ from (5.12a) as

$$\begin{aligned}
\mathscr{P}_j^{vac} &= \int_{-\infty}^{\infty} \frac{dk}{4\pi\omega_k} \int_{-\infty}^{\infty}\int_{-\infty}^{\infty} d\tau_j\, d\tau_j'\, e^{-i\Delta E(\tau_j - \tau_j')} e^{-i(\omega_k - k v_j)\gamma_j(\tau_j - \tau_j')} \\
&= \int_{-\infty}^{\infty} \frac{\pi\, dk}{\omega_k} \left\{\delta[\gamma_j(\omega_k - k v_j) + \Delta E]\right\}^2 \\
&= \int_0^{\infty} \frac{\pi\, d\omega_k}{\omega_k} \left[\left\{\delta[\gamma_j \omega_k(1 - v_j) + \Delta E]\right\}^2 + \left\{\delta[\gamma_j \omega_k(1 + v_j) + \Delta E]\right\}^2 \right],
\end{aligned} \tag{5.19}$$

where $\omega_k = |k|$ has been used. Here we obtained square of a Dirac delta functions due to the two proper time integrals. In this calculation of ω_k-integral, one of the delta functions is treated in the usual way, while the other is considered as a general function. The integration is then performed over the delta function. The final expression in Eq. (5.19) vanishes as we have $0 \leq v_j \leq 1$ and $\Delta E > 0$. The reason behind is, in that situation the argument of the Dirac delta distribution is always positive in the considered integration range of ω_k. The transition probability can be also calculated using the transition amplitude (see discussion in Sec. 3.3 of [24]). The transition amplitude is $A_j = i\langle e_j, \psi | \int d\tau \hat{m}(\tau)\hat{\phi}(x) | g_j, 0_M \rangle$, where ψ is an excited field state. To calculate the transition probability, one need to square the modulus of A_j and sum it over all possible ψ. For inertial motion of the detector, transition amplitude is obtained as $(4\pi\omega_k)^{-1/2}\delta(\Delta E + \gamma_j(\omega_k - k v_j))$. Again the transition probability will have square of Dirac delta functions with positive argument and it will vanish. This is expected as an inertial detector does not experience excitations due to vacuum fluctuation of fields.

On the other hand, if one uses the expression of $\Phi_{\rm eff}(x)$ from Eq. (5.8) for $(1+1)$ dimensions, then the quantity $\mathscr{A}(\Delta E)$, given by Eq. (5.16a), becomes

$$\begin{aligned}\mathscr{A}(\Delta E) &= \int_{-\infty}^{\infty} \frac{f(\omega_k)dk}{4\pi\omega_k} \int_{-\infty}^{\infty} d\tau'_j\, e^{i[\Delta E-(\omega_k - k\,v_j)\gamma_j]\tau'_j} \\ &= \int_{-\infty}^{\infty} \frac{dk}{2\omega_k} f(\omega_k)\delta[\gamma_j(\omega_k - k\,v_j) - \Delta E] \\ &= \frac{1}{2\,\Delta E}\left\{f(D_j\,\Delta E) + f(\Delta E/D_j)\right\}\,, \end{aligned} \tag{5.20}$$

where, $D_j = \sqrt{1+v_j}/\sqrt{1-v_j}$. In a similar manner one can find out the other quantity from (5.16b) as

$$\begin{aligned}\mathscr{B}(\Delta E) &= \int_{-\infty}^{\infty} \frac{f(\omega_k)dk}{4\pi\omega_k} \int_{-\infty}^{\infty} d\tau'_j\, e^{i[\Delta E+(\omega_k - k\,v_j)\gamma_j]\tau'_j} \\ &= \int_{-\infty}^{\infty} \frac{dk}{2\omega_k} f(\omega_k)\delta[(\omega_k - k\,v_j)\gamma_j + \Delta E] \\ &= 0\,, \end{aligned} \tag{5.21}$$

for $\Delta E > 0$. Therefore, in $(1+1)$ dimensions with two detectors in uniform velocities the quantity $\mathscr{P}_j$ from Eq. (5.10) is entirely given by $\mathscr{A}(\Delta E)$, specifically as $\mathscr{P}_j(\Delta E) = |\mathscr{A}(\Delta E)|^2$. Once the explicit form of distribution function $f(\omega_k)$ is given, then we will be able to know $\mathscr{P}_j(\Delta E)$. One may look into Appendix 5.A.1 for the expressions of a few possible distribution functions $f(\omega_k)$ in $(1+1)$ dimensions. We choose them to be similar that have been adopted in [191] to investigate the single detector's response function in an accelerated frame.

Note that the quantities $\mathscr{P}_j$ denote the single detector transition probabilities. In Fig. 5.1 and 5.2 we have plotted these quantities for the specific distribution functions $f(\omega_k) = C\,\omega_k\, e^{-\alpha\omega_k}$ and $f(\omega_k) = C\,\omega_k\; e^{-(\omega_k-\omega_0)^2/2\sigma^2}$ respectively. Here C is the normalization constant and its explicit form, which is imperative for obtaining the numerical value of $\mathscr{P}_j$, is determined in Appendix 5.A.1.

From these figures, with both the exponentially damping and Gaussian distribution functions, one can observe that in different regions of ΔE the transition probability varies differently with the velocity v_j of the detector. For example, the upper plots of Fig. 5.1 and 5.2 signify that for very low and high ΔE the transition increases with increasing v_j. While in the intermediate range of ΔE, transition decreases with increasing v_j. The behavior of the transition probability with respect to the velocity v_j in different ΔE regimes is further elucidated in the lower plots of the concerned figures. From those plots, one further can observe that in the low and high ΔE regime, when $\Delta E/\kappa = 0.2$ and $\Delta E/\kappa = 4$ (here κ can be σ or $1/\alpha$ depending on the considered distribution function), the

transition rate initially increases with increasing velocity v_j up to certain values of v_j and then decreases. While this characteristic is different in the intermediate transition energy regimes, *e.g.,* when $\Delta E/\kappa = 2$. In the later case transition probability decreases with the increase of v_j.

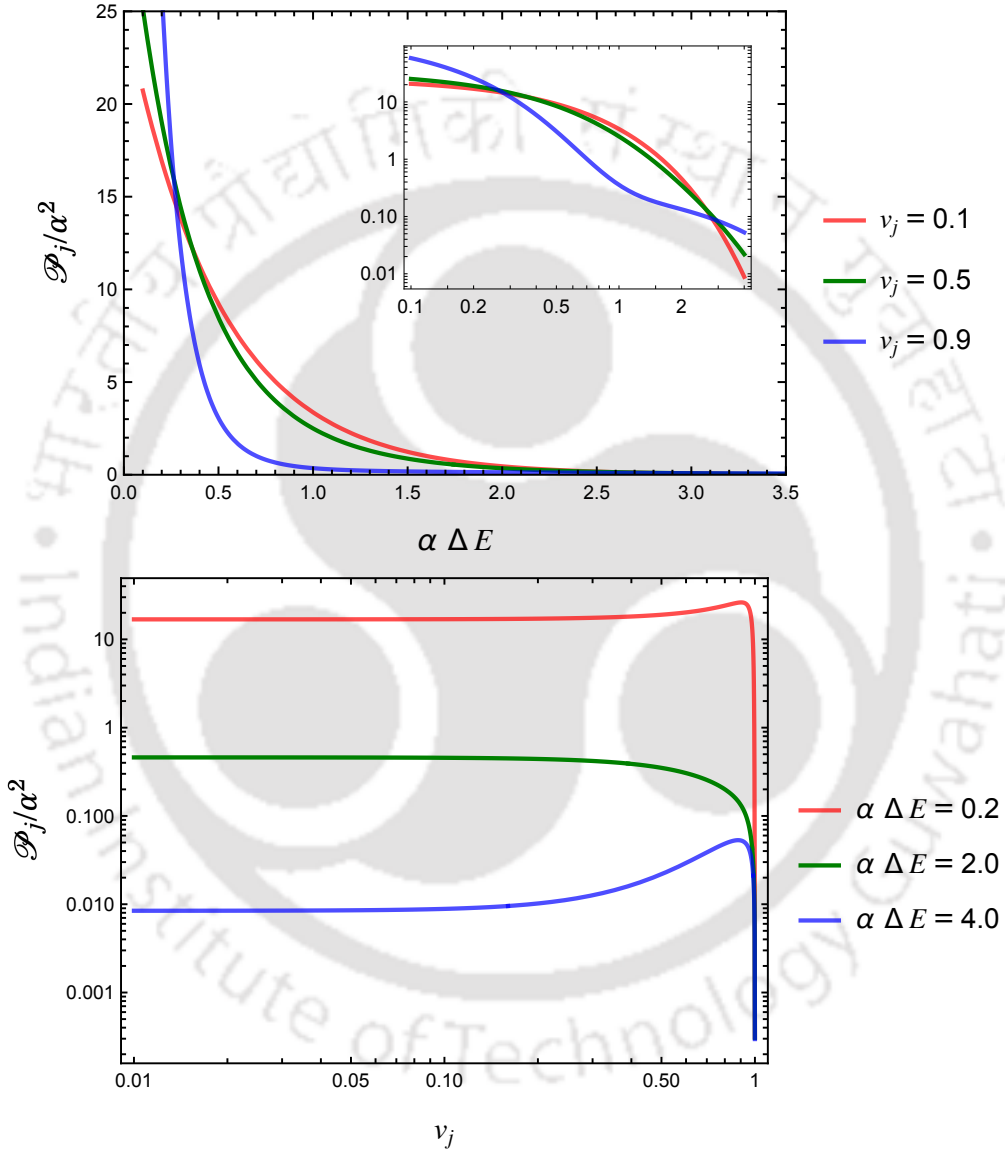

Figure 5.1: The dimensionless transition probability $\mathscr{P}_j/\alpha^2$ is plotted as functions of $\alpha\,\Delta E$ and v_j in the upper and the lower figures respectively in $(1+1)$ dimensions with the distribution function $f(\omega_k) = C\,\omega_k\,e^{-\alpha\omega_k}$. We mention that the upper inner and the lower plots are presented in *Log-Log* fashion.

Let us now elucidate on the reasoning behind the specific features of the lower plots

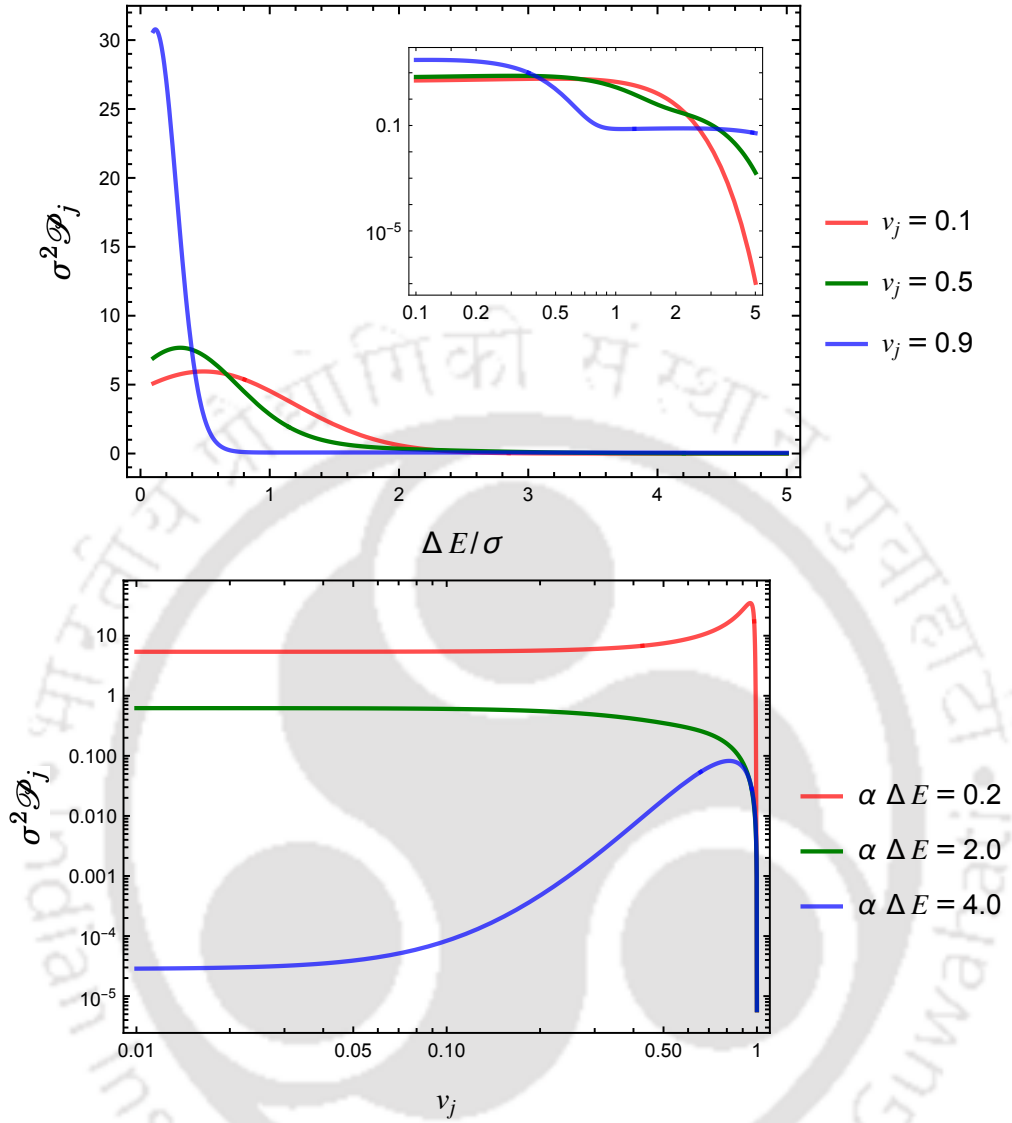

Figure 5.2: The dimensionless transition probability $\sigma^2\mathscr{P}_j$ is plotted as functions of $\Delta E/\sigma$ and v_j in the upper and the lower figures respectively in $(1+1)$ dimensions. For both the cases we considered the distribution function $f(\omega_k) = C\,\omega_k\, e^{-(\omega_k-\omega_0)^2/2\sigma^2}$, with $\omega_0/\sigma = 0.5$. Here also we have presented the upper inner and the lower plots in *Log-Log* fashion.

in Figs. 5.1 and 5.2, which is due to the appearance of two terms in Eq. (5.20). One is providing red shift in ΔE while the other one induces blue shift. In order to understand influence of these two effects in the transition amplitude, it is convenient to pay attention on a particular distribution of $f(\omega_k)$. Here we consider the exponentially damping one,

where $\mathscr{A}(\Delta E)$ is given by

$$\mathscr{A}(\Delta E) = \frac{C}{2}\left[\sqrt{\frac{1+v_j}{1-v_j}}\, e^{-\alpha\Delta E\sqrt{\frac{1+v_j}{1-v_j}}} + \sqrt{\frac{1-v_j}{1+v_j}}\, e^{-\alpha\Delta E\sqrt{\frac{1-v_j}{1+v_j}}}\right]. \tag{5.22}$$

Since we have $v_j < 1$, the above can be expanded in Taylor series. Keeping terms up to leading order in v_j (which is here v_j^2) one finds

$$\mathscr{A}(\Delta E) \simeq Ce^{-\alpha\Delta E}\left[1 + \left(\alpha^2\Delta E^2 - 3\alpha\Delta E + 1\right)v_j^2\right]. \tag{5.23}$$

Therefore when $\left(\alpha^2\Delta E^2 - 3\alpha\Delta E + 1\right) > 0$, the magnitude of the transition amplitude will increase with the increase of v_j. But if $\left(\alpha^2\Delta E^2 - 3\alpha\Delta E + 1\right) < 0$, then second term in the above expression provides diminishing effect in amplitude. As a result the transition amplitude decreases with the increase in v_j. This discussion provides explanation for the nature of curves for $\alpha\Delta E = 0.2, 2.0$ and 4.0. But when v_j is large, i.e., $v_j \to 1$, this approximation is not valid. In that case it is noted that the first term in (5.22) decays exponentially with the increase of v_j. Because of the pre-factor in the second exponential, the whole term also decreases. Hence effectively the amplitude decreases with the increase of v_j. Furthermore, one can check by taking the limit $v_j \to 1$ that the transition amplitude $\mathscr{A}(\Delta E)$ vanishes. Similar things are also happening for the Gaussian distribution in the lower plot of Fig. 5.2.

Entangling term and the concurrence:

Let us now proceed to evaluate the integral $\mathscr{E}$. We first consider the expression of $\mathscr{E}$ from Eq. (5.11) and evaluate $\mathscr{E}^{vac}$, which again is expressed as (5.13). In Eq. (5.13) the term containing only the Wightman function can be expressed as

$$\begin{aligned}\mathscr{E}_W^{vac} &= -\frac{1}{\gamma_A\gamma_B}\int_{-\infty}^{\infty}\frac{dk}{4\pi\omega_k}\int_{-\infty}^{\infty}dt_B\int_{-\infty}^{\infty}dt_A \\ &\quad\times e^{-i(\omega_k - k v_B)t_B + i(\omega_k - k v_A)t_A}\, e^{i\Delta E(t_B/\gamma_B + t_A/\gamma_A)} \\ &= -\frac{\pi}{\gamma_A\gamma_B}\int_{-\infty}^{\infty}\frac{dk}{\omega_k}\delta[(\omega_k - k v_A) + \Delta E/\gamma_A]\,\delta[(\omega_k - k v_B) - \Delta E/\gamma_B].\end{aligned} \tag{5.24}$$

This quantity vanishes due to the first Dirac-delta distribution for $\Delta E > 0$ and $0 \le v_A \le 1$. We also mention that here we have used the relation $t_j = \gamma_j\tau_j$ from Eq. (5.17). On the other hand, from Eq. (5.13) the term containing the retarded Green's function can be expressed as

$$\begin{aligned}\mathscr{E}_R^{vac} = \frac{i}{\gamma_A\gamma_B}\int_{-\infty}^{\infty}\frac{dk}{2\omega_k}\Bigg[&\frac{\delta[k(v_A - v_B) - \Delta E(1/\gamma_A + 1/\gamma_B)]}{\omega_k - k v_B - \Delta E/\gamma_B} \\ &+ \frac{\delta[k(v_A - v_B) + \Delta E(1/\gamma_A + 1/\gamma_B)]}{\omega_k - k v_B + \Delta E/\gamma_B}\Bigg].\end{aligned} \tag{5.25}$$

See Appendix 5.B for an explicit derivation of this expression. Here for $v_A > v_B$ this expression leads to

$$\mathscr{E}_R^{vac} = \frac{i\gamma_A\gamma_B(v_A - v_B)D_AD_B}{\Delta E^2(D_A + D_B)^2} \ . \tag{5.26}$$

On the other hand, for $v_B > v_A$ the integral from Eq. (5.25) becomes

$$\mathscr{E}_R^{vac} = \frac{i\gamma_A\gamma_B(v_B - v_A)D_AD_B}{\Delta E^2(D_A + D_B)^2} \ , \tag{5.27}$$

which is basically the same compared to the expression from $v_A > v_B$ case with a change in sign. From the previous sub-section we have seen that the integral of the form $\int_{-\infty}^{\infty} d\tau\, e^{i\Delta E\tau}\, \Phi^{\star}_{\text{eff}}(\tau)$ vanishes for detectors in uniform velocity in $(1+1)$ dimensions (see Eq. (5.21)). Then, one can perceive that the quantity $\mathscr{E}^{nv}$ from Eq. (5.15b) will also vanish in this scenario. Therefore, in this case we have $\mathscr{E}$ entirely given by $\mathscr{E}_R^{vac}$, *i.e.,* $\mathscr{E} = \mathscr{E}_R^{vac}$. Moreover, since there is only a sign change between the expressions from Eq. (5.26) and (5.27), in both the cases $v_A > v_B$ and $v_A < v_B$ the quantity $|\mathscr{E}|$ appearing in (5.4) yields the same feature. Also observe from Eq. (5.26) and (5.27) that when $v_A = v_B$ the integral $\mathscr{E}$ vanishes and so vanishes the concurrence. Thus in a situation when the two UD detectors are co-moving in $(1+1)$ dimensions there will be no entanglement harvesting. On the other hand, when the velocity of detector A approaches the velocity of light, *i.e.,* when $v_A \to 1$, the quantity $|\mathscr{E}_R^{vac}| = 1/(2\Delta E^2)$. Therefore, in this limit there is an upper bound in the value of the concurrence depending on the value of v_B and ΔE. This expressions also suggests that in this limit the amount of harvested concurrence (see Eq. (5.4)) should be increasing with decreasing ΔE.

In Fig. 5.3 and 5.4 we have plotted the concurrence denoting quantity $\mathscr{C}_{\mathscr{J}}$ as described in Eq. (5.4) considering the exponentially damping and Gaussian distribution functions respectively. For a discussion on these distributions in $(1+1)$ dimensions see Appendix 5.A.1. We also mention that if the detectors were to interact with the field vacuum rather than the singly excited field state, the quantities $\mathscr{P}_j$ denoting single detectors' transition probabilities would have been zero. In that scenario the concurrence is entirely given by $\mathscr{C}_{\mathscr{J}}^{vac} = |\mathscr{E}| = |\mathscr{E}_R^{vac}|$, a depiction of which is also included in these plots. From these figures, one notices that when $v_A = v_B$, the entanglement harvesting, like vacuum field state, ceases to exist for non-vacuum field state as well. Fig. 5.3 and 5.4 also confirms the possibility of entanglement harvesting between inertial UD detectors even from the single particle field states in $(1+1)$ dimensions. However, comparing the plots for $\mathscr{C}_{\mathscr{J}}$ and $\mathscr{C}_{\mathscr{J}}^{vac}$ from these figures, one can clearly see that entanglement harvesting is reduced in the non-vacuum case. In the non-vacuum situation the reduction

happens not only in magnitude of concurrence, also the range of velocity decreases. A common feature observed with both the distributions (the exponential damping and Gaussian distributions) is that the regime of low detector transition energy corresponds to quantitatively higher entanglement extraction. One should also note that for large fixed transitions energies there is no entanglement harvesting from the low velocity regimes. However, the amount of the harvested entanglement in the high velocity regime keeps decreasing with increasing ΔE. This is because in the very large v_A limit the entangling term varies as $\sim 1/(\Delta E)^2$ and hence $\mathscr{E}$ increase more than $\mathscr{P}_j$ with the decrease of ΔE.

5.4 Entanglement harvesting: motion in $(1+3)$ dimensions

Now we are going to investigate the same in $(1+3)$ dimensions. Since there are three spatial directions, the observers can move in more than one possible directions. We mainly concentrate on following motions of the two detectors – both are moving along the same direction and one is moving in the perpendicular direction of the other's motion.

5.4.1 Parallel motion

In this part we we are going to consider Unruh-DeWitt detectors in parallel uniform velocities in $(1+3)$ dimensions. For simplicity we shall consider the detectors to be in motion along the z direction. In particular, the observer with detector A is assumed to have an inertial motion such that its coordinates are related to its proper time as

$$t_A = \gamma_A \tau_A; \;\; x_A = 0; \;\; y_A = 0; \;\; z_A = \gamma_A v_A \tau_A. \tag{5.28}$$

On the other hand, the trajectory of detector B is

$$t_B = \gamma_B \tau_B; \;\; x_B = x_0; \;\; y_B = y_0; \;\; z_B = \gamma_B v_B \tau_B, \tag{5.29}$$

such that $r_0 = \sqrt{x_0^2 + y_0^2}$ is the perpendicular distance between the trajectories of two detectors A and B. In $(1+3)$ dimensions the effective field Φ_{eff} with respect to the Minkowski modes is given as

$$\Phi_{\text{eff}}(x) = \int \frac{d^3k}{(2\pi)^3} \frac{f(\omega_{\mathbf{k}})}{2\omega_{\mathbf{k}}} e^{ik\cdot x} \;, \tag{5.30}$$

where, $k\cdot x \equiv k_a x^a = -\omega_{\mathbf{k}} t + \mathbf{k}\cdot\mathbf{x}$. We shall see that unlike the previous $(1+1)$ dimensional scenario, here the expressions of $\mathscr{P}_A$ and $\mathscr{P}_B$ are not the same due to a finite non-zero

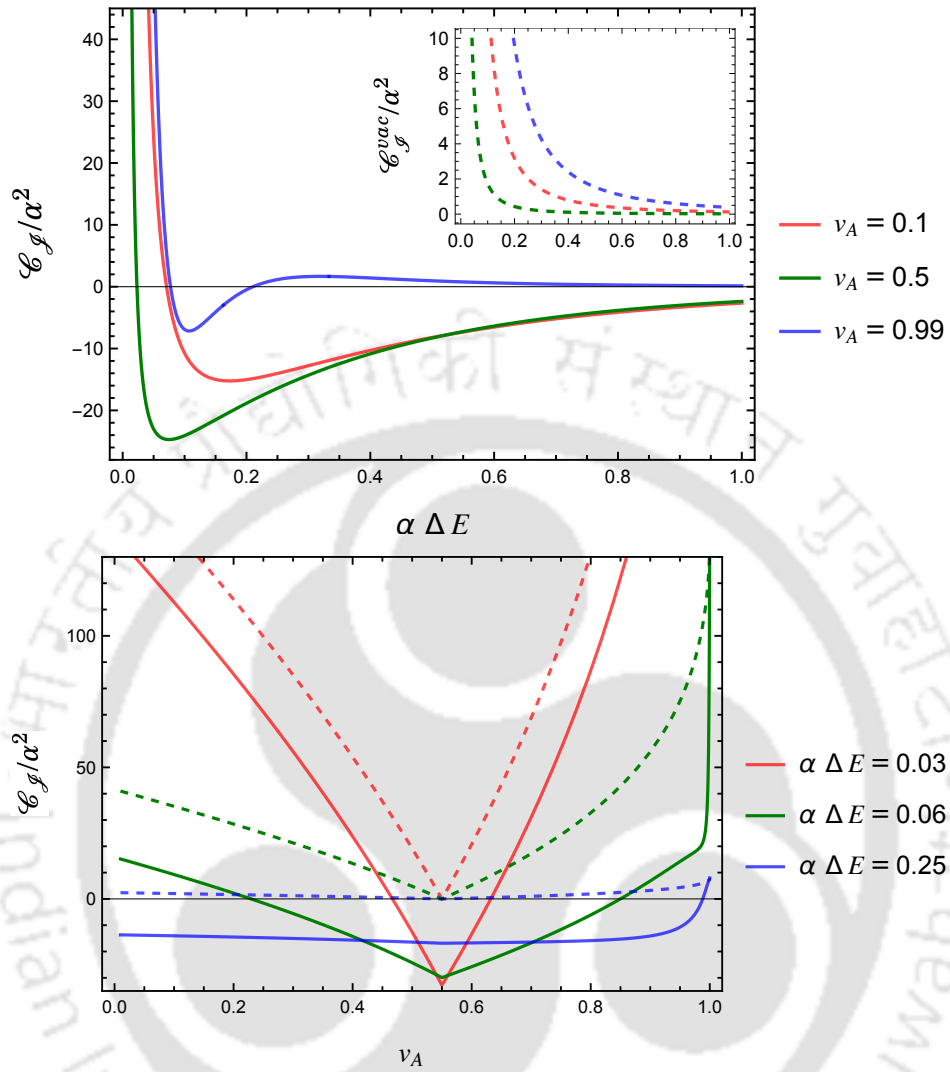

Figure 5.3: The dimensionless concurrence quantity $\mathscr{C}_{\mathscr{J}}/\alpha^2$ (the solid lines) is plotted as functions of $\alpha\,\Delta E$ and v_A in the upper and the lower plots respectively in $(1+1)$ dimensions with the distribution function $f(\omega_k) = C\,\omega_k\,e^{-\alpha\omega_k}$. Here the velocity of detector B is fixed at $v_B = 0.55$. We also mention that $\mathscr{C}_{\mathscr{J}}^{vac}/\alpha^2$, denoted by the dashed lines, indicates the concurrence if the detectors were interacting with the field vacuum. In the lower plot we have chosen the fixed parameter values for $\alpha\,\Delta E$ conveniently as suggested from the upper plot.

initial separation between the two detectors.

Transition probability:

Let us consider evaluating the integral $\mathscr{P}_B$ first, and one may expect that the expres-

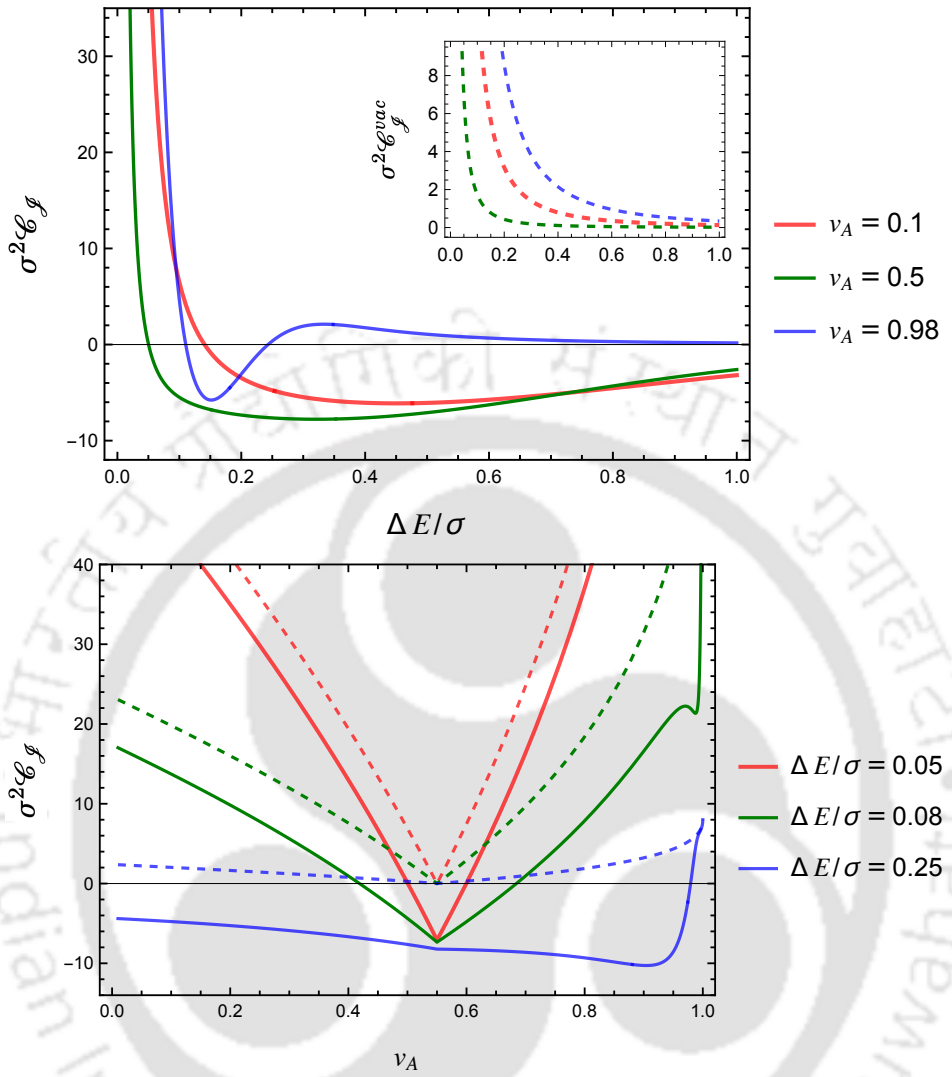

Figure 5.4: The dimensionless concurrence quantity $\sigma^2\mathscr{C}_{\mathscr{J}}$ (the solid lines) is plotted as functions of $\Delta E/\sigma$ and v_A in the upper and the lower plots respectively in $(1+1)$ dimensions. We have considered the distribution function $f(\omega_k) = C\,\omega_k\; e^{-(\omega_k-\omega_0)^2/2\sigma^2}$ in this case with $\omega_0/\sigma = 0.5$ and $v_B = 0.55$. Here also $\sigma^2\mathscr{C}^{vac}_{\mathscr{J}}$ (the dashed lines) indicates the concurrence if the detectors were interacting with the field vacuum.

sion of the integral $\mathscr{P}_A$ will arrive as a special case when $r_0 = 0$. For trajectory given in (5.29) the integral $\mathscr{P}_B$ can be evaluated considering the wave-vector in the spherical polar coordinates such that

$$\begin{aligned} k\cdot x &= -\omega_k t + \mathbf{k}.\mathbf{x} \\ &= \omega_k(-\gamma_B\tau_B + x_0\sin\theta\cos\phi + y_0\sin\theta\sin\phi + v_B\gamma_B\tau_B\cos\theta)\,, \end{aligned} \tag{5.31}$$

where we have used

$$\mathbf{k} = \omega_k \left(\sin\theta\cos\phi\,\hat{x} + \sin\theta\sin\phi\,\hat{y} + \cos\theta\,\hat{z}\right) ,$$
$$\mathbf{x} = x\,\hat{x} + y\,\hat{y} + z\,\hat{z} , \tag{5.32}$$

with $\omega_{\mathbf{k}} = |\mathbf{k}|$. Then in this case one can obtain the quantity from Eq. (5.16a) as

$$\mathscr{A}_B(\Delta E) = \int_{-1}^{1} \frac{du}{4\pi} \frac{\Delta E\, f\left(\frac{\Delta E}{\gamma_B(1-v_B u)}\right)}{\left[\gamma_B(1-v_B u)\right]^2} J_0\left(\frac{r_0 \Delta E\sqrt{1-u^2}}{\gamma(1-v_B u)}\right) , \tag{5.33}$$

where $J_n(x)$ denotes the Bessel function of the first kind, and $r_0 = \sqrt{x_0^2 + y_0^2}$. A detailed derivation of this expression is presented in Appendix 5.C. From this expression one can easily find out the value of $\mathscr{A}(\Delta E)$ for detector A by making $r_0 = 0$ as is also evident from the trajectories (5.28) and (5.29). When $r_0 = 0$ and $v_B \to v_A$ one may consider a change of variables $z = \Delta E/\gamma_A(1 - v_A u)$ in the previous equation such that it reduces to

$$\mathscr{A}_A(\Delta E) = \frac{1}{4\pi v_A \gamma_A} \int_{\Delta E/D_A}^{D_A \Delta E} dz\, f(z) . \tag{5.34}$$

where we have used the fact that $J_0(0) = 1$. This expression matches exactly with the one obtained explicitly for the detector A with trajectory (5.28), and is provided in Appendix 5.C. The relevant expression is derived in Eq. (5.A.8) of the Appendix. One should notice that in Eq. (5.34) and (5.33) we have included subscript A and B to signify the specific detectors. One may find out the respective $\mathscr{P}_j$ from $\mathscr{P}_j = |\mathscr{A}_j(\Delta E)|^2$ as here also $\mathscr{P}_j^{vac} = 0$ and $\mathscr{B}(\Delta E) = 0$ (see Appendix 5.C for details).

In (1+3) dimensions one may use the expressions of a few possible distribution functions as given in Appendix 5.A.2 to obtain $\mathscr{P}_j$. In particular, in Appendix 5.A.2 the explicit forms of the normalization constants (C) in the exponential damping and the Gaussian distribution functions are obtained, which are essential for procuring a numerical value for the above mentioned integral. Here also, these quantities $\mathscr{P}_j$ correspond to individual detector transition probabilities with a non-vacuum singly excited field state in the background. We have plotted this transition probability in Fig. 5.5 and 5.6 for the exponential decaying and Gaussian distribution functions, respectively. To be specific, we have plotted the quantity $\mathscr{P}_B$ with respect to the velocity v_B (when $r_0 \neq 0$), where the special case of $r_0 = 0$ produces the transition probability $\mathscr{P}_A$ with v_B now becoming v_A. The curves in these plots have somewhat similar features to the ones from (1+1) dimensions. Specifically, for low and high transition energy ΔE, the transition probability

increases with increasing velocity, and in the intermediate ΔE regimes this nature is reversed. Also visible from these plots is that the transition probability decreases with increasing r_0.

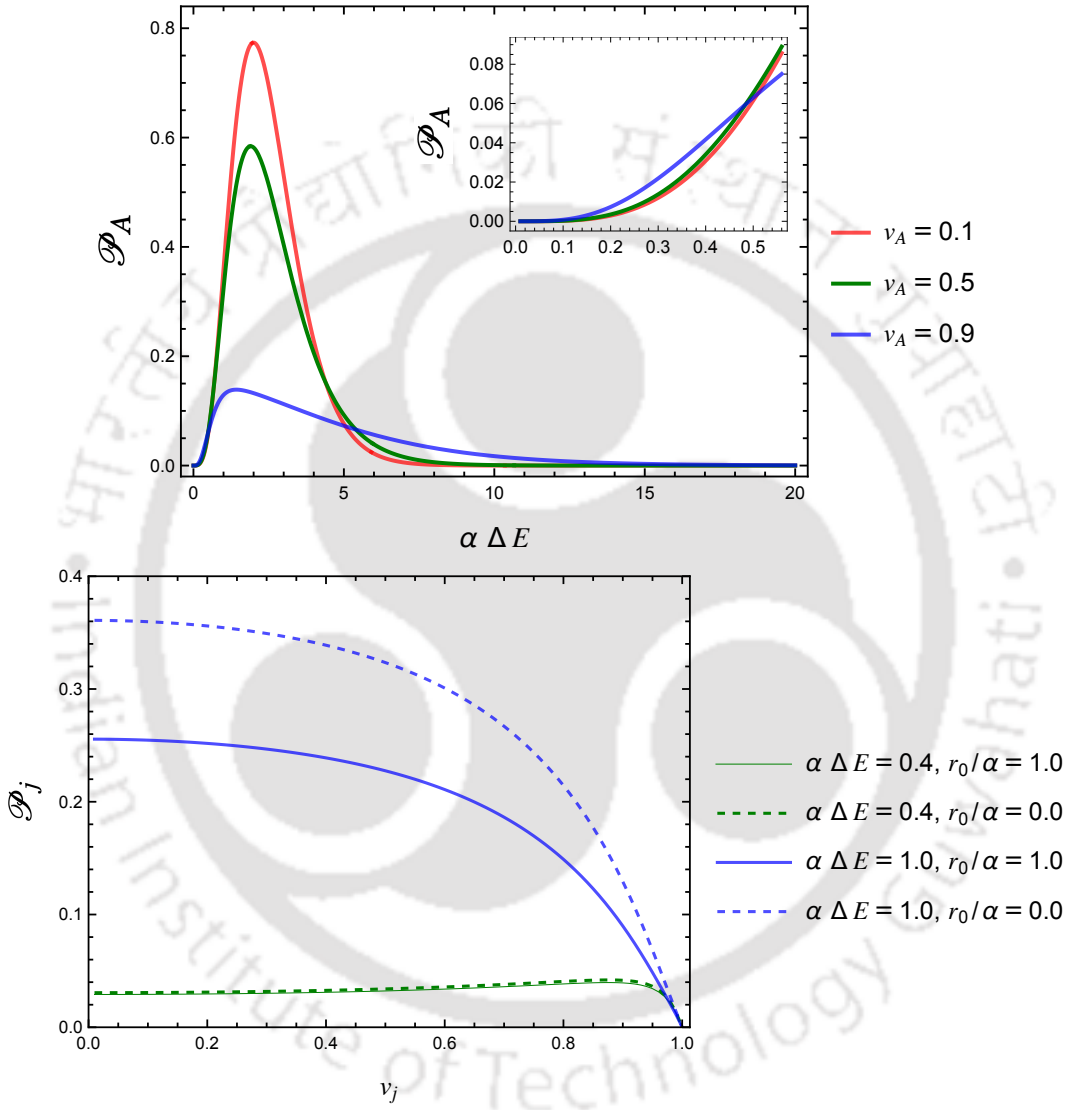

Figure 5.5: In the upper figure the quantity $\mathscr{P}_A$ is plotted as a function of $\alpha\,\Delta E$ for fixed values of v_A in $(1+3)$ dimensions. On the other hand, in the lower figure $\mathscr{P}_j$ is plotted with respect to v_j for different fixed values of $\alpha\,\Delta E$ and r_0/α. In both of these figures we have considered the distribution function $f(\omega_{\mathbf{k}}) = C\ \omega_{\mathbf{k}}\ e^{-\alpha\omega_{\mathbf{k}}}$. It is to be noted that in the lower plot $r_0/\alpha = 1$ corresponds to detector B and $r_0/\alpha = 0$ corresponds to detector A.

Entangling term and the concurrence:

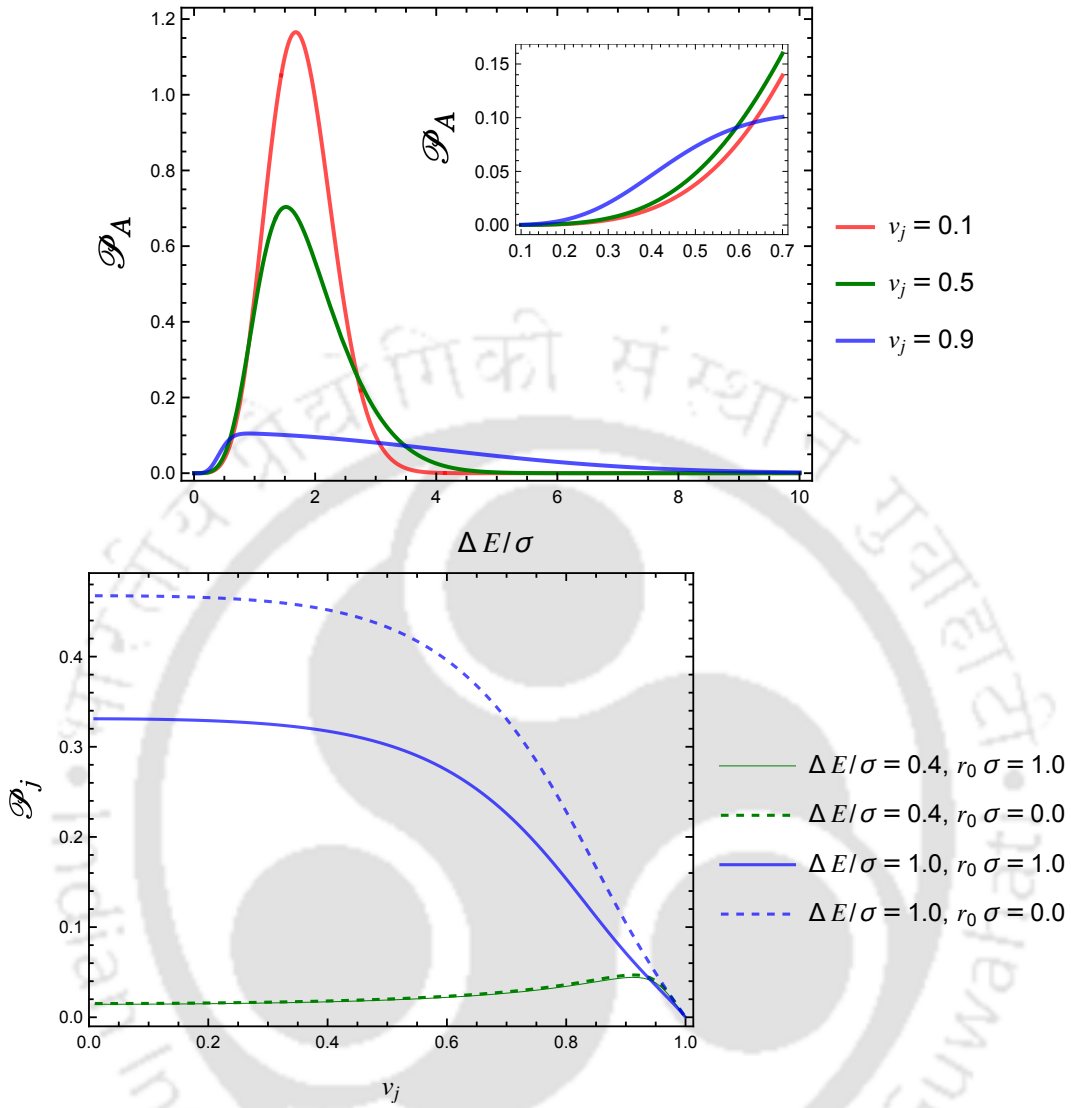

Figure 5.6: In the upper figure $\mathscr{P}_A$ is plotted as a function of $\Delta E/\sigma$ for fixed values of v_A in $(1+3)$ dimensions. On the other hand, in the lower figure $\mathscr{P}_j$ is plotted with respect to v_j for different fixed values of $\Delta E/\sigma$ and $r_0\sigma$. In both of these figures we have considered the distribution function $f(\omega_{\mathbf{k}}) = C\ \omega_{\mathbf{k}}\ e^{-(\omega_{\mathbf{k}}-\omega_0)^2/2\sigma^2}$ with $\omega_0/\sigma = 0.5$. Here also in the lower plot $r_0\sigma = 1$ corresponds to detector B and $r_0\sigma = 0$ corresponds to detector A.

Let us now evaluate the integral $\mathscr{E}$ for these two detectors which are in parallel inertial motion. In this scenario the quantities $\mathscr{E}^{nv}$ and $\mathscr{E}^{vac}_W$ vanish. The detailed calculation is provided in Appendix 5.C. The only non-vanishing contribution is given by the integral $\mathscr{E}^{vac}_R$. Using the representation from Eq. (5.14b) and with the help of Eqs. (5.28) and

(5.29) one can express this integral as

$$\mathscr{E}_R^{vac} = -\int_{-\infty}^{\infty}\int_{-\infty}^{\infty} \frac{dp\, dq}{2v_A v_B' \gamma_A \gamma_B} e^{i\Delta E(a_1 p + a_2 q)} \theta(a_3 p - q) \times \int_{-1}^{1} du \int_0^{\infty} \frac{\omega_k d\omega_k}{2(2\pi)^2} \left[e^{-i\omega_k a_4 (a_3 p - q) + i\omega_k \sqrt{p^2 + r_0^2}\, u} - e^{i\omega_k a_4 (a_3 p - q) - i\omega_k \sqrt{p^2 + r_0^2}\, u} \right], \tag{5.35}$$

where we have considered the change of variables $p = v_A\gamma_A\tau_A - v_B\gamma_B\tau_B$ and $q = v_A\gamma_A\tau_A + v_B\gamma_B\tau_B$. The Jacobian of this transform is given by $|J| = 1/(2v_A v_B \gamma_A \gamma_B)$. Whereas, the other variable is $u = \cos\theta$, and we have considered the redefined parameters $a_1 = 1/(2v_A\gamma_A) - 1/(2v_B\gamma_B)$, $a_2 = 1/(2v_A\gamma_A) + 1/(2v_B\gamma_B)$, $a_3 = (v_A + v_B)/(v_A - v_B)$, and $a_4 = (v_A - v_B)/2v_A v_B$. One may notice that due to the Heaviside step function the upper limit of the q integration transforms to $a_3 p$. Then one may evaluate this entire quantity $\mathscr{E}_R^{vac}$ in a step by manner with first carrying out the integration over q. Subsequently the integrals over u and ω_k can be performed in a likewise manner. After carrying out all these steps the integral looks like

$$\mathscr{E}_R^{vac} = \int_{-\infty}^{\infty} dp \, \frac{i\, e^{i\Delta E p(a_1 + a_2 a_3)} \cos\left(\frac{a_2 \Delta E \sqrt{p^2 + r_0^2}}{a_4} \right)}{8\pi v_A v_B \gamma_A \gamma_B a_4 \sqrt{p^2 + r_0^2}}. \tag{5.36}$$

To perceive a detailed procedure to arrive at this expression one may look into Appendix 5.C.3.2. This integral can be carried out to give a further simplified expression with the help of the integral representations of the modified Bessel function of the second kind $K_n(z)$ (see Eq. (3.876) of [250]), which are

$$\begin{aligned} &\int_0^{\infty} \frac{\cos\left(\varrho\sqrt{\xi^2 + a^2}\right)}{\sqrt{\xi^2 + a^2}} \cos(\beta\xi)\, \mathrm{d}\xi = K_0\left(a\sqrt{\beta^2 - \varrho^2}\right); \\ &\int_0^{\infty} \frac{\sin\left(\varrho\sqrt{\xi^2 + a^2}\right)}{\sqrt{\xi^2 + a^2}} \cos(\beta\xi)\, \mathrm{d}\xi = 0, \ [\beta > \varrho > 0]. \end{aligned} \tag{5.37}$$

Now one can observe that the exponential in the integral (5.36) can be written in terms of sin and cos functions so that the previous forms of Eq. (5.37) can be perceived. In our case, a comparison with Eq. (5.37) reveals $\beta = \Delta E(a_1 + a_2 a_3)$ and $\varrho = a_2 \Delta E/a_4$. Then from the consideration of a positive transition frequency ΔE (which is true in our case) and the explicit expressions of a_1, a_2, a_3, and a_4 one can confirm the satisfaction of the condition $\beta > \varrho > 0$ even with the integral (5.36). In particular, the integral of Eq. (5.36)

now becomes

$$\begin{aligned}\mathscr{E}_R^{vac} &= i\int_0^\infty dp\,\frac{\cos\left(\frac{a_2\Delta E}{a_4}\sqrt{p^2+r_0^2}\right)}{2\pi(v_A-v_B)\gamma_A\gamma_B\sqrt{p^2+r_0^2}}\cos\{\Delta E\,p(a_1+a_2a_3)\}\\ &= \frac{i\,K_0\left(r_0\Delta E\sqrt{(a_1+a_2a_3)^2-(a_2/a_4)^2}\right)}{2\pi(v_A-v_B)\gamma_A\gamma_B}\\ &= \frac{-i}{2\pi\gamma_A\gamma_B(v_A-v_B)}K_0\left(\frac{r_0\Delta E}{\gamma_B}\sqrt{\left(\frac{\frac{1}{\gamma_A}+\gamma_B(1-v_Av_B)}{v_A-v_B}\right)^2-\gamma_B^2}\right),\end{aligned} \tag{5.38}$$

where we have used (5.37) along with the relation $2v_Av_Ba_4=(v_A-v_B)$.

As a side remark and for comparison with the earlier result (given in [108]) we mention that in the limit $v_B\to 0$ we have $(a_1+a_2a_3)^2-(a_2/a_4)^2=2(1+\gamma_A)/v_A^2\gamma_A^2$, and thus the expression of $\mathscr{E}$ (which is entirely determined by $\mathscr{E}_R^{vac}$) is given by

$$|\mathscr{E}| = \frac{1}{2\pi v_A\gamma_A}K_0\left(\frac{r_0\Delta E}{v_A\gamma_A}\sqrt{2(1+\gamma_A)}\right). \tag{5.39}$$

This result matches correctly with the one from [108] (see Eq. (74) of [108] with $\theta=\pi/2$, where θ is the angle between $\mathbf{v}$ and $\mathbf{x}_0$), where one of the detectors was taken to be static.

We should emphasize here that in our present case the quantities $\mathscr{E}_W^{vac}$ and $\mathscr{E}^{nv}$ vanish (see Appendix 5.C for detailed estimations of these integrals). Here one may notice that in the limit of $(v_A-v_B)\to 0$ Eq. (5.38) leads to vanishing result. Therefore, for two parallel co-moving detectors the quantity dictating entanglement harvesting vanishes and one can assert that in this situation there will be no entanglement harvesting. A similar conclusion can also be made starting from Eq. (5.39), where one of the two observers is static, that the quantity $|\mathscr{E}|$ vanishes in the limit $v_A\to 0$.

In Fig. 5.7, 5.8, 5.9, and 5.10 we have plotted the concurrence denoting quantity $\mathscr{C}_{\mathscr{J}}$ for different distribution functions of the single particle field state. One can notice from these figures (specifically Fig. 5.7 and 5.9) that with decreasing ΔE the concurrence quantitatively increases, signifying an increase in the measure of the harvested entanglement. While from Fig. 5.8 and 5.10 it is evident that when $v_A\to v_B$ the entanglement harvesting vanishes. Moreover, when the detector transition energy ΔE becomes larger we observe a wide region of no harvesting around $v_A=v_B$ and this increases with the increase of ΔE. When the ΔE value is very large the entanglement harvesting is happening only in high velocity regimes. From Eq. (5.39) one can observe that in the limit $v_A\to 1$ the quantity $|\mathscr{E}|$ vanishes, and this feature is apparent from these figures too. One should also note that if the detectors were interacting with the field vacuum rather

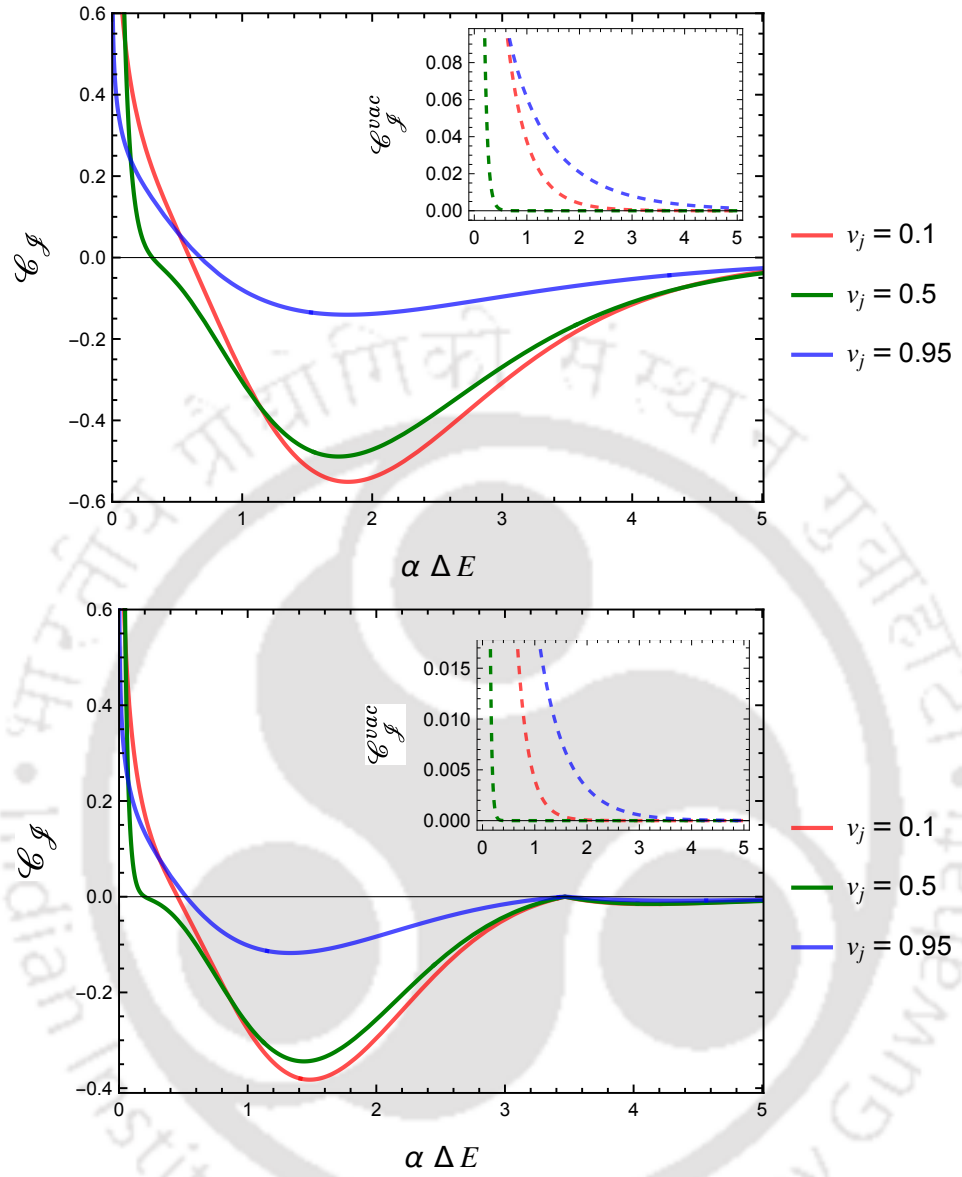

Figure 5.7: In (1+3) dimensions the quantity $\mathscr{C}_{\mathscr{J}}$, signifying the concurrence is plotted as a function of $\alpha\,\Delta E$ for different fixed values of v_A with two detectors in parallel inertial motion. In this plot we have considered the distribution function $f(\omega_{\mathbf{k}}) = C\,\omega_{\mathbf{k}}\,e^{-\alpha\omega_{\mathbf{k}}}$. Here the velocity of detector B is fixed at $v_B = 0.55$ and the other parameter is $r_0/\alpha = 0.5$ and $r_0/\alpha = 1$ respectively in the upper and lower plots. The inner plots correspond to $\mathscr{C}^{vac}_{\mathscr{J}}$, the concurrence, if the detectors were interacting with the field vacuum.

than the non-vacuum state, the quantity $\mathscr{P}_j$ would have been zero and the concurrence would have been completely given by $\mathscr{C}^{vac}_{\mathscr{J}} = |\mathscr{E}|$. We have included the plots of these $\mathscr{C}^{vac}_{\mathscr{J}}$ in the above mentioned figures. Here also, like the (1+1) dimensional case, the

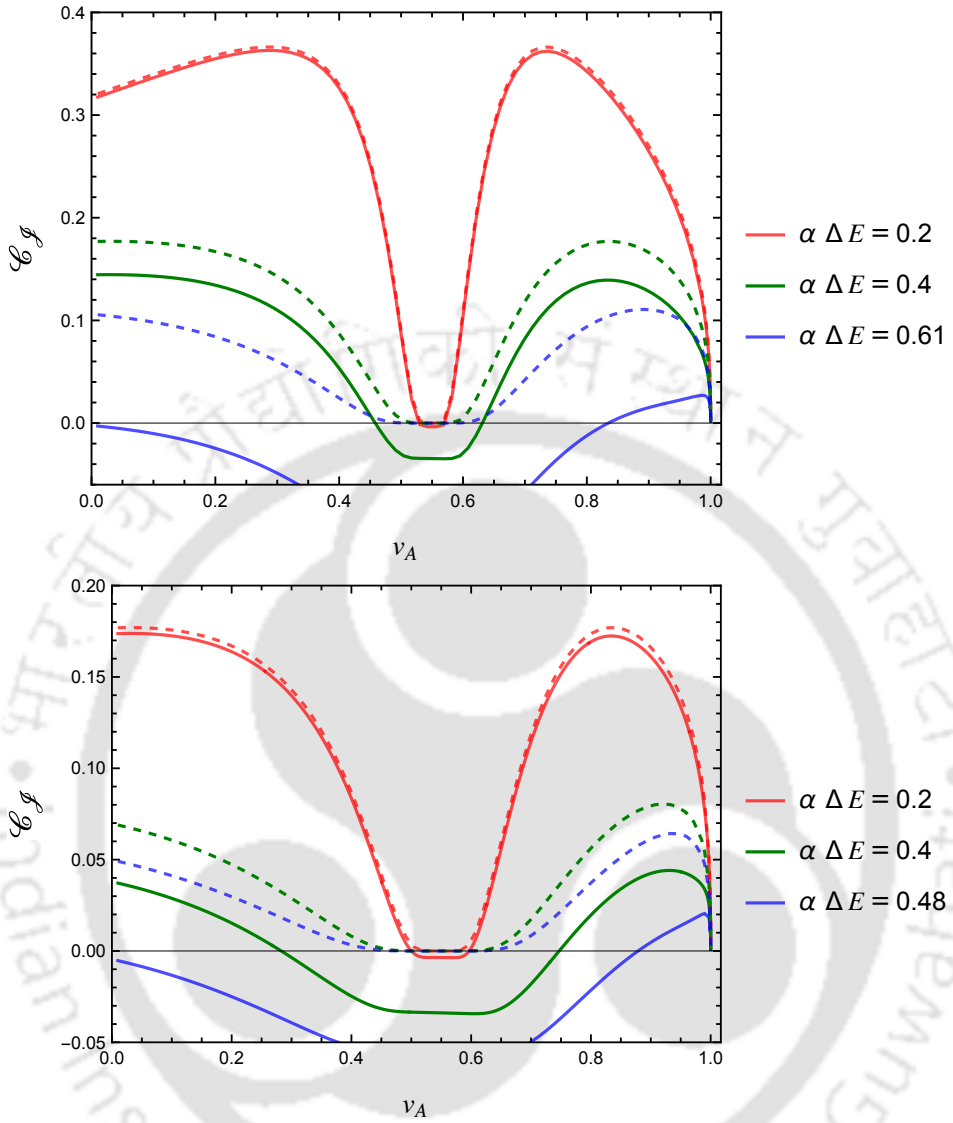

Figure 5.8: In (1 + 3) dimensions the integral $\mathscr{C}_{\mathscr{J}}$ signifying the concurrence is plotted as a function of v_A for two detectors in parallel inertial motion. The upper and the lower plots respectively correspond to $r_0/\alpha = 0.5$ and $r_0/\alpha = 1$. In both of these plots we have considered the distribution function $f(\omega_{\mathbf{k}}) = C\,\omega_{\mathbf{k}}\,e^{-\alpha\omega_{\mathbf{k}}}$ and the velocity of detector B is fixed at $v_B = 0.55$. The solid lines denote the contributions from $\mathscr{C}_{\mathscr{J}}$, while the dashed lines denote $\mathscr{C}^{vac}_{\mathscr{J}}$.

entanglement harvesting is suppressed due to non-vacuum fluctuations as compared to vacuum effect. Here both the magnitude of concurrence and valid region of the value of v_A for entanglement harvesting decreases. From these figures we also observe that entanglement harvesting is decreasing with increasing distance r_0/α between the parallel

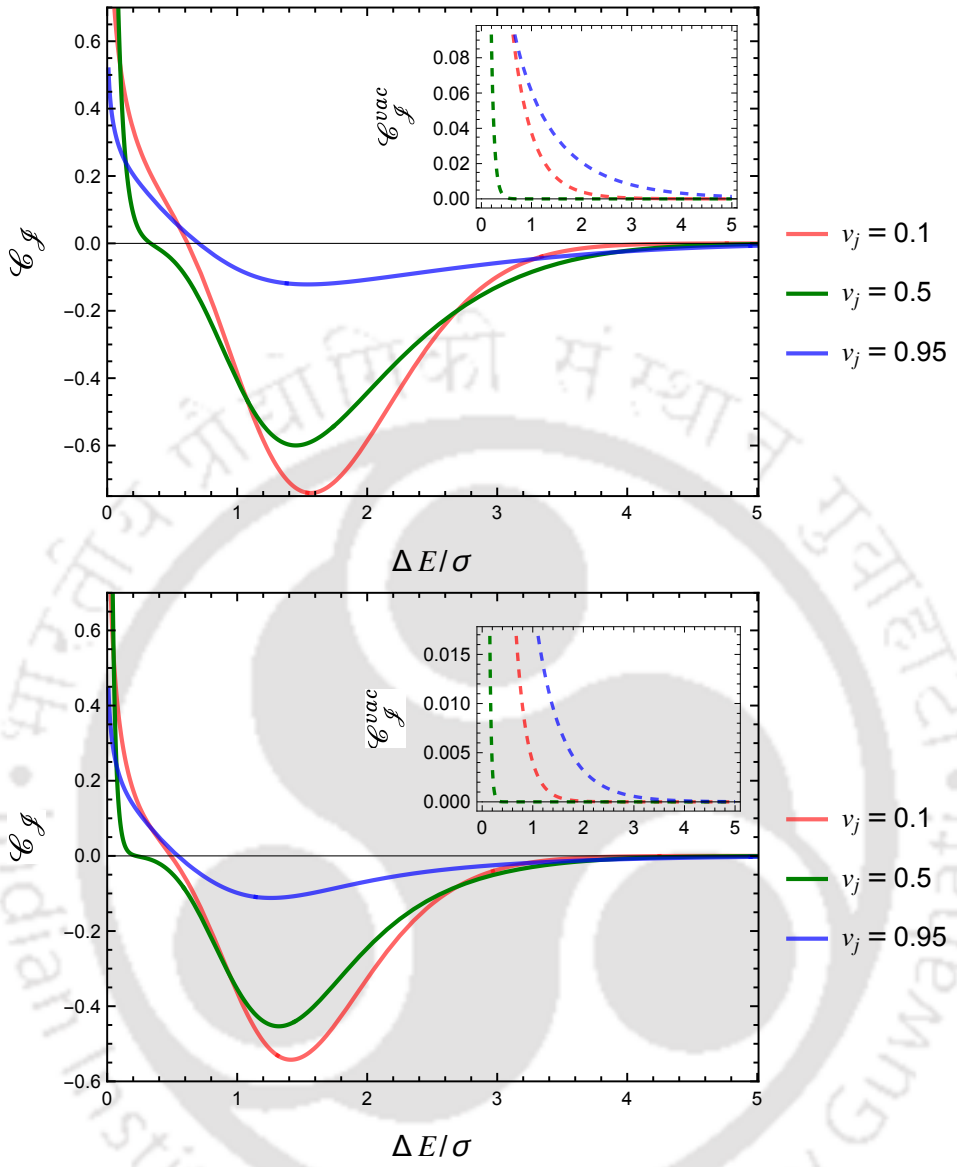

Figure 5.9: In (1+3) dimensions the quantity $\mathscr{C}_{\mathscr{J}}$ signifying the concurrence is plotted as a function of $\Delta E/\sigma$ for different fixed values of v_A with two detectors in parallel inertial motion. In this plot we have considered the distribution function $f(\omega_{\mathbf{k}}) = C\,\omega_{\mathbf{k}}\; e^{-(\omega_{\mathbf{k}}-\omega_0)^2/2\sigma^2}$. The velocity of detector B is fixed at $v_B = 0.55$ and the other fixed parameters are $r_0\sigma = 0.5$ and $r_0\sigma = 1$ (respectively for the upper and lower figures), $\omega_0/\sigma = 0.5$. The inner plots correspond to $\mathscr{C}^{vac}_{\mathscr{J}}$, the concurrence, if the detectors were interacting with the field vacuum.

paths, and with increasing detector transition energy ΔE.

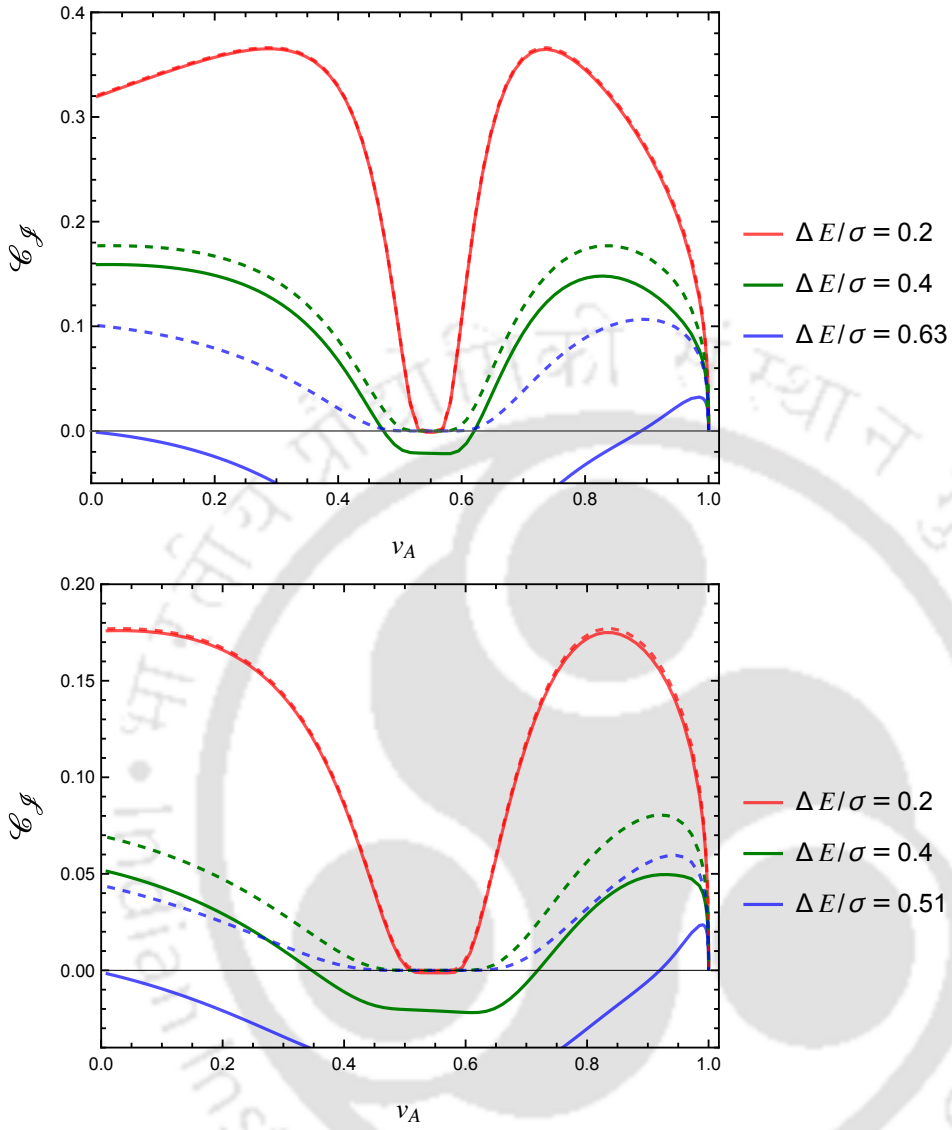

Figure 5.10: In (1+3) dimensions the quantity $\mathscr{C}_{\mathscr{J}}$ signifying the concurrence is plotted as a function of v_A for two detectors in parallel inertial motion. The upper and the lower plots respectively correspond to $r_0\sigma = 0.5$ and $r_0\sigma = 1$. In both of these plots we have considered the distribution function $f(\omega_{\mathbf{k}}) = C\,\omega_{\mathbf{k}}\, e^{-(\omega_{\mathbf{k}}-\omega_0)^2/2\sigma^2}$. Here the velocity of detector B is fixed at $v_B = 0.55$, and the other parameter $\omega_0/\sigma = 0.5$. The solid lines denote the contributions from $\mathscr{C}_{\mathscr{J}}$, while the dashed lines denote $\mathscr{C}^{vac}_{\mathscr{J}}$.

5.4.2 Perpendicular motion

In this part we consider two Unruh-DeWitt detectors in motion perpendicular to each other. We consider detector A with an uniform velocity along the x-axis and detector B with an uniform velocity along the z direction starting from a constant displacement in

the y direction. The trajectory of detector A is

$$t_A = \gamma_A \tau_A;\;\; x_A = \gamma_A v_A \tau_A;\;\; ;\;\; y_A = 0;\;\; z_A = 0\,. \tag{5.40}$$

On the other hand, the trajectory of detector B is given by

$$t_B = \gamma_B \tau_B;\;\; x_B = 0;\;\; y_B = r_0;\;\; z = \gamma_B v_B \tau_B\,. \tag{5.41}$$

These trajectories signify that the motion of the detectors are confined to the $x-z$ plane, while there is a perpendicular initial separation between them in the y direction.

Transition probability:

One may observe that the trajectory of the detector A in this case and the previous case of the parallel motion are physically the same. Therefore, the expressions of the integral $\mathscr{P}_A$ will also be the same. In fact this indeed comes to be true and one can look into Appendix 5.D.1 for a derivation of the expression of $\mathscr{P}_A$ with the trajectory (5.40). Here we recall the expression of $\mathscr{A}_A(\Delta E)$ from Eq. (5.34), which is relevant to estimate $\mathscr{P}_A$, as

$$\mathscr{A}_A(\Delta E) = \frac{1}{4\pi v_A \gamma_A}\int_{\Delta E/D_A}^{D_A \Delta E} dz\, f(z)\,. \tag{5.42}$$

On the other hand, in a similar manner one can also find out the quantity $\mathscr{A}_B(\Delta E)$ relevant for estimating $\mathscr{P}_B$ with the trajectory (5.41) as

$$\mathscr{A}_B(\Delta E) = \int_{-1}^{1} \frac{du}{4\pi} \frac{\Delta E\; f\left(\frac{\Delta E}{\gamma_B(1-v_B u)}\right)}{[\gamma_B(1-v_B u)]^2} J_0\left(\frac{r_0 \Delta E \sqrt{1-u^2}}{\gamma_B(1-v_B u)}\right). \tag{5.43}$$

This expression can be obtained from Eq. (5.33) as the trajectories of detector B from the parallel and perpendicular motion cases are physically equivalent. In this regard, compare the trajectories of detector B from Eq. (5.29) and (5.41). Furthermore, one can find that here also $\mathscr{P}_j^{vac} = 0$ and $\mathscr{B}_j(\Delta E) = 0$, see Appendix 5.D for details. Then the previous integral signifying individual detector transition probability for the detectors A and B are given by $\mathscr{P}_j = |\mathscr{A}_j(\Delta E)|^2$.

Here with the two detectors in inertial motion perpendicular to each other in $(1+3)$ dimensions, the integrals $\mathscr{P}_j$ are the same as the previous parallel case (see Eq. (5.34) and (5.33) and compare them with the expressions here). Therefore the individual detector's response function will have the same features as shown in Fig. 5.5 and 5.6.

Entangling term and the concurrence:

Now we shall evaluate the quantity $\mathscr{E}$ for two detectors in perpendicular inertial motion with trajectories given in (5.40) and (5.41). In particular, here also one can observe that the $\mathscr{E}^{nv}$ part of this quantity vanishes, so does the $\mathscr{E}_W^{vac}$. Then $\mathscr{E} = \mathscr{E}^{nv} + \mathscr{E}_W^{vac} + \mathscr{E}_R^{vac}$ is completely given by $\mathscr{E}_R^{vac}$. In Eq. (5.14b) we have seen that this integral is dependent on the retarded Green's function $G_R(x_A, x_B)$. This retarded Green function $G_R(x_A, x_B)$ for a massless, minimally coupled, free scalar field in the Minkowski spacetime (see [108]) is expressed as

$$\begin{aligned} G_R(x_A, x_B) &= -\frac{1}{2\pi}\,\theta(t_A - t_B)\,\delta\left((t_A - t_B)^2 - |\boldsymbol{x}_A - \boldsymbol{x}_B|^2\right) \\ &= -\frac{1}{2\pi}\theta(t_A - t_B)\,\delta(g(t_A, t_B))\,. \end{aligned} \tag{5.44}$$

For the considered trajectories of detector A and B from Eq. (5.40) and (5.41) one can find the solution of $g(t_A, t_B) = t_A^2(1 - v_A^2) + t_B^2(1 - v_B^2) - 2t_A t_B - r_0^2 = 0$ with respect to t_B as

$$t_B = \gamma_B^2(t_A \pm u(t_A)) \equiv t_\pm\,, \tag{5.45}$$

with,

$$u(t_A) = \sqrt{t_A^2(v_A^2 + v_B^2 - v_A^2 v_B^2) + r_0^2(1 - v_B^2)}\,, \tag{5.46}$$

where, for $0 \leq v_j \leq 1$ one can confirm that,

$$\begin{aligned} \gamma_B^2(t_A + u(t_A)) &> t_A \\ \gamma_B^2(t_A - u(t_A)) &< t_A\,. \end{aligned} \tag{5.47}$$

Now it is imperative to use the property of Dirac delta distributions

$$\begin{aligned} \delta(g(t_A, t_B)) &= \left[\frac{\delta(t_B - t_+)}{|g'(t_A, t_B)|_{t_B = t_+}} + \frac{\delta(t_B - t_-)}{|g'(t_A, t_B)|_{t_B = t_-}}\right] \\ &= \frac{1}{2u(t_A)}[\delta(t_B - t_+) + \delta(t_B - t_-)]\,. \end{aligned} \tag{5.48}$$

Then the integral $\mathscr{E}_R^{vac}$ from Eq. (5.14b), with a change of variable from τ_j to t_j, can be expressed as

$$\begin{aligned} \mathscr{E}_R^{vac} &= \frac{-i}{2\pi}\int_{-\infty}^{\infty}\frac{dt_A}{\gamma_A}\int_{-\infty}^{t_A}\frac{dt_B}{\gamma_B}\,e^{i\Delta E\left(\frac{t_A}{\gamma_A} + \frac{t_B}{\gamma_B}\right)}\delta(g(t_A, t_B)) \\ &= \frac{-i}{4\pi}\int_{-\infty}^{\infty}\frac{dt_A}{\gamma_A\gamma_B\,u(t_A)}\,e^{i\Delta E\left(\frac{t_A}{\gamma_A} + \gamma_B(t_A - u(t_A))\right)} \\ &= \frac{-i}{2\pi\gamma_A\gamma_B}\int_0^{\infty}\frac{dt_A e^{-i\Delta E\gamma_B u(t_A)}}{u(t_A)}\cos\left\{\Delta E t_A\left(\frac{1}{\gamma_A} + \gamma_B\right)\right\}\,. \end{aligned} \tag{5.49}$$

Furthermore, one can expand the exponential in this integral in terms of sin and cos functions and then by comparing them with the integral representations of the Bessel functions (5.37), can recognize

$$a = r_0/\gamma_B; \;\; p = \gamma_B \Delta E; \;\; b = \frac{\Delta E\left(\frac{1}{\gamma_A}+\gamma_B\right)}{\sqrt{v_A^2+v_B^2(1-v_A^2)}}; \tag{5.50}$$

and as one has $0 \leq v_j \leq 1$, this also satisfies the condition among the parameters from (5.37), which is $b > p$. Thus, the integration in Eq. (5.49) can be evaluated. One can provide the simplified form as

$$\mathscr{E}_R^{vac} = \frac{-i}{2\pi\gamma_A\gamma_B\sqrt{v_A^2+v_B^2(1-v_A^2)}}\, K_0\left(r_0\Delta E\sqrt{\frac{\left(\frac{1}{\gamma_A\gamma_B}+1\right)^2}{v_A^2+v_B^2(1-v_A^2)}-1}\right). \tag{5.51}$$

Moreover, one can check that when $v_B = 0$ (in that situation $\gamma_B = 1$), this expression reduces to (5.39) as obtained in the parallel case. Here also the quantities $\mathscr{E}_W^{vac}$ and $\mathscr{E}^{nv}$ vanish and we refer the reader to go through Appendix 5.D for detailed estimations of these integrals.

The plots from Figs. 5.11 and 5.13 of $\mathscr{C}_{\mathscr{I}}$ with respect to the transition energy ΔE in this perpendicular case represent nature similar to the parallel case (see Fig. 5.7 and 5.9). From these figures we observe that with increasing detector transition energy ΔE the harvesting decreases (only when $\mathscr{C}_{\mathscr{I}}$ is positive). In Fig. 5.12 and 5.14 we have plotted $\mathscr{C}_{\mathscr{I}}$ as functions of v_A for fixed $v_B \neq 0$. We have also plotted the quantity $\mathscr{C}_{\mathscr{I}}^{vac} = |\mathscr{E}|$ in these figures, which denotes the concurrence if the detectors were interacting with the field vacuum rather than the non-vacuum state. From these plots one can observe that entanglement harvesting from the single particle excited state is suppressed compared to the vacuum fluctuations. Here also, one can observe that in the limit of $v_A \to 1$, the quantity $|\mathscr{E}|$ vanishes, leading to a vanishing concurrence, and this feature is evident in these figures. When the ΔE value is large the entanglement harvesting is happening in discrete intermediate and high velocity regimes. Like the parallel case here also entanglement harvesting decreases with increasing distance r_0/α between the perpendicular paths, and with increasing transition energy ΔE. Here when the two detectors are in perpendicular inertial motion in $(1+3)$ dimensions the integral $\mathscr{E}_R^{vac}$ does not vanish in the $v_A \to v_B$ limit unlike the parallel case. However, its expression in the $v_B \to 0$ limit is the same as the parallel case. We also observe that in the $v_B = 0$ situation (plots corresponding to this situation are given in Fig. 5.15) the plots are the

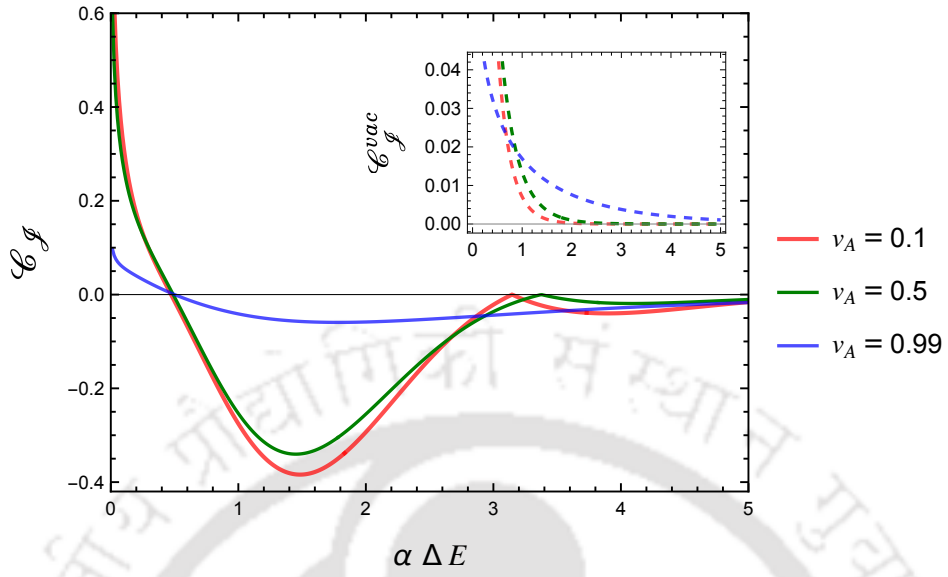

Figure 5.11: In $(1+3)$ dimensions for perpendicular motion of the detectors the integral $\mathscr{C}_{\mathscr{J}}$ signifying the concurrence is plotted as a function of $\alpha\,\Delta E$ for different fixed values of v_A. In this plot we have considered the distribution function $f(\omega_{\mathbf{k}}) = C\,\omega_{\mathbf{k}}\,e^{-\alpha\omega_{\mathbf{k}}}$ for the singly excited background field state. Here the velocity of detector B is fixed at $v_B = 0.55$ and the other parameter is $r_0/\alpha = 1$. The inner plot correspond to $\mathscr{C}^{vac}_{\mathscr{J}}$, the concurrence, if the detectors were interacting with the field vacuum.

same as the parallel case (done in [108], where one detector is taken to be stationary). While for $v_B \neq 0$ they are much different.

5.5 Summary and Discussions

In the earlier chapters, we have studied entanglement harvesting, considering the detectors interacting with the field vacuum. However, in nature, one cannot expect that the background field will always be in a vacuum state. Then, the consideration of non-vacuum field states in understanding entanglement harvesting becomes essential from the practical point of view. The present work has considered single-particle background field excitations to investigate the entanglement harvesting between inertial Unruh-DeWitt detectors in $(1+1)$ and $(1+3)$ dimensions. Choice of single particle state is motivated from the earlier work [191], and to build an analytically simple, tractable model. We have presented a thorough formulation for understanding entanglement harvesting from non-vacuum field states. Our main observation is that in both $(1+1)$ and $(1+3)$ dimensions, the entanglement harvested due to the single-particle background

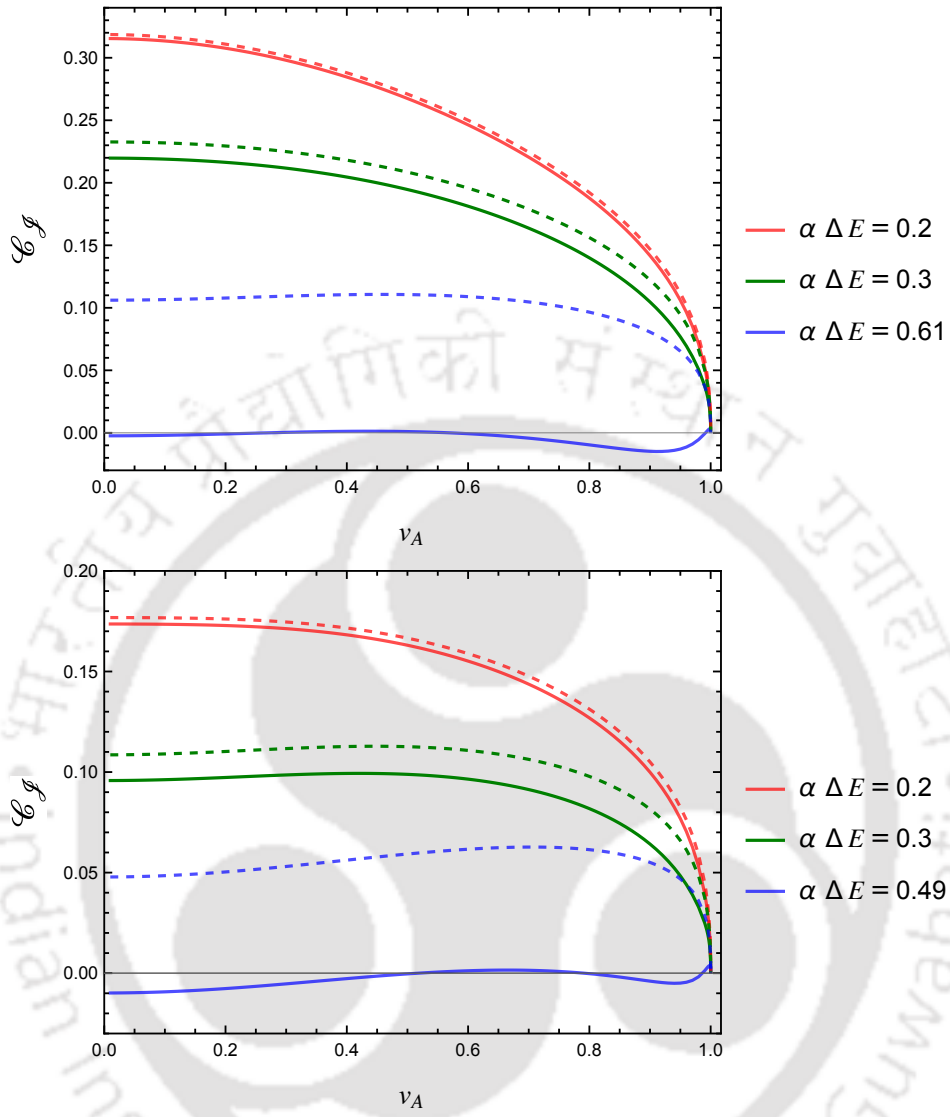

Figure 5.12: In $(1+3)$ dimensions for the detectors' perpendicular motion the quantity $\mathscr{C}_{\mathscr{J}}$, signifying the concurrence, is plotted as a function of v_A. The upper and the lower plots respectively correspond to $r_0/\alpha = 0.5$ and $r_0/\alpha = 1$. In both of these plots we have considered the distribution function $f(\omega_{\mathbf{k}}) = C\,\omega_{\mathbf{k}}\,e^{-\alpha\omega_{\mathbf{k}}}$ and the velocity of detector B is fixed at $v_B = 0.55$. The solid lines denote the contributions from $\mathscr{C}_{\mathscr{J}}$, while the dashed lines denote $\mathscr{C}^{vac}_{\mathscr{J}}$.

fluctuations is reduced compared to the vacuum fluctuations. The transition probability for inertial detectors interacting with the non-vacuum field state is non-zero and non-trivial (see Figs. 5.1, 5.2, 5.5, and 5.6). This non-zero transition probability is expected even if the detectors are inertial as they interact with non-vacuum field states. We also observed, both in $(1+1)$ and $(1+3)$ dimensions with detectors in parallel motion,

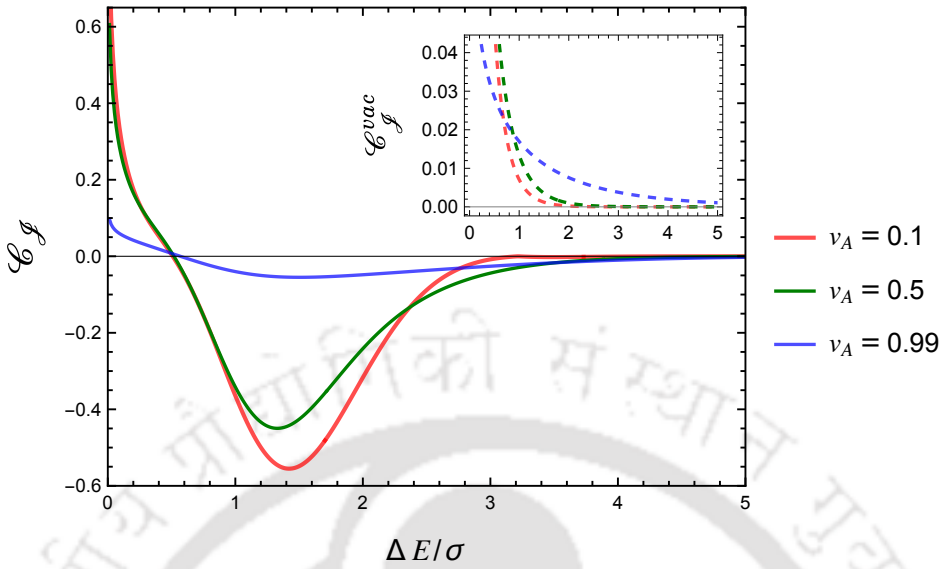

Figure 5.13: In $(1+3)$ dimensions for perpendicular motion of the detectors the quantity $\mathscr{C}_{\mathscr{J}}$ signifying the concurrence is plotted as a function of $\Delta E/\sigma$ for different fixed values of v_A. In this plot we have considered the distribution function $f(\omega_{\mathbf{k}}) = C\,\omega_{\mathbf{k}}\, e^{-(\omega_{\mathbf{k}}-\omega_0)^2/2\sigma^2}$ for the singly excited background field state. Here the velocity of detector B is fixed at $v_B = 0.55$ and the other fixed parameters are $r_0\sigma = 1$ and $\omega_0/\sigma = 0.5$. The inner plot correspond to $\mathscr{C}_{\mathscr{J}}^{vac}$, the concurrence, if the detectors were interacting with the field vacuum.

that two detectors with the same velocity ($v_A = v_B$) do not harvest any entanglement among themselves when interacting with the single particle field state. This phenomenon was true even when the detectors interacted with the field vacuum. However, a similar situation with detectors in perpendicular inertial motion in $(1+3)$ dimensions is not observed. One observes increasing entanglement harvesting with decreasing detector transition energy in both these dimensions, for parallel and perpendicular motions, and the considered system parameters. In particular, in $(1+1)$ dimensions, there is visible occurrence of entanglement harvesting in low detector transition energy and high-velocity regimes (see Figs. 5.3 and 5.4). While in $(1+3)$ dimensions (both with detectors in parallel and perpendicular motion), one notices that entanglement harvesting stops when the velocity of detector A approaches the velocity of light, i.e., when $v_A \to 1$ (see Figs. 5.8, 5.10, 5.12, 5.14, and 5.15). In $(1+3)$ dimensions the entanglement harvesting decreases with increasing perpendicular distance (r_0) between the two detectors.

We want to provide a few final comments, which are as follows. First, we emphasize that entanglement harvesting is possible only when $|\mathscr{E}|^2 > \mathscr{P}_A\mathscr{P}_B$. The nonnegative

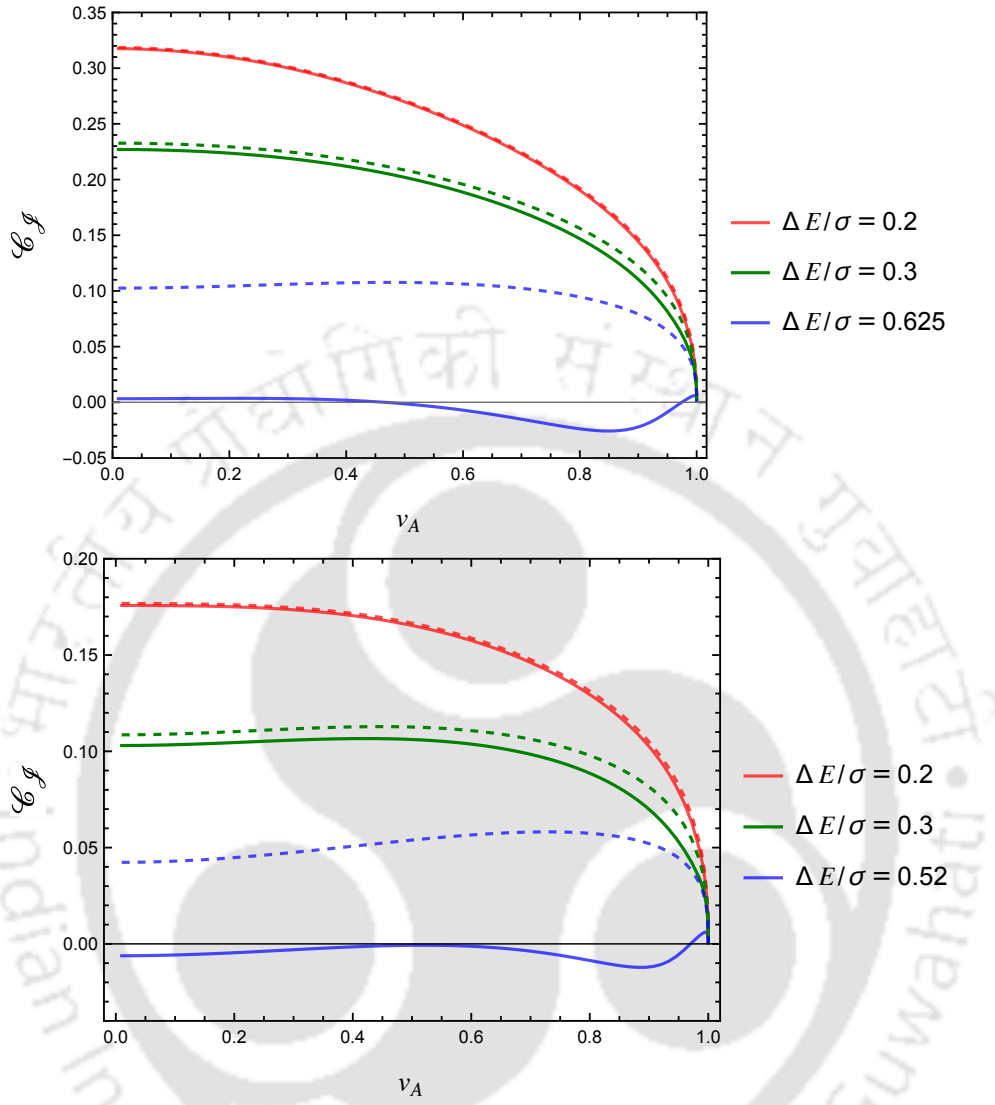

Figure 5.14: In $(1+3)$ dimensions for the detectors in perpendicular inertial motion, the integral $\mathscr{C}_{\mathscr{J}}$ signifying the concurrence is plotted as a function of v_A. The upper and the lower plots respectively correspond to $r_0/\sigma = 0.5$ and $r_0/\sigma = 1$. In both of these plots we have considered the distribution function $f(\omega_{\mathbf{k}}) = C\ \omega_{\mathbf{k}}\ e^{-(\omega_{\mathbf{k}}-\omega_0)^2/2\sigma^2}$. Here the velocity of detector B is fixed at $v_B = 0.55$, and the other fixed parameter is $\omega_0/\sigma = 0.5$. The solid lines denote the contributions from $\mathscr{C}_{\mathscr{J}}$, while the dashed lines denote $\mathscr{C}_{\mathscr{J}}^{vac}$.

measure of $\mathscr{C}_{\mathscr{J}} = |\mathscr{E}| - \sqrt{\mathscr{P}_A \mathscr{P}_B}$ quantifies the harvested entanglement. Interestingly the local terms $\mathscr{P}_j$ (with j being either A or B) denote individual detector transition probabilities. These terms have a vanishing contribution to inertial detectors interacting with the vacuum background scalar field. While for the background field in any excited state, these local terms for the similar detector motion are finite and nonzero. Therefore,

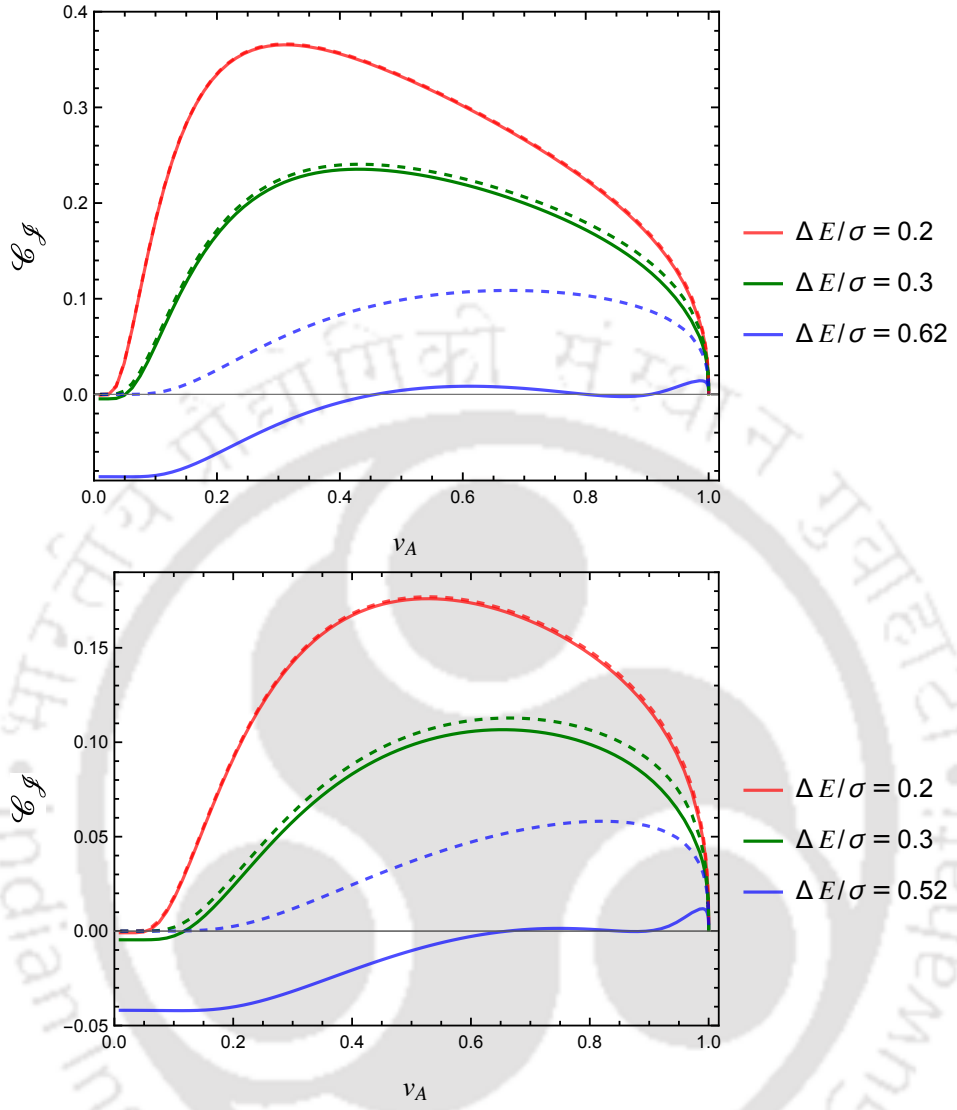

Figure 5.15: In $(1+3)$ dimensions the integral $\mathscr{C}_{\mathscr{J}}$ signifying the concurrence is plotted as a function of v_A for $v_B = 0$. The upper and the lower plots respectively correspond to $r_0\sigma = 0.5$ and $r_0\sigma = 1$. In both of these plots we have considered the distribution function $f(\omega_{\mathbf{k}}) = C\ \omega_{\mathbf{k}}\ e^{-(\omega_{\mathbf{k}}-\omega_0)^2/2\sigma^2}$ with $\omega_0/\sigma = 0.5$. It should be mentioned that with the exponential decaying distribution function also one gets similar plots with the same characteristics. The dashed lines denote the contributions from $\mathscr{C}^{vac}_{\mathscr{J}}$, while the solid lines denote $\mathscr{C}_{\mathscr{J}}$.

1

the harvesting from the nonvacuum states is always expected to be lesser compared to the field vacuum if the entangling term $\mathscr{E}$ does not change much. In our current work, we found that this is indeed the case with single-particle excited states, as the entangling

term $\mathscr{E}$ remains the same for the vacuum and nonvacuum field states.

Furthermore, we found some additional distinct features with the single-particle excited states compared to the vacuum field state. For example, for two inertial detectors moving at different velocities, entanglement harvesting from the field vacuum always seems possible as one varies the detector transition energy ΔE. While the same is not true from the single-particle excited state as one can perceive ranges of no-harvesting in ΔE. One observes this phenomenon in both $(1+1)$ and $(1+3)$ dimensions and for parallel and perpendicular cases. In this regard, see the plots of concurrence as a function of ΔE in Figs. 5.3, 5.4, 5.7, 5.9, 5.11, and 5.13. When examining the results with a varying velocity v_A of the detector A, one may point out a similarly interesting distinguishing feature in the perpendicular motion case. In this scenario, one can observe discrete regions of entanglement harvesting in v_A from the single-particle field states for larger detector transition energies. In comparison, in similar scenarios, entanglement harvesting from the vacuum is possible in the whole range $0 < v_A < 1$, see Figs. 5.12 and 5.14. These specific observations provide additional distinctions between the vacuum and single-particle entanglement harvesting cases other than the expected diminishing phenomenon observed for the latter case. Finally, one should notice that in nature, it is not guaranteed that the background field state will be in a vacuum. In fact, it is natural to believe that the fields will be in some excited state due to the presence of various constituents. Then, these specific features of harvesting shall provide some valuable distinctions of identification. Moreover, for the physical realization of entanglement harvesting from the single-particle field state, there is a restriction in the range of system parameters (prominently visible in ΔE), unlike the vacuum. Therefore, contrary to the vacuum case, to observe the entanglement harvesting, one needs to construct a detector such that the transition energy must live within the allowed range of values.

Entanglement harvesting from the non-vacuum field states with non-inertial detectors remains an interesting arena to venture further. In particular, some of our preliminary observations, corresponding to the uniformly accelerated linear motion of the detectors, are as follows. The excess contribution due to the non-vacuum fluctuations in the individual detector transition probability $\mathscr{P}_j$ is finite for detectors with infinite switching. In comparison, one observes that the same contribution $\mathscr{P}_j$ due to the vacuum fluctuation has a Dirac delta zero multiplying factor (see the transition probabilities of non-inertial Unruh-DeWitt detectors from [113, 159, 216]), which results in a finite transition rate for infinite time. Therefore, in concurrence per unit time, the different effects of vacuum and non-vacuum fluctuations will not be evident. Considering detectors

with finite time switching functions may be beneficial to circumvent this inconvenience, which provides finite transition probabilities.

Appendices

5.A Normalized distribution functions for singly excited states

5.A.1 In $(1+1)$ dimensions

One may consider qualitatively different distribution functions $f(\omega_k)$ (see [191]). In $(1+1)$ dimensions a few examples follow, and we also provide their respective normalization constants. It should be noted that to evaluate the normalization constant in $f(\omega_k)$, here one has to use the $(1+1)$ dimensional form of the normalization condition (5.6).

Exponential damping, $f(\omega_k) = C\,\omega_k\, e^{-\alpha\omega_k}$:

In this case the distribution function is of the form $f(\omega_k) = C\,\omega_k\, e^{-\alpha\omega_k}$. Using the normalization condition (5.6) of $f(\omega_k)$ for $(1+1)$ dimensions one can find out the value of the constant C as $C = 2\sqrt{2\pi}\,\alpha$.

Gaussian distribution, $f(\omega_k) = C\,\omega_k\, e^{-(\omega_k-\omega_0)^2/2\sigma^2}$:

In this case the distribution function is of the form $f(\omega_k) = C\,\omega_k\, e^{-(\omega_k-\omega_0)^2/2\sigma^2}$. Using the normalization condition (5.6) of $f(\omega_k)$ for $(1+1)$ dimensions one can find out the value of the constant C here, as $C = \left\{4\sqrt{\pi}/\left[\omega_0\,\sigma\left(2 - Q\left(-1/2, \omega_0^2/\sigma^2\right)\right)\right]\right\}^{1/2}$. Here $Q(a,z)$ denotes the Regularized Gamma Function.

5.A.2 In $(1+3)$ dimensions

In $(1+3)$ dimensions also one may consider similar distribution functions $f(\omega_{\mathbf{k}})$. However, here one has to use the $(1+3)$ dimensional form of the normalization condition (5.6) to find out the respective normalization constants. Naturally the normalization constants C obtained here will be different than the ones obtained for $(1+1)$ dimensional case.

Exponential damping, $f(\omega_{\mathbf{k}}) = C\,\omega_{\mathbf{k}}\, e^{-\alpha\omega_{\mathbf{k}}}$:

Like the $(1+1)$ dimensional case here also we consider the same exponentially damping distribution function

$$f(\omega_{\mathbf{k}}) = C\ \omega_{\mathbf{k}}\ e^{-\alpha\omega_{\mathbf{k}}}\ . \tag{5.A.1}$$

However, here the normalization constant C is obtained from Eq. (5.6) by putting $d = 3$,

which corresponds to three spatial dimensions of our present case. Then this constant C is given by $C = 4\pi\alpha^2\sqrt{2/3}$.

Gaussian distribution, $f(\omega_{\mathbf{k}}) = C\,\omega_{\mathbf{k}}\,e^{-(\omega_{\mathbf{k}}-\omega_0)^2/2\sigma^2}$:

We consider the Gaussian distribution function for a singly excited state in $(1+3)$ dimensions as

$$f(\omega_{\mathbf{k}}) = C\;\omega_{\mathbf{k}}\;e^{-(\omega_{\mathbf{k}}-\omega_0)^2/2\sigma^2}. \tag{5.A.2}$$

Here also one has to use the normalization condition (5.6) with $d = 3$ to evaluate the value of the normalization constant C, which is given by

$$C = 4\pi\Big/\left\{\sqrt{\pi}\,\omega_0\left(3\sigma^2+2\omega_0^2\right)\sigma\left(\mathrm{Erf}\left(\frac{\omega_0}{\sigma}\right)+1\right)+2\sigma^2 e^{-\frac{\omega_0^2}{\sigma^2}}\left(\sigma^2+\omega_0^2\right)\right\}^{1/2}, \tag{5.A.3}$$

where, Erf(z) denotes the error function.

5.B Evaluations of the integrals in $(1+1)$ dimensions

In this section of the Appendix we provide an explicit derivation of the integral $\mathscr{E}_R^{vac}$. In particular, we shall be obtaining its expression as provided in Eq. (5.25) for two inertial detectors in (1+1) dimensions. In this regard we consider the form of the integral from Eq. (5.14b) with the consideration that t_j are now the Minkowski times. Then this integral becomes

$$\begin{aligned}
\mathscr{E}_R^{vac} &= \frac{1}{\gamma_A\gamma_B}\int_{-\infty}^{\infty}\frac{dk}{4\pi\omega_k}\int_{-\infty}^{\infty}dt_A\int_{-\infty}^{\infty}dt_B\,\theta(t_A-t_B)\\
&\quad\times e^{i\Delta E(t_B/\gamma_B+t_A/\gamma_A)}\left[e^{-i(\omega_k-k\,v_B)t_B+i(\omega_k-k\,v_A)t_A}-e^{i(\omega_k-k\,v_B)t_B-i(\omega_k-k\,v_A)t_A}\right]\\
&= \frac{1}{\gamma_A\gamma_B}\int_{-\infty}^{\infty}\frac{dk}{4\pi\omega_k}\int_{-\infty}^{\infty}dt_A\int_{-\infty}^{t_A}dt_B\\
&\quad\times e^{i\Delta E(t_B/\gamma_B+t_A/\gamma_A)}\left[e^{-i(\omega_k-k\,v_B)t_B+i(\omega_k-k\,v_A)t_A}-e^{i(\omega_k-k\,v_B)t_B-i(\omega_k-k\,v_A)t_A}\right]\\
&= \frac{i}{\gamma_A\gamma_B}\int_{-\infty}^{\infty}\frac{dk}{4\pi\omega_k}\int_{-\infty}^{\infty}dt_A\,e^{i\Delta E\,t_A(1/\gamma_B+1/\gamma_A)}\\
&\quad\times\left[\frac{e^{-i\{k(v_A-v_B)+i\epsilon\}t_A}}{\omega_k-k\,v_B-\Delta E/\gamma_B}+\frac{e^{ik\{(v_A-v_B)-i\epsilon\}t_A}}{\omega_k-k\,v_B+\Delta E/\gamma_B}\right],
\end{aligned} \tag{5.A.4}$$

where one can observe that a $e^{\epsilon t_B}$ regulator, with positive small ϵ, was introduced to make the t_B integral convergent in the lower limit of negative infinity. The actual integral

is obtained in the limit of $\epsilon \to 0$. After performing the t_A integration now one can obtain

$$\mathscr{E}_R^{vac} = \frac{i}{\gamma_A \gamma_B} \int_{-\infty}^{\infty} \frac{dk}{2\omega_k} \left[\frac{\delta\left[k(v_A - v_B) - \Delta E\left(\frac{1}{\gamma_A} + \frac{1}{\gamma_B}\right)\right]}{\omega_k - k\, v_B - \Delta E/\gamma_B} + \frac{\delta\left[k(v_A - v_B) + \Delta E\left(\frac{1}{\gamma_A} + \frac{1}{\gamma_B}\right)\right]}{\omega_k - k\, v_B + \Delta E/\gamma_B} \right]. \quad (5.A.5)$$

This expression is the same as the one presented in Eq. (5.25).

5.C Evaluations of the integrals in $(1+3)$ dimensions for detectors in parallel motion

5.C.1 Explicit evaluation of $\mathscr{P}_A$

Here we consider evaluating the necessary integrals for entanglement harvesting for two detectors in parallel inertial motion in $(1+3)$ dimensions. To derive the expression of the quantity $\mathscr{P}_A$ corresponding to detector A we consider the trajectory from Eq. (5.28) and the $\mathscr{A}(\Delta E)$ part of it becomes

$$\begin{aligned}
\mathscr{A}(\Delta E) &= \int_{-\infty}^{\infty} d\tau_A e^{i\Delta E \tau_A} \Phi_{\text{eff}}(x) \\
&= \int_{-\infty}^{\infty} d\tau_A e^{i\Delta E \tau_A} \int_0^{\pi} \int_0^{\infty} \frac{2\pi \sin\theta \omega_{\mathbf{k}}^2 d\omega_{\mathbf{k}} d\theta}{(2\pi)^3} \frac{f(\omega_{\mathbf{k}})}{2\omega_{\mathbf{k}}} e^{-i\omega_{\mathbf{k}}\gamma_A \tau_A + i\omega_{\mathbf{k}}\gamma_A v \tau_A \cos\theta} \\
&= -\frac{i}{2(2\pi)^2 \gamma_A v_A} \int_0^{\infty} d\omega_{\mathbf{k}} f(\omega_{\mathbf{k}}) \int_{-\infty}^{\infty} \frac{d\tau_A}{\tau_A} [e^{i\tau_A(\Delta E - \omega_{\mathbf{k}}/D_A)} - e^{i\tau_A(\Delta E - \omega_{\mathbf{k}} D_A)}], \quad (5.A.6)
\end{aligned}$$

where $D_j = \sqrt{(1+v_j)/(1-v_j)}$ and θ-integration is done to obtain the final result. Now it is known that [251]

$$P \int_{-\infty}^{\infty} d\tau \frac{e^{i\tau\alpha}}{\tau} = i\pi\, \text{sgn}(\alpha), \quad (5.A.7)$$

Here P stands for principal value. The value of $\text{sgn}(\alpha)$ is ± 1 depending on positive or negative sign of the α, or *zero* for $\alpha = 0$. Thus the expression of (5.A.6) is non-zero only when, $1/D_A \leq \omega_{\mathbf{k}}/\Delta E \leq D_A$, *i.e.,* when $(\Delta E - \omega_{\mathbf{k}}/D_A) > 0$ with $(\Delta E - \omega_{\mathbf{k}} D_A) < 0$. Therefore (5.A.6) becomes

$$\mathscr{A}(\Delta E) = \frac{1}{4\pi \gamma_A v_A} \int_{\Delta E/D_A}^{D_A \Delta E} d\omega_{\mathbf{k}} f(\omega_{\mathbf{k}})\,. \quad (5.A.8)$$

Similarly one can check that

$$\begin{aligned}
\mathscr{B}(\Delta E) &= \int_{-\infty}^{\infty} d\tau_A\, e^{i\Delta E\, \tau_A} \Phi^{\star}_{\text{eff}}(x) \\
&= -\frac{i}{2(2\pi)^2 \gamma_A v_A} \int d\omega_{\mathbf{k}} f(\omega_{\mathbf{k}}) [i\pi - i\pi] \\
&= 0\,. \quad (5.A.9)
\end{aligned}$$

5.C.2 Explicit evaluation of $\mathscr{P}_B$

The quantity $\mathscr{A}(\Delta E)$ for detector B from Eq. (5.16a) can be evaluated as

$$\begin{aligned}
\mathscr{A}(\Delta E) &= \int_{-\infty}^{\infty} d\tau_B e^{i\Delta E\tau_B}\Phi_{\text{eff}}(x_B) \\
&= \int_{-\infty}^{\infty} d\tau_B e^{i\Delta E\tau_B}\int_0^{2\pi}\int_0^{\pi}\int_0^{\infty}\frac{d\phi\sin\theta\omega_{\mathbf{k}}^2 d\omega_{\mathbf{k}} d\theta}{(2\pi)^3}\frac{f(\omega_{\mathbf{k}})}{2\omega_{\mathbf{k}}} \\
&\quad\times e^{-i\omega_{\mathbf{k}}\gamma_B\tau_B + i\omega_{\mathbf{k}}\sin\theta(x_0\cos\phi + y_0\sin\phi) + i\omega_{\mathbf{k}}v_B\gamma_B\tau_B\cos\theta} \\
&= \int_{-\infty}^{\infty} d\tau_B e^{i\Delta E\tau_B}\int_0^{\pi}\int_0^{\infty}\frac{\sin\theta d\theta\omega_{\mathbf{k}} d\omega_{\mathbf{k}}}{(2\pi)^2}\frac{f(\omega_{\mathbf{k}})}{2} \\
&\quad\times e^{-i\omega_{\mathbf{k}}\gamma_B\tau_B(1-v_B\cos\theta)}J_0(\omega_{\mathbf{k}}r_0\sin\theta) \\
&= \int_{-1}^{1} du\int_0^{\infty}\frac{\omega_{\mathbf{k}} d\omega_{\mathbf{k}}}{(2\pi)}\frac{f(\omega_{\mathbf{k}})}{2}\delta(\Delta E - \omega_{\mathbf{k}}\gamma_B(1-v_B u))J_0\left(\omega_{\mathbf{k}}r_0\sqrt{1-u^2}\right) \\
&= \int_{-1}^{1}\frac{du}{4\pi}\frac{\Delta E\; f\left(\frac{\Delta E}{\gamma_B(1-v_B u)}\right)}{\{\gamma_B(1-v_B u)\}^2}J_0\left(\tfrac{r_0\Delta E\sqrt{1-u^2}}{\gamma_B(1-v_B u)}\right),
\end{aligned} \tag{5.A.10}$$

where after the third equality we have defined $u = \cos\theta$. We can evaluate the integration over u in (5.A.10) numerically using the expressions of $f(\omega_{\mathbf{k}})$ given in (5.A.1) and (5.A.2), with the appropriate forms of the normalization constant C separately in $(1+1)$ and $(1+3)$ dimensions.

5.C.3 Explicit evaluation of $\mathscr{E}$

5.C.3.1 Considering the expression of the Green's function in position space

Here we consider the position space representation of the Green's function appearing in the expression of the integral

$$\mathscr{E}_R^{vac} = -i\int_{-\infty}^{\infty} d\tau_B\int_{-\infty}^{\infty} d\tau_A e^{i\Delta E(\tau_A+\tau_B)}G_R(x_A,x_B). \tag{5.A.11}$$

The retarded Green function $G_R(x_A,x_B)$ corresponding to a massless, minimally coupled free scalar field in the Minkowski spacetime is

$$\begin{aligned}
G_R(x_A,x_B) &= -\frac{1}{2\pi}\,\theta(t_A-t_B)\,\delta\left((t_A-t_B)^2 - |\boldsymbol{x}_A-\boldsymbol{x}_B|^2\right) \\
&= -\frac{1}{2\pi}\theta(t_A-t_B)\delta(g(t_A,t_B))\,.
\end{aligned} \tag{5.A.12}$$

For two detectors moving in parallel inertial trajectories (see Eq. (5.28) and (5.29)) in $(1+3)$ dimensions the argument of the Dirac delta distribution becomes zero when

$$\begin{aligned}
g(t_A,t_B) &= A^2(1-v_A^2) + t_B^2(1-v_B^2) - 2t_A t_B(1-v_A v_B) - r_0^2 \\
&= 0\,.
\end{aligned} \tag{5.A.13}$$

This equation has solutions for t_B as

$$t_B = \gamma_B^2(t_A(1-v_Av_B) \pm u(t_A)) \equiv t_\pm, \tag{5.A.14}$$

where

$$u(t_A) = \sqrt{t_A^2(v_A-v_B)^2 + r_0^2(1-v_B^2)}\,. \tag{5.A.15}$$

Now, with the general condition $0 \le v_j \le 1$, one can check that

$$\begin{aligned} t_+ &> t_A\ , \\ t_- &< t_A\ . \end{aligned} \tag{5.A.16}$$

Then using the property of Dirac delta functions, we have

$$\begin{aligned} \delta(g(t_A,t_B)) &= \left[\frac{\delta(t_B-t_+)}{|g'(t_A,t_B)|_{t_B=t_+}} + \frac{\delta(t_B-t_-)}{|g'(t_A,t_B)|_{t_B=t_-}}\right] \\ &= \frac{1}{2u(t_A)}[\delta(t_B-t_+)+\delta(t_B-t_-)]. \end{aligned} \tag{5.A.17}$$

Therefore one may express the integral of Eq. (5.A.11) as

$$\begin{aligned} \mathscr{E}_R^{vac} &= \frac{-i}{2\pi}\int_{-\infty}^{\infty}\frac{dt_A}{\gamma_A}\int_{-\infty}^{t_A}\frac{dt_B}{\gamma_B}e^{i\Delta E\left(\frac{t_A}{\gamma_A}+\frac{t_B}{\gamma_B}\right)}\delta(g(t_A,t_B)) \\ &= \frac{-i}{4\pi}\int_{-\infty}^{\infty}\frac{dt_A}{\gamma_A\gamma_B\,u(t_A)}e^{i\Delta E\left(\frac{t_A}{\gamma_A}+\gamma_B(t_A(1-v_Av_B)-u(t_A))\right)} \\ &= \frac{-i}{2\pi}\int_0^{\infty}\frac{dt_Ae^{-i\Delta E\gamma_Bu(t_A)}}{\gamma_A\gamma_B\,u(t_A)}\cos\left(\Delta Et_A\left(\frac{1}{\gamma_A}+\gamma_B(1-v_Av_B)\right)\right)\,. \end{aligned} \tag{5.A.18}$$

Now expanding the exponential in (5.A.18) in terms of *sin* and *cos* functions and by comparing with (5.37), we can recognise

$$\begin{aligned} a &= \frac{r_0}{\gamma_B|v_A-v_B|};\ \ \varrho = \gamma_B|v_A-v_B|\Delta E; \\ \beta &= \Delta E\left(\frac{1}{\gamma_A}+\gamma_B(1-v_Av_B)\right); \end{aligned} \tag{5.A.19}$$

as we know $0 \le v_j \le 1$, this satisfies the criteria for (5.37), *i.e.,*

$$\begin{aligned} &\beta > \varrho \text{ or, } \left(\frac{1}{\gamma_A}+\gamma_B(1-v_Av_B)\right) > \gamma_B|v_A-v_B| \\ &\text{or, } \frac{1}{\gamma_A(1-v_Av_B)}+\gamma_B > \gamma_B|v_{rel}|. \end{aligned} \tag{5.A.20}$$

Thus $\beta > \varrho > 0$ is satisfies as the relative velocity (v_{rel}) between the detectors is always less than *one*. Therefore, from (5.A.18), we obtain

$$\mathscr{E}_R^{vac} = \frac{-i}{2\pi\gamma_A\gamma_B|v_A-v_B|}K_0\left(\frac{r_0\Delta E}{\gamma_B}\sqrt{\left(\frac{\frac{1}{\gamma_A}+\gamma_B(1-v_Av_B)}{v_A-v_B}\right)^2-\gamma_B^2}\right)\,. \tag{5.A.21}$$

If $v_A = v_B$ then from (5.A.14) and (5.A.15), we obtain $u(t_A)$ is t_A independent and $t_- = t_A - r_0\gamma_B$. Therefore, the t_A-integration after the second last line of (5.A.18) gives a delta function of form $\delta\left(\Delta E\left(1/\gamma_A + 1/\gamma_B\right)\right)$. This is always *zero* for $v_A = v_B$, as both γ_A and ΔE are always positive. One can also simply take the limit $(v_A - v_B) \to 0$ and observe that this quantity readily vanishes from Eq. (5.A.21).

5.C.3.2 Considering the expression of the Green's function in momentum space

On the other hand, considering the expression of the Green's function in momentum space on can express the integral $\mathscr{E}_R^{vac}$ from Eq. (5.A.11) as

$$\begin{aligned}
\mathscr{E}_R^{vac} = &-\int_{-\infty}^{\infty} d\tau_A \int_{-\infty}^{\infty} d\tau_B\, e^{i\Delta E(\tau_A+\tau_B)}\theta(\gamma_A\tau_A - \gamma_B\tau_B) \\
&\times \int_0^{\pi} \sin\theta d\theta \int_0^{\infty} \frac{\omega_{\mathbf{k}} d\omega_{\mathbf{k}}}{2(2\pi)^2}\Big[e^{-i\omega_{\mathbf{k}}(\gamma_A\tau_A-\gamma_B\tau_B)} e^{i\omega_{\mathbf{k}}\sqrt{(\gamma_A\tau_A v_A - \gamma_B\tau_B v_B)^2 + r_0^2}\cos\theta} \\
&\qquad - e^{i\omega_{\mathbf{k}}(\gamma_A\tau_A-\gamma_B\tau_B) - i\omega_{\mathbf{k}}\sqrt{(\gamma_A\tau_A v_A - \gamma_B\tau_B v_B)^2 + r_0^2}\cos\theta}\Big] \\
= &-\int_{-\infty}^{\infty}\int_{-\infty}^{\infty} \frac{dp\, dq}{2v_A v_B' \gamma_A\gamma_B} e^{i\Delta E(a_1 p + a_2 q)}\theta(a_3 p - q) \\
&\times \int_{-1}^{1} du \int_0^{\infty} \frac{\omega_{\mathbf{k}} d\omega_{\mathbf{k}}}{2(2\pi)^2}\Big[e^{-i\omega_{\mathbf{k}} a_4(a_3 p - q) + i\omega_{\mathbf{k}}\sqrt{p^2+r_0^2}u} - e^{i\omega_{\mathbf{k}} a_4(a_3 p - q) - i\omega_{\mathbf{k}}\sqrt{p^2+r_0^2}u}\Big].
\end{aligned} \tag{5.A.22}$$

As we have already discussed in sec. 5.4.1, here we defined a change of variables, $p = v_A\gamma_A\tau_A - v_B\gamma_B\tau_B$ and $q = v_A\gamma_A\tau_A + v_B\gamma_B\tau_B$. The Jacobian of the transform is given by $|J| = 1/(2v_A v_B\gamma_A\gamma_B)$. Under this transform the quantities $(\gamma_A\tau_A - \gamma_B\tau_B)$ and $(\tau_A + \tau_B)$, can be expressed as

$$\begin{aligned}
\gamma_A\tau_A - \gamma_B\tau_B &= \frac{p+q}{2v_A} - \frac{q-p}{2v_B} = \frac{p(v_B+v_A)+q(v_B-v_A)}{2v_A v_B} \\
&= \frac{v_A - v_B}{2v_A v_B}\left(p\frac{v_A+v_B}{v_A-v_B} - q\right) = a_4(a_3 p - q); \\
\tau_A + \tau_B &= p\left(\frac{1}{2v_A\gamma_A} - \frac{1}{2v_B\gamma_B}\right) + q\left(\frac{1}{2v_A\gamma_A} + \frac{1}{2v_B\gamma_B}\right) \\
&= a_1 p + a_2 q;
\end{aligned} \tag{5.A.23}$$

In Eq. (5.A.22) the step function provides the upper limit of q-integration, which is $a_3 p$. After evaluating the q-integral, we obtain

$$\begin{aligned}
\mathscr{E}_R^{vac} = &-\int_{-\infty}^{\infty} \frac{dp\, e^{i\Delta E a_1 p}}{2vv'\gamma'\gamma}\int_{-1}^{1} du \int_0^{\infty}\frac{\omega_{\mathbf{k}} d\omega_{\mathbf{k}}}{8\pi^2} \\
&\times\left[\frac{e^{i\Delta E a_2 a_3 p}}{i(\Delta E a_2 + a_4\omega_{\mathbf{k}})} e^{i\omega_{\mathbf{k}}\sqrt{p^2+r_0^2}u} - \frac{e^{i\Delta E a_2 a_3 p}}{i(\Delta E a_2 - a_4\omega_{\mathbf{k}})} e^{-i\omega_{\mathbf{k}}\sqrt{p^2+r_0^2}u}\right].
\end{aligned} \tag{5.A.24}$$

Then we perform the u-integral and after some re-arrangement we obtain

$$\mathscr{E}_R^{vac} = \int_{-\infty}^{\infty} \frac{dp\ e^{i\Delta E p(a_1+a_2a_3)}}{16\pi^2 v v' \gamma' \gamma \sqrt{p^2+r_0^2}} \left[\int_{-\infty}^{\infty} \frac{d\omega_{\mathbf{k}}\ e^{i\omega_{\mathbf{k}}\sqrt{p^2+r_0^2}}}{a_4\omega_{\mathbf{k}} + a_2\Delta E} + \int_{-\infty}^{\infty} \frac{d\omega_{\mathbf{k}}\ e^{i\omega_{\mathbf{k}}\sqrt{p^2+r_0^2}}}{a_4\omega_{\mathbf{k}} - a_2\Delta E} \right]. \quad (5.A.25)$$

To evaluate the ω_k-integration we change the integration variable to $a_4\omega_k \pm a_2\Delta E$ for first and second integration, respectively. The integration limit remain unchanged as the quantities a_4, $a_2\Delta E$ are finite. Then we will use an identity from complex variable theory, that is [251]

$$P\int_{-\infty}^{\infty} dx \frac{e^{i\alpha x}}{x} = i\pi\ \mathrm{sgn}(\alpha)\ , \quad (5.A.26)$$

then the expression from (5.A.25) will become

$$\begin{aligned}
\mathscr{E}_R^{vac} &= i\int_{-\infty}^{\infty} \frac{dp\ e^{i\Delta E p(a_1+a_2a_3)}}{8\pi v_A v_B \gamma_A \gamma_B a_4 \sqrt{p^2+r_0^2}} \cos\left(\frac{a_2\Delta E\sqrt{p^2+r_0^2}}{a_4}\right) \\
&= i\int_0^{\infty} \frac{dp\ \cos\left(\frac{a_2\Delta E}{a_4}\sqrt{p^2+r_0^2}\right)}{2\pi(v_A-v_B)\gamma_A\gamma_B\sqrt{p^2+r_0^2}} \cos(\Delta E p(a_1+a_2a_3)) \\
&= \frac{i\ K_0\left(r_0\Delta E\sqrt{(a_1+a_2a_3)^2-(a_2/a_4)^2}\right)}{2\pi(v_A-v_B)\gamma_A\gamma_B}\ ,
\end{aligned} \quad (5.A.27)$$

where we have used the integral representation from Eq. (5.37).

In a manner similar to the previous case one can also express the integral $\mathscr{E}_W^{vac}$ as

$$\begin{aligned}
\mathscr{E}_W^{vac} &= -\int_{-\infty}^{\infty} d\tau_A \int_{-\infty}^{\infty} d\tau_B e^{i\Delta E(\tau_A+\tau_B)} G_W(x_A,x_B) \\
&= -\int_{-\infty}^{\infty} d\tau_A \int_{-\infty}^{\infty} d\tau_B e^{i\Delta E(\tau_A+\tau_B)} \int_0^{\pi} \sin\theta\, d\theta \\
&\times \int_0^{\infty} \frac{\omega_{\mathbf{k}} d\omega_{\mathbf{k}}}{2(2\pi)^2} e^{-i\omega_{\mathbf{k}}(\gamma_A\tau_A-\gamma_B\tau_B)} e^{i\omega_{\mathbf{k}}\sqrt{(\gamma_A\tau_A v_A-\gamma_B\tau_B v_B)^2+r_0^2}\cos\theta}\ .
\end{aligned} \quad (5.A.28)$$

Using the previously mentioned coordinate transformation, related to Eq. (5.A.23), the quantity from Eq. (5.A.28) can be evaluated as

$$\begin{aligned}
&\mathscr{E}_W^{vac} \\
&= -\int_{-\infty}^{\infty}\int_{-\infty}^{\infty} \frac{dp\ dq\ e^{i\Delta E(a_1p+a_2q)}}{2v_Av_B\gamma_A\gamma_B} \int_0^{\pi} \sin\theta d\theta \int_0^{\infty} \frac{\omega_{\mathbf{k}} d\omega_{\mathbf{k}}}{2(2\pi)^2} e^{-i\omega_{\mathbf{k}}a_4(a_3p-q)+i\omega_{\mathbf{k}}\sqrt{p^2+r_0^2}\cos\theta} \\
&= -\int_{-1}^{1} du \int_0^{\infty} \frac{\omega_{\mathbf{k}} d\omega_{\mathbf{k}}}{8\pi^2} \int_{-\infty}^{\infty} \frac{dp\ e^{i\Delta E a_1 p}}{2v_Av_B\gamma_A\gamma_B} e^{-i\omega_{\mathbf{k}}a_3a_4p+i\omega_{\mathbf{k}}\sqrt{p^2+r_0^2}u} \int_{-\infty}^{\infty} dq\ e^{i(a_2\Delta E+a_4\omega_{\mathbf{k}})q} \\
&= -\int_{-1}^{1} du \int_0^{\infty} \frac{\omega_{\mathbf{k}} d\omega_{\mathbf{k}}}{4\pi} \int_{-\infty}^{\infty} \frac{dp}{2v_Av_B\gamma_A\gamma_B} e^{i\omega_{\mathbf{k}}\sqrt{p^2+r_0^2}u}\ e^{ip(a_1\Delta E-a_3a_4\omega_{\mathbf{k}})}\ \delta(a_2\Delta E+a_4\omega_{\mathbf{k}}) \\
&= 0\ .
\end{aligned} \quad (5.A.29)$$

5.D Evaluations of the integrals in $(1+3)$ dimensions for detectors in perpendicular motion

5.D.1 Explicit evaluation of $\mathscr{P}_A$

We will evaluate $\mathscr{P}_A^{nv}$ for trajectory (5.40). In particular, the $\mathscr{A}(\Delta E)$ part of this quantity becomes

$$\begin{aligned}
\mathscr{A}(\Delta E) &= \int_{-\infty}^{\infty} d\tau_A e^{i\Delta E\tau_A}\phi_{eff}(x_A) \\
&= \int_{-\infty}^{\infty} d\tau_A e^{i\Delta E\tau_A}\int_0^{\infty}\frac{\omega_{\mathbf{k}}d\omega_{\mathbf{k}}}{2(2\pi)^3}\int_0^{\pi}\sin\theta d\theta\int_0^{2\pi}d\phi e^{-i\omega_{\mathbf{k}}t_A+i\omega_{\mathbf{k}}v_At_A\sin\theta\cos\phi}f(\omega_{\mathbf{k}}) \\
&= \int_{-\infty}^{\infty} d\tau_A e^{i\Delta E\tau_A}\int_0^{\infty}\frac{\omega_{\mathbf{k}}d\omega_{\mathbf{k}}}{2(2\pi)^2}\int_{-1}^{1}du\; e^{-i\omega_{\mathbf{k}}t_A}f(\omega_{\mathbf{k}})J_0\left(|\omega_{\mathbf{k}}v_At_A\sqrt{1-u^2}|\right) \\
&= \int_{-\infty}^{\infty}\frac{dt_A}{\gamma}e^{i\Delta Et_A/\gamma_A}\int_0^{\infty}\frac{\omega_{\mathbf{k}}d\omega_{\mathbf{k}}}{2(2\pi)^2}e^{-i\omega_kt_A}f(\omega_{\mathbf{k}})\;\frac{2\sin\omega_{\mathbf{k}}v_At_A}{\omega_{\mathbf{k}}v_At_A} \\
&= \int_0^{\infty}\frac{d\omega_{\mathbf{k}}\;f(\omega_{\mathbf{k}})}{i2(2\pi)^2v_A\gamma_A}\int_{-\infty}^{\infty}\frac{dt_A}{t_A}\left[e^{i(\Delta E-\frac{\omega_{\mathbf{k}}}{D_A})t_A/\gamma_A}-e^{i(\Delta E-\omega_{\mathbf{k}}D_A)t_A/\gamma_A}\right] \\
&= \int_0^{\infty}\frac{d\omega_{\mathbf{k}}}{i2(2\pi)^2v_A\gamma_A}f(\omega_{\mathbf{k}})i\pi\left[\mathrm{sgn}(D_A\Delta E-\omega_{\mathbf{k}})-\mathrm{sgn}(\Delta E/D_A-\omega_{\mathbf{k}})\right] \\
&= \frac{1}{4\pi v_A\gamma_A}\int_{\Delta E/D_A}^{\Delta ED_A}d\omega_{\mathbf{k}}\,f(\omega_{\mathbf{k}})\,. \qquad (5.A.30)
\end{aligned}$$

As all other quantities in $\mathscr{P}_A$ are zero, one can express $\mathscr{P}_A = |\mathscr{A}(\Delta E)|^2$. This expression is same as the one from Eq. (5.A.8) for two detectors in parallel inertial motion in $(1+3)$ dimensions, as expected.

5.D.2 Explicit evaluation of $\mathscr{E}$

Now let us evaluate $\mathscr{E}_W^{vac}$ for two detectors in perpendicular inertial motions. For $t_A > t_B$, we have positive frequency Wightman function

$$\begin{aligned}
G_W(x_A,x_B) &= -\frac{1}{4\pi^2}\frac{1}{(t_A-t_B-i\epsilon)^2-|\boldsymbol{x}_A-\boldsymbol{x}_B|^2} \\
&= -\frac{1}{4\pi^2}\frac{1}{g(t_A,t_B)-i\epsilon}\,. \qquad (5.A.31)
\end{aligned}$$

No contribution for $t_B > t_A$, will be taken. Now, solving for $g(t_A,t_B)-i\epsilon=0$ gives, $t_B = \gamma_B^2(t_A \pm u(t_A)(1+i\epsilon)) = t_\pm(1\pm i\epsilon)$. We already know that $t_B = t_+ > t_A$ and $t_B = t_- < t_A$. When $t_A > t_B$ satisfied, we have pole in the lower half of the complex t_B-plane. Thus

$$\begin{aligned}
\mathscr{E}_W^{vac} &= -\int_{-\infty}^{\infty}\int_{-\infty}^{\infty}d\tau_Ad\tau_Be^{i\Delta E(\tau_A+\tau_B)}G_W(x_A,x_B) \\
&= 0\,. \qquad (5.A.32)
\end{aligned}$$

Part III

Entanglement Leakage

CHAPTER 6

SPONTANEOUS LEAKAGE OF ENTANGLEMENT

6.1 Introduction and Motivation

Study of quantum entanglement in the relativistic framework can provide a broader perspective towards the reality. Interestingly the existence of entanglement in vacuum state of a quantum field is capable of harvest entanglement between a pair of two-level atomic detectors. This process of swapping field entanglement to two initially-uncorrelated detectors is extensively discussed in chapters 3, 4 and 5, where we observed that this process is sensitive to the type of motion of UDW detectors [96, 107, 108, 113, 152] as well as the nature of the background fields [133, 149, 159], *etc*. Moreover, the quantum entanglement phenomenon appears to be frame dependent – the measure of entanglement changes as one describes with respect to other reference frames [92–94, 96, 97, 110, 253].

In this chapter we intend to address a fundamentally important question – whether entanglement between systems remain intact when they are not isolated from the environment? In our environment the background fields always contain vacuum fluctuation energy and as the entanglement in vacuum state of the background fields swaps to a pair of UDW detectors (see *e.g.* [100, 107, 108, 113, 126, 133, 134, 138, 139, 141, 142, 147, 149, 150, 152, 159])), it is natural to investigate whether the swapping of vacuum entanglement has any influence on entangled systems. To get the answer to this we consider a relativistic model where two initially entangled UDW detectors are individually interacting with the background fields. For simplicity the fields are chosen to be real

scalar ones and the interaction is monopole type. In order to avoid the effect of motion we consider both the detectors to be static eternally with respect to the lab frame in Minkowski spacetime. Also, to avoid transient switching effects and to simplify the calculations, we choose eternal interaction between the field and detectors. The investigation, like earlier various analysis, is done till second order in perturbation series.

We observe that even if the detectors are eternally static with respect to the lab frame, they lose entanglement communication while interacting with the environment (here the background scalar field). This feature is a bit unexpected as previous results are in favour of entanglement harvesting due to entanglement swapping (like mentioned in [100, 107, 108, 113, 126, 133, 134, 138, 139, 141, 142, 147, 149, 150, 152, 159]). Therefore, if two entangled qubit are left open in the environment, they will lose entanglement. We find that such leakage of entanglement within this simple model is caused by collective effects of spontaneous emission of the individual detector and vacuum fluctuation of quantum field. Moreover, we argue that the leakage is unavoidable even for other type of switching function related to interaction. In the latter situation other effects (like excitation of detectors, *etc*.) may also contribute. Interestingly, if any one of the detectors is kept shielded from the environment (while the other one is open to environment quantum field) then also the composite system suffers from entanglement degradation. But in the latter situation the same will be less than the situation where both the detectors are switched on.

This chapter is organized as follows. In Sec. 6.2 we discuss the model consisting of two static UDW detectors interacting with a minimally coupled, massive scalar field through monopole coupling. This section contains the discussion on the general density matrix elements for two initially entangled detectors. In Sec. 6.3 we shall consider two entanglement measures negativity and concurrence to study the fate of entanglement at later times. We have discussed how spontaneous emission and vacuum fluctuations lead to entanglement leakage of the system. Subsequently, we conclude by discussing our findings and implications in Sec. 6.4.

6.2 Density matrix elements

Consider a pair of UDW detectors, A and B, with energy gap ΔE^j ($j = A, B$). The detectors are at rest in $(3+1)$-dimensional Minkowski spacetime and hence their trajectories are

denoted as

$$\begin{aligned} t_A &= \tau_A,\ \mathbf{x}_A = 0\ ; \\ t_B &= \tau_B,\ \mathbf{x}_B = \mathbf{d}\ , \end{aligned} \tag{6.1}$$

where $\mathbf{d}$ is a constant vector (measures the distance between the detectors) and τ_j is proper time of j^{th} detector. The detectors are initially entangled and the initial quantum state is taken to be (see Eq. (2.44))

$$|D\rangle = \alpha|g_A g_B\rangle + \gamma|e_A e_B\rangle\ , \tag{6.2}$$

with α and γ are chosen to be real and satisfy $\alpha^2+\gamma^2=1$. Here $|g_j\rangle$ and $|e_j\rangle$ are the ground and exited states of j^{th} detector, respectively. Therefore the density matrix is (see Eq. (2.64))

$$\hat{\rho}_{AB} = \begin{pmatrix} a_1 & 0 & 0 & a_2 \\ 0 & b_1 & b_2 & 0 \\ 0 & h_1 & h_2 & 0 \\ d_1 & 0 & 0 & d_2 \end{pmatrix} + O(c^4); \tag{6.3}$$

The general density matrix elements are given in Eq. (2.65) and the integral quantities are given in Eq. (2.46), (2.47), (2.48), (2.49), (2.58) and (2.59).

Considering the detectors are identical (*i.e.,* $\Delta E^A = \Delta E^B = \Delta E$) and the coupling strength is equal of both detectors (*i.e.,* $c_A = c_B = c$), we have $\mathscr{P}_A(-\Delta E) = \mathscr{P}_B(-\Delta E) = \mathscr{P}_-$ and $M_A(\Delta E) = M_B(\Delta E) = M$. Therefore, we obtain the density matrix elements as (with $\chi_j = 1$)

$$\begin{aligned} a_1 &= \gamma^2(1-2c^2\mathscr{P}_-); \\ b_1 &= \gamma^2 c^2 \mathscr{P}_- = h_2; \\ a_2 &= \alpha\gamma(1-2c^2 M^\star) = d_1^\star; \\ b_2 &= \gamma^2 c^2 \mathscr{P}_{AB}^\star(-\Delta E) = h_1^\star; \\ d_2 &= \alpha^2, \end{aligned} \tag{6.4}$$

where

$$\begin{aligned} \mathscr{P}_j(-\Delta E^j) &= \int\int d\tau_j d\tau'_j e^{-i\Delta E^j(\tau_j-\tau'_j)} G_W(x'_j, x_j); \\ \mathscr{P}_{AB}(\Delta E) &= \int\int d\tau_A \tau_B e^{i(\Delta E^A \tau_A - \Delta E^B \tau_B)} G_W(x_B, x_A); \\ M_j(\Delta E) &= \int\int d\tau_j d\tau'_j e^{i\Delta E^j(\tau_j-\tau'_j)} \theta(\tau_j-\tau'_j)\Big(G_W(x'_j,x_j) + G_W(x_j,x'_j)\Big). \end{aligned} \tag{6.5}$$

Here, $G_W(x'_j, x_j)$ is the positive frequency Wightman function. These quantities are evaluated in Appendix 6.A, and the final expressions are obtained as

$$\begin{aligned}
\mathscr{P}_j(-\Delta E^j) &= \frac{\delta(0)}{2}\sqrt{\Delta E^2 - m^2} \equiv \mathscr{P}_- \ ; \\
\mathrm{Re}\{M_j(\Delta E)\} &= \frac{\delta(0)}{4}\sqrt{\Delta E^2 - m^2} \equiv \mathrm{Re}\{M\} \ ; \\
\mathscr{P}_{AB}(-\Delta E) &= \frac{\delta(0)}{d}\,\sin\left(d\sqrt{\Delta E^2 - m^2}\right),
\end{aligned} \tag{6.6}$$

where 'Re' denotes the real part only. These expressions are obtained under the assumption that $\Delta E \geq m$. If $0 < \Delta E < m$, the de-excitation probability ($\mathscr{P}_j$) will become imaginary, hence the whole analysis will not be valid anymore.

Since $\mathscr{P}_j(\Delta E^j)$ signifies the excitation probability of j^{th} detector from the ground state to the excited state ($|g_j\rangle \to |e_j\rangle$) [24]. Here, the quantity $\mathscr{P}_j(-\Delta E^j)$ corresponds to the de-excitation of it. Since the detectors are static, therefore $\mathscr{P}_j(-\Delta E^j)$ does not have any contribution due to the relative motion of the detectors. Therefore it is completely denoting the *spontaneous emission probability* [254]. On the other hand, $G_W(x'_j, x_j) + G_W(x_j, x'_j)$ in the second term can be realised as $\langle 0_M|\{\hat{\phi}(x'_j), \hat{\phi}(x_j)\}|0_M\rangle$. Therefore M_j is determined from the anti-commutator of the scalar field and as the expectation value of anti-commutator depends on the field state under consideration (contrary to the commutator of field, whose expectation value is independent of state), M_j arises purely due to the *vacuum fluctuation* of field.

6.3 Entanglement leakage

There are two well established quantities, negativity and concurrence, which fruitfully measure the entanglement between two qubits. The relevant expressions of these quantities for our density matrix in Eq. (6.3) are already discussed in chapter 2. Here we will use the final expressions obtained in chapter 2.

6.3.1 Negativity

Negativity is defined as absolute value of the sum of negative eigenvalues of the partially transposed density matrix, derived from the PPT criterion [72]. The analysis in chapter 2 shows that the only negative eigenvalue for $\hat{\rho}_{AB}^{T_A} = (\hat{T}_A \otimes \hat{\mathbf{1}}_B)\hat{\rho}_{AB}$ can be λ_4 with *negative* sign, which is given by (2.80)

$$\lambda_4 = \frac{1}{2}\left\{b_1 + h_2 - \sqrt{(b_1 + h_2)^2 + 4(a_2 d_1 - b_1 h_2)}\right\}. \tag{6.7}$$

Hence Negativity is given by (2.88) can be expressed as (see Appendix 6.B)

$$\mathcal{N} = max\left\{0, |\alpha\gamma| - c^2\left(\gamma^2\mathscr{P}_- + 2|\alpha\gamma|\text{Re}\{M\}\right)\right\} . \tag{6.8}$$

Note that since $\mathscr{P}_-$ and $\text{Re}\{M\}$ are non-vanishing, even though the detectors are static, hence negativity will decrease. Therefore if an entangled pair of two-level detectors are kept at rest in the environment, there will be entanglement leakage and that phenomenon is driven by two effects – spontaneous emission of individual detector and the vacuum fluctuation of the background field.

6.3.2 Concurrence

Another independent measure of entanglement is concurrence [75]. The importance of this quantity is due to its connection with the entanglement of formation. The concurrence is (using Eq. (2.96))

$$\mathscr{C}(\hat{\rho}) = \max\{0, (\lambda_1 - \lambda_2 - \lambda_3 - \lambda_4)\} . \tag{6.9}$$

where the λ's are the square-root of eigenvalues of the matrix $\hat{\rho}_{AB}(\hat{\sigma}_y \otimes \hat{\sigma}_y)\hat{\rho}^{\star}_{AB}(\hat{\sigma}_y \otimes \hat{\sigma}_y)$ and λ_1 is the largest of them. For our density matrix (2.64), λ's are calculated in Appendix 6.C. The final expression of concurrence is obtained as

$$\mathscr{C}(\rho) = max\left\{0, 2|\alpha\gamma| - c^2\Big((|\alpha\gamma| + 2\gamma^2)\mathscr{P}_- + 2|\alpha\gamma|\text{Re}\{M\}\Big)\right\} . \tag{6.10}$$

It decreases from the initial value. So again it is confirmed that there will be leakage of entanglement between the two UD detectors when they are not isolated from the environment and such is due to two phenomenon – spontaneous emission of individual detector and vacuum fluctuation of quantum field.

Note that for this model both $\mathscr{P}_-$ and M contain Dirac-delta function $\delta(0)$ and therefore are divergent. This is due to consideration of interaction for infinite time and such issue always arises naturally for the choice of switching function as unity. The same has also appeared in the original calculation for transition probability of an accelerated detector. In this situation, making an analogy with the Fermi's golden rule, the transition probability per unit time (known as detector's response function) is considered to be the relevant physical quantity (see for example section 3.3 of [24]). In the same sprit to tackle the present situation we define the change in negativity or concurrence per unit time as follows. Using the fact (6.8) and (6.10) one defines the change in negativity and concurrence per unit time as

$$\delta\dot{\mathcal{N}} = (\text{finite quantity}) \times \lim_{T\to\infty} \frac{1}{2\pi T}\int_{-T/2}^{T/2} du \ , \tag{6.11}$$

and

$$\delta\dot{\mathscr{C}} = (\text{finite quantity}) \times \lim_{T\to\infty} \frac{1}{2\pi T} \int_{-T/2}^{T/2} du \ , \tag{6.12}$$

respectively, where the "finite quantity" in $\delta\dot{\mathscr{N}}$ is determined from $c^2(\gamma^2\mathscr{P}_- + 2|\alpha\gamma|\text{Re}\{M\})$ by removing the common factor $\delta(0)$ in it and so on. In this case to make the perturbative calculation viable we satisfy the condition – initial negativity and concurrence per unit interaction time is greater than their rate of change. Then non-vanishing positive value of $\delta\dot{\mathscr{N}}$ or $\delta\dot{\mathscr{C}}$ can be regarded as the signature of degradation of initial entanglement (the same has been proposed earlier in [110] as well). Introduction of this idea of measuring the entanglement for the present model then shows the unavoidable leakage of initial entanglement which here depends on the energy gap ΔE of the detectors and mass of the scalar field m under the condition $\Delta E > mc^2$ (c is taken to be 1) . Moreover, the entanglement leakage will decrease with increasing mass (m) of the scalar field till $m \sim \Delta E$. Also note that such is independent of the intra-distance ($|\mathbf{d}| = d$) between the detectors and hence situation remains same even if they sit together. Moreover no change will occur when $\Delta E = m$. Interestingly, for massless field one finds degradation for all values of ΔE. The latter discussion seems to indicate that when two entangled detectors are illuminated by photon, that will lead to decrease of quantum communication between them. Additionally it may also be noted that if only one detector (say, A) is switched on while other one (say, B) is shielded from environment, then also entanglement degradation will happen. But in this case $\mathscr{P}_B(-\Delta E)$ and M_B will not contribute and hence degradation will be half of the earlier one.

6.4 Discussion and implications

Within this simple model we observed that two static entangled UD detectors looses communication when they are open to environment. This has been confirmed through negativity as well as concurrence of the two detectors system. Such phenomenon is driven by the spontaneous emissions of the individual detectors and the vacuum fluctuation of the background quantum fields. In this regard it may be mentioned that in literature it is already pointed out that in open quantum systems, the environment causes decoherence for the quantum systems (*e.g.* see [255, 256]). Therefore, it is natural to expect that this may cause entanglement leakage (*e.g.* see [257]), which is observed here as well. On the other hand in the detector context, it is well known that coupling with the background scalar field favours the generation of entanglement between two initially non-entangled detectors due to entanglement swapping from the field vacuum (see

e.g. [100, 107, 108, 113, 126, 133, 134, 138, 139, 141, 142, 147, 149, 150, 152, 159]). Interestingly here we observe the negative effect of vacuum fluctuation which was observed to be providing entanglement harvesting between two un-entangled UD detector. This degradation can be decreased by shielding one of the detectors from the environment. Although the calculation has been done for eternal interaction between the detector and fields, but other types of switching function should not change the nature of the result. In the latter situation other terms in (6.A.1) will contribute, but in any case one can always find a negative eigenvalue and so negativity will decrease. For example, Gaussian type switching function yields non-vanishing value for $\mathscr{P}_j(\Delta E)$ and in that case the leakage will be driven by transition of detectors from ground state to excited state as well. Hence the phenomenon of entanglement leakage is quite unavoidable and therefore two entangled systems will suffer a spontaneous drainage of communication due to their surroundings.

Finally, we mention that the present model can have significant impact to understand more about black hole spacetimes. A Minkowski observer is equivalent to a freely-falling observer in black hole spacetime. Therefore the present result indicates that two initially entangled qubits' communication gets fade during their free-fall towards the horizon. Since the quantum nature of a black hole (particularly the black hole information paradox problem) is now being investigated in the light of quantum information, we feel that the present observation can be important in this field of study. This is not more than a suggestive one.

Appendices

6.A Elements of the time evolved density matrix Eq. (6.3)

The explicit forms of the elements of the later time density matrix (6.3) (also (2.64)), upto second order perturbation expansion, are already calculated in chapter 2. The elements are given in Eq. (2.65) as

$$\begin{aligned}
a_1 &= \gamma^2 - \gamma^2(c_A^2\mathscr{P}_A(-\Delta E) + c_B^2\mathscr{P}_B(-\Delta E)) + \alpha\gamma c_A c_B(\mathscr{E}^\star(\Delta E) + \mathscr{E}(\Delta E)),\\
a_2 &= \alpha\gamma - \alpha\gamma(c_A^2 M_A^\star + c_B^2 M_B^\star) + \gamma^2 c_A c_B \mathscr{E}^\star(-\Delta E) + \alpha^2 c_A c_B \mathscr{E}(\Delta E),\\
d_1 &= \alpha\gamma - \alpha\gamma(c_A^2 M_A + c_B^2 M_B) + \alpha^2 c_A c_B \mathscr{E}^\star(\Delta E) + \gamma^2 c_A c_B \mathscr{E}(-\Delta E),\\
d_2 &= \alpha^2 - \alpha^2(c_A^2\mathscr{P}_A(\Delta E) + c_B^2\mathscr{P}_B(\Delta E)) + \alpha\gamma c_A c_B(\mathscr{E}^\star(-\Delta E) + \mathscr{E}(-\Delta E)),\\
b_1 &= \alpha^2 c_A^2\mathscr{P}_A(\Delta E) + \gamma^2 c_B^2\mathscr{P}_B(-\Delta E) + \alpha\gamma c_A c_B(\bar{\mathscr{P}}_{AB}(\Delta E) + \bar{\mathscr{P}}^\star_{AB}(\Delta E)),\\
b_2 &= \alpha\gamma(c_A^2\bar{\mathscr{P}}_{AA}(\Delta E) + c_B^2\bar{\mathscr{P}}_{BB}(-\Delta E)) + c_A c_B(\alpha^2\mathscr{P}_{AB}(\Delta E) + \gamma^2\mathscr{P}^\star_{AB}(-\Delta E)),\\
h_1 &= \alpha\gamma(c_A^2\bar{\mathscr{P}}_{AA}(-\Delta E) + c_B^2\bar{\mathscr{P}}_{BB}(\Delta E)) + c_A c_B(\alpha^2\mathscr{P}^\star_{AB}(\Delta E) + \gamma^2\mathscr{P}_{AB}(-\Delta E)),\\
h_2 &= \gamma^2 c_A^2\mathscr{P}_A(-\Delta E) + \alpha^2 c_B^2\mathscr{P}_B(\Delta E) + \alpha\gamma c_A c_B(\bar{\mathscr{P}}_{AB}(-\Delta E) + \bar{\mathscr{P}}^\star_{AB}(-\Delta E)).
\end{aligned} \tag{6.A.1}$$

The positive frequency Wightman function in Minkowski spacetime this is given by

$$G_W(x,x') = \frac{1}{16\pi^3}\int \frac{d^3k}{\omega_{\mathbf{k}}} e^{-i\omega_{\mathbf{k}}(t-t')+i\mathbf{k}\cdot\mathbf{x}}. \tag{6.A.2}$$

Whereas $iG_F(x,x')$ is the Feynman propagator and it is related to $G_W(x,x')$ by the relation $iG_F(x_A,x'_B) = \theta(t-t')G_W(x,x') + \theta(t'-t)G_W(x',x)$. For our choice of trajectories (see (6.1)), $G_W(x,x')$ is time translational invariant with respect to detector's proper time. Using infinite switching $\chi_j(\tau_j) = 1$, we can evaluate the expressions of the integral quantities as follows:

$$\begin{aligned}
\mathscr{P}_j(\Delta E^j) &= \int\int d\tau_j d\tau'_j e^{i\Delta E^j(\tau_j-\tau'_j)} G_W(x'_j,x_j)\\
&= \frac{1}{16\pi^3}\int\frac{d^3k}{\omega_{\mathbf{k}}}\int\int\frac{du\,dv}{2} e^{i\Delta E^j u} e^{i\omega_{\mathbf{k}}u}\\
&= \frac{1}{16\pi^3}\int\frac{d^3k}{\omega_{\mathbf{k}}}\int\frac{dv}{2} 2\pi\delta(\Delta E^j + \omega_{\mathbf{k}}) = 0
\end{aligned} \tag{6.A.3}$$

Here we used the coordinate transform $u = \tau_j - \tau'_j$ and $v = \tau_j + \tau'_j$, with $|J| = 1/2$. The same is also used for the following integral.

$$\begin{aligned}
\mathscr{P}_j(-\Delta E^j) &= \int\int d\tau_j d\tau'_j e^{-i\Delta E^j(\tau_j-\tau'_j)} G_W(x'_j, x_j) \\
&= \frac{1}{16\pi^3}\int \frac{d^3k}{\omega_{\mathbf{k}}}\int\int \frac{du\,dv}{2} e^{-i\Delta E^j u} e^{i\omega_{\mathbf{k}} u} \\
&= \frac{1}{16\pi^3}\int \frac{d^3k}{\omega_{\mathbf{k}}}\int \frac{dv}{2} 2\pi\delta(\Delta E^j - \omega_{\mathbf{k}}) \\
&= \frac{\delta(0)}{8\pi}\int_0^\infty \frac{4\pi k^2 dk}{\sqrt{k^2+m^2}}\delta(\Delta E^j - \sqrt{k^2+m^2}) \\
&= \frac{\delta(0)}{2}\int_0^\infty \frac{k^2 dk}{\sqrt{k^2+m^2}} \frac{\delta\left(k - \sqrt{\left(\Delta E^j\right)^2 - m^2}\right)}{\frac{\sqrt{(\Delta E^j)^2-m^2}}{\Delta E}} \\
&= \frac{\delta(0)}{2}\frac{\left(\sqrt{\left(\Delta E^j\right)^2 - m^2}\right)^2}{\Delta E}\frac{1}{\frac{\sqrt{(\Delta E^j)^2-m^2}}{\Delta E}} \\
&= \frac{\delta(0)}{2}\sqrt{\left(\Delta E^j\right)^2 - m^2}\ ; \qquad (6.A.4)
\end{aligned}$$

$$\begin{aligned}
\bar{\mathscr{P}}_{jj}(\pm\Delta E^j) &= \int\int d\tau_j d\tau'_j e^{\pm i\Delta E^j(\tau_j+\tau'_j)} G_W(x'_j, x_j) \\
&= \frac{1}{16\pi^3}\int \frac{d^3k}{\omega_{\mathbf{k}}}\int\int \frac{du\,dv}{2} e^{\pm i\Delta E^j v} e^{i\omega_{\mathbf{k}} u} \\
&= \frac{1}{16\pi^3}\int \frac{d^3k}{\omega_{\mathbf{k}}}\frac{1}{2}(2\pi)^2\delta(\Delta E^j)\delta(\omega_{\mathbf{k}}) = 0; \qquad (6.A.5)
\end{aligned}$$

$$\begin{aligned}
\mathscr{P}_{AB}(\Delta E) &= \int\int d\tau_A \tau_B e^{i(\Delta E^A \tau_A - \Delta E^B \tau_B)} G_W(x_B, x_A) \\
&= \frac{1}{16\pi^3}\int \frac{d^3k}{\omega_{\mathbf{k}}}\int\int d\tau_A \tau_B e^{i(\Delta E^A \tau_A - \Delta E^B \tau_B)} e^{i\mathbf{k}\cdot\mathbf{d} - i\omega_{\mathbf{k}}(\tau_B - \tau_A)} \\
&= \frac{1}{16\pi^3}\int \frac{d^3k}{\omega_{\mathbf{k}}} e^{i\mathbf{k}\cdot\mathbf{d}}(2\pi)^2\delta(\Delta E^A + \omega_{\mathbf{k}})\delta(\Delta E^B + \omega_{\mathbf{k}}) = 0\ ; \qquad (6.A.6)
\end{aligned}$$

$$
\begin{aligned}
\mathscr{P}_{AB}(-\Delta E) &= \int\int d\tau_A \tau_B e^{-i(\Delta E^A \tau_A - \Delta E^B \tau_B)} G_W(x_B, x_A) \\
&= \frac{1}{16\pi^3}\int \frac{d^3k}{\omega_{\mathbf{k}}} \int\int d\tau_A \tau_B e^{-i(\Delta E^A \tau_A - \Delta E^B \tau_B)} e^{i\mathbf{k}\cdot\mathbf{d} - i\omega_{\mathbf{k}}(\tau_B - \tau_A)} \\
&= \frac{1}{16\pi^3}\int \frac{d^3k}{\omega_{\mathbf{k}}} \int\int \frac{du\,dv}{2} e^{-i\left(\frac{(\Delta E^A - \Delta E^B)v}{2} + \frac{(\Delta E^A + \Delta E^B)u}{2}\right)} e^{i\mathbf{k}\cdot\mathbf{d} + iu\omega_{\mathbf{k}}} \\
&= \frac{1}{16\pi^3}\frac{1}{2}\int \frac{d^3k}{\omega_{\mathbf{k}}} e^{i\mathbf{k}\cdot\mathbf{d}} (2\pi)^2 \delta\left(\frac{\Delta E^A - \Delta E^B}{2}\right)\delta\left(\overline{\Delta E} - \omega_{\mathbf{k}}\right) \\
&= \frac{1}{4}\delta\left(\frac{\Delta E^A - \Delta E^B}{2}\right)\int_0^\pi \int_0^\infty \frac{\sin\theta\, d\theta\, k^2 dk}{\omega_{\mathbf{k}}} e^{ikd\cos\theta} \frac{\delta\left(k - \sqrt{\overline{\Delta E}^2 - m^2}\right)}{\left(\sqrt{\overline{\Delta E}^2 - m^2}\right)/\overline{\Delta E}} \\
&= \frac{1}{2}\delta\left(\frac{\Delta E^A - \Delta E^B}{2}\right)\int_0^\infty k dk \frac{\sin(kd)}{\omega_{\mathbf{k}} d} \frac{\delta(k - \sqrt{\overline{\Delta E}^2 - m^2})}{\left(\sqrt{\overline{\Delta E}^2 - m^2}\right)/\overline{\Delta E}} \\
&= \frac{\sin\left(d\sqrt{\overline{\Delta E}^2 - m^2}\right)}{2d}\delta\left(\frac{\Delta E^A - \Delta E^B}{2}\right). \qquad \text{(6.A.7)}
\end{aligned}
$$

where $\overline{\Delta E} = \frac{\Delta E^A + \Delta E^B}{2}$.

$$
\begin{aligned}
\bar{\mathscr{P}}_{AB}(\Delta E) &= \int\int d\tau_A \tau_B e^{i(\Delta E^A \tau_A + \Delta E^B \tau_B)} G_W(x_B, x_A) \\
&= \frac{1}{16\pi^3}\int \frac{d^3k}{\omega_{\mathbf{k}}} \int\int d\tau_A \tau_B e^{i(\Delta E^A \tau_A + \Delta E^B \tau_B)} e^{i\mathbf{k}\cdot\mathbf{d} - i\omega_{\mathbf{k}}(\tau_B - \tau_A)} \\
&= \frac{1}{16\pi^3}\int \frac{d^3k}{\omega_{\mathbf{k}}} e^{i\mathbf{k}\cdot\mathbf{d}} (2\pi)^2 \delta(\Delta E^A + \omega_{\mathbf{k}})\delta(\Delta E^B - \omega_{\mathbf{k}}) = 0\,; \qquad \text{(6.A.8)}
\end{aligned}
$$

$$
\begin{aligned}
M_j(\Delta E) &= \int\int d\tau_j d\tau'_j e^{i\Delta E^j(\tau_j-\tau'_j)}\theta(\tau_j-\tau'_j)\Big(G_W(x'_j,x_j)+G_W(x_j,x'_j)\Big)\\
&= \frac{1}{16\pi^3}\int\frac{d^3k}{\omega_{\mathbf{k}}}\int\int\frac{du\,dv}{2}e^{i\Delta E^j u}\theta(u)\Big(e^{i\omega_{\mathbf{k}}u}+e^{-i\omega_{\mathbf{k}}u}\Big)\\
&= \frac{1}{16\pi^3}\int\frac{4\pi k^2 dk}{\omega_{\mathbf{k}}}\frac{1}{2}\int_{-\infty}^{\infty}dv\int_0^{\infty}du\left(e^{i(\Delta E^j+\omega_{\mathbf{k}}+i\epsilon)u}+e^{i(\Delta E^j-\omega_{\mathbf{k}}+i\epsilon)u}\right)\\
&= \frac{\delta(0)}{4\pi}\int\frac{k^2dk}{\omega_{\mathbf{k}}}\left(PV\left(\frac{i}{\Delta E^j+\omega_{\mathbf{k}}}\right)+\pi\delta(\Delta E^j+\omega_{\mathbf{k}})+PV\left(\frac{i}{\Delta E^j-\omega_{\mathbf{k}}}\right)+\pi\delta(\Delta E^j-\omega_{\mathbf{k}})\right)\\
&= \frac{\delta(0)}{4}\int\frac{k^2dk}{\omega_{\mathbf{k}}}\delta(\Delta E^j-\omega_{\mathbf{k}})+i\frac{\delta(0)}{4\pi}\int_0^{\infty}\frac{k^2dk}{\omega_{\mathbf{k}}}PV\left(\frac{2\Delta E^j}{(\Delta E^j)^2-\omega_{\mathbf{k}}^2}\right)\\
&= \frac{\delta(0)}{4}\sqrt{(\Delta E^j)^2-m^2}+i\frac{\delta(0)}{4\pi}\int_0^{\infty}\frac{k^2dk}{\omega_{\mathbf{k}}}PV\left(\frac{2\Delta E^j}{(\Delta E^j)^2-\omega_{\mathbf{k}}^2}\right);
\end{aligned}
\tag{6.A.9}
$$

where $PV\left(\frac{1}{x}\right)$ represents the principal value of $\frac{1}{x}$. Here we used the coordinate transform $u=\tau_j-\tau'_j$ and $v=\tau_j+\tau'_j$, with $|J|=1/2$. We only need real part of M_j to calculate negativity and concurrence.

$$
\begin{aligned}
\mathcal{E}(\Delta E) &= -\int\int d\tau_A d\tau_B e^{i(\Delta E^B\tau_B+\Delta E^A\tau_A)}\{iG_F(x_A,x_B)\}\\
&= \int\int d\tau_A d\tau_B e^{i(\Delta E^B\tau_B+\Delta E^A\tau_A)}\Bigg\{\frac{1}{16\pi^2}\int\frac{d^3k}{\omega_{\mathbf{k}}}\\
&\times[\theta(\tau_B-\tau_A)e^{i\mathbf{k}\cdot\mathbf{d}-i\omega_{\mathbf{k}}(\tau_B-\tau_A)}+\theta(\tau_A-\tau_B)e^{-i\mathbf{k}\cdot\mathbf{d}-i\omega_{\mathbf{k}}(\tau_A-\tau_B)}]\Bigg\}\\
&= \frac{1}{2}\int\int dv\,du\,e^{i\left(\frac{\Delta E^B+\Delta E^A}{2}v+\frac{\Delta E^A-\Delta E^B}{2}u\right)}\Bigg\{\frac{1}{16\pi^2}\int\frac{d^3k}{\omega_{\mathbf{k}}}\\
&\times[\theta(-u)e^{i\mathbf{k}\cdot\mathbf{d}+i\omega_{\mathbf{k}}u}+\theta(u)e^{-i\mathbf{k}\cdot\mathbf{d}-i\omega_{\mathbf{k}}u}]\Bigg\}\\
&= 2\pi\delta\left(\frac{\Delta E^B+\Delta E^A}{2}\right)\frac{1}{2}\int du\,e^{iu\left(\frac{-\Delta E^B+\Delta E^A}{2}\right)}\Bigg\{\frac{1}{16\pi^2}\int\frac{d^3k}{\omega_{\mathbf{k}}}\\
&\times[\theta(-u)e^{i\mathbf{k}\cdot\mathbf{d}+i\omega_{\mathbf{k}}u}+\theta(u)e^{-i\mathbf{k}\cdot\mathbf{d}-i\omega_{\mathbf{k}}u}]\Bigg\}\\
&= 0;
\end{aligned}
\tag{6.A.10}
$$

as $\Delta E^B>0$ and $\Delta E^A>0$. Here we used the coordinate transform $u=\tau_A-\tau_B$ and $v=\tau_A+\tau_B$, with $|J|=1/2$.

6.B Negativity

The only eigenvalue of $\hat{\rho}_{AB}^{T_A} = (\hat{T}_A \otimes \hat{\mathbf{1}}_B)\hat{\rho}_{AB}$, that can be *negative*, is given by (see Eq. (2.80))

$$\lambda_4 = \frac{1}{2}\left\{(b_1+h_2) - \sqrt{(b_1-h_2)^2 + 4a_2d_1}\right\}. \tag{6.A.11}$$

We know $|a_2|^2 = |d_1|^2 = a_2d_1$ and $|b_2|^2 = |h_1|^2 = b_2h_1$. Thus the eigenvalue becomes

$$\begin{aligned}
\lambda_4 &= \frac{1}{2}\left\{2\gamma^2c^2\mathscr{P}_- - 2|\alpha\gamma|\sqrt{(1-2c^2M^\star)(1-2c^2M)}\right\} \\
&= \gamma^2c^2\mathscr{P}_- - |\alpha\gamma|\sqrt{1-2c^2M^\star-2c^2M+\mathscr{O}\left(c^4\right)} \\
&\simeq \gamma^2c^2\mathscr{P}_- - |\alpha\gamma|\left\{1-\frac{1}{2}\left(2c^2M^\star+2c^2M+\mathscr{O}\left(c^4\right)\right)\right\} \\
&\simeq c^2\left(\gamma^2\mathscr{P}_- + |\alpha\gamma|\mathrm{Re}\{M\}\right) - |\alpha\gamma|.
\end{aligned} \tag{6.A.12}$$

6.C Concurrence

The square-root of the eigenvalues of $\hat{\rho}_{AB}(\hat{\sigma}_y\otimes\hat{\sigma}_y)\hat{\rho}_{AB}^\star(\hat{\sigma}_y\otimes\hat{\sigma}_y)$ are given as (see Eq. 2.96)

$$\begin{aligned}
\lambda_{1,2} &= \left(|a_2|^2 + a_1d_2 \pm 2|a_2|\sqrt{a_1d_2}\right)^{1/2}; \\
\lambda_{3,4} &= \left(|b_2|^2 + b_1h_2 \pm 2|b_2|\sqrt{2b_1h_2}\right)^{1/2}.
\end{aligned} \tag{6.A.13}$$

$$\begin{aligned}
\lambda_{1,2}^2 &= \left(|a_2|^2 + a_1d_2 \pm 2|a_2|\sqrt{a_1d_2}\right); \\
&= \left(|\alpha\gamma(1-2c^2M)|^2 + \alpha^2\gamma^2(1-2c^2\mathscr{P}_-) \pm 2\alpha^2\gamma^2|(1-2c^2M)|\sqrt{(1-2c^2\mathscr{P}_-)}\right) \\
&\simeq \alpha^2\gamma^2\left(|(1-2c^2M)|^2 + (1-2c^2\mathscr{P}_-) \pm 2|(1-2c^2M)|(1-c^2\mathscr{P}_-)\right)
\end{aligned} \tag{6.A.14}$$

$$\begin{aligned}
\lambda_{1,2} &= |\alpha\gamma|\sqrt{|(1-2c^2M)|^2 + (1-2c^2\mathscr{P}_-) \pm 2|(1-2c^2M)|(1-c^2\mathscr{P}_-)} \\
&= |\alpha\gamma|\sqrt{(2-4c^2\mathrm{Re}\{M\} - 2c^2\mathscr{P}_- + \mathscr{O}(c^4)) \pm 2(1-2c^2\mathrm{Re}\{M\} - c^2\mathscr{P}_- + \tilde{\mathscr{O}}(c^4))} \\
&\simeq 2|\alpha\gamma|\left(1 - c^2\mathrm{Re}\{M\} - \frac{1}{2}c^2\mathscr{P}_-\right), 0.
\end{aligned} \tag{6.A.15}$$

and

$$\begin{aligned}
\lambda_{3,4}^2 &= \left(|b_2|^2 + b_1h_2 \pm 2|b_2|\sqrt{2b_1h_2}\right) \\
&= \gamma^4c^4\left(\left(|\mathscr{P}_{AB}(-\Delta E)|^2 + \mathscr{P}_-^2\right) \pm 2\mathscr{P}_-|\mathscr{P}_{AB}(-\Delta E)|\right) \\
&= \gamma^4c^4(\mathscr{P}_- \pm |\mathscr{P}_{AB}(-\Delta E)|)^2
\end{aligned} \tag{6.A.16}$$

Since we always have $|\mathscr{P}_{AB}(-\Delta E)| \leq \mathscr{P}_{-}$ as $\frac{\sin x}{x} \leq 1$ (see Eq. (6.A.4) and (6.A.7)). The eigenvalues $\lambda_{3,4}$ are obtained as

$$\lambda_{3,4} = \gamma^2 c^2 (\mathscr{P}_{-} \pm |\mathscr{P}_{AB}(-\Delta E)|) \,. \tag{6.A.17}$$

CHAPTER 7

CONCLUSIONS AND OUTLOOK

7.1 Conclusions

In recent years, there has been growing interest in understanding the entangling nature of background field states in connection with entanglement extraction from the background field into a composite system of two atomic detectors. These studies reveal several characteristics of entanglement harvesting or extraction from the vacuum of the field, depending on atoms' motions, nature of background fields and spacetime, boundary conditions, *etc*. However, the results obtained for a particular situation (say, accelerating motion) vary among the studies upon consideration of models for the detector (two-level atom, harmonic oscillator, *etc*), consideration of the switching functions, *etc*. At later times, the atomic detectors are found to be entangled in some cases but not entangled in others, depending on the models under consideration. Therefore, one can not clearly understand the elementary physical processes behind the various entanglement harvesting or leakage phenomena. In this thesis, we aimed to understand the elementary physical processes behind this. In this regard, we consider a simplistic Unruh DeWitt atomic detector with two energy levels. This detector is coupled to the background field such that any transition in the field's state will be reflected as a transition in the detector atom's state (in other words, detectors will beep). Since the spatial profile of the detector does not play in atom-field interactions, we choose the detector atom to be point-like. From the path integral formalism, we know that the classical trajectory of a particle mostly dominates over other possible trajectories. Here, we consider the

detectors following classical paths. In many entanglement harvesting-related works, people have considered finite time switching functions (χ) for the interactions since, in reality, no interaction can continue for infinite periods. However, considering these finite time switching functions introduces transient effects. Consequently, the detector can beep even if there is no transition in the field's state, *e.g., the* inertially moving detector will beep for a finite time switching function even though there is no particle production in the background field. Also, two parallel accelerated detectors can extract entanglement for finite time switching functions, which vanishes for a much larger period of interaction. To avoid this kind of transient effects, one can start with an adiabatic interaction switching function $\chi_j(\tau_j) = e^{-s|\tau_j|}$ to build up a model (*e.g.,* see [24, 89]). This helps to suppress spurious transient effects. The interaction is switched on for duration $\tau_j \sim s^{-1}$ with the restriction $s << \Delta E$. Moreover, the interaction is switched on and off in an infinitely slow process to satisfy the adiabatic condition. Then if the interaction starts at $t_{in} = \tau_j^{in} = -\tau_0$ and ended at $t = \tau_j^f = \tau_0$, one must take the limits $\tau_0 \to \infty$ and $s \to 0$. In that case, the limits of integrations are from $-\infty$ to ∞, and χ_j can be chosen to unity. Using this spirit, we have chosen $\chi_j = 1$ in our analysis so that the interaction starts at the asymptotic infinite-past (same has also been done in [24]). Therefore, in this thesis, we have tried to understand the underlying physical processes in entanglement harvesting or leakage phenomena and to find out the roles played by the vacuum of the field in different systems under consideration. The chapter-wise findings of the thesis are the following:

Starting with the second chapter, where we have briefly reviewed the quantum field theory in Minkowski and curved spacetimes. Due to the non-uniqueness of the vacuum in curved spacetime, two observers quantising in different frames will not generally agree on the particle content of the field. This is the reason behind the Unruh effect and the Hawking radiation. One observer can see particles in the vacuum of another observer. The idea of atomic Unruh DeWitt detectors was introduced to realise these particles operationally. The main focus of this chapter is to discuss the formalism of entanglement harvesting or leakage. We considered two atomic detectors that are initially uncorrelated or correlated and coupled to the background field. Due to this coupling, the initial composite state of two detectors will evolve, and their reduced density state after a sufficiently large time is discussed. Once we have the final density matrix, we can study the conditions for the entanglement harvesting or leakage phenomena. We finally discussed the quantitative measures of entanglement, such as the negativity and concurrence for our systems under consideration.

In the second chapter, we learned about the formalism of entanglement harvesting. In the third chapter, we apply this formalism to accelerated systems. Since it is almost impossible to exclude the thermal effects completely from a realistic setup, we consider a background thermal bath (by considering the thermal fields). This chapter studied entanglement harvesting with two accelerated detectors interacting with a background thermal massless scalar field. Now, let us summarize the results of this chapter.

- We have constructed Green's functions corresponding to accelerated observers in a thermal bath considering the Rindler modes with the vacuum for the Unruh modes instead of the Minkowski vacuum. This consideration is due to the fact that the Green's function for accelerated observers in thermal bath with Minkowski vacuum will not be time translational invariant. Then using the Green's functions, we calculated the density matrix elements.

- We found that entanglement extraction from the field to the detectors is not possible for parallel accelerations of the detectors. Even though the thermal bath can influence the individual detectors' transition probabilities, the entangling term remains vanishing for any temperature of the thermal bath.

- Entanglement harvesting is possible for the detectors in anti-parallel motion. For *equal magnitude of accelerations*, entanglement harvesting is always possible at a temperature of zero. However, as background temperature increases, the magnitude of the harvested entanglement decreases, and also requires higher accelerations to satisfy the condition for entanglement harvesting (2.83), which is expected as thermal fluctuations are known to have a demoting effect on quantum entanglement in low acceleration regime [211, 212]. However, after a specific (critical) acceleration, the magnitude of the harvested entanglement increases due to the interplay between the background and Unruh thermal baths. However, the Unruh thermal bath dominates for extremely large accelerations, and entanglement harvesting is suppressed due to Unruh thermality. This is true for both $(1+1)$ and $(1+3)$-dimensions as contributions of the retarded Green's function in entangling term vanishes.

- For *different magnitudes of accelerations* of the detectors, we observe the monotonic nature of entanglement in the $(1+1)$-dimension. However, in $(1+3)$-dimension, there are multiple critical accelerations (α_c), and around a α_c-point nature of entan-

glement under the influence of bath temperature is the opposite. Also, in this case, entanglement harvesting is possible for various discrete ranges of accelerations.

- We have also studied the quantity known as mutual information, which increases with background temperature for parallel motion of the detectors and vanishes for anti-parallel motion.

We learned in the third chapter that two uniformly accelerated detectors can harvest entanglement from the vacuum only when they are in anti-parallel motion. In that case, the detectors are in two causally disconnected regions. We have seen that for equal accelerations of the detectors, thermal effects depreciate entanglement extraction in lower accelerations, which is more achievable in actual experimental setups. It is always desirable to achieve higher degrees of entanglement at lower accelerations. In this chapter, we aim to understand if one can harvest more entanglement in the presence of multiple (single and double) reflecting boundaries than in free space. The findings from the fourth chapter are listed below;

- As in the previous chapter, we found that entanglement harvesting is only possible for the anti-parallel motion of the detectors. Here, the acceleration of identical detectors with the same energy gap must have the same magnitude.

- Here, we studied for only the $(1+3)$-dimension. We observe that detectors' entanglement increases as the perpendicular separation between them decreases. This is true for any number of boundaries.

- For the single and double boundary systems, the entanglement gets suppressed if any one or both of the detectors are near the boundary or boundaries. As the separation increases, the boundary influence on the detectors decreases; the concurrence rate approaches the same for no-boundary system. Entanglement degradation is much higher for the double boundary system than the single boundary system.

- There is enhancement in harvesting for some specific parameter values compared to the free space case. In that case, enhancement for a double boundary system is higher than a single boundary system. Due to reflecting boundaries, this enhancement is more favoured in lower acceleration regimes.

Therefore, the presence of reflecting boundaries can both enhance or suppress entanglement harvesting. Enhancing or suppressing is higher for double boundaries than for

a single boundary.

In the earlier chapters, we have studied entanglement harvesting in accelerated systems, considering the background field is in the vacuum state. However, in nature, it is not guaranteed that the background field will always be in a vacuum state. Then, understanding how entanglement harvesting is influenced by consideration of non-vacuum field states becomes crucial. The fifth chapter considers single-particle background field states to investigate the entanglement harvesting between inertial Unruh-DeWitt detectors in $(1+1)$ and $(1+3)$ dimensions. This analysis has been concluded with the following results;

- When the detectors interact with the non-vacuum field states, the density matrix elements have contributions due to non-vacuum as well as vacuum fluctuations. The vacuum contributions for the transition probability of inertial detectors vanish. However, the total transition probability remains due to non-vacuum contributions. The entangling term has only non-zero contributions from vacuum fluctuations.
- Since the entangling term remains the same and the transition probabilities are enhanced compared to the vacuum counterpart, the harvesting from the non-vacuum states is always expected to be less compared to the field vacuum.
- When the field is in a vacuum state, entanglement harvesting is possible for all energy gaps of the detectors (ΔE), although it decreases with increasing ΔE. However, when the background field is in a non-vacuum state, there are disconnected ranges of ΔE for which entanglement harvesting is possible.
- We observe that in both $(1+1)$ and $(1+3)$ dimensions with detectors in parallel motion, two detectors with the same velocity ($v_A = v_B$) do not harvest any entanglement. However, a similar situation with detectors in perpendicular inertial motion in $(1+3)$ dimensions is not observed.
- For a fixed v_B, there are discrete ranges of v_A for entanglement harvesting from the single-particle field states for larger ΔE. In comparison, in similar scenarios, entanglement harvesting from the vacuum is possible in the whole range of velocities $0 < v_A < 1$.
- In high-velocity regimes $v_A \to 1$, there is visible occurrence of entanglement harvesting with lower ΔE in $(1+1)$ dimensions. While in $(1+3)$ dimensions, entanglement harvesting stops in the limit $v_A \to 1$.

These specific observations provide distinctions between entanglement harvesting from vacuum and single-particle field states.

In the previous chapters, we have studied the phenomenon of entanglement harvesting from the background field state to two initially uncorrelated detectors. In the sixth chapter, we studied the degradation of entanglement of two initially entangled atomic detectors open to the environment (coupled to the background scalar field). This analysis has been concluded with the following results;

- Two initially entangled, static detectors lose entanglement when they interact with the background (massive) scalar field provided the mass of the scalar field (m) is less than the energy gap of the detectors (ΔE) *i.e.,* $\Delta E > m$. If $\Delta E = m$, then the entangled state of detectors will remain the same.

- For our simple model with an infinite switching function, we investigated the elementary physical processes behind this phenomenon. We observe that the spontaneous emission probability of the individual detectors and vacuum fluctuations of the background field lead to this entanglement leakage. Both of these quantities are local in nature and specific to the individual detectors.

- Entanglement degradation between the detectors shall also happen even if one considers finite time switching functions. However, in that case, some additional terms in the density matrix elements will arise due to the switching effects. Also, one would be unable to figure out the fundamental processes behind the entanglement leakage phenomenon.

In earlier chapters, we observe that the vacuum fluctuations of the field favour the generation of entanglement between two initially non-entangled detectors. In contrast, we observe the negative effect of vacuum fluctuation, which was observed to provide entanglement harvesting between two un-entangled atomic detectors.

In this scenario, where researchers seek to understand gravity's influence on quantum information systems (especially on quantum entanglement), which can reveal several intriguing features of the quantum nature of gravity, it also may shed some light on the famous black hole information paradox. A significant amount of effort has been put into uncovering the entangling nature of the vacuum of quantum fields in the context of two atomic detectors, which were initially introduced to capture the notion of particle production in non-inertial or gravitational systems. It was known that a vacuum is a

maximally entangled state from a local observer's point of view. In accelerated systems, the Minkowski vacuum is an entangled state of the left and right Rindler field states (3.1). In our considered simple model setup, we also observe that entanglement extraction is only possible when one detector is in the left and another in the right Rindler wedge. Also, we notice that for excited field states, entanglement harvesting is suppressed compared to vacuum, which also supports the fact that vacuum is the maximally entangled state. Additionally, we observe that for two static entangled detectors, the effect of vacuum fluctuations on individual detectors leads to leakage in entanglement. In this case, non-local terms do not play any roles. The way we have studied here revealed the elementary physical process behind this phenomenon. With the progress of these present investigations, the role of the field's vacuum in entanglement phenomena may be revealed, and further exploration in this direction may uncover various quantum signatures of gravity. In the following, we provide the areas where people can explore further to better understand the subject.

7.2 Scope for future works

7.2.1 Role of Horizon in entanglement harvesting

Since accelerating systems are related to local gravitational systems, entanglement phenomenon in accelerating systems attract a lot of attention in recent years. This phenomenon of entanglement harvesting has been studied in accelerated systems with various set-ups under considerations. There another possible configuration for entanglement harvesting with one observer in the right Rindler wedge and another observer in the future Rindler wedge. This set-up closely resembles the black hole scenario where one particle in outside of event horizon and another particle moving inside the horizon. Studying entanglement between these two observers or particles can help us to understand the role of horizon in quantum entanglement.

7.2.2 Entanglement harvesting or leakage between two accelerated detectors in cavity systems

There has lots of studies to capture how non-inertial effects can influence a quantum system. In this regard, utilization of cavity systems is known to modify the quantum field's density of modes significantly. A recent study [198] has shown that considering a cylindrical cavity magnificently amplifies the transition rate of an accelerated detector at much lower accelerations. On the other hand, entanglement harvesting is related to particle production or absorption in the background quantum field. Hence one may expect that two initially non-entangled detectors, accelerating inside a cylindrical cavity can get sufficiently entangled at lower accelerations.

7.2.3 Can accelerated observers harvest entanglement from Rindler vacuum?

In Chapter 5, we studied that two inertial observers can harvest entanglement from the Minkowski vacuum. They can harvest entanglement from it when there is relative velocity between them. Similarly, one can ask for an equivalent set-up with accelerated observers. Can two uniformly accelerated observers confined in a particular Rindler wedge harvest entanglement from the Rindler vacuum? This became interesting because

accelerated observers do not see particles in the Rindler vacuum in the same way as inertial observers do not see particles in the Minkowski vacuum. The possibility of entanglement harvesting from the Rindler vacuum can broaden our understanding of the equivalence between these two systems.

BIBLIOGRAPHY

[1] K. Schwarzschild, "On the gravitational field of a mass point according to Einstein's theory," *Sitzungsber. Preuss. Akad. Wiss. Berlin (Math. Phys.)*, vol. 1916, pp. 189–196, 1916.

[2] J. Droste, "The field of a single centre in Einstein's theory of gravitation, and the motion of a particle in that field," *Koninklijke Nederlandse Akademie van Wetenschappen Proceedings Series B Physical Sciences*, vol. 19, pp. 197–215, Jan. 1917.

[3] H. Reissner, "Über die Eigengravitation des elektrischen Feldes nach der Einsteinschen Theorie," *Annalen der Physik*, vol. 355, pp. 106–120, jan 1916.

[4] G. Nordström, "On the Energy of the Gravitation field in Einstein's Theory," *Koninklijke Nederlandse Akademie van Wetenschappen Proceedings Series B Physical Sciences*, vol. 20, pp. 1238–1245, jan 1918.

[5] J. L. Synge, "The gravitational field of a particle," in *Proceedings of the Royal Irish Academy. Section A: Mathematical and Physical Sciences*, vol. 53, pp. 83–114, JSTOR, 1950.

[6] D. Finkelstein, "Past-future asymmetry of the gravitational field of a point particle," *Physical Review*, vol. 110, no. 4, p. 965, 1958.

[7] C. Fronsdal, "Completion and embedding of the Schwarzschild solution," *Physical Review*, vol. 116, no. 3, p. 778, 1959.

[8] M. D. Kruskal, "Maximal extension of Schwarzschild metric," *Physical review*, vol. 119, no. 5, p. 1743, 1960.

[9] G. Szekeres, "On the singularities of a Riemannian manifold," *Publicationes Mathematicae Debrecen 7*, vol. 7, p. 285, 1960.

[10] I. Novikov, "On the evolution of a semiclosed world," *Astronomicheskii Zhurnal*, vol. 40, p. 772, 1963.

[11] I. Novikov, "R-and t-regions in space-time with spherically symmetric space," *General Relativity and Gravitation*, vol. 33, no. 12, pp. 2259–2295, 2001.

[12] R. P. Kerr, "Gravitational field of a spinning mass as an example of algebraically special metrics," *Phys. Rev. Lett.*, vol. 11, pp. 237–238, Sep 1963.

[13] B. P. Abbott *et al.*, "Observation of Gravitational Waves from a Binary Black Hole Merger," *Phys. Rev. Lett.*, vol. 116, no. 6, p. 061102, 2016.

[14] B. P. Abbott *et al.*, "GW151226: Observation of Gravitational Waves from a 22-Solar-Mass Binary Black Hole Coalescence," *Phys. Rev. Lett.*, vol. 116, no. 24, p. 241103, 2016.

[15] B. P. Abbott *et al.*, "Binary Black Hole Mergers in the first Advanced LIGO Observing Run," *Phys. Rev.*, vol. X6, no. 4, p. 041015, 2016.

[16] B. P. Abbott *et al.*, "GW170104: Observation of a 50-Solar-Mass Binary Black Hole Coalescence at Redshift 0.2," *Phys. Rev. Lett.*, vol. 118, no. 22, p. 221101, 2017.

[17] K. Akiyama *et al.*, "First M87 Event Horizon Telescope Results. I. The Shadow of the Supermassive Black Hole," *Astrophys. J. Lett.*, vol. 875, p. L1, 2019.

[18] J. D. Bekenstein, "Black holes and entropy," *Phys. Rev. D*, vol. 7, pp. 2333–2346, Apr 1973.

[19] S. W. Hawking, "Particle creation by black holes," *Communications in Mathematical Physics*, vol. 43, pp. 199–220, 1975.

[20] S. W. HAWKING, "Black hole explosions?," *Nature*, vol. 248, no. 5443, pp. 30–31, 1974.

[21] S. A. Fulling, "Nonuniqueness of Canonical Field Quantization in Riemannian Space-Time," *Phys. Rev. D*, vol. 7, pp. 2850–2862, May 1973.

[22] P. Davies, "Scalar production in Schwarzschild and Rindler metrics," *Journal of Physics A: Mathematical and Theoretical*, vol. 8, pp. 609–616, 1975.

[23] W. G. Unruh, "Notes on black hole evaporation," *Phys. Rev. D*, vol. 14, p. 870, 1976.

[24] N. D. Birrell and P. C. W. Davies, *Quantum fields in curved space*. Cambridge Monographs on Mathematical Physics, Cambridge University Press, 1982.

[25] S. D. Mathur, "The Information paradox: A Pedagogical introduction," *Class. Quant. Grav.*, vol. 26, p. 224001, 2009.

[26] A. Almheiri, D. Marolf, J. Polchinski, and J. Sully, "Black Holes: Complementarity or Firewalls?," *JHEP*, vol. 02, p. 062, 2013.

[27] O. Lunin and S. D. Mathur, "AdS/CFT duality and the black hole information paradox," *Nuclear Physics B*, vol. 623, pp. 342–394, 2002.

[28] S. D. Mathur, "The fuzzball proposal for black holes: an elementary review," *Fortschritte der Physik*, vol. 53, pp. 793–827, 2005.

[29] S. B. Giddings, "Black holes and massive remnants," *Phys. Rev. D*, vol. 46, pp. 1347–1352, 1992.

[30] P. Chen, Y. C. Ong, and D. h. Yeom, "Black hole remnants and the information loss paradox," *Physics Reports*, vol. 603, pp. 1–45, 2015.

[31] S. K. Modak, L. Ortíz, I. Peña, and D. Sudarsky, "Black hole evaporation: information loss but no paradox," *General Relativity and Gravitation*, vol. 47, p. 120, 2015.

[32] A. Almheiri, T. Hartman, J. Maldacena, E. Shaghoulian, and A. Tajdini, "Replica Wormholes and the Entropy of Hawking Radiation," *JHEP*, vol. 05, p. 013, 2020.

[33] G. Penington, S. H. Shenker, D. Stanford, and Z. Yang, "Replica wormholes and the black hole interior," 2020.

[34] A. Almheiri, R. Mahajan, J. Maldacena, and Y. Zhao, "The Page curve of Hawking radiation from semiclassical geometry," *JHEP*, vol. 03, p. 149, 2020.

[35] S. Bose, A. Mazumdar, G. W. Morley, H. Ulbricht, M. Toros, M. Paternostro, A. A. Geraci, P. F. Barker, M. S. Kim, and G. Milburn, "Spin entanglement witness for quantum gravity," *Phys. Rev. Lett.*, vol. 119, p. 240401, 2017.

[36] C. Marletto and V. Vedral, "Gravitationally Induced Entanglement between Two Massive Particles is Sufficient Evidence of Quantum Effects in Gravity," *Physical Review Letters*, vol. 119, p. 240402, 2017.

[37] L. Susskind, L. Thorlacius, and J. Uglum, "The stretched horizon and black hole complementarity," *Phys. Rev. D*, vol. 48, pp. 3743–3761, Oct 1993.

[38] S. L. Braunstein, S. Pirandola, and K. Życzkowski, "Better late than never: Information retrieval from black holes," *Phys. Rev. Lett.*, vol. 110, p. 101301, Mar 2013.

[39] S. W. Hawking, M. J. Perry, and A. Strominger, "Soft hair on black holes," *Phys. Rev. Lett.*, vol. 116, p. 231301, Jun 2016.

[40] D. Marolf, "The black hole information problem: past, present, and future," *Reports on Progress in Physics*, vol. 80, p. 092001, jul 2017.

[41] R. Brustein, M. B. Einhorn, and A. Yarom, "Entanglement interpretation of black hole entropy in string theory," *JHEP*, vol. 01, p. 098, 2006.

[42] S. N. Solodukhin, "Entanglement entropy of black holes," *Living Rev. Rel.*, vol. 14, p. 8, 2011.

[43] J. S. Bell, "On the Einstein Podolsky Rosen paradox," *Physics Physique Fizika*, vol. 1, pp. 195–200, Nov 1964.

[44] A. Einstein, B. Podolsky, and N. Rosen, "Can quantum-mechanical description of physical reality be considered complete?," *Phys. Rev.*, vol. 47, pp. 777–780, May 1935.

[45] J. F. Clauser, M. A. Horne, A. Shimony, and R. A. Holt, "Proposed experiment to test local hidden-variable theories," *Phys. Rev. Lett.*, vol. 23, pp. 880–884, Oct 1969.

[46] C. A. Kocher and E. D. Commins, "Polarization correlation of photons emitted in an atomic cascade," *Phys. Rev. Lett.*, vol. 18, pp. 575–577, Apr 1967.

[47] G. Weihs, T. Jennewein, C. Simon, H. Weinfurter, and A. Zeilinger, "Violation of Bell's Inequality under Strict Einstein Locality Conditions," *Phys. Rev. Lett.*, vol. 81, pp. 5039–5043, Dec 1998.

[48] W. Tittel, J. Brendel, H. Zbinden, and N. Gisin, "Violation of Bell Inequalities by Photons More Than 10 km Apart," *Phys. Rev. Lett.*, vol. 81, pp. 3563–3566, Oct 1998.

[49] W. Tittel, J. Brendel, N. Gisin, and H. Zbinden, "Long-distance Bell-type tests using energy-time entangled photons," *Phys. Rev. A*, vol. 59, pp. 4150–4163, Jun 1999.

[50] Z. Y. Ou and L. Mandel, "Violation of Bell's Inequality and Classical Probability in a Two-Photon Correlation Experiment," *Phys. Rev. Lett.*, vol. 61, pp. 50–53, Jul 1988.

[51] S. J. Freedman and J. F. Clauser, "Experimental test of local hidden-variable theories," *Phys. Rev. Lett.*, vol. 28, pp. 938–941, Apr 1972.

[52] P. G. Kwiat, K. Mattle, H. Weinfurter, A. Zeilinger, A. V. Sergienko, and Y. Shih, "New high-intensity source of polarization-entangled photon pairs," *Phys. Rev. Lett.*, vol. 75, pp. 4337–4341, Dec 1995.

[53] A. Aspect, J. Dalibard, and G. Roger, "Experimental Test of Bell's Inequalities Using Time-Varying Analyzers," *Phys. Rev. Lett.*, vol. 49, pp. 1804–1807, Dec 1982.

[54] J.-W. Pan, D. Bouwmeester, H. Weinfurter, and A. Zeilinger, "Experimental entanglement swapping: Entangling photons that never interacted," *Phys. Rev. Lett.*, vol. 80, pp. 3891–3894, May 1998.

[55] Y. Hasegawa, R. Loidl, G. Badurek, M. Baron, and H. Rauch, "Violation of a Bell-like inequality in neutron optical experiments: quantum contextuality," *Journal of Optics B: Quantum and Semiclassical Optics*, vol. 6, pp. S7–S12, Mar. 2004.

[56] R. Ursin, F. Tiefenbacher, T. Schmitt-Manderbach, H. Weier, T. Scheidl, M. Lindenthal, B. Blauensteiner, T. Jennewein, J. Perdigues, P. Trojek, B. Ömer, M. Fürst, M. Meyenburg, J. Rarity, Z. Sodnik, C. Barbieri, H. Weinfurter, and A. Zeilinger, "Entanglement-based quantum communication over 144km," *Nature Physics*, vol. 3, pp. 481–486, June 2007.

[57] B. Hensen *et al.*, "Loophole-free Bell inequality violation using electron spins separated by 1.3 kilometres," *Nature*, vol. 526, pp. 682–686, 2015.

[58] J. Handsteiner, A. S. Friedman, D. Rauch, J. Gallicchio, B. Liu, H. Hosp, J. Kofler, D. Bricher, M. Fink, C. Leung, A. Mark, H. T. Nguyen, I. Sanders, F. Steinlechner, R. Ursin, S. Wengerowsky, A. H. Guth, D. I. Kaiser, T. Scheidl, and A. Zeilinger, "Cosmic Bell Test: Measurement Settings from Milky Way Stars," *Phys. Rev. Lett.*, vol. 118, p. 060401, Feb 2017.

[59] B. T. Kirby and J. D. Franson, "Nonlocal interferometry using macroscopic coherent states and weak nonlinearities," *Phys. Rev. A*, vol. 87, p. 053822, May 2013.

[60] M. Hotta, "Quantum measurement information as a key to energy extraction from local vacuums," *Phys. Rev. D*, vol. 78, p. 045006, 2008.

[61] M. Hotta, "Quantum energy teleportation in spin chain systems," *Journal of the Physical Society of Japan*, vol. 78, no. 3, p. 034001, 2009.

[62] J. Matson, "Quantum teleportation achieved over record distances," *Nature*, 2012.

[63] M. Frey, K. Funo, and M. Hotta, "Strong local passivity in finite quantum systems," *Phys. Rev. E*, vol. 90, p. 012127, Jul 2014.

[64] A. K. Ekert, "Quantum cryptography based on Bell's theorem," *Phys. Rev. Lett.*, vol. 67, pp. 661–663, Aug 1991.

[65] D. Salart, A. Baas, C. Branciard, N. Gisin, and H. Zbinden, "Testing the speed of 'spooky action at a distance'," *Nature*, vol. 454, no. 7206, pp. 861–864, 2008.

[66] J. Yin, Y.-H. Li, S.-K. Liao, M. Yang, Y. Cao, L. Zhang, J.-G. Ren, W.-Q. Cai, W.-Y. Liu, S.-L. Li, R. Shu, Y.-M. Huang, L. Deng, L. Li, Q. Zhang, N.-L. Liu, Y.-A. Chen, C.-Y. Lu, X.-B. Wang, F. Xu, J.-Y. Wang, C.-Z. Peng, A. K. Ekert, and J.-W. Pan, "Entanglement-based secure quantum cryptography over 1,120 kilometres," *Nature*, vol. 582, no. 7813, pp. 501–505, 2020.

[67] G. J. Mooney, C. D. Hill, and L. C. L. Hollenberg, "Entanglement in a 20-qubit superconducting quantum computer," *Scientific Reports*, vol. 9, no. 1, p. 13465, 2019.

[68] E. Schrödinger, "Die gegenwärtige situation in der quantenmechanik," *Naturwissenschaften*, vol. 23, no. 48, pp. 807–812, 1935.

[69] J. VonNeumann, *Mathematische Grundlagen der Quantenmechanik*. Springer, 1932.

[70] R. F. Werner, "Quantum states with Einstein-Podolsky-Rosen correlations admitting a hidden-variable model," *Phys. Rev. A*, vol. 40, pp. 4277–4281, Oct 1989.

[71] M. Horodecki, P. Horodecki, and R. Horodecki, "Separability of mixed states: necessary and sufficient conditions," *Physics Letters A*, vol. 223, pp. 1–8, Nov. 1996.

[72] A. Peres, "Separability criterion for density matrices," *Phys. Rev. Lett.*, vol. 77, pp. 1413–1415, 1996.

[73] G. Vidal and R. F. Werner, "Computable measure of entanglement," *Phys. Rev. A*, vol. 65, p. 032314, 2002.

[74] C. H. Bennett, H. J. Bernstein, S. Popescu, and B. Schumacher, "Concentrating partial entanglement by local operations," *Phys. Rev. A*, vol. 53, pp. 2046–2052, Apr 1996.

[75] W. K. Wootters, "Entanglement of formation of an arbitrary state of two qubits," *Phys. Rev. Lett.*, vol. 80, pp. 2245–2248, 1998.

[76] S. Hill and W. K. Wootters, "Entanglement of a pair of quantum bits," *Phys. Rev. Lett.*, vol. 78, pp. 5022–5025, 1997.

[77] W. K. Wootters, "Entanglement of formation and concurrence," *Quant. Inf. Comput.*, vol. 1, no. 1, pp. 27–44, 2001.

[78] J. Schwinger, "On gauge invariance and vacuum polarization," *Phys. Rev.*, vol. 82, pp. 664–679, Jun 1951.

[79] Y. Li, Y. Dai, and Y. Shi, "Pairwise mode entanglement in Schwinger production of particle-antiparticle pairs in an electric field," *Phys. Rev. D*, vol. 95, p. 036006, Feb 2017.

[80] D.-C. Dai, "State of a particle pair produced by the Schwinger effect is not necessarily a maximally entangled Bell state," *Phys. Rev. D*, vol. 100, p. 045015, Aug 2019.

[81] Z. Ebadi and B. Mirza, "Entanglement generation by electric field background," *Annals of Physics*, vol. 351, pp. 363–381, 2014.

[82] S. J. Summers and R. Werner, "The vacuum violates Bell's inequalities," *Physics Letters A*, vol. 110, no. 5, pp. 257–259, 1985.

[83] S. J. Summers and R. Werner, "Maximal Violation of Bell's Inequalities Is Generic in Quantum Field Theory," *Commun. Math. Phys.*, vol. 110, pp. 247–259, 1987.

[84] S. J. Summers and R. Werner, "Bell's inequalities and quantum field theory. II. Bell's inequalities are maximally violated in the vacuum," *Journal of Mathematical Physics*, vol. 28, pp. 2448–2456, 10 1987.

[85] S. J. Summers and R. Werner, "Bell's inequalities and quantum field theory. i. general setting," *Journal of Mathematical Physics*, vol. 28, no. 10, pp. 2440–2447, 1987.

[86] W. G. Unruh and R. Schützhold, "Universality of the Hawking effect," *Phys. Rev. D*, vol. 71, p. 024028, Jan 2005.

[87] W. G. Unruh and R. M. Wald, "What happens when an accelerating observer detects a Rindler particle," *Phys. Rev. D*, vol. 29, pp. 1047–1056, Mar 1984.

[88] L. C. B. Crispino, A. Higuchi, and G. E. A. Matsas, "The Unruh effect and its applications," *Rev. Mod. Phys.*, vol. 80, pp. 787–838, 2008.

[89] S. Takagi, "Vacuum Noise and Stress Induced by Uniform Acceleration: Hawking-Unruh Effect in Rindler Manifold of Arbitrary Dimension," *Progress of Theoretical Physics Supplement*, vol. 88, pp. 1–142, 1986.

[90] A. Higuchi, S. Iso, K. Ueda, and K. Yamamoto, "Entanglement of the Vacuum between Left, Right, Future, and Past: The Origin of Entanglement-Induced Quantum Radiation," *Phys. Rev. D*, vol. 96, no. 8, p. 083531, 2017.

[91] A. Peres and D. R. Terno, "Quantum information and relativity theory," *Rev. Mod. Phys.*, vol. 76, pp. 93–123, Jan 2004.

[92] A. Peres, P. F. Scudo, and D. R. Terno, "Quantum entropy and special relativity," *Phys. Rev. Lett.*, vol. 88, p. 230402, May 2002.

[93] M. Czachor, "Einstein-Podolsky-Rosen-Bohm experiment with relativistic massive particles," *Phys. Rev. A*, vol. 55, pp. 72–77, Jan 1997.

[94] R. M. Gingrich and C. Adami, "Quantum entanglement of moving bodies," *Phys. Rev. Lett.*, vol. 89, p. 270402, Dec 2002.

[95] S. Weinberg, *The Quantum Theory of Fields*. Cambridge University Press, 1995.

[96] I. Fuentes-Schuller and R. B. Mann, "Alice falls into a black hole: Entanglement in noninertial frames," *Phys. Rev. Lett.*, vol. 95, p. 120404, Sep 2005.

[97] P. M. Alsing and G. J. Milburn, "Teleportation with a uniformly accelerated partner," *Phys. Rev. Lett.*, vol. 91, p. 180404, Oct 2003.

[98] A. Valentini, "Non-local correlations in quantum electrodynamics," *Physics Letters A*, vol. 153, no. 6, pp. 321–325, 1991.

[99] B. Reznik, "Entanglement from the vacuum," *Foundations of Physics*, vol. 33, no. 1, pp. 167–176, 2003.

[100] B. Reznik, A. Retzker, and J. Silman, "Violating Bell's inequalities in the vacuum," *Phys. Rev. A*, vol. 71, no. 4, p. 042104, 2005.

[101] D. Braun, "Creation of entanglement by interaction with a common heat bath," *Phys. Rev. Lett.*, vol. 89, p. 277901, Dec 2002.

[102] M. S. Kim, J. Lee, D. Ahn, and P. L. Knight, "Entanglement induced by a single-mode heat environment," *Phys. Rev. A*, vol. 65, p. 040101, Apr 2002.

[103] S. Schneider and G. J. Milburn, "Entanglement in the steady state of a collective-angular-momentum (Dicke) model," *Phys. Rev. A*, vol. 65, p. 042107, Mar 2002.

[104] A. M. Basharov, "Decoherence and entanglement in radiative decay of a diatomic system," *Journal of Experimental and Theoretical Physics*, vol. 94, no. 6, pp. 1070–1079, 2002.

[105] F. Benatti, R. Floreanini, and M. Piani, "Environment Induced Entanglement in Markovian Dissipative Dynamics," *Phys. Rev. Lett.*, vol. 91, p. 070402, Aug 2003.

[106] F. Benatti and R. Floreanini, "Entanglement generation in uniformly accelerating atoms: Reexamination of the Unruh effect," *Phys. Rev. A*, vol. 70, no. 1, p. 012112, 2004.

[107] G. Salton, R. B. Mann, and N. C. Menicucci, "Acceleration-assisted entanglement harvesting and rangefinding," *New J. Phys.*, vol. 17, no. 3, p. 035001, 2015.

[108] J.-I. Koga, G. Kimura, and K. Maeda, "Quantum teleportation in vacuum using only Unruh-DeWitt detectors," *Phys. Rev. A*, vol. 97, no. 6, p. 062338, 2018.

[109] K. K. Ng, R. B. Mann, and E. Martín-Martínez, "New techniques for entanglement harvesting in flat and curved spacetimes," *Phys. Rev. D*, vol. 97, no. 12, p. 125011, 2018.

[110] P. Chowdhury and B. R. Majhi, "Fate of entanglement between two Unruh-DeWitt detectors due to their motion and background temperature," *JHEP*, vol. 05, p. 025, 2022.

[111] S.-Y. Lin and B. Hu, "Entanglement creation between two causally disconnected objects," *Phys. Rev. D*, vol. 81, p. 045019, 2010.

[112] T. Li, B. Zhang, and L. You, "Would quantum entanglement be increased by anti-Unruh effect?," *Phys. Rev. D*, vol. 97, no. 4, p. 045005, 2018.

[113] J.-i. Koga, K. Maeda, and G. Kimura, "Entanglement extracted from vacuum into accelerated Unruh-DeWitt detectors and energy conservation," *Phys. Rev. D*, vol. 100, no. 6, p. 065013, 2019.

[114] A. P. C. M. Lima, G. Alencar, and R. R. Landim, "Asymptotic states of accelerated qubits in nonzero background temperature," *Phys. Rev. D*, vol. 101, no. 12, p. 125008, 2020.

[115] Y. Pan and B. Zhang, "Influence of acceleration on multibody entangled quantum states," *Phys. Rev. A*, vol. 101, no. 6, p. 062111, 2020.

[116] J. Zhang and H. Yu, "Entanglement harvesting for Unruh-DeWitt detectors in circular motion," *Phys. Rev. D*, vol. 102, no. 6, p. 065013, 2020.

[117] Z. Liu, J. Zhang, and H. Yu, "Entanglement harvesting in the presence of a reflecting boundary," *JHEP*, vol. 08, p. 020, 2021.

[118] Z. Liu, J. Zhang, R. B. Mann, and H. Yu, "Does acceleration assist entanglement harvesting?," *Phys. Rev. D*, vol. 105, p. 085012, Apr 2022.

[119] Z. Liu, J. Zhang, and H. Yu, "Entanglement harvesting of accelerated detectors versus static ones in a thermal bath," *Phys. Rev. D*, vol. 107, no. 4, p. 045010, 2023.

[120] M. S. Soares, G. Menezes, and N. F. Svaiter, "Entanglement dynamics: Generalized master equation for uniformly accelerated two-level systems," *Phys. Rev. A*, vol. 106, no. 6, p. 062440, 2022.

[121] J. Yan and B. Zhang, "Effect of spacetime dimensions on quantum entanglement between two uniformly accelerated atoms," *JHEP*, vol. 10, p. 051, 2022.

[122] C. Suryaatmadja, R. . B. Mann, and W. Cong, "Entanglement harvesting of inertially moving Unruh-DeWitt detectors in Minkowski spacetime," *Phys. Rev. D*, vol. 106, no. 7, p. 076002, 2022.

[123] D. Wu, S.-C. Tang, and Y. Shi, "Birth and death of entanglement between two accelerating Unruh-DeWitt detectors coupled with a scalar field," *JHEP*, vol. 12, p. 037, 2023.

[124] Y. Pan, J. Yan, S. Yang, and B. Zhang, "Influence of field mass and acceleration on entanglement generation," *Eur. Phys. J. C*, vol. 84, no. 10, p. 1111, 2024.

[125] Mayank, K. Hari, S. Barman, and D. Kothawala, "Entanglement between accelerated probes in de Sitter," 2 2025.

[126] A. Pozas-Kerstjens and E. Martin-Martinez, "Harvesting correlations from the quantum vacuum," *Phys. Rev. D*, vol. 92, no. 6, p. 064042, 2015.

[127] A. Pozas-Kerstjens, J. Louko, and E. Martin-Martinez, "Degenerate detectors are unable to harvest spacelike entanglement," *Phys. Rev. D*, vol. 95, no. 10, p. 105009, 2017.

[128] L. J. Henderson and N. C. Menicucci, "Bandlimited Entanglement Harvesting," *Phys. Rev. D*, vol. 102, no. 12, p. 125026, 2020.

[129] E. Martín-Martínez, E. G. Brown, W. Donnelly, and A. Kempf, "Sustainable entanglement production from a quantum field," *Phys. Rev. A*, vol. 88, no. 5, p. 052310, 2013.

[130] K. Lorek, D. Pecak, E. G. Brown, and A. Dragan, "Extraction of genuine tripartite entanglement from the vacuum," *Phys. Rev. A*, vol. 90, no. 3, p. 032316, 2014.

[131] A. Pozas-Kerstjens and E. Martin-Martinez, "Entanglement harvesting from the electromagnetic vacuum with hydrogenlike atoms," *Phys. Rev. D*, vol. 94, no. 6, p. 064074, 2016.

[132] A. Sachs, R. B. Mann, and E. Martín-Martínez, "Entanglement harvesting and divergences in quadratic unruh-dewitt detector pairs," *Phys. Rev. D*, vol. 96, p. 085012, Oct 2017.

[133] T. R. Perche, C. Lima, and E. Martín-Martínez, "Harvesting entanglement from complex scalar and fermionic fields with linearly coupled particle detectors," *Phys. Rev. D*, vol. 105, no. 6, p. 065016, 2022.

[134] L. J. Henderson, R. A. Hennigar, R. B. Mann, A. R. Smith, and J. Zhang, "Harvesting Entanglement from the Black Hole Vacuum," *Class. Quant. Grav.*, vol. 35, no. 21, p. 21LT02, 2018.

[135] W. Zhou and H. Yu, "Resonance interatomic energy in a Schwarzschild spacetime," *Phys. Rev. D*, vol. 96, no. 4, p. 045018, 2017.

[136] G. Menezes, "Entanglement dynamics in a Kerr spacetime," *Phys. Rev.*, vol. D97, no. 8, p. 085021, 2018.

[137] W. Cong, E. Tjoa, and R. B. Mann, "Entanglement Harvesting with Moving Mirrors," *JHEP*, vol. 06, p. 021, 2019.
[Erratum: JHEP 07, 051 (2019)].

[138] E. Tjoa and R. B. Mann, "Harvesting correlations in Schwarzschild and collapsing shell spacetimes," *JHEP*, vol. 08, p. 155, 2020.

[139] W. Cong, C. Qian, M. R. R. Good, and R. B. Mann, "Effects of Horizons on Entanglement Harvesting," *JHEP*, vol. 10, p. 067, 2020.

[140] M. P. G. Robbins, L. J. Henderson, and R. B. Mann, "Entanglement amplification from rotating black holes," *Class. Quant. Grav.*, vol. 39, no. 2, p. 02LT01, 2022.

[141] K. Gallock-Yoshimura, E. Tjoa, and R. B. Mann, "Harvesting entanglement with detectors freely falling into a black hole," *Phys. Rev. D*, vol. 104, p. 025001, Jul 2021.

[142] S. Barman, D. Barman, and B. R. Majhi, "Entanglement harvesting from conformal vacuums between two Unruh-DeWitt detectors moving along null paths," *JHEP*, vol. 09, p. 106, 2022.

[143] S. Barman and B. R. Majhi, "Optimization of entanglement depends on whether a black hole is extremal," *Gen. Rel. Grav.*, vol. 56, no. 6, p. 70, 2024.

[144] I. J. Membrere, K. Gallock-Yoshimura, L. J. Henderson, and R. B. Mann, "Tripartite Entanglement Extraction from the Black Hole Vacuum," 4 2023.

[145] S. Wang, M. R. P. Rivas, and R. B. Mann, "Harvesting Information Across the Horizon," 3 2025.

[146] J. L. Ball, I. Fuentes-Schuller, and F. P. Schuller, "Entanglement in an expanding spacetime," *Phys. Lett. A*, vol. 359, pp. 550–554, 2006.

[147] G. L. Ver Steeg and N. C. Menicucci, "Entangling power of an expanding universe," *Phys. Rev. D*, vol. 79, p. 044027, 2009.

[148] E. Martin-Martinez and N. C. Menicucci, "Cosmological quantum entanglement," *Class. Quant. Grav.*, vol. 29, p. 224003, 2012.

[149] S. Kukita and Y. Nambu, "Harvesting large scale entanglement in de Sitter space with multiple detectors," *Entropy*, vol. 19, no. 9, p. 449, 2017.

[150] L. J. Henderson, R. A. Hennigar, R. B. Mann, A. R. H. Smith, and J. Zhang, "Entangling detectors in anti-de Sitter space," *JHEP*, vol. 05, p. 178, 2019.

[151] H. Cai and Z. Ren, "Transition processes of a static multilevel atom in the cosmic string spacetime with a conducting plane boundary," *Sci. Rep.*, vol. 8, no. 1, p. 11802, 2018.

[152] E. Martin-Martinez, A. R. H. Smith, and D. R. Terno, "Spacetime structure and vacuum entanglement," *Phys. Rev. D*, vol. 93, no. 4, p. 044001, 2016.

[153] J. Trevison, K. Yamaguchi, and M. Hotta, "Spatially Overlapped Partners in Quantum Field Theory," *J. Phys. A*, vol. 52, no. 12, p. 125402, 2019.

[154] Q. Xu, S. A. Ahmad, and A. R. H. Smith, "Gravitational waves affect vacuum entanglement," *Phys. Rev. D*, vol. 102, no. 6, p. 065019, 2020.

[155] H. K, S. Barman, and D. Kothawala, "Universal role of curvature in vacuum entanglement," *Phys. Rev. D*, vol. 109, no. 6, p. 065017, 2024.

[156] S. Barman, I. Chakraborty, and S. Mukherjee, "Entanglement harvesting for different gravitational wave burst profiles with and without memory," *JHEP*, vol. 09, p. 180, 2023.

[157] F. He, Y. Pan, and B. Zhang, "Harvesting entanglement from the cylindrical gravitational wave spacetime," 4 2025.

[158] D. J. Stargen, "Finite-time Unruh effect: Waiting for the transient effects to fade off," 1 2025.

[159] D. Barman, S. Barman, and B. R. Majhi, "Role of thermal field in entanglement harvesting between two accelerated Unruh-DeWitt detectors," *JHEP*, vol. 07, p. 124, 2021.

[160] D. Barman, S. Barman, and B. R. Majhi, "Entanglement harvesting between two inertial Unruh-DeWitt detectors from nonvacuum quantum fluctuations," *Phys. Rev. D*, vol. 106, no. 4, p. 045005, 2022.

[161] D. Barman and B. R. Majhi, "Are multiple reflecting boundaries capable of enhancing entanglement harvesting?," *Phys. Rev. D*, vol. 108, p. 085007, Oct 2023.

[162] D. Barman, A. Choudhury, B. Kad, and B. R. Majhi, "Spontaneous entanglement leakage of two static entangled Unruh-DeWitt detectors," *Phys. Rev. D*, vol. 107, no. 4, p. 045001, 2023.

[163] S. A. Fulling, "Aspects of Quantum Field Theory in Curved Space-time," *London Math. Soc. Student Texts*, vol. 17, pp. 1–315, 1989.

[164] N. N. Bogoljubov, "On a new method in the theory of superconductivity," *Il Nuovo Cimento (1955-1965)*, vol. 7, no. 6, pp. 794–805, 1958.

[165] L. Parker, "Particle creation in expanding universes," *Phys. Rev. Lett.*, vol. 21, pp. 562–564, Aug 1968.

[166] L. Parker, "Quantized fields and particle creation in expanding universes. i," *Phys. Rev.*, vol. 183, pp. 1057–1068, Jul 1969.

[167] L. Parker, "Quantized fields and particle creation in expanding universes. ii," *Phys. Rev. D*, vol. 3, pp. 346–356, Jan 1971.

[168] L. Parker, "Quantized fields and particle creation in expanding universes. ii," *Phys. Rev. D*, vol. 3, pp. 2546–2546, May 1971.

[169] L. Parker, "Particle creation in isotropic cosmologies," *Phys. Rev. Lett.*, vol. 28, pp. 705–708, Mar 1972.

[170] L. Parker, "Particle creation in isotropic cosmologies," *Phys. Rev. Lett.*, vol. 28, pp. 1497–1497, May 1972.

[171] R. U. Sexl and H. K. Urbantke, "Production of particles by gravitational fields," *Phys. Rev.*, vol. 179, pp. 1247–1250, Mar 1969.

[172] B. S. DeWitt, "QUANTUM GRAVITY: THE NEW SYNTHESIS," in *General Relativity: An Einstein Centenary Survey*, pp. 680–745, Cambridge University Press, 1980.

[173] E. Martín-Martínez and P. Rodriguez-Lopez, "Relativistic quantum optics: The relativistic invariance of the light-matter interaction models," *Phys. Rev. D*, vol. 97, p. 105026, May 2018.

[174] A. Higuchi, G. E. A. Matsas, and C. B. Peres, "Uniformly accelerated finite time detectors," *Phys. Rev. D*, vol. 48, pp. 3731–3734, 1993.

[175] L. Sriramkumar and T. Padmanabhan, "Response of finite time particle detectors in noninertial frames and curved space-time," *Class. Quant. Grav.*, vol. 13, pp. 2061–2079, 1996.

[176] J. Louko and A. Satz, "Transition rate of the Unruh-DeWitt detector in curved spacetime," *Class. Quant. Grav.*, vol. 25, p. 055012, 2008.

[177] C. Rodríguez-Camargo, N. Svaiter, and G. Menezes, "Finite-time response function of uniformly accelerated entangled atoms," *Annals Phys.*, vol. 396, pp. 266–291, 2018.

[178] B. F. Svaiter and N. F. Svaiter, "Inertial and noninertial particle detectors and vacuum fluctuations," *Phys. Rev. D*, vol. 46, pp. 5267–5277, Dec 1992.

[179] S. Barman, B. R. Majhi, and L. Sriramkumar, "Radiative processes of single and entangled detectors on circular trajectories in (2+1)-dimensional Minkowski spacetime," *Phys. Rev. D*, vol. 109, no. 10, p. 105025, 2024.

[180] C. R. D. Bunney and J. Louko, "Circular motion analogue Unruh effect in a thermal bath: robbing from the rich and giving to the poor," *Class. Quant. Grav.*, vol. 40, no. 15, p. 155001, 2023.

[181] L. Sriramkumar, "On the response of Unruh-DeWitt detectors in classical electromagnetic backgrounds," *Mod. Phys. Lett. A*, vol. 14, p. 1869, 1999.

[182] L. Sriramkumar and T. Padmanabhan, "Probes of the vacuum structure of quantum fields in classical backgrounds," *Int. J. Mod. Phys. D*, vol. 11, pp. 1–34, 2002.

[183] J. Louko and A. Satz, "How often does the Unruh-DeWitt detector click? Regularisation by a spatial profile," *Class. Quant. Grav.*, vol. 23, pp. 6321–6344, 2006.

[184] J. Louko and A. Satz, "A New expression for the transition rate of an accelerated particle detector," in *11th Marcel Grossmann Meeting on General Relativity*, pp. 2659–2661, 11 2006.

[185] L. Hodgkinson and J. Louko, "How often does the Unruh-DeWitt detector click beyond four dimensions?," *J. Math. Phys.*, vol. 53, p. 082301, 2012.

[186] L. Hodgkinson and J. Louko, "Unruh-DeWitt detector on the BTZ black hole," *Springer Proc. Phys.*, vol. 157, pp. 523–530, 2014.

[187] L. Hodgkinson and J. Louko, "Static, stationary and inertial Unruh-DeWitt detectors on the BTZ black hole," *Phys. Rev. D*, vol. 86, p. 064031, 2012.

[188] K. K. Ng, L. Hodgkinson, J. Louko, R. B. Mann, and E. Martin-Martinez, "Unruh-DeWitt detector response along static and circular geodesic trajectories for Schwarzschild-AdS black holes," *Phys. Rev. D*, vol. 90, no. 6, p. 064003, 2014.

[189] J. Louko, "Unruh-DeWitt detector response across a Rindler firewall is finite," *JHEP*, vol. 09, p. 142, 2014.

[190] L. Hodgkinson, J. Louko, and A. C. Ottewill, "Static detectors and circular-geodesic detectors on the Schwarzschild black hole," *Phys. Rev. D*, vol. 89, no. 10, p. 104002, 2014.

[191] K. Lochan and T. Padmanabhan, "Inertial nonvacuum states viewed from the Rindler frame," *Phys. Rev. D*, vol. 91, no. 4, p. 044002, 2015.

[192] J. Louko and V. Toussaint, "Unruh-DeWitt detector's response to fermions in flat spacetimes," *Phys. Rev. D*, vol. 94, no. 6, p. 064027, 2016.

[193] L. Sriramkumar, "What do detectors detect?," *Fundam. Theor. Phys.*, vol. 187, pp. 451–478, 2017.

[194] K. Lochan, H. Ulbricht, A. Vinante, and S. K. Goyal, "Detecting Acceleration-Enhanced Vacuum Fluctuations with Atoms Inside a Cavity," *Phys. Rev. Lett.*, vol. 125, p. 241301, 2020.

[195] M. S. Ali, S. Bhattacharya, and K. Lochan, "Unruh-DeWitt detector responses for complex scalar fields in de Sitter spacetime," *JHEP*, vol. 03, p. 220, 2021.

[196] S. Biermann, S. Erne, C. Gooding, J. Louko, J. Schmiedmayer, W. G. Unruh, and S. Weinfurtner, "Unruh and analogue Unruh temperatures for circular motion in 3+1 and 2+1 dimensions," *Phys. Rev. D*, vol. 102, no. 8, p. 085006, 2020.

[197] K. K. Ng, C. Zhang, J. Louko, and R. B. Mann, "A little excitement across the horizon," *New J. Phys.*, vol. 24, no. 10, p. 103018, 2022.

[198] D. J. Stargen and K. Lochan, "Cavity Optimization for Unruh Effect at Small Accelerations," *Phys. Rev. Lett.*, vol. 129, no. 11, p. 111303, 2022.

[199] A. Dhanuka and K. Lochan, "Unruh DeWitt probe of late time revival of quantum correlations in Friedmann spacetimes," *Phys. Rev. D*, vol. 106, no. 12, p. 125006, 2022.

[200] H. K and D. Kothawala, "Rotating detectors in dS and AdS spacetimes," *Phys. Rev. D*, vol. 109, no. 10, p. 104073, 2024.

[201] M. R. Preciado-Rivas, M. Naeem, R. B. Mann, and J. Louko, "More excitement across the horizon," *Phys. Rev. D*, vol. 110, no. 2, p. 025002, 2024.

[202] A. S. Wilkinson and J. Louko, "Local quantum detection of the cosmological expansion: Unruh-DeWitt detectors in spatially compact Milne cosmology," *Phys. Rev. D*, vol. 111, no. 2, p. 025008, 2025.

[203] D. Bhattacharya, J. Louko, and R. B. Mann, "Probing hidden topology with quantum detectors," *Phys. Rev. D*, vol. 111, no. 4, p. 045005, 2025.

[204] H. S. Sahota and K. Lochan, "Are accelerated detectors sensitive to Planck scale changes?," *Phys. Rev. D*, vol. 111, no. 4, p. 045023, 2025.

[205] Peskin and Schroeder, *An Introduction to Quantum Field Theory*. Westview Press, 1 ed., 2015.

[206] I. L. C. Michael A. Nielsen, *Quantum computation and quantum information*. Cambridge Series on Information and the Natural Sciences, Cambridge University Press, 1 ed., 2004.

[207] M. Horodecki, P. Horodecki, and R. Horodecki, "On the necessary and sufficient conditions for separability of mixed quantum states," *Phys. Lett. A*, vol. 223, p. 1, 1996.

[208] C. H. Bennett, D. P. DiVincenzo, J. A. Smolin, and W. K. Wootters, "Mixed state entanglement and quantum error correction," *Phys. Rev. A*, vol. 54, pp. 3824–3851, 1996.

[209] F. Mintert, M. Kuś, and A. Buchleitner, "Concurrence of mixed bipartite quantum states in arbitrary dimensions," *Phys. Rev. Lett.*, vol. 92, p. 167902, Apr 2004.

[210] J. Hu and H. Yu, "Entanglement dynamics for uniformly accelerated two-level atoms," *Phys. Rev. A*, vol. 91, no. 1, p. 012327, 2015.

[211] E. G. Brown, "Thermal amplification of field-correlation harvesting," *Phys. Rev. A*, vol. 88, no. 6, p. 062336, 2013.

[212] P. Simidzija and E. Martín-Martínez, "Harvesting correlations from thermal and squeezed coherent states," *Phys. Rev. D*, vol. 98, no. 8, p. 085007, 2018.

[213] S. S. Costa and G. E. A. Matsas, "Background thermal contributions in testing the Unruh effect," *Phys. Rev. D*, vol. 52, pp. 3466–3471, 1995.

[214] S. Kolekar and T. Padmanabhan, "Quantum field theory in the Rindler-Rindler spacetime," *Phys. Rev. D*, vol. 89, no. 6, p. 064055, 2014.

[215] C. Chowdhury, S. Das, S. Dalui, and B. R. Majhi, "How robust is the indistinguishability between quantum fluctuation seen from noninertial frame and real thermal bath," *Phys. Rev. D*, vol. 99, no. 4, p. 045021, 2019.

[216] S. Barman and B. R. Majhi, "Radiative process of two entangled uniformly accelerated atoms in a thermal bath: a possible case of anti-Unruh event," *JHEP*, vol. 03, p. 245, 2021.

[217] D. Ghosh and B. R. Majhi, "Influence of thermal bath on Pancharatnam-Berry phase in an accelerated frame," *Phys. Lett. B*, vol. 858, p. 139015, 2024.

[218] S. Carroll, *Spacetime and geometry. An introduction to general relativity*.
AW, 2004.

[219] G. Compère, J. Long, and M. Riegler, "Invariance of Unruh and Hawking radiation under matter-induced supertranslations," *JHEP*, vol. 05, p. 053, 2019.

[220] J. J. Bisognano and E. H. Wichmann, "On the Duality Condition for a Hermitian Scalar Field," *J. Math. Phys.*, vol. 16, pp. 985–1007, 1975.

[221] J. J. Bisognano and E. H. Wichmann, "On the Duality Condition for Quantum Fields," *J. Math. Phys.*, vol. 17, pp. 303–321, 1976.

[222] R. Chatterjee, S. Gangopadhyay, and A. S. Majumdar, "Resonance interaction of two entangled atoms accelerating between two mirrors," *The European Physical Journal D*, vol. 75, no. 6, p. 179, 2021.

[223] S. Haroche and J.-M. Raimond, *Exploring the Quantum: Atoms, Cavities, and Photons*.
Oxford Graduate Texts, Oxford university press, 2006.

[224] I. Akal, Y. Kusuki, N. Shiba, T. Takayanagi, and Z. Wei, "Holographic moving mirrors," *Class. Quant. Grav.*, vol. 38, no. 22, p. 224001, 2021.

[225] Z. Huang and H. Situ, "Protection of quantum dialogue affected by quantum field," *Quantum Information Processing*, vol. 18, p. 37, Jan. 2019.

[226] Z. Huang and Z. He, "Deterministic secure quantum communication under vacuum fluctuation," *European Physical Journal D*, vol. 74, p. 176, Sept. 2020.

[227] M. R. R. Good, A. Lapponi, O. Luongo, and S. Mancini, "Quantum communication through a partially reflecting accelerating mirror," *Phys. Rev. D*, vol. 104, no. 10, p. 105020, 2021.

[228] R. Messina and R. Passante, "Fluctuations of the casimir-polder force between an atom and a conducting wall," *Phys. Rev. A*, vol. 76, p. 032107, Sep 2007.

[229] L. Rizzuto, "Casimir-polder interaction between an accelerated two-level system and an infinite plate," *Phys. Rev. A*, vol. 76, p. 062114, Dec 2007.

[230] Z. Zhu and H. Yu, "Position-dependent energy-level shifts of an accelerated atom in the presence of a boundary," *Phys. Rev. A*, vol. 82, p. 042108, Oct 2010.

[231] M. O. Scully, V. V. Kocharovsky, A. Belyanin, E. Fry, and F. Capasso, "Enhancing Acceleration Radiation from Ground-State Atoms via Cavity Quantum Electrodynamics," *Phys. Rev. Lett.*, vol. 91, p. 243004, 2003.

[232] H. W. Yu and S. Lu, "Spontaneous excitation of an accelerated atom in a spacetime with a reflecting plane boundary," *Phys. Rev. D*, vol. 72, p. 064022, 2005. [Erratum: Phys.Rev.D 73, 109901 (2006)].

[233] H. Yu, H. W. Yu, and Z. Zhu, "Spontaneous absorption of an accelerated hydrogen atom near a conducting plane in vacuum," *Phys. Rev. D*, vol. 74, p. 044032, 2006.

[234] A. Belyanin, V. V. Kocharovsky, F. Capasso, E. Fry, M. S. Zubairy, and M. O. Scully, "Quantum electrodynamics of accelerated atoms in free space and in cavities," *Phys. Rev. A*, vol. 74, p. 023807, Aug 2006.

[235] L Rizzuto and S Spagnolo, *Energy level shifts of a uniformly accelerated atom in the presence of boundary conditions*, vol. 161 of *012031*. https://dx.doi.org/10.1088/1742-6596/161/1/012031,: Journal of Physics: Conference Series, apr 2009.

[236] E. Arias, J. Dueñas, G. Menezes, and N. Svaiter, "Boundary effects on radiative processes of two entangled atoms," *JHEP*, vol. 07, p. 147, 2016.

[237] C. Zhang and W. Zhou, "Radiative processes of two accelerated entangled atoms near boundaries," *Symmetry*, vol. 11, no. 12, 2019.

[238] H. Zhai, J. Zhang, and H. Yu, "Geometric phase of an accelerated two-level atom in the presence of a perfectly reflecting plane boundary," *Annals of Physics*, vol. 371, pp. 338–347, 2016.

[239] J. Zhang and H. W. Yu, "The Unruh effect and entanglement generation for accelerated atoms near a reflecting boundary," *Phys. Rev. D*, vol. 75, p. 104014, 2007.

[240] S. Cheng, H. Yu, and J. Hu, "Entanglement dynamics for uniformly accelerated two-level atoms in the presence of a reflecting boundary," *Phys. Rev. D*, vol. 98, no. 2, p. 025001, 2018.

[241] L. S. Brown and G. J. Maclay, "Vacuum stress between conducting plates: An image solution," *Phys. Rev.*, vol. 184, pp. 1272–1279, Aug 1969.

[242] L. García-Álvarez, S. Felicetti, E. Rico, E. Solano, and C. Sabín, "Entanglement of superconducting qubits via acceleration radiation," *Scientific Reports*, vol. 7, no. 1, p. 657, 2017.

[243] J. R. Johansson, G. Johansson, C. M. Wilson, and F. Nori, "Dynamical casimir effect in superconducting microwave circuits," *Phys. Rev. A*, vol. 82, p. 052509, Nov 2010.

[244] S. Felicetti, C. Sabín, I. Fuentes, L. Lamata, G. Romero, and E. Solano, "Relativistic motion with superconducting qubits," *Phys. Rev. B*, vol. 92, p. 064501, Aug 2015.

[245] B. R. Majhi, "Are non-vacuum states much relevant for retrieving shock wave memory of spacetime?," *Phys. Lett. B*, vol. 808, p. 135640, 2020.

[246] K. Lochan and T. Padmanabhan, "Extracting information about the initial state from the black hole radiation," *Phys. Rev. Lett.*, vol. 116, no. 5, p. 051301, 2016.

[247] K. Lochan, S. Chakraborty, and T. Padmanabhan, "Information retrieval from black holes," *Phys. Rev. D*, vol. 94, no. 4, p. 044056, 2016.

[248] S. Chakraborty and K. Lochan, "Black Holes: Eliminating Information or Illuminating New Physics?," 2017.

[249] A. Chen, "Generalized Unruh effect: A potential resolution to the black hole information paradox," *Phys. Rev. D*, vol. 107, no. 5, p. 056014, 2023.

[250] I. S. Gradshteyn and I. M. Ryzhik, *Table of Integrals, Series, and Products*. Academic Press, 2014.

[251] P. Dennery and A. Krzywicki, *Mathematics for Physicists*. Dover Books on Physics, Dover Publications, 2012.

[252] M. J. Ablowitz and A. S. Fokas, *Complex Variables: Introduction and Applications*. Cambridge Texts in Applied Mathematics, Cambridge University Press, 2 ed., 2003.

[253] M. Czachor, "Comment on "quantum entropy and special relativity"," *Phys. Rev. Lett.*, vol. 94, p. 078901, Feb 2005.

[254] E. T. Akhmedov and D. Singleton, "On the physical meaning of the Unruh effect," *Pisma Zh. Eksp. Teor. Fiz.*, vol. 86, pp. 702–706, 2007.

[255] W. H. Zurek, "Decoherence and the transition from quantum to classical," *Physics Today*, vol. 44, no. 10, p. 36, 1991.

[256] W. H. Zurek, "Decoherence, einselection, and the quantum origins of the classical," *Rev. Mod. Phys.*, vol. 75, pp. 715–775, May 2003.

[257] F. Mintert, A. R. R. Carvalho, M. Kuś, and A. Buchleitner, "Measures and dynamics of entangled states," *Physics Reports*, vol. 415, pp. 207–259, Aug. 2005.